2006

SYNTHESIS AND EVALUATION OF PYRIDINIUM DERIVATIVES AS CENTRAL NERVOUS SYSTEM NICOTINIC ACETYLCHOLINE RECEPTOR LIGANDS

Joshua Thomas Longen Ayers
University of Kentucky, josh-uk@coffeegrinder.org

ABSTRACT OF DISSERTATION

Joshua Thomas Longen Ayers

The Graduate School

University of Kentucky

2006

SYNTHESIS AND EVALUATION OF PYRIDINIUM DERIVATIVES AS CENTRAL NERVOUS SYSTEM NICOTINIC ACETYLCHOLINE RECEPTOR LIGANDS

ABSTRACT OF DISSERTATION

A dissertation submitted in partial fulfillment of the
requirements for the degree of Doctor of Philosophy
in the College of Pharmacy at the University of Kentucky

By
Joshua Thomas Longen Ayers

Lexington, Kentucky

Director: Dr. Peter A. Crooks,

Professor of Pharmaceutical Sciences, College of Pharmacy

Lexington, Kentucky

2006

ABSTRACT OF DISSERTATION

SYNTHESIS AND EVALUATION OF PYRIDINIUM DERIVATIVES AS CENTRAL NERVOUS SYSTEM NICOTINIC ACETYLCHOLINE RECEPTOR LIGANDS

This project utilized synthesis and in vitro assays to generate antagonist SARs at various nAChR subtypes. Alkylation of the pyridino nitrogen of the nicotine molecule afforded subtype specific antagonists at a4ß2* nAChR subtypes and nAChR subtypes that mediate nicotine-evoked dopamine release. Using this data, a series of *mono*-azaaromatic quaternary salts were produced and evaluated in binding and functional assays for a4ß2* and a7* nAChR subtypes and nAChR subtypes that mediate nicotine-evoked dopamine release. Additionally, *bis*-azaaromatic quaternary salts were synthesized and evaluated in the same assays. Two potent lead compounds were identified. *N*-n-dodecylnicotinium iodide (NDDNI) was found to be very potent at both a4ß2* nAChR subtypes and nAChR subtypes that mediate nicotine-evoked dopamine release. And the most promising candidate was *N-N'-bis*-dodecylpicolinium dibromide (bDDPiB), which was selective for the nAChR subtypes that mediate nicotine-evoked dopamine release (IC_{50} = 9 nM).

Additionally, using the data from the SARs, predictive computer models were generated to assist in future compound assessment without in vitro assays. Three self-organizing map (SOMs) models were generated from three different sets of compounds. The groups consisted of the *mono*-substituted compounds, the *bis*-substituted compounds, and both sets combined. The models were able to successfully "bin" the test set of compounds after developing a model from a similar set of training compounds. Additionally, using genetic functional activity (GFA) algorithms an evolutionary approach to generating predictive model equations was

applied to the compounds. Three separate equations were generated in order to form a predictive method for evaluating affinities at the $\alpha 4\beta 2^*$ receptor subtype.

In addition to the modeling and SAR work of the quaternary ammonium compounds, novel synthetic methods were also employed to develop enantiomerically pure nicotine analogs. Efficient enantioselective syntheses of (S)- and R-(+)-nornicotine, (S)-and R-(+)-anabasine, and (S)-and R-(+)-anatabine have been developed, affording isomers in high enantiomeric excess.

KEYWORDS: Nicotinic receptors, Antagonists, Nicotine, Enantiomeric synthesis, Self-organizing maps

Joshua T. L. Ayers

07 July 2006

SYNTHESIS AND EVALUATION OF PYRIDINIUM DERIVATIVES AS CENTRAL NERVOUS SYSTEM NICOTINIC ACETYLCHOLINE RECEPTOR LIGANDS

By

Joshua Thomas Longen Ayers

Peter A. Crooks

Director of Dissertation

James Pauly

Director of Graduate Studies

07 July 2006

RULES FOR THE USE OF DISSERTATIONS

Unpublished dissertations submitted for the Doctor's degree and deposited in the University of Kentucky Library are as a rule open for inspection, but are to be used only with due regard to the rights of the authors. Bibliographical references may be noted, but quotations or summaries of parts may be published only with the permission of the author, and with the usual scholarly acknowledgments.

Extensive copying or publication of the dissertation in whole or in part also requires the consent of the Dean of the Graduate School of the University of Kentucky.

A library that borrows this dissertation for use by its patrons is expected to secure the signature of each user.

Name Date

_____

_____

_____

_____

_____

_____

_____

_____

_____

DISSERTATION

Joshua Thomas Longen Ayers

The Graduate School

University of Kentucky

2006

SYNTHESIS AND EVALUATION OF PYRIDINIUM DERIVATIVES AS CENTRAL NERVOUS SYSTEM NICOTINIC ACETYLCHOLINE RECEPTOR LIGANDS

DISSERTATION

A dissertation submitted in partial fulfillment of the
requirements for the degree of Doctor of Philosophy
in the College of Pharmacy at the University of Kentucky

By
Joshua Thomas Longen Ayers

Lexington, Kentucky

Director: Dr. Peter A. Crooks,

Professor of Pharmaceutical Sciences, College of Pharmacy

Lexington, Kentucky

2006

In Memory of my Grandfather
Lawrence N. Longen

ACKNOWLEDGEMENTS

I would like to thank my mentor and advisor Dr. Peter Crooks for his guidance, advice, and friendship. I owe much of my development as a scientist to his training and direction. I appreciate the opportunity to work on a project with such a variety of aspects and having the freedom to explore those that held specific interest to me. It was truly an honor to work under his supervision. I would also like to thank my committee members: Dr. Linda Dwoskin, Dr. George Digenis, Dr. Kyung Kim, and Dr. Lowell Bush for their insights and guidance. Additionally, I appreciate the willingness of Dr. Mark Lovell to serve as my outside examiner. I want to express my gratitude to my undergraduate advisor Dr. Shelby Anderson, who urged me to explore and fulfill my research potential in graduate school. I also want to thank the University of Kentucky and the National Institutes of Health for their financial support.

In my graduate career, I have interacted with excellent scientists and trusted friends. Thank you to Dr. Crooks' lab group for your support and tolerance during my tenure at the university. I would especially like to thank Rui and Guangrong for their assistance and encouragement. I also would like to thank Dr. Dwoskin and her lab group, especially Dr. Vladimir Grinevich, Dr. Jun Zhu, Dr. Sangeetha Sumithran, A. Gabriela Deaciuc, Aaron Haubner, David Eaves, and Lisa Price for their work in the pharmacological assays presented within. Additionally, I am grateful to Dr. Jeffery Schmitt, Dr. Rebecca Harris, and Aaron Clauset of Targacept Inc. for their assistance with the modeling work. I want to thank Aimee, Lisa, Bethel, and Josh for their encouragement, advice, and friendship.

I would like to thank my family, whose unending understanding and encouragement have allowed me to be everything that I am today. I thank my mother for always being there for me as both an intellectual guide, as well as a loving parent. I thank my brother, Matt, for his support and steadfast belief in me. I would also like to thank all my friends that have listened, encouraged, and cheered me along the way. Finally, I would like to thank my wife, Lindsey, for her incredible patience and love, they have meant the world to me.

TABLE OF CONTENTS

LIST OF TABLES

LIST OF FIGURES

Chapter 1: Overview and Research Plan

1.1. Overview

In order to bring a drug to market, it first must go through two major areas of research: drug discovery and drug development. Drug discovery incorporates both chemical and biological methodologies in order to identify a compound or a group of compounds, which exhibit favorable *in vitro* activity in specific pharmacological assays. After the initial identification of a lead compound, the development process then incorporates formulation studies and human clinical trials to assess the bioavailability, stability, and safety of the drug candidate (Figure 1.1).

Within the discovery process, there are several important issues to assess. The first is the determination of an active compound. Once a structure is determined to be bioactive in *in vitro* screens, a series of structurally similar compounds are synthesized and evaluated and structure-activity relationships (SAR) are defined in an attempt to optimize biological activity, since the initial compound "hit" is rarely the most efficacious. The synthetic compounds are prioritized according to their bioactivity, and a lead candidate is then identified. The data obtained can be compiled to form a library of information or an SAR database relating the structure of the compounds to their bioactivities. From this information, computer-assisted models of the compound's interaction with the receptor may be developed.

Depending on the system being evaluated, a variety of techniques may be used to generate computer models for assessing biological activity. Those compounds that

interact with a biological target that previously has been crystallized, e.g. an enzyme or protein molecule, can be modeled in the active site using *in silico* methods involving molecular modeling and docking to the crystallized target. For those biological targets that have not been identified crystallographically, e.g. receptors, several methodologies can be utilized in order to achieve a three-dimensional model of the molecular recognition site from SAR data. Pharmacophore models (three-dimensional approximation of the active binding site) can be generated from large numbers of compounds and their activities predicted using comparative molecular field analysis (CoMFA). Additionally, mathematical models, genetic functional approximation algorithms (GFAs), and self-organizing maps (SOMs) can be used as methodologies to predict activities or trends at a given receptor or enzyme active site.

Further drug development includes the pre-clinical processes associated with toxicity screening, formulation, and characterization of the absorption, distribution, metabolism, and elimination (ADME) properties of the potential drug molecule. After full characterization of the compound, as well as determination of dosing parameters, drug candidates enter human clinical studies. In order to obtain approval for clinical studies, an Investigational New Drug application (IND) must be filed. This document contains all pertinent data to the drug's safety and efficacy as determined in the studies mentioned above. If accepted, trials in healthy human volunteers (Phase I) may begin followed by patient volunteers (Phase II-IV). After all information on safety, efficacy, and dosage regimes is collected, drug approval is sought from the Food and Drug Administration (FDA) through a New Drug Application (NDA).

In addition to their therapeutic uses, the development of compounds may also be useful as diagnostic and pharmacological tools in the analysis of perspective drug candidates. In *in vitro* binding assays, a test ligand that interacts with the receptor binding site is used as a measurement tool in order to assess the relative affinities of the drug candidates for the target binding site. These ligands must be selective and potent at their site of action in order to be used as diagnostic tools.

An objective of this research is to involve aspects of the drug discovery process to aid in identifying potential drug candidates for therapeutic use or as analytical tools to help determine biological functions.

Figure 1.1 Components of the Drug Discovery and Drug Development Process

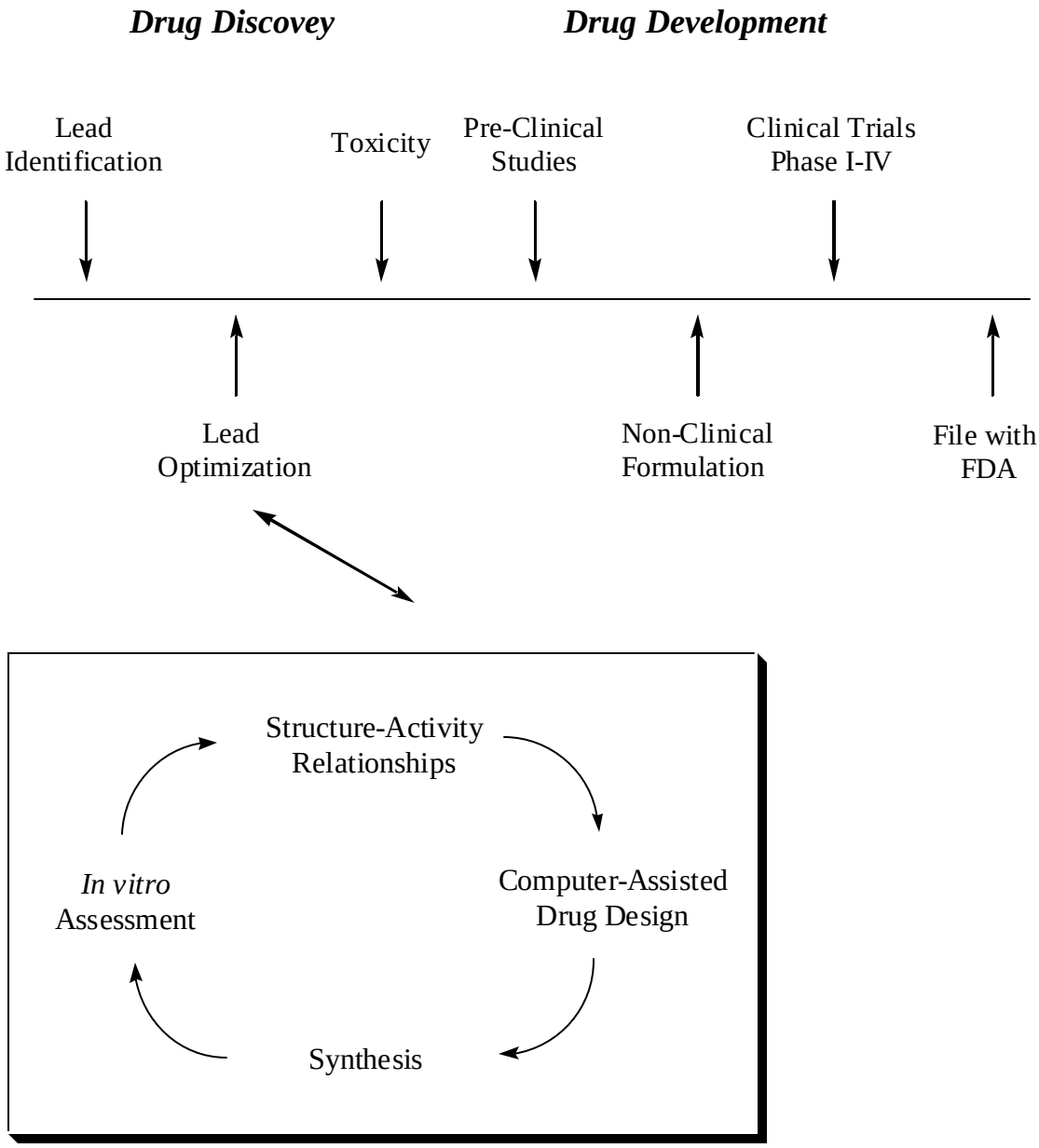

1.2. Molecular Target and Lead Identification

Nicotinic acetylcholine receptors (nAChRs) belong to a ligand-gated ion channel superfamily of receptors located in both the peripheral and central nervous systems. Neuronal nAChRs are composed of five subunits that assemble in both heterologous (α- and β-subunits) and homologous forms (α-subunits). Several different nAChR combinations, or subtypes, have been identified, with the $\alpha4\beta2$* being the most studied heterologous subtype and the $\alpha7$* being the most studied homologous subtype. Since definitive subunit combinations have yet to be determined, an asterisk (*) is used following subtype nomenclature to indicate the reported subunit make-up. In addition to the above receptor subtypes, which are thought to produce a pharmacological effect without other nAChR subtypes, there are other receptor populations where multiple subtypes contribute to one pharmacological response. While these heterologous subunit combinations have not yet been fully assigned, they are referred to by their biological function that they initiate (e.g. the nicotinic receptor that facilitates dopamine (DA) release. These subtypes, which have recently begun to be identified as the $\alpha4\beta2$*, $\alpha4\alpha5\beta2$*, $\alpha6\beta2\beta3$*, and $\alpha6\alpha4\beta2\beta3$*, all contributing to nicotine-evoked DA release. Research in the field of nAChRs has focused mainly on the development of receptor agonists, and to a lesser extent antagonists, that act at specific nicotinic receptor subtypes in order to elucidate function, as well as to serve as potential drug therapies in disease states such as Alzheimer's and Parkinson's disease, schizophrenia, pain management, and nicotine addiction.

Previous research in the Crooks and Dwoskin laboratories has focused on the development of ligands, specifically antagonists that may be more efficacious and specific than the more established "classical" antagonists (e.g. DHßE). In this respect, alkylation of the pyridyl nitrogen of the nicotine (NIC) molecule afforded two lead compounds, *N*-octylnicotinium iodide (NONI), an antagonist at the nAChR subtypes that facilitate DA release, and *N*-decylnicotinium iodide (NDNI), an antagonist at the $\alpha4\beta2^*$ receptor subtype (Crooks *et al.* 1995; Dwoskin *et al.* 1999). Thus, quaternary ammonium compounds of this type were considered as useful lead candidates for exploring the complex biological activities at the molecular level through SAR studies at individual nAChR receptor subtypes.

1.3. Hypothesis and Specific Aims of Research

The nicotinic receptor has been implicated in many disease states, including Alzheimer's and Parkinson's disease and schizophrenia. With the diverse subtype architecture of the nicotinic receptor, novel selective ligands are needed for both furthering research and use as treatments for diseases. Current research has focused in the development of agonists for these purposes. However, the development of novel antagonists at various nAChR subtypes should also give insight into the pharmacology of these receptors. This research will utilize synthesis and in vitro assays to generate antagonist SARs at various nAChR subtypes. These SARs will be used to develop potent and selective antagonists at individual nicotinic receptor subtypes. Additionally, using the data from the SARs, predictive computer models will be generated to assist in future compound assessment without in vitro assays.

Specific Aim 1

SARs directed at alteration of the nicotine molecule will result in optimization of the potency, activity, and nicotinic receptor subtype selectivity of these novel classes of nicotinic receptor ligands. Alterations will include changing the pyridino head group, e.g. pyridinium and picolinium groups, increasing the carbon chain length, and creating both *mono*- and *bis*-substituted molecules.

Specific Aim 2

Utilizing the SARs developed in specific aim 1, computer generated models can be developed for screening of compounds at $\alpha 4\beta 2^*$ receptor subtypes. Modeling techniques will include GFA and SOM model generation.

Specific Aim 3

The synthesis of quaternary ammonium salts outlined in specific aim 1, which utilize commercially available pyridine moieties, e.g. pyridine and S-(-)-nicotine, are useful for discovering new nAChR antagonists. In addition to those commercially available compounds, new potential nicotinic receptor ligands head groups will be developed. Novel enantioselective synthetic procedures of nornicotine, anabasine, and anatabine will be developed and optimized.

Chapter 2: Background

2.1. Molecular Pharmacology

Nicotinic acetylcholine receptors (nAChRs) are members of the ligand-gated ion channel superfamily of receptors, activated by endogenous acetylcholine (ACh), and are widely distributed throughout the body. Other members of this superfamily include, gamma-aminobutyric acid ($GABA_A$), serotonin (5-HT), glycine, and several glutamate receptors (e.g. *N*-methyl-D-aspartate (NMDA), α-amino-3-hydroxy-5-methyl-4-isoxazolepropionate (AMPA), and kinate). Members of this family of receptors all share a pair of disulphide-bonded cystines in their N-terminus extracellular halves that are separated by 13 residues (Kao and Karlin 1986; Karlin and Akabas 1995; Ortells and Lunt 1995). Nicotinic receptors modulate a wide range of physiological areas, including the central and peripheral nervous systems and the function of the cardiovascular, immune, and neuromuscular systems and are located at the neuromuscular junction in autonomic ganglia, and in the central nervous system (CNS) (Sargent 1993; Lloyd and Williams 2000). nAChRs are preferentially located presynaptically, where they play a role in neurotransmitter release (McGehee and Role 1995; Wonnacott 1997). Postsynaptic nAChRs, however, have also been identified in brain regions, although their function and importance is still being investigated (Colquhoun and Patrick 1997).

2.2. Structure of the nAChR

It is generally accepted that nAChRs are membrane-bound pentameric complexes composed of individual protein subunits. When activated by interaction with acetylcholine or other appropriate agonists, the receptor allows passage of cations, e.g.

Na^+, Ca^{2+}, and K^+, through the central pore. These complexes have an approximate molecular weight of 300 kDa. The protein subunits assemble with a 5-fold axis of symmetry and form the ion conduction pathway of the receptor (Karlin and Akabas 1995; Schmitt 2000) (Figure 2.1A). Each subunit is composed of a large N-terminus loop followed by four transmembrane spanning hydrophobic regions, M1-M4 (Claudio *et al.* 1983; Leonard *et al.* 1988). The portions of the M1 and the complete segments of the M3 and M4 transmembrane regions interact with the lipid bilayer, separating the pore from the hydrophobic membrane (Karlin 2002; Miyazawa *et al.* 2003). M2 has a high degree of segregated hydrophilic and hydrophobic portions of the amino acid helical cylinder and forms the inner portion of the ion channel with some sections of the M1 (Leonard *et al.* 1988; Changeux *et al.* 1998; Grutter and Changeux 2001; Karlin 2002; Miyazawa *et al.* 2003). Additionally, alterations to the amino acid sequence of the M2 portion affect the ion selectivity of the channel (Imoto *et al.* 1988; Adcock *et al.* 1998) (Figure 2.1B).

Smit *et al.* (2001) provided the high-resolution structure of the Acetylcholine Binding Protein (AChBP), which provided a number of insights into the structure and function of nAChRs. AChBP is a soluble protein synthesized in snail neuronal glial cells and modulates synaptic transmissions (Brejc *et al.* 2001; Smit *et al.* 2001). This protein binds many of the same ligands as the peripheral and neuronal nAChRs, including nicotine, epibatidine, (+)-tubocurarine, and α-bungarotoxin. The affinities for these ligands closely resemble those found in the α7* subtype, though with higher overall affinities. This similarity can be attributed in part to the AChBP's similar amino acid residues and a

significant sequence alignment (20 - 24%, α7 ~ 24%) with the extracellular portions of the α subunits (Grutter and Changeux 2001; Karlin 2002; Smit *et al.* 2003).

As stated above, several of the nAChR subtypes have a conserved 13 residue Cys-loop at the N-terminus. This loop is present in the AChBP; it is only 12 amino acid residues and is not conserved. The nAChR subunits are typically hydrophobic residues that make up the loop, while the AChBP's subunits are mostly hydrophilic (Karlin 2002; Smit *et al.* 2003). It has been proposed that differences in the 13 amino acid sequence of the Cys-loop are because nAChR subtypes are membrane bound and interacting with the transmembrane domain of the receptor. The AChBP is not membrane bound, therefore, it would not need to have the conserved residues in order to function (Karlin 2002; Smit *et al.* 2003). The AChBP also provided insight into the binding site of the nAChR. Examination of the peripheral nAChR ACh-binding site by mutagenesis and photoaffinity labeling studies identified the residues involved in ACh-binding (Corringer *et al.* 2000). When compared to the peripheral nAChR subtype, the AChBP has high conservation of residues that line the ACh-binding site (Smit *et al.* 2001; Karlin 2002). It was originally thought that the position of the binding site was contained within the α-subunit within the ion channel (Miyazawa *et al.* 1999). The binding site of the AChBP, however, was found to be at the outside of the complex approximately midway in between the top and bottom of the receptor. Additionally, access to receptor binding site was found to be from the outside not through the ion channel (Changeux and Edelstein 2001; Karlin 2002). Studies of the AChBP binding site also demonstrated that the site was located at the interface of two subunits. The same binding phenomenon was

determined for peripheral and neuronal nAChR subtypes (Corringer *et al.* 2000). Luetje and Patrick (1991) demonstrated that both the α- and β-subunits are important in agonist, as well as antagonist, sensitivity to nAChRs. The heteropentamer's interfacial binding site was split into two components, the principal (α-subunit) and the complementary (the neighboring subunit, e.g. β-subunits in the CNS and γ/δ in the periphery). Homopentamer's binding sites are also split into the principle and complementary components but both are contributed by the α-subunits. The principal component is composed of three loops, A (Tyr93, α1-numbering), B (Trp149), and C (Tyr190, Cys 192, Cys 193, and Tyr 198). The complementary component is also composed of three loops, D (Trp55 and Glu57, γ-numbering), E (Leu109, Tyr111, Tyr117, and Leu119), and F (Asp 174 and Glu176) (Smit *et al.* 2003; Grutter *et al.* 2004). Tyr93 (methyl groups), Trp149 (ammonium ion), and Loop C (ester moiety) all interact with the binding of ACh (Cohen *et al.* 1991; Zhong *et al.* 1998; Grutter *et al.* 2000). Additionally, Sine *et al.* (2002) have reported that the AChBP binding of HEPES has been crystallized and the charged ammonium group was found to interact with the Trp143 (Trp149 in the peripheral nAChR) residue, confirming the calculations of Zhong *et al.* (1998). Docking experiments using models of the extracellular domains of nAChR subtypes based on the AChBP structure have been performed with success (Zhong *et al.* 1998; Fruchart-Gaillard *et al.* 2002; Le Novere *et al.* 2002; Schapira *et al.* 2002). The use of such experiments may lead to increased understanding of the nAChR; however, without crystallized structures of each individual subtype, data collected will not be definitive.

2.3. NAChR Subunit Nomenclature and Composition

Nicotinic receptors have been characterized into two different classes, peripheral and neuronal. The peripheral muscle-type nicotinic receptor has been extensively characterized due to the abundance and reproducibility of the receptor. When various toxins were found to bind to the acetylcholine binding site of the muscle nicotinic receptor, radiolabeled forms of these toxins were utilized to identify, quantitate, and purify these receptors. From these studies, the major binding subunit of the nicotinic receptor has become known as the α subunit. This subunit is identified by two adjacent cysteine residues (residues 192 and 193) (Figure 2.1A), as well as a highly conserved binding domain possessing aromatic amino acids involved in π-interactions (Grutter and Changeux 2001; Sharpless and Wonnacott 2001). From the information gathered using these criteria, ten such subunits have been identified, α1-α10, in various peripheral and central nervous systems (Sargent 1993; Elgoyhen *et al.* 2001).

Figure 2.1 Subunit designation and composition

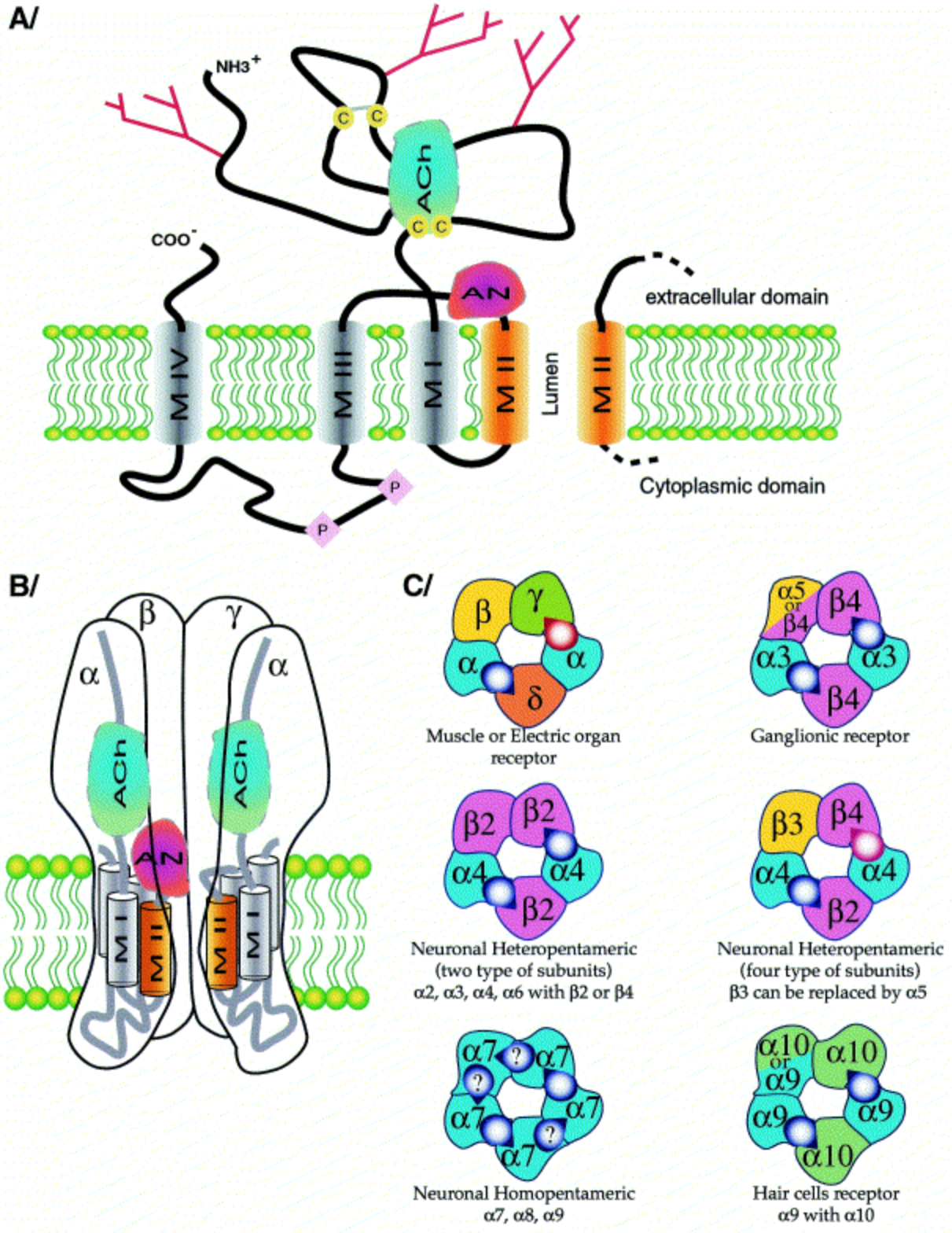

Reprinted from Brain Res Bull, 57(2), Tassonyi E. *et al*., The role of nicotinic acetylcholine receptors in the mechanisms of anesthesia, 133-150, Copyright (2002), with permission from Elsevier

The α subunit has been found in combination with other subunits, β, γ, ε, and δ, in the periphery. These other subunits were initially identified as structural subunits. Similarly, α subunits in the central nervous system were found with subunits that lacked the disulfide bridge. These non-alpha or β subunits have been identified as β1-β4 for heterologolously expressed neuronal receptors (Sargent 1993). Additionally, homologolously expressed neuronal receptors that only contain the α subunit have also been discovered. The various subunits found have been further organized into four subfamilies, I-IV. Subfamilies I and II contain the homologously expressed subunits, α9 and α10 (subfamily I) and α7 and α8 (subfamily II). The peripheral muscle-type receptor subunits (α1, β1, γ, ε, and δ) compose subfamily IV. Finally the largest of the subfamilies, subfamily III (α2-α6 and β2-β4), has been further subdivided into three tribes. Tribe 1 contains the binding subunits, α2, α3, α4, and α6. The β subunits, β2 and β4, make up tribe 2. Tribe 3 is composed of α5 and β3 (Corringer *et al.* 2000).

Skeletal muscle nicotinic receptors were found to have a subunit composition of $(\alpha 1)_2$:β1:γ:δ or $(\alpha 1)_2$:β1:ε:δ depending on the age of the receptor subtype (Karlin and Akabas 1995). The ε subunit replaces the γ subunit in adult mammalian muscle receptors. The pentameric structure of this subtype is α1:γ:α1:δ:β1 or α1:ε:α1:δ:β1. Additionally, contrary to the initial findings of the ACh binding site, the α1, γ or ε, and δ all contributing to the binding of acetylcholine, with the majority of the binding sites located in the α1 subunit (Adcock *et al.* 1998) (Figure 2.1C).

As stated above, CNS nicotinic receptor subunits tend to associate in two modes, e.g. heterologously and homologously. However, in contrast to the significant amount of information on the muscle-type receptors, the subunit make-up and stoichiometries of the neuronal nAChRs are not as well characterized. Members of subfamilies I and IV and the α8 subunit (subfamily II) are not expressed in the mammalian brain (Corringer *et al.* 2000; Elgoyhen *et al.* 2001). A number of researchers have isolated cDNA or gene clones of several α subunits, α2, α3, α4, α5, α6, and α7, as well as three β subunits, β2, β3, and β4 (Boulter *et al.* 1987; Goldman *et al.* 1987; Deneris *et al.* 1988; Wada *et al.* 1988; Deneris *et al.* 1989; Boulter *et al.* 1990; Seguela *et al.* 1993). Subunit mRNA for different α and β subunits have been identified in various overlapping brain regions, suggesting subunit complexity (Wilkens 2001). The binding site of the heterologously expressed nAChR subtypes is formed from both tribe 1 (α2, α3, α4, and α6) and tribe 2 (β2 and β4). Additionally, the function of the receptors requires that at least one subunit of α and one of β be present. Tribe 3 subunits (α5 and β3) have also been proposed to exist in such multi α or β complexes as modulators of the other paired subunits (Lin and Meyer 1998; Girod *et al.* 1999) (Figure 2.1C). Therefore, the subunit composition of the pentameric system is two binding site pairs and a fifth subunit from tribes 2 or 3 (Luetje 2004).

Homologously expressed receptor subtypes demonstrated a five α subunit binding site structure (suggesting a pentameric structure), each of which may exhibit different affinities for nicotinic ligands (Palma *et al.* 1996; Orr-Urtreger *et al.* 1997; Rakhilin *et al.* 1999). Only the α7 subunit from the homomeric subfamily II exists in the CNS.

Therefore, the only homologously expressed subtype is often referred to as the α7* nAChR subtype.

2.4. nAChR Subtype Formation

It should be noted that before there is any discussion about subunit assembly, there is still much to be learned about the composition of naturally expressed nAChR subtypes. Although many researchers have presented compelling evidence towards a particular subtype combination, other more complex assemblies may exist *in vivo*, and therefore an asterisk (*) follows native subtypes that are putatively assigned, after the convention adopted by Lukas *et al.* (Lukas *et al.* 1999).

Heterologously expressed nAChR Subtypes

Affinity labeling, immunoprecipitation, [^{3}H]-nicotine binding, *in situ* hybridization, and constitutive gene knockout studies all demonstrate that the α4β2* receptor subtype is the predominant neuronal nicotinic receptor for which nicotine has high affinity (Clarke *et al.* 1985; Marks *et al.* 1986; Whiting *et al.* 1987; Wada *et al.* 1989; Flores *et al.* 1992; Picciotto *et al.* 1998; Zoli *et al.* 1998). *Xenopus* oocytes express α4β2 receptors with a stoichiometry of $(\alpha4)_2(\beta2)_3$, with the presumed order being α4:β2:α4:β2:β2 (Anand *et al.* 1991; Cooper *et al.* 1991). Two identical agonist binding sites exist at the α4 and β2 subunit interfaces. It has also been proposed that an α5 subunit may be associated with some populations of α4β2* receptors (Conroy *et al.* 1992; Sharpless and Wonnacott 2001). α4β2* nAChR have been associated with anxiety, depression, pain, cognition, and neurodegeneration (Lloyd and Williams 2000).

Another form of heterologously expressed nAChR subtype is the nicotinic receptors that mediate NIC-evoked DA release. Although not as prevalent in brain tissue as $\alpha4\beta2^*$ subtypes (Schulz *et al.* 1991), these subunit assemblies are very important in regulation of dopamine release, as determined from antagonist studies involving several known compounds that interact at the nAChR subtype (Schulz and Zigmond 1989; Grady *et al.* 1992; Crooks *et al.* 1995; Cartier *et al.* 1996). The existence of DA release facilitating nAChR subtypes is further supported by autoradiography studies, where a potent, non-specific agonist, [^{3}H](±)-epibatidine, is proposed to bind to areas of the brain containing $\alpha4\beta2^*$ nAChR subtypes as well as a second receptor class that were also marked by [^{125}I]neuronal bungarotoxin, a sensitive ligand to the nAChR subtype facilitating DA release (Holladay *et al.* 1997). Although, initially defined as one subtype, $\alpha3\beta2^*$, the exact assignment of the subunit composition of these DA releasing nAChR subtypes was uncertain for many years. mRNA of several nAChR subunits were shown to be present in areas of the brain associated with dopamine release, including $\alpha4$, $\alpha5$, $\alpha6$, $\alpha7$, $\beta3$, and $\beta4$ subunits located in the substantia nigra, which projects to the striatum, a known area involved in dopamine release (Deneris *et al.* 1989; Wada *et al.* 1989; Wonnacott 1997; Charpantier *et al.* 1998). Additionally, mRNA of the modulatory subunits $\alpha6$ and $\beta3$ had high expression levels in the substantia nigra (Deneris *et al.* 1989; Goldner *et al.* 1997; Charpantier *et al.* 1998). Studies involving $\alpha5$ subunits (closely related structurally to β subunits) revealed that the replacement of the non-binding $\beta4$ subunit with an $\alpha5$ subunit leads to a change in the pore Ca^{2+} permeabilities and desensitization rates (Wang *et al.* 1996; Gerzanich *et al.* 1998) (Figure 2.1C). Moreover, increased agonist potencies were

observed when incorporating α5 into the oocyte α3β2 subunit assembly to yield a subunit composition of α3:β2:α5:β2:α3 (Gerzanich *et al.* 1998). These findings generated considerable debate as to the exact subunit composition of nAChR subtypes mediating NIC-evoked DA release (Klink *et al.* 2001; Azam *et al.* 2002; Champtiaux *et al.* 2002; Whiteaker *et al.* 2002; Zoli *et al.* 2002), and there remained a large focus on elucidating the specific nAChR subtypes responsible for DA release. The discovery and use of the α-conotoxins (α-ctx), particularly α-ctx MII, has greatly increased understanding of this receptor class. Two receptor classes, α-ctx MII sensitive and α-ctx MII resistant, have been determined using α-ctx MII. The α-ctx MII sensitive receptors were identified as an α3β2* subtype due to α-ctx MII sensitivity for oocytes expressing the α3β2 subtype. However, α3 knockout mice studies did not eliminate [^{125}I]α-ctx MII binding in the brain (Whiteaker *et al.* 2002). Further studies found that deletion of α6 and β3 subunits led to a loss of [^{125}I]α-ctx MII binding (Champtiaux *et al.* 2003; Cui *et al.* 2003). α6 containing receptors were found to be sensitive to α-ctx MII, neuronal bungarotoxin, and α-ctx PnIa, all reported α3β2* subtype antagonists (Kuryatov *et al.* 2000; Dowell *et al.* 2003; Everhart *et al.* 2003). In addition to the α6 subunit investigations, knockout mice have been used to determine which individual subunits are responsible for functional receptor subtypes. Loss of function was demonstrated for α4-, α5-, α6-, β2-, and β3-null mutant mice, implicating their role modulating NIC-evoked DA release (Grady *et al.* 2001; Champtiaux *et al.* 2003; Cui *et al.* 2003; Salminen *et al.* 2004). Salminen *et al.* (2004) also determined that β4- and α7-null mutant mice have no loss of receptor function. By coupling the knockout mice data with the α-ctx MII data, Luetje (2004) has

identified four distinct DA releasing subtypes: α-ctx MII sensitive subtypes, α6β2β3 and α6α4β2β3, where α6 and α4 form with the β2 subunit to form the binding sites and α-ctx MII resistant subtypes consisting of α4β2 and α4α5β2 with the α4 and β2 subunits forming the agonist binding sites (Luetje 2004). For purposes of this publication, this family of receptors will be referred to by its functional designation, e.g. the receptors that mediate NIC-evoked DA release.

Homologously expressed nAChR Subtypes

In addition to heterologously expressed nAChR subtypes, there exists a second class of homologously expressed receptor subtypes. Originally, these homomers were identified using the same methods utilized in identifying muscle-type nAChRs. Using radiolabeled α-bungarotoxin, a known α1β1γδ ligand (Lee 1972), researchers found a receptor population which demonstrated a high affinity for the compound (Marks *et al.* 1986). Using α7 mRNA brain distributions as well as the autoradiographic binding data, this receptor subtype was identified as an α7 homomer (Clarke *et al.* 1985; Wada *et al.* 1989; Seguela *et al.* 1993; Chen and Patrick 1997). This class of homomeric receptor subtype is almost as prevalent as the α4β2* population of nAChRs in the brain. However, these receptors are expressed differently in different brain regions (Holladay *et al.* 1997). The α7* receptor subtypes are highly permeable to Ca^{2+} ions (Seguela *et al.* 1993; de Fiebre *et al.* 1995), and rapidly desensitize in the presence of agonists (Castro and Albuquerque 1993). Synapse formation, mediation of nicotine-induced seizures, and modulation of neurotransmitter release are some functions potentially regulated by the α7* nAChR (Orr-Urtreger *et al.* 1997).

2.5. Pharmacology of Nicotine at the nAChR

As stated above, nicotinic receptors mediate a wide variety of effects on many systems in the body. Nicotine, the principal alkaloid and active compound in tobacco, has been found to interact with the acetylcholine binding site on nicotinic receptor subtypes. Nicotine exposure has been shown to enhance memory and attention, increase arousal, decrease anxiety, and cause weight loss (Arneric and Brioni 1999). Additionally, nicotine has been shown to be highly addictive due to its ability to affect the modulation of dopamine release. Like acetylcholine and other agonists, nicotine has been shown to first activate the opening of the receptor ion channel. After activation, nicotine exposure causes a second conformational change in which the receptor becomes refractory or desensitized (Corringer *et al.* 1998). In its desensitized state, the ion channel is closed, and the receptor is in a resting state. Before activation by an agonist, the receptor has a high affinity for binding nicotine or other agonist molecules. Interestingly, after binding of nicotine, the subsequent desensitized state also has an increased affinity for nicotine, even though it is unable to function (Sharpless and Wonnacott 2001). Additionally, at the binding site, the ß-subunit may control the extent of desensitization or inactivation of the receptor after long-term agonist exposure (Fenster *et al.* 1997; Kuryatov *et al.* 2000; Kuo *et al.* 2005). Concentrations needed to desensitize the receptor are also much less then those required to activate the receptor (Rowell and Hillebrand 1994; Fenster *et al.* 1997; Grady *et al.* 1997). An increase in receptor number, or up-regulation, also occurs when a4ß2* receptors are exposed to chronic nicotine treatments (Wonnacott *et al.* 1990). However, this upregulation is not due to an increase in receptor mRNA production, and

may be due to a recruitment of nicotinic receptors from a reserve pool (Marks *et al.* 1992; Bencherif *et al.* 1995). It should also be noted that different nAChR subtypes respond to agonists differently, and their desensitization rates and function can vary when exposed long term to NIC (Nguyen *et al.* 2004; Grilli *et al.* 2005). As stated above, α7 receptors are characterized by their very rapid desensitization, whereas receptors modulating DA release are more resistant to desensitization (Castro and Albuquerque 1993; Gray *et al.* 1996; Yu *et al.* 1996). Interestingly, the opposite is true for regulation of these receptor subtypes using chronic NIC infusion. a7* receptor subtypes are more resistant to regulation by NIC, where as a6* containing receptors (DA mediating nAChR subtypes) are down-regulated when exposed to chronic NIC (Collins *et al.* 1994; Lai *et al.* 2005). Desensitization, as well as up-regulation, has allowed researchers not only to search for agonists that are selective for various subtypes, but also to explore subtype-selective antagonists as therapeutic agents (Arneric and Brioni 1999).

2.6. Existing Assays for Evaluating Affinity and Functional Responses at nAChRs

Radioligand Binding Studies

Only a limited number of pharmacological tools are available to evaluate affinity and function at the various nicotinic receptors. Radioligand binding assays are often used as the first step in determining ligand affinity for individual nAChRs, due to methodological ease and the capacity for rapid screening. These assays are carried out using native tissue, or utilizing receptors expressed in *Xenopus* oocytes or other stably-transfected cell lines.

Ligand binding assays developed for the α4β2* receptor subtype are performed using several different ligands, including [^{3}H]S-(-)-nicotine (NIC), [^{3}H]cytisine, [^{3}H](±)-epibatidine, and [^{3}H]ACh. Several different brain regions may be used to obtain native tissue nAChRs, including the thalamus, cortex, and striatum. Cell line K-177, a line of human embryonic kidney (HEK) 293 cells that stably express the human α4β2 nAChR, has also been utilized in binding assays (Gopalakrishnan *et al.* 1996). α7* nAChR subtypes are also assayed *via* radioligand binding methods; the most widely used ligands for these studies have been [^{3}H]-α-bungarotoxin and [^{3}H]-methyllycaconitine. Native tissue receptors, as well as stable cell lines expressing a7 receptors have been used in these binding assays (Gopalakrishnan *et al.* 1995; Quik *et al.* 1996; Whiteaker *et al.* 1999). A third class of neuronal nAChRs, the subtypes that mediate NIC-evoked DA release, has primarily utilized [^{3}H]-(+)-epibatidine as the radioligand in the binding assay. However, due to its non-specificity (α4β2 activity), this radioligand must be used in conjunction with unlabeled cytisine to block [^{3}H](+)-epibatidine binding to the α4β2* subtype (Marks *et al.* 1998). Cloned cell lines have revealed several possible candidates for these studies. α3α5β2, α3β2, and α3β4 nAChR clones have all shown an affinity for n-bungarotoxin and epibatidine (Lin and Meyer 1998). [^{125}I]-α-ctx MII has also been used as a ligand for the nAChR subtype mediating NIC-evoked DA release (Holladay *et al.* 1997).

Functional Assays

In order to differentiate between agonists and antagonist at nAChR subtypes, functional studies must be utilized in addition to the binding studies. These functional assays must also be used to assess what is occurring at the actual receptor site. Binding studies only represent the affinity of ligands for the desensitized form of the receptor and may not give an accurate indication of the ligand's interaction with a functional receptor (e.g. the non-desensitized form). As in the binding studies, functional assays must be subtype specific. Current approaches incorporate the use of slices or synaptosomes from various brain regions, as well as recombinant receptors expressed in *Xenopus* oocytes, or in stably-transfected cell lines. $\alpha4\beta2^*$ subtypes have traditionally been assayed using ion flux assays involving the radioactive ion [$^{86}Rb^+$]. $^{86}Rb^+$ is an ion considered to be equivalent to the endogenous cation K^+. Rodent brain synaptosomes or stably transfected cell lines (K177 cells or IMR-32 cells) are preloaded with $^{86}Rb^+$ and superfusion systems in the presence of agonist are used to efflux the radiolabel through the ion channel. Functional response is designated once the compound either elicits efflux (agonist), or inhibits efflux when NIC is introduced into the system as an agonist (antagonist). Data from $^{86}Rb^+$ efflux and [^{3}H]-nicotine binding assays have shown correlative EC_{50} and IC_{50} values for agonist-induced efflux, respectively, as well as correlation of similar sites of action within brain regions. It is important to note that $\alpha7$ [^{125}I]-α-bungarotoxin binding data does not correlate with $^{86}Rb^+$ efflux brain regions, offering further proof that $^{86}Rb^+$ efflux is a functional assay for $\alpha4\beta2^*$ nAChRs (Marks *et al.* 1998).

Generally, ion flux functional assays for α7 subunits have proven to be unsuccessful, due to rapid α7* receptor desensitization, which has been reported to occur over several milliseconds (Seguela *et al.* 1993). Consequently, electrophysiology studies have been used to characterize these homomeric receptor subtypes. Whole-cell voltage clamp experiments using either hippocampal interneurons or *Xenopus* oocytes expressing α7 subtypes have been shown to be useful in determining functional activity before the receptor is desensitized (Frazier *et al.* 1998; Papke and Thinschmidt 1998; Papke *et al.* 2000).

As mentioned above, the nAChR has been implicated in the mediation of NIC-evoked dopamine release. Therefore, nAChR subtypes that mediate NIC-evoked DA release have been assayed utilizing neurotransmitter (NT) release methodologies. These assays, usually utilize brain slices or synaptosomes, oocytes, or stably-transfected cell lines, which are preloaded with [^{3}H]-dopamine and superfused to monitor the efflux of the radiolabel in the presence of agonist. Drug candidates can be added to the system to measure their intrinsic (agonist) activity, and compounds can also be tested against a known agonist (e.g. NIC) to determine the ability of the compound to inhibit agonist-evoked dopamine response (antagonist response). Native tissues, such as striatum, as well as cell lines, including IMR-32 human neuroblastoma cells and rat PC12 cells, both of which are ganglionic in nature and express an α3-containing subtype (possibly α3β4), have been employed using this assay method (Lukas 1993; Donnelly-Roberts *et al.* 1998). Although this assay does not differentiate between the four possible subtypes that

mediate DA release, it has been invaluable in identifying non-$\alpha 4\beta 2$ and non-$\alpha 7$ selective ligands.

Researchers may choose to use several types of tissues when conducting any of the assays outlined above. However, both native tissue and expressed cells have benefits and limitations. Using neuronal tissue affords a more accurate representation of the native receptor but limits the effective determination of nAChR subtype compositions, due to the complexity of the neuronal tissue, as well as the limitations of the pharmacological assays. Additionally, the rodent brain (e.g. rat or mouse) is small, and large amounts of tissue may be needed in order to fully assess a series of compounds, adding a high cost to the process. Expressed cells, in contrast, can be grown in large quantities, are quite easy to manipulate, and provide an accurate determination of subunit composition. These cells are also cost-effective, when screening large numbers of compounds. However, perceived strengths of homogeneity and basic cell function are also weaknesses for these tissue preparations. In addition, while the subunit composition of nAChRs is known in both *Xenopus* oocytes and transfected cells, they are not necessarily identical to the corresponding native receptor subtypes, with regard to subunit combination, stoichiometry, post-translational modification, and placement within the brain regions.

2.7. Nicotinic Ligands of the nAChR

2.7.1. Agonists

Alkaloids

The tobacco plant, *Nicotinia tobacum*, contains many different naturally occurring alkaloids. The most abundant, NIC (**1**), has a varied pharmacological profile, as discussed above, throughout the body, both peripherally and centrally. R-(+)-Nicotine (R-NIC, **2**), the enantiomer of NIC, which is formed during pyrolysis of tobacco products and is present in tobacco smoke, also has activity at nAChRs. In addition to NIC, *N. tobacum* contains several other alkaloids, including, S-(-)-nornicotine (**3**), S-(-)-cotinine (**4**), S-(-)-anabasine (**5**), and S-(-)-anatabine (**6**). R-NIC has lower affinity for the $\alpha4\beta2^*$ receptor subtype than that reported for (**1**), as determined by inhibition of [^{3}H]-NIC binding (Ki = 46 and 2 nM, respectively) (Crooks *et al.* 1995). Stimulation of DA release in striatal tissue with (**2**) afforded an equivalent efficacy but a lower potency than (**1**) (Garvey *et al.* 1994). Compounds **3** and **4** have been evaluated in the NIC-evoked [^{3}H]-DA release assay and both evoked [^{3}H]-DA release but neither was as potent as NIC. S-(-)-Nornicotine (EC_{50} = 1.0 μM) was more potent than S-(-)-cotinine (EC_{50} = 30.0 μM) (Teng *et al.* 1997; Dwoskin *et al.* 1999). [^{3}H]-NIC binding affinities for (**3**) and (**4**) were also determined in comparison to that of NIC and were 259-fold and 3900-fold lower in affinity, respectively (Garvey *et al.* 1994; Lin and Meyer 1998). Compound **5** exhibits a 30-fold decrease in affinity when compared to NIC in the [^{3}H]-NIC binding assay, a 40% efficacy in the $^{86}Rb^+$ efflux assay compared to NIC, and an EC_{50} value of 15.4 μM in the NIC-evoked [^{3}H]-DA release assay (Marks *et al.* 1993; Dwoskin *et al.* 1995).

Figure 2.2 Structures of Alkaloid Molecules and Pyridine Ring Modified NIC Molecules

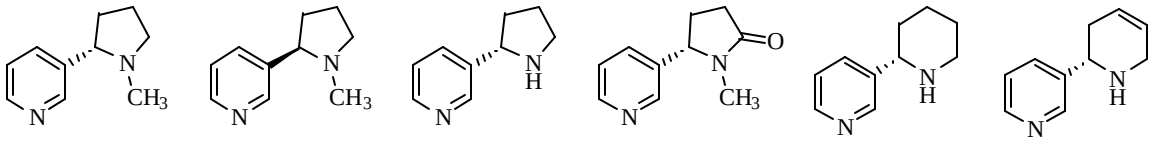

1 NIC **2** R-NIC **3** Nornicotine **4** Cotinine **5** Anabasine **6** Anatabine

Anabaseine and Anabaseine Analogs

Anabaseine (**7**) is a 1', 2'-dehydroanabasine analog. It is found in cured tobacco and in the marine worm *Hoponemetines hydrobiologia*. Compound **7** affords about a 20-fold decrease in rat brain [^{3}H]-NIC binding affinity when compared to NIC, and has a similar selectivity for $\alpha4\beta2$* nAChR subtypes (Ki = 32 nM) over $\alpha7$* nAChR subtypes (Ki = 58 nM) (de Fiebre *et al.* 1995; Kem *et al.* 1997). However, intrinsic $\alpha7$ activity is 200% higher for (**7**) over NIC in expressed oocytes. A 3'-substituted anabaseine analog, GTS-21 (**8**), exhibits partial agonist activity at rat $\alpha7$ receptors expressed in *Xenopus* oocytes (ca. 28% of the ACh response) and low activities at $\alpha4\beta2$ oocyte-expressed receptors. In contrast, human $\alpha7$ receptor activity elicited by (**8**), when compared to that elicited at rat $\alpha7$ nAChRs, was less efficacious (Briggs *et al.* 1997; Meyer *et al.* 1998). 4-OH-GTS-21 (**9**), a GTS-21 metabolite, showed a similar increase in affinity for the $\alpha7$ receptor subtype when compared to (**8**) in rat oocyte PC-12 cells utilizing the [^{125}I]α-Btx binding assay [e.g. Ki = 45 nM (4-OH-GTS-21) and 31 nM (GTS-21)]. Additionally, the 4-OH metabolite had more affinity for the binding sites of human SK-N-SH cells when assayed

in the [^{125}I]α-Btx binding assay (Ki = 170 nM (**9**) and 23 μM (**8**)) (Meyer *et al.* 1998; Papke *et al.* 2000).

Figure 2.3 Structures of Anabaseine and Modified Anabaseine Molecules

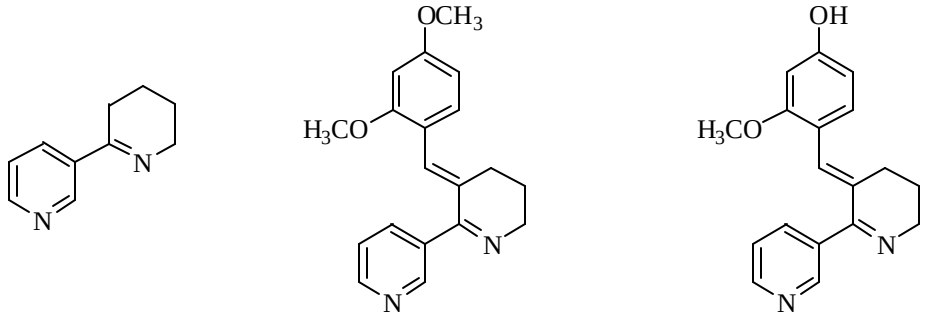

7 Anabaseine **8** GTS-21 **9**

Two series of restricted nicotine analogs (**10-12**) have affinities for nAChRs. A *syn*-rotamers of NIC (**10a**) elicited antinociceptive effects in the tail flick assay (a purported α4β2* mediated effect), with the (+)-enantiomer having a 12-fold greater effect over the (-)-enantiomer (Sabey *et al.* 1999; Sarkar *et al.* 2004). Interestingly, affinity values of these enantiomers in the [^{3}H]-NIC binding assay were reversed; the (+)- and (-)-enantiomers of 10) having Ki values of >10,000 and 605 nM, respectively. The racemic desmethyl analog (**10b**) had a higher affinity for α4β2* nAChRs (Ki = 167 nM) when compared to the *N*-methyl enantiomers (Chavadarian *et al.* 1983; Glassco *et al.* 1993). Xu *et al.* (2001) obtained similar values for the *syn*-rotamer compounds **10a** and **10b** (Ki = 400 and 220 nM, respectively) in the [^{3}H]-NIC binding assay, and these compounds demonstrated different affinities in the [^{3}H]-MLA binding assay, Ki = 590 nM (**10a**) and 20.2 μM (**9b**). Binding affinities for the anti-rotameric analogs (**11a** and **11b**) of NIC and

nornicotine indicated no appreciable affinity of these compounds at the α7 receptor subtype (Ki >100 μM for both compounds) and only weak micromolar affinity in the [^{3}H]-NIC binding assay (Ki = 12.2 and 10.5 μM, respectively) (Xu *et al.* 2001). Compound **12**, a racemic 6-methoxy substituted analog of (**10b**), had a much lower affinity (Ki = 1.9 μM) than that of NIC in the [^{3}H]-NIC binding assay using rat brain homogenate, but exhibited strong antinociceptive effects in the rat tail flick assay (McDonald *et al.* 1996).

Figure 2.4 Structures of Conformationally Restricted NIC Analogs

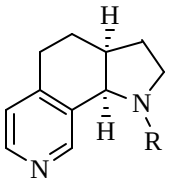

10a R = CH_3
10b R = H

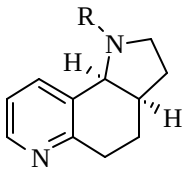

11a R = CH_3
11b R = H

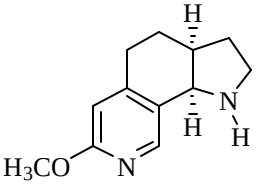

12

Cytisine

Cytisine (Cyt, **13**), an alkaloid found in laburnum of the *Leguminosae* family, has exhibited selectivity for neuronal nAChR subtypes over those in the periphery (Astles *et al.* 2002). Cyt has demonstrated high affinity and activity at α4β2* nAChRs. In [^{3}H]-NIC binding assays, Ki values ranging from 0.14-2.7 nM for Cyt have been reported (Marks *et al.* 1993; Court *et al.* 1994; Whiteaker *et al.* 1998). Cyt has been shown to favor α4-containg subtypes over the a7* nAChR subtype (Astles *et al.* 2002). Functional studies have revealed that Cyt elicits ion flux in both brain thalamic synaptosomes, as well as in cells expressing α4β2* nicotinic receptors (EC_{50} = 0.019 – 71.4 nM) (Marks *et*

al. 1993; Peng *et al.* 1994; Marks *et al.* 1996). Cyt has low μM affinity (Ki = 1.6 μM) in the [^{125}I]-α-Btx binding assay using rat brain preparations (α7* nAChRs) (Marks *et al.* 1993). In the [^{3}H]-DA release assay from rat striatal slices, Cyt was a partial agonist (Sacaan *et al.* 1995). However, Grady *et al.* (1992) reported that Cyt was a full agonist when evaluating DA release from mouse striatal synaptosomes (Grady *et al.* 1992). Cyt is also able to distinguish between the β4 and β2 subunits using oocyte-expressed cells systems, with the α4β4 nAChR subtype eliciting a much larger agonist response than the α4β2 subtype (Luetje and Patrick 1991).

Epibatidine

Epibatidine (Epi, **14**), an alkaloid originally isolated from *Epipedobates tricolour* (an Ecuadorian poisonous frog), was first structurally determined by Daly *et al.* (1991) to be an azabicycloheptane (Daly *et al.* 1991; Spande *et al.* 1992; Badio and Daly 1994). To date, Epi is the most potent natural agonist at nAChRs. Epi has demonstrated very little enantioselectivity at various nAChRs (Badio and Daly 1994; Gerzanich *et al.* 1995). In rat homogenate binding assays using various specific radiolabeled ligands, Epi had picomolar affinities at α4β2* receptor subtypes (Ki = 70 pM), low nanomolar affinities at α7* (Ki = 21 nM), and low micromolar affinities at α1βγδ receptor subtypes (2.7 μM, respectively) (Gopalakrishnan *et al.* 1996; Sullivan and Bannon 1996). Cell expressed nAChRs demonstrated similar α4β2 affinities (Ki =19 pM) and slightly weaker α7 affinities (Ki = 200 nM). Affinities for α3β2 and α3β4 nAChRs were determined to be over 10-fold lower than for α4β2 nAChRs (Ki = 230 and 380 pM, respectively) (Gerzanich *et al.* 1995; Xiao *et al.* 1998). In functional assays, Epi has been evaluated in

the NIC-evoked [$^{86}Rb^{+}$] efflux assay using K177 cells expressing the $\alpha4\beta2^*$ nAChR (EC_{50} = 17 nM), as well as oocyte-expressed $\alpha7$ nAChRs (EC_{50} = 1.3 μM) (Gopalakrishnan *et al.* 1996; Sullivan and Bannon 1996). Epi was also 150-fold more potent (EC_{50} = 0.4 nM) than nicotine (EC_{50} = 60 nM) in evoking DA release from rat striatal slices, and 40% more efficacious (Sullivan *et al.* 1994).

Figure 2.5 Structures of Cytisine, Epibatidine, Anatoxin-a

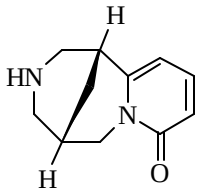

13 Cystine

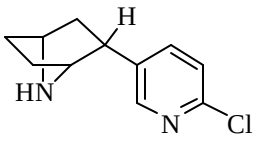

14 (±)-Epibatidine

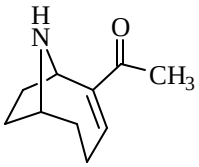

15 (+)-Anatoxin-a

Anatoxin-a

(+)-Anatoxin-a (Atx, **15**), isolated from the freshwater blue-green algae *Anabaena flos-aquae*, has an azabicyclononene skeleton and exhibits a wide variety of nAChR activities. Atx has a similar affinity to NIC (Atx, Ki = 3.5 nM; NIC, Ki = 1-3 nM) in the [^{3}H]-NIC binding assay using rat brain homogenate (Wonnacott *et al.* 1991). Binding studies using rat $\alpha7^*$ native receptors and [^{125}I]-α-Btx revealed that (+)-Atx had a 60-fold higher binding affinity than NIC at this receptor subtype. Using mouse thalamic synaptosomes and M10 cells, **15** has been shown to be more efficacious than NIC in the NIC-evoked [$^{86}Rb^{+}$] efflux assay (EC_{50} = 48 - 93 nM and 180 - 2500 nM, respectively) (Thomas *et al.* 1993; Marks *et al.* 1996). Using $\alpha7$ receptors expressed in *Xenopus* oocyte cells, ion flux assays demonstrated a 50-fold increase in potency for Atx over NIC (Thomas *et al.*

1993). Additionally, (+)-anatoxin is 10-fold more potent than NIC in PC-12 cells expressing a ganglionic-type receptor (Daly *et al.* 1991). The (-)-Atx enantiomer has 1000-fold less affinity for $\alpha4\beta2^*$ receptors and 50-fold less affinity for $\alpha7^*$ receptors, compared to (+)-Atx, when assaying rat brain tissue (Macallan *et al.* 1988). Reduction of the olefinic bond in the octene ring of (+)-Atx causes a 20-fold decrease in affinity at both [^{3}H]-NIC ($\alpha4\beta2^*$) and α-Btx ($\alpha7^*$) binding sites in rat brain tissue.

2.7.2. Antagonists

Competitive Antagonists

d-Tubocurarine (d-TC, **16**) is a classical nAChR antagonist isolated from the South American bush *Chondodendron tomentosum*. Originally used as a poison on the tips of arrows, d-TC was found to be a potent antagonist at muscle type nAChR [$(\alpha1)_2\beta\gamma\delta$ or $(\alpha1)_2\beta\varepsilon\delta$] (Sharpless and Wonnacott 2001). d-TC binds to many different peripheral and neuronal nicotinic receptor subtypes with a low micromolar affinity, and is able to antagonize several different functional responses of nicotinic receptors at micromolar concentrations in *Xenopus* oocytes (Chiappinelli *et al.* 1993; Cachelin and Rust 1995; Chavez-Noriega *et al.* 1997). Similar activities were seen in native neuronal receptor assays for $\alpha4\beta2^*$ nAChR subtypes and receptor subtypes mediating DA release (Grady *et al.* 1992), further supporting the observation that d-TC is not a selective ligand at nAChR subtypes. It should also be noted that, while d-TC does exhibit competitive antagonistic properties in the systems mentioned above, it also may have a non-competitive component to its receptor inhibition profile (Cachelin and Rust 1994; Chavez-Noriega *et al.* 1997).

Dihydro-β-erythroidine (DHβE, **17**), an alkaloid isolated from *Erythrina* seeds, competitively binds to nAChRs, with affinities in the nanomolar range, at both α4β2* nAChR subtypes and receptor subtypes mediating DA release (Crooks *et al.* 1995; Khiroug *et al.* 2004). Characterization of DHβE in a number of oocyte expression systems demonstrated selectivity between nAChR subtypes. A 3-fold selectivity α4β2 receptor subtype over the α2β2 receptor subtype and a 10-fold selectivity for the α4β4 receptor subtype over the α4β2 receptor subtype. Additionally, an approximate 100-fold increase in selectivity for α4β4 receptors over α3β4 receptors was observed (Harvey and Luetje 1996; Chavez-Noriega *et al.* 1997; Khiroug *et al.* 2004). DHβE binds similarly to NIC, and the receptor blockade can be overcome with high concentrations of NIC or another agonist. DHβE does not act as an antagonist at α7* receptor subtypes (McQuinston and Madison 1999). Erysodine (**18**), a structurally related DHβE analog, also isolated from *Erythrina* seeds, has also been investigated. Erysodine is more active at α4β2* receptor subtypes than DHβE, but like DHβE has relatively weak affinity for α7* nAChRs (Decker *et al.* 1995). Erysodine also exhibits antagonistic properties similar to those of DHβE at nAChR subtypes mediating DA release.

Methyllycaconitine (MLA, **19**) isolated from *Delphinium brownii*, is a tertiary diterpenoid alkaloid. It is a potent and competitive antagonist at the homologously expressed and native α7* nAChR subtypes with a low nanomolar affinity (Ki =1 nM). MLA also has the ability to block α7 mediated currents recorded from *Xenopus* oocytes or hippocampal neurons (Alkondon *et al.* 1992; Palma *et al.* 1996; Davies *et al.* 1999). In

addition to the homomeric α7* nAChR subtypes, MLA has been shown to inhibit a population of α7-like nAChR subtypes which are not labeled by other α7 antagonists (Yum *et al.* 1995; Davies *et al.* 1999). When compared to other receptor subtypes, both muscle and α4β2* subtypes require micromolar concentrations of MLA to achieve inhibition of nAChR function (Wonnacott *et al.* 1993). Early studies have shown MLA has little antagonistic activity in the nicotine-evoked dopamine release assay (Drasdo *et al.* 1992). However, more recent studies have demonstrated that MLA may antagonize α6-containing nAChR subtypes, one of the purported nAChR subtypes involved in mediating DA release (Mogg *et al.* 2002; Karadsheh *et al.* 2004). SAR on the MLA molecule reveals the ring E moiety is an important feature for activity, specifically the succinimide moiety of the multi-ring structure. Removal of various portions of the succinimide moiety significantly decreases binding affinity 20- to 2000-fold (Hardick *et al.* 1995). In addition, Ring E racemic analogs of MLA exhibited moderate to equivalent activity compared to that of MLA, and demonstrates the importance of the methyl group in the succinimide moiety (Jacyno *et al.* 1996; Bergmeier *et al.* 1999).

Figure 2.6 Structures of Competitive nAChR Antagonists and Neurotoxins

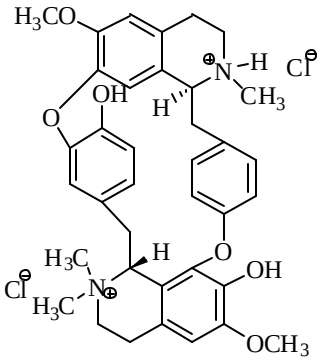

16 d-Tubocurarine

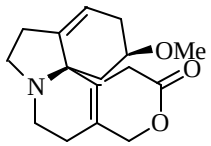

17 DHβE

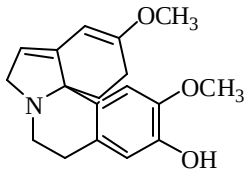

18 Erysodine

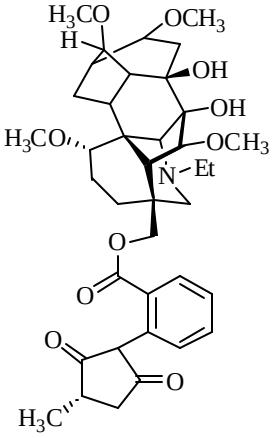

19 MLA

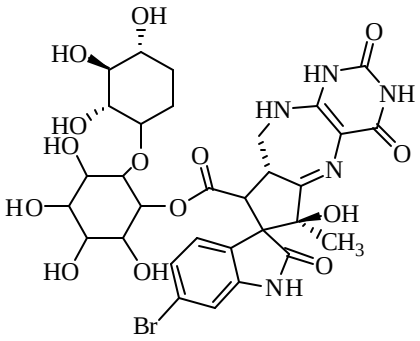

20 Neosurugatoxin

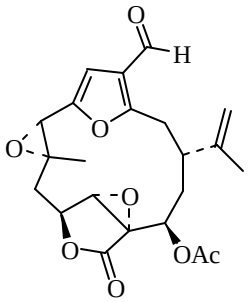

21 Lophotoxin

Gly-Cys-Cys-Ser-Asn-Pro-Val-Cys-His-Leu-Glu-His-Ser-Asn-Leu-Cys
22a a-conotoxin MII
Gly-Cys-Cys-Ser-Asp-Pro-Arg-Cys-Ala-Trp-Arg-Cys
22b a-conotoxin ImI
Gly-Cys-Cys-Ser-Tyr-Pro-Pro-Cys-Phe-Ala-Thr-Asn-Ser-Asp-Cys
22c a-conotoxin AuIB
Gly-Cys-Cys-Ser-Thr-Pro-Pro-Cys-Ala-Val-Leu-Tyr-Cys
22da-conotoxin BuIA

Neurotoxins

Several small peptide antagonists have been identified from the venom of *Bungarus multicinctus*, the Formosan banded krait. α-Bungarotoxin (α-Btx), the most studied of these peptides, is an 8kDa protein that was found to have high affinity at neuronal α7* homomeric nAChR subtypes (Ki = 1 nM) (Marks *et al.* 1986; Davies *et al.* 1999). Homomeric avian α8* nAChRs and α9* nAChRs of cochlear hair cells are also inhibited with low nanomolar concentrations of α-Btx (Gotti *et al.* 1994; Elgoyhen *et al.* 2001). α-

Btx does not seem to antagonize any neuronal heteromeric nAChR assemblies (McGehee and Role 1995).

A minor component of the venom of *Bungarus multicinctus*, is neuronal bungarotoxin (n-Btx or κ-Btx). n-Btx has been shown to inhibit some α3*- and α6*- containing neuronal nicotinic receptor subtypes, as well as α7* subtypes (Chiappinelli 1983; Luetje *et al.* 1998; Luetje 2004). n-Btx inhibits nicotine-evoked dopamine release, as well as inhibiting [^{3}H]-(+)-epibatidine non-α4β2* binding sites (Grady *et al.* 1992; Houghtling *et al.* 1995). Due to its limited availability and non-selective pharmacological profile, n-Btx is not as widely utilized in research as other nAChR antagonists.

Other neurotoxins exist in nature that act at various nAChRs, including neosurugatoxin (NSTX, **20**) from the Japanese mollusk *Babylonia japonica*, which exhibits non-competitive antagonism at several different nAChR subtypes and lophotoxin (LTX, **21**) and its analog LTX-1 are cyclic diterpenes isolated from coral, which block neurotransmission of muscle type and ganglionic nAChRs (Abramson *et al.* 1988; Groebe and Abramson 1995). Additionally, other toxins identified, include α-cobratoxin (α-CBT), erabutoxin-a (ETX-a) and erabutoxin-b (ETX-b), and histrionicotoxin, all of which have been isolated from various species of snake (Luetje *et al.* 1990; Adams and Olivera 1994). ETX-a has been identified as an inhibitor of NIC-evoked DA release in rat striatal tissue, while α-CBT had no inhibitory effect in the same system (Dajas-Bailador *et al.* 1998).

a-Conotoxins

Venoms from the *Conus* marine snails have been isolated and found to target various nAChR subtypes. The α-conotoxin compounds are peptides of 12-19 amino acids in length and contain key disulphide bonds integral to maintaining their structure (Janes 2005). α-Conotoxin MII (**22a**) has been shown to potently and selectively antagonize α3β2 nAChRs expressed in *Xenopus* oocytes at concentrations of 100 nM, which was 2 to 4 orders of magnitude higher than any other subtype tested (Harvey *et al.* 1997; Kaiser *et al.* 1998). Partial inhibition of nicotine-evoked dopamine release was observed when rat striatal synaptosomes were exposed to α-conotoxin MII (Kaiser *et al.* 1998). This partial inhibition was due to the presence of two classes of nAChR subtypes involved in mediating DA release. The α6-containing α-ctx MII sensitive receptor subtypes are blocked by α-ctx MII (Salminen *et al.* 2004). Related α-conotoxins, α-conotoxin ImI (**22b**) and α-conotoxin AuBI (**22c**), were shown to be selective for α7 and α3β4 receptors, respectively (Johnson *et al.* 1995; Grady *et al.* 2001). However, recent evaluation of a-ImI and a close analog, a-ImII (75% homology), both demonstrate activity at a3ß2 (IC_{50} = 40.8 nM and 9.61 µM, respectively) and a7 (IC_{50} = 595 nM and 571 nM, respectively) receptor subtypes expressed in *Xenopus* oocytes. Therefore, the evaluation of the selectivity of a-ImI is undecided at this time. a-ImII did act at a different a7 binding region than traditional a7 antagonists, including a-ImI. This a-conotoxin could act as a potential probe for a novel a7 binding site (Ellison *et al.* 2003; Ellison *et al.* 2004). a-Conotoxin BuIA (**22d**), isolated from *Conus bullatus*, demonstrated a broad spectrum of activity at several nAChR subtypes expressed in *Xenopus* oocytes. BuIA was most active in the inhibiting a6/a3ß2 nAChRs (IC_{50} = 0.258

nM) followed by a6/a3ß4 nAChRs (IC_{50} = 1.54 nM). a7 and a4ß2 nAChR subtypes were not as active with IC_{50} values of 272 nM and 10.4 μM, respectively. Additionally, BuIA was able to differentiate between ß2- and ß4-containing subtypes due to different dissociation rates when a common a-subunit was used (Azam *et al.* 2005).

Nicotinium Salts

N-*n*-alkylnicotinium iodide salts have been prepared by regioselective *N*-alkylation of the S-(-)-nicotine pyridino-*N* moiety (Crooks *et al.* 1995; Dwoskin *et al.* 1999). These compounds exhibited a range of inhibitory potency at various nAChR subtypes. Compounds **23a-d** were the most potent inhibitors. In [^{3}H]-NIC binding experiments utilizing rat striatal slices, NDNI (Ki = 93 nM) and NDDNI (140 nM) had similar affinities for the $\alpha4\beta2$* receptor subtype, with NNNI (840 nM) having moderate affinity, and NONI (20 μM) demonstrating weaker affinity for this receptor subtype. Functional responses (IC_{50}) were also determined in NIC-evoked $^{86}Rb^+$ efflux assays, IC_{50} values obtained were: NDNI (14 nM) = NNNI (9 nM) > NDDNI (40 nM) > NONI (10 μM). Nicotine-evoked [^{3}H]-DA release assays, these *N*-alkylnicotinium salts exhibited a different inhibitory profile than that observed in the $^{86}Rb^+$ efflux assays, with inhibitory potencies (IC_{50}) ranging from the low nanomolar to high micromolar range; IC_{50} values were as follows: NDDNI (9 nM) > NNNI (140 nM) > NONI (620 nM) > NDNI (>100 μM). From the functional and binding data, it can be concluded that NNNI and NDDNI are nonselective antagonists at $\alpha4\beta2$* nAChR subtypes and at nAChR subtypes mediating NIC-evoked DA release, while NDNI and NONI, due to their functional profiles, are selective and competitive receptor antagonists at $\alpha4\beta2$* nAChR subtypes

and at nAChR subtypes mediating NIC-evoked DA release, respectively. In addition, none of the *N*-alkylated compounds **23a-d** had any affinity for α7 [^{3}H]-MLA binding sites (Wilkins *et al.* 2003). When unsaturation was introduced to the alkyl chains of the *N*-*n*-alkylnicotinium salts, the NONI analogs gained affinity for α4β2* nAChR subtypes (0.08 – 4.49 μM), while maintaining or increasing their activity at nAChR subtypes mediating NIC-evoked DA release (80 – 250 nM). Additionally, the NDNI analogs maintained or lost affinity for α4β2* nAChR subtypes (0.05 – 7.47 μM), but demonstrated antagonist activity at nAChR subtypes mediating NIC-evoked DA release (20 – 140 nM) (Sumarithan *et al.* 2005).

Figure 2.7 Structures of Nicotinium and Structurally Modified Nicotinium Salts

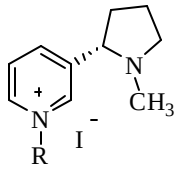

23a NONI R=$(CH_2)_7CH_3$
23b NNNI R=$(CH_2)_8CH_3$
23c NDNI R=$(CH_2)_9CH_3$
23d NDDNI R=$(CH_2)_{11}CH_3$

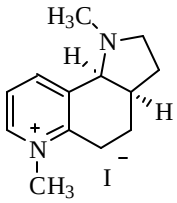

24a BCO R=$(CH_2)_7CH_3$
24b BCN R=$(CH_2)_8CH_3$
24c BCD R=$(CH_2)_9CH_3$
24d BCUD R=$(CH_2)_{10}CH_3$
24e BCDD R=$(CH_2)_{11}CH_3$

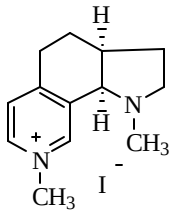

25a ACO R=$(CH_2)_7CH_3$
25b ACN R=$(CH_2)_8CH_3$
25c ACD R=$(CH_2)_9CH_3$
25d ACUD R=$(CH_2)_{10}CH_3$
25e ACDD R=$(CH_2)_{11}CH_3$

A second series of conformationally restricted nicotinium analogs (**24 and 25**) were alkylated with various long carbon chain lengths (Crooks *et al.* 2000). Restriction of the pyrrolidine ring rotation about the pyridine moiety caused complete loss of affinity for the α4β2* nAChR subtype, and none of these compounds had any activity in the [^{3}H]-MLA binding assay. However, analysis of these compounds in the [^{3}H]-nicotine-evoked dopamine release assay demonstrated that a general increase in carbon chain length from

C_8 to C_{12} produced a nearly 100-fold increase in antagonism at the nAChR mediating DA release (IC_{50} = 30 – 660 nM). The sole exception was the dodecyl analog BCDD, which was devoid of inhibitory activity at this receptor, although interestingly the isomeric analog ACDD exhibited an IC_{50} of 220 nm.

Other Antagonists

Lobeline (LOB, **26**), an alkaloid found in *Lobelia inflata* plants is the active ingredient in what is referred to as "Indian tobacco". LOB has many pharmacological effects related to those of nicotine, and has historically been regarded as an agonist at nicotinic receptors; however, it may bind to the nicotinic receptor in a novel manner (Decker *et al.* 1995; Damaj *et al.* 1997). Both LOB and nicotine bind to the $\alpha4\beta2$* nAChR with low nanomolar affinity (Ki = 4 - 30 nM), while exhibiting little or no $\alpha7$ affinity (>10,000 nM) (Abood *et al.* 1988; Reavill *et al.* 1990; Bhat *et al.* 1991; Court *et al.* 1994; Brioni *et al.* 1997). LOB has recently been shown to competitively inhibit NIC-evoked [^{3}H]dopamine overflow (IC_{50} = 300 nM), as well as inhibiting NIC-evoked $^{86}Rb^+$ efflux (IC_{50} = 700 nM) in rat striatal slices and in rat thalamus synaptosomes, respectively (Miller *et al.* 2000). It should be noted that at concentrations greater than 1 μM, LOB potently releases dopamine from rat striatal slices in a manner that is not nAChR mediated, since the release cannot be inhibited by mecamylamine (Teng *et al.* 1997). These data lead to the classification of LOB as a competitive, nonselective antagonist at $\alpha4\beta2$* nAChR subtypes and at nAChR subtypes mediating NIC-evoked DA release.

Strychnine (**27**) has been shown to competitively inhibit the α7* nAChR subtype, in addition to its original use as an antagonist at the glycine-gated chloride channel (Matsubayashi *et al.* 1998). In *Xenopus* oocytes expressing nAChRs individually composed of homomeric α7, α8, and α9 nAChR subtypes, strychnine acts as an inhibitor at toxicologically relevant concentrations (Gerzanich *et al.* 1994; Peng *et al.* 1994). Additionally, strychnine has also been found to block α4β2* nAChRs non-competitively (Matsubayashi *et al.* 1998).

bis-Isoquinolines, tetrandrine, hernandezine and E_6-berbamine were evaluated as ligands to block ACh-evoked currents at α3* and α7 nAChR subtypes endogenously expressed in PC12 cells. Tetrandrine, hernandezine and E_6-berbamine exhibited antagonistic activity at the α3* nAChR subtypes (IC_{50} = 8.1, 5.8, and 5.1 μM, respectively). [^{3}H]MLA binding studies revealed that all three compounds displaced the radiolabeled ligand (IC_{50} = 8.1 μM (tetrandrine), 5.8 μM (hernandezine), and 5.1 μM (E_6-berbamine)). Additionally, the functional assay demonstrated that tetrandrine and hernandezine inhibited ACh-evoked currents at α7 nAChR subtypes (IC_{50} = 407 and 372 nM, respectively) (Virginio *et al.* 2005).

Figure 2.8 Structures of nAChR Antagonists

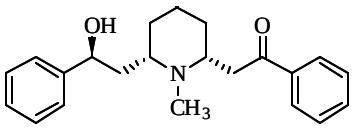

26 LOB

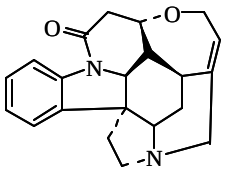

27 Strychnine

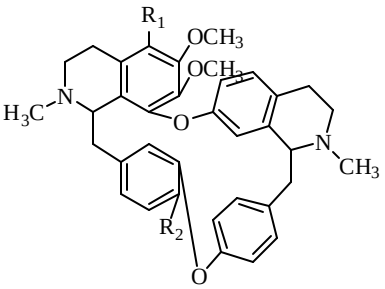

28a Tetrandrine
R_1 = H R_2 = OCH_3
28b Hernandezine
R_1 = H R_2 = OH
28c E_6-Berbamine
R_1 = H R_2 =

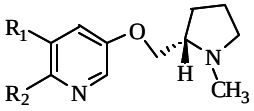

29a R_1= CH=CH_2, R_2= H
29b R_1= H, R_2= Br

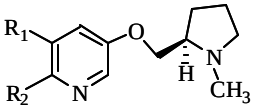

30a R_1= Br, R_2= Cl
30b R_1= R_2= Cl

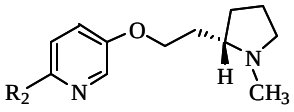

31a R_1= CH_3, R_2= H
31b R_1= H, R_2= Cl

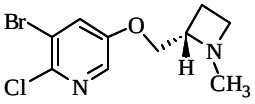

32

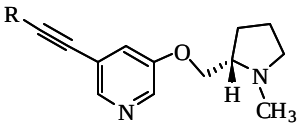

33a R= $C(CH_3)_3$
33b R= $(CH_2)_3CH_2C_6H_5$

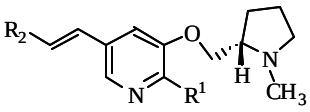

34a R_1= H, R_2= *trans*-CH=CH-CH_2CH$(CH_3)_2$
34b R_1= Cl, R_2= 4-pyridyl

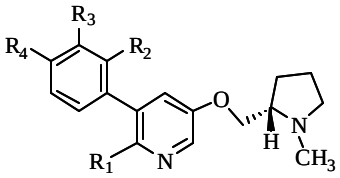

35a R_1= Cl, R_2= R_3= R_4= H
35b R_1= H, R_2= R_4= Cl, R_3= H
35c R_1= R_2= R_3= R_4= H

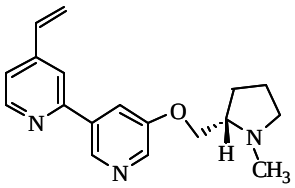

36

Prevailing drug discovery endeavors have lead researchers to explore structural modifications of tobacco alkaloids in an attempt to find novel agonists that are potent and subtype-selective. More recently, there has been a growing interest in the development of novel receptor antagonists that are selective and potent at various nAChR subtypes. Abbot laboratories have disclosed several antagonist candidates that have stemmed from

their development of a series of pyridyl ether agonists. Compounds **29-36** have been evaluated in the IMR-32 expressed cell assay utilizing the nicotine-evoked $^{86}Rb^{+}$ efflux assay to determine the extent of $\alpha3\beta4^*$ nAChR antagonist activity. Compound **29a** and **29b** inhibited 50% of the $^{86}Rb^{+}$ efflux at concentrations of 1 μM, although **29b** had 15% intrinsic activity at the same concentration implying that it is a partial agonist. Under the same conditions, compound **30a** produced 50% inhibition (1 μM) and 60% inhibition (10 μM), while compound **30b** exhibited 20-90% inhibition over the concentration range 1-10 μM. Two compounds in the 3-(2-pyrrolidinylethoxy)pyridine series (**31a and 31b)** produced moderate antagonist activity (IC_{50} = 75 and 6 μM, respectively), with no observed intrinsic activity and compound **32** (1 μM) also exhibited 55% inhibition of NIC-evoked $^{86}Rb^{+}$ efflux and produced no intrinsic activity. Therefore, a pyridyl ether linkage can demonstrate antagonist activities at the $\alpha3\beta4^*$ nAChR subtype. The substituted pyridyl ethers **(33-36)** were also assessed using IMR-32 expressed cells in nicotine (100 μM)-evoked $^{86}Rb^{+}$ efflux assays. Compound **33a** at a 1 μM exhibited 66% inhibition of NIC-evoked $^{86}Rb^{+}$ efflux, while compound **33b** at 10 μM exhibited 100% inhibition, indicating potent $\alpha3\beta4^*$ antagonism. The 5-substituted pyridyl ethers **34a** and **34b** were found to inhibit 90% of NIC-evoked $^{86}Rb^{+}$ efflux at 10 μM; while **34b** exhibited an IC_{50} = 2 μM. Compounds **35a** and **35b**, exhibited ~50% inhibition, while the R- and S- enantiomers of **35c** (only S-(-) shown) had comparable IC_{50} values of 9 μM. Compound **36** (1 μM) produced 50% inhibition of NIC-evoked $^{86}Rb^{+}$ efflux. Taken together the substituted pyridyl ethers demonstrate an ability to inhibit $\alpha3\beta4^*$ nAChR subtypes at the μM level. The inclusion of a chlorine molecule on either aromatic ring in compounds **33a** or **33b** resulted in the most potent compounds in this series.

Additionally, this series of compounds demonstrates that the 5-position of the pyridine ring can be altered with large substituents and still fit into the binding site.

Figure 2.9 Conformationally Restricted Pyridyl Ether Analogs

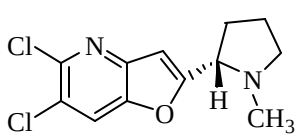

37

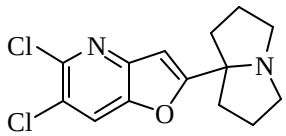

38

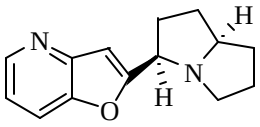

39

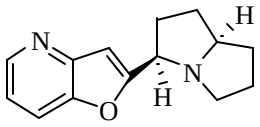

40

Compounds **37-40** were assayed in the IMR-32 cell assay described above and/or in K177 cells expressing the $\alpha 4\beta 2^*$ nAChR subtype. A rigid aromatic analog of compound **30b**, compound **37**, exhibits nonselective antagonist activity in both the K177 cell assay (55% inhibition and 6% intrinsic activity) and the IMR cell assay (38% inhibition and 7% intrinsic activity). This indicates a significant difference in inhibitory capability, since **30b** was assayed in the IMR cell assay at 10 μM (90% inhibition). The difference in IMR cell assay activities between **37** and **30b** may be attributed to increased aromatic characteristics of **37** as well as the additional flexibility of **30b**. Compounds **38-40** incorporate an extra degree of conformational rigidity, due to the substitution of a hexahydro-1H-pyrrolizine moiety for the N-methyl pyrrolidine ring. The 7a-substituted hexahydro-1H-pyrrolizine analog, **38**, was a low-potency antagonist (43% inhibition,

with minimal intrinsic activity). Compound **39** (30 μM), a dehalogenated, rigid analog of **37**, exhibited no intrinsic activity, while exhibiting 50% inhibition in the IMR cell assay. The 55% inhibition produced by compound **40** is not significantly different from that afforded by its stereoisomer **39** in the IMR cell assay.

Figure 2.10 Structural Analogs of Anabaseine and NIC

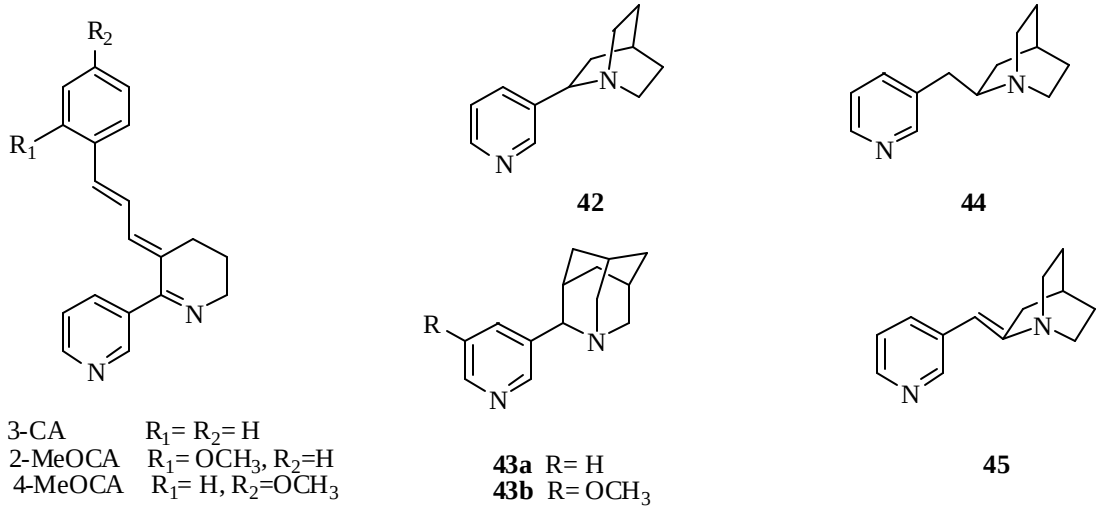

41a 3-CA $R_1 = R_2 = H$
41b 2-MeOCA $R_1 = OCH_3$, $R_2 = H$
41c 4-MeOCA $R_1 = H$, $R_2 = OCH_3$

42

44

43a R= H
43b R= OCH_3

45

In addition to the structural modifications of the agonist molecules listed above, other researchers have attempted to structurally modify the minor tobacco alkaloids, anabaseine and anabasine, in order to identify possible new nAChR antagonists. The partial agonist GTS-21 (**7**; also known as DMXB) is a structural analog of anabaseine and has been discussed previously in this chapter (de Fiebre *et al.* 1995; Meyer *et al.* 1997; Meyer *et al.* 1998). 3-*Trans*-cinnamylidene analogs have been developed to alter the agonist/antagonist profile of GTS-21 in an attempt to create antagonists that are more potent. Using an *Xenopus* oocyte α7 expression system, compounds **41a, 41b,** and **41c** were shown to exhibit nanomolar affinities for [^{125}I]-α-Btx binding sites (IC_{50} = 8-80

nM), and cause activation of α7 receptor channels (EC_{50} = 3.2 – 15.9 μM). These compounds also inhibited acetylcholine-elicited electrical responses after incubation for five minutes with various concentrations of the analog. The following order of potencies (IC_{50}) was obtained: 2-MeOCA (**41b**) (2.3 μM) > 4-MeOCA (**41c**) (5.0 μM) > 3-CA (**41a**) (15 μM). Due to the similar concentration ranges for both IC_{50} and EC_{50} values, these compounds have antagonist characteristics but are viewed as partial agonists, rather than antagonists (Meyer *et al.* 1998).

Conformationally restricted piperidine ring analogs of anabasine have been shown to be potent antagonists at α4β2* nAChRs. Compound **42** has high affinity for the [^{3}H]-nicotine binding site (Ki = 1 nM) in rat brain membranes, and blocks nicotine (10μM)-evoked $^{86}Rb^+$ efflux in rat thalamic synaptosomes (IC_{50} = 154 nM) (Crooks *et al.* 1998). However, in the nicotine-evoked [^{3}H]-dopamine release assay using rat striatal synaptosomes, compound **42** had an EC_{50} of 2 nM, E_{max} = 40%, and this compound activated α3β4* (EC_{50} = 1100 nM) and muscle-type (EC_{50} = 59 nM) nAChRs (Bencherif *et al.* 1998). Therefore, **42** is potent antagonist at α4β2* nAChRs and an agonist at other nAChR subtypes. The R-isomer appears to be the more active of the two enantiomers, with a Ki value of 0.5 μM at α4β2* nAChRs, and an EC_{50} value of 9 nM, E_{max} = 55% at nAChR subtypes mediating NIC-evoked DA release (Dwoskin and Crooks 2001). Compounds **43a** and **43b** are adamantane analogs of anabasine, developed by R. J. Reynolds (Co. 1999, 1999, 1999, 2000). Compound **43b** was found to antagonize NIC (100 μM)-evoked $^{86}Rb^+$ efflux in rat thalamic synaptosomes with an IC_{50} value of 630 nM. Additionally, both **43a** and **43b** were found to inhibit NIC-evoked [^{3}H]-DA release

using rat striatal synaptosomes with values in the high nanomolar range (IC_{50} =659 and 846 μM respectively) and were devoid of intrinsic activity. Thus, these 1-aza-2-(5-ethoxy-(3-pyridyl))tricyclo-[3.3.1.1^{3,7}]decanes appear to be nonselective and potent antagonist at α4β2* nAChR subtypes and nAChR subtypes mediating NIC-evoked DA release. Compounds **44** and **45** are methylene bridged analogs of 2-(3-pyridyl-)-1-azabicyclo[2.2.2]octane (**42**) and have high affinity for the [^{3}H]-NIC binding site in rat cortical membranes (Ki = 37 and 73 nM respectively). Although no functional antagonism has been reported in the $^{86}Rb^+$ efflux assay, no agonist activity was observed in the $^{86}Rb^+$ efflux assay, using rat thalamic synaptosomes. Also, no agonist activity was observed in either muscle-type (α1β1γδ) or α3β4* nAChRs (Dwoskin *et al.* 2000; Dwoskin and Crooks 2001).

2.8. Channel Blockers

One of the first nAChR open channel blockers (OCB) was identified as hexamethonium (HEX, **46**), a six-carbon *bis*-trimethylammonium alkyl compound, which acts within the pores of nAChR subtypes on autonomic ganglia (Paton and Zaimis 1951; Blackman *et al.* 1963; Ascher *et al.* 1979). HEX is considered a prototypical OCB, since it meets the following criteria: (1) it causes a voltage dependent blocking effect, (2) it displays a use-dependent mode of action, and (3) it produces a more pronounced inhibitory effect when there is an increase in agonist concentrations (Ascher *et al.* 1979; Buisson and Bertrand 1998). Compound **46** has also been shown to exhibit antagonist effects on reconstituted chick and rat α4β2* nAChRs (Bertrand *et al.* 1990; Charnet *et al.* 1992).

Figure 2.11 Structures of Open Channel Blockers of the nAChR

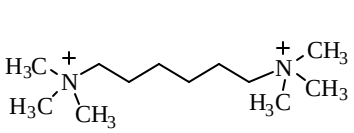

46 HEX

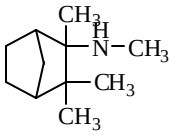

47 MEC

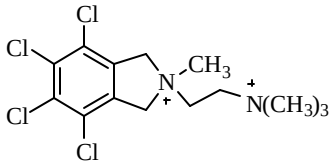

48 Chlorisondramine

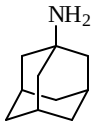

49 Amantidine

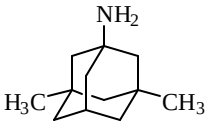

50 Memantine

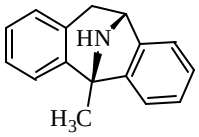

51 (+)-MK-801

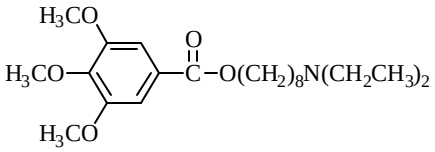

52 TMB-8

Mecamylamine (MEC, **47**) has become one of the most utilized nAChR blockers due to its ability to block the physiological, behavioral, and reinforcing effects of nicotine (Papke *et al.* 2001). MEC, a neuronal and peripheral OCB, has been shown to block several neuronal nAChR subtypes at low micromolar affinities, but has lower activities at muscle-like nAChRs (Cachelin and Rust 1995; Briggs and McKenna 1996). Moderate nanomolar inhibition (IC_{50} = 150 – 190 nM) of rat and *Xenopus* oocyte-expressed $\alpha3\beta4$ nAChRs has been observed (Cachelin and Rust 1995; Webster *et al.* 1999). Separation of the R- and S-enantiomers of MEC demonstrated very little pharmacological benefit. However, S-(+)-MEC enantiomer appears to dissociate more slowly than R-(-)-MEC at $\alpha4\beta3$* and $\alpha4\beta2$* nAChRs (Papke *et al.* 2001). Suchocki *et al.* (1991) prepared a series of C1, C2, C3, and C7 analogs of MEC and showed that compounds with methyl substituents at the C3 position were important for channel blockage activity (Suchocki *et al.* 1991). Creasy *et al.* (1996) determined that substitutions on the C2 amino functionality with large groupings were detrimental to antinociception and hypomotility

activities (Creasy *et al.* 1996). Webster *et al.* (1999) found that point mutations of the M2 region of the β4 subunit in *Xenopus* oocytes expressing ganglionic (α4β3) neuronal nAChRs, caused a decrease in sensitivity to MEC, indicating a possible binding location of MEC. Another well studied OCB is the *bis*-quaternary antagonist, chlorisondamine (**48**). This compound has no effect on [^{3}H]-ACh or [^{3}H]-NIC binding to rat brain (Schwartz *et al.* 1982). However, chlorisondamine does block NIC-evoked DA release from rat striatal synaptosomes both *in vitro* and when administered over a period of weeks *in vivo* (10 mg/kg/day) (el-Bizri and Clarke 1994, 1994). This suggests that the quaternary ammonium molecule is able to pass the blood brain barrier, although the exact mechanism is not known. In addition, it is not known if metabolic changes could account for its CNS activity. Central nervous system accumulation of chlorisondamine has been suggested to explain the blockade effects; however, this cannot provide a complete explanation of the long-term blockade effects of the drug (el-Bizri and Clarke 1994; Reuben *et al.* 1998). Buisson and Bertrand have demonstrated that several OCBs have activity at human α4β2* receptors. Classical NMDA OCBs, amantadine (**49**), memantine (**50**), and dizocilipine ((+)-MK-801, **51**), as well as, the Ca^{2+} channel antagonist 8-(*N*,*N*-diethylamino)-octyl 3,4,5,-trimethoxybenzoate (TMB-8, **52**) were evaluated using stably expressed α4β2* receptors from embryonic kidney 293 cells. ACh-elicited electrophysiological current blockade was measured in the presence of various concentrations of each of a number of antagonist molecules. Potency values (IC_{50}) were as follows: amantadine (3 μM) > memantine (7 μM) > TMB-8 (15 μM) ~ MK-801 (15 μM). These studies demonstrated that OCBs tested non-competitively antagonized α4β2* nAChRs and were supported by a mechanism of action mathematical

model detailing the interaction between the nAChR and OCBs (Buisson and Bertrand 1998). TMB-8 has also been shown to potently inhibit agonist-induced flux through muscle-type and ganglionic type nAChRs (IC_{50} ~400 nM), as well as, exhibiting potent inhibition (IC_{50} ~500 nM) in NIC-evoked [^{3}H]DA release assays using rat brain synaptosomes (Bencherif *et al.* 1995). However, all nAChR binding affinities for TMB-8 were in the moderate to high micromolar range (IC_{50} = 30 - 200 μM). Additionally, in the muscle-type nAChR ion flux assay, in the presence of TMB-8, increased agonist (ACh) concentration caused a more potent blockade of the receptor. MK-801 was also examined in human α7 nAChRs expressed in *Xenopus* oocytes, and exhibited a non-competitive inhibition of ACh elicited currents (IC_{50} = 14 - 15 μM). Stereoselectivity was not a criteria for blockade since both the (+)- and (-)-MK-801 isomers had similar activities and the blockade observed was dependent on cell potential, a hallmark of channel blockade (Briggs and McKenna 1996).

2.9. The Nicotinic Pharmacophore

The nicotinic pharmacophore has been studied for over fifty years. Theories in the early 1950s and 60s suggested a positive center located near an onium site (e.g. N^+) (Hey 1952; Sekul and Holland 1961). In the late sixties, the theory was revised to include a partially negative site near (4.85 Å) an onium site (Kier 1968). Beers and Reich proposed a model that is considered to be the first for the nicotinic pharmacophore. They proposed a two element system using both agonist and antagonist molecules: element 1- a protonated nitrogen, and element 2- an electronegative atom that can act as a hydrogen bond acceptor. They also proposed a specific distance of 5.9 Å as the optimum length between

the center of the charged moiety and a van derWaals interaction area in the receptor binding site (Beers and Reich 1970). Sheridan *et al.* (1986) suggested that a third element, an aryl centroid moiety, was needed for binding site recognition, a point or atom that was close to the H-bond acceptor site and that was in-line with the acceptor atom, in addition to altering the Beers-Reich distance to 4.8 Å (See Figure 2.12A) (Sheridan *et al.* 1986). Over the last decade, several nAChR ligands have been identified and modifications to the Sheridan model have been necessary. One major issue was some compounds with affinity for the nAChR were not in accordance the Sheridan distance. Therefore, a model had to be developed for "long" and "short" ligands. It is also important to note that stereochemistry plays an important part in receptor recognition, and since several enantiomerically pure ligands have dramatically different affinities compared to their optical isomers (Hacksell and Mellin 1989). Tonder *et al.* (2001) proposed the following nAChR pharmacophore: 1- interaction between the protonated atom of the ligand (N^+) with an anionic site (a) located on the receptor, 2- a hydrogen bond acceptor moiety (X) on the ligand that is paired with a H-bond donator (b) on the receptor surface, 3- π-system interaction of the ligand with π-systems (or positively charged residues) of the receptor (aryl centroid, c), 4- interactions between a protonated *N*-atom in the ligand and π-systems of the receptor (possibly Trp-149), and steric interactions around the aliphatic and heteroaromatic portions of the molecule (Figure 2.12b) (Tonder and Olesen 2001; Tonder *et al.* 2001; Glennon and Dukat 2004). Another model proposed involved the use of a water molecule to change "short" ligands into "long" ligands. This water molecule may interact with the protonated atom or the hydrogen bonding acceptor (Glennon *et al.* 2004). Many ligands, however, have shown

different affinities and activities at various nAChRs. Therefore, different pharmacophore models may need to be developed for each individual receptor subtype, and maybe even for the assays as well, due to the varied characteristics of the pharmacological tools used.

Figure 2.12 Pharmacophore models proposed for the α4β2* receptor subtype

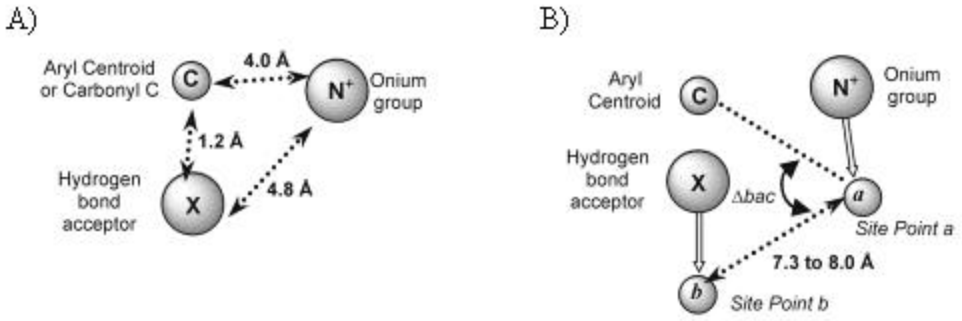

Reprinted from Bioorg Med Chem Lett, 14, Glennon and Dukat, a4ß2 nACh Receptor pharmacophore models, 1841-1844, Copyright (2004), with permission from Elsevier

The pharmacological tools themselves pose a challenge as it is unclear which molecular species is interacting with the binding site. Huang *et al.* (2005) modeled multiple free base and protonation states of NIC and (R)-descholoroepibatidine (DCEH) using a variety of molecular modeling and docking techniques to explore a general strategy of "from-microscopic-to-phenomenological" approach. This procedure involved prediction of binding energies to each of the different states of NIC and DCEH. Furthermore, hydrogen-bonding and cation-π interactions were found to be the dominant forces that differentiated the binding strengths of the molecular states of NIC and DCEH. These types of studies increase modeling ability beyond a static structure to a more dynamic

approach that can correlate binding energies with multiple states of molecule (Huang *et al.* 2005).

2.10. Disease States

Alzheimer's Disease

Alzheimer's disease (AD) is diagnosed as the loss of ability to learn by memory and attention deficits and usually affect the population over the age of 65 years and older (Lindstrom 1997; Tuppo and Arias 2005). As mentioned above, NIC improves cognitive function in healthy humans. Additionally, treatment of Alzheimer's patients with nicotine has attenuated the decline of cognitive deficits (Everitt and Robbins 1997; Lawrence and Sahakian 1998). Diagnosed Alzheimer's patients also had a decreased number of high affinity [^{3}H]-NIC binding sites in various brain regions (Flynn and Mash 1986; Whitehouse *et al.* 1988; Sugaya *et al.* 1990; Nordberg *et al.* 1995; Rusted *et al.* 2000). On a genetic level, $\beta 2$ knockout mice (e.g. mice unable to express $\beta 2$ subunits) lack high affinity nicotine binding sites. In addition, these knockout mice demonstrated learning and memory abnormalities, implicating the $\alpha 4\beta 2$* receptor subtype as playing a key role in cognitive function (Picciotto *et al.* 1995; Zoli *et al.* 1999). Neuroinflammation has also been linked to the onset of Alzheimer's disease, although the role it plays is not fully understood (Tuppo and Arias 2005). $\alpha 7$* binding sites are unaffected in Alzheimer's patients; however, a high concentration of Ca^{2+} ions may implicate this receptor subtype in neurodegeneration, due to the high Ca^{2+} permeability of the $\alpha 7$* nAChR (Sugaya *et al.* 1990; Perry *et al.* 2000). Additionally, strong correlations have been found between expression of $\alpha 7$* nAChR subtypes and the presence and rate

of accumulation of amyloid beta (1-42), the predominant Aβ species in amyloid plaques. The two proteins strongly interact and interference in this interaction may lead to the neurodegeneration. With this information, α7* nAChR subtypes may be targets for the treatment of Alzheimer's disease (D'Andrea *et al.* 2002; D'Andrea and Nagele 2006). To date, several subtype selective nAChR ligands are being investigated for their potential therapeutic value. Among them are ABT-418 (Abbott Laboratories), RJR-2403 (R. J. Reynolds/Targacept), and GTS-21 (Decker *et al.* 1994; Lippiello *et al.* 1996; Kem 1997; Gotti *et al.* 2000). Administration of the nAChR channel blocker, mecamylamine, decreased cognitive function in all populations tested. This blockade of the channel is over come by administration of NIC. Interestingly, younger healthy volunteers had a decreased sensitivity to the mecamylamine induced cognitive deficits, while AD patients had the highest sensitivity (Rusted *et al.* 2000)

Parkinson's Disease

Parkinson's disease (PD) has been closely associated with Alzheimer's disease in that patients in both disease states are found to have deficiencies in neurotransmitter systems, as well as decreased nAChR expression within the CNS. Parkinsonian patients suffer from an inability to control hyper-motor function. This is manifested as difficulties in initiating and sustaining motions (Lloyd *et al.* 1975; Olanow 2004; Samii *et al.* 2004). These motor control problems occur due to loss of dopaminergic neurons in the substantia nigra (German *et al.* 1989). L-Dihydroxyphenylanine (L-DOPA), a dopamine prodrug, treatments have been used as a form of dopamine substitute therapy, after conversion of L-DOPA to dopamine in the CNS. Although not a cure for the disease, L-

DOPA treatments can retard the degenerative effects for three to five years before peripheral side effects prevent it use. Nicotine has also been linked to the treatment of Parkinson's disease. Monkeys given NIC with L-DOPA experienced a synergistic effect to reverse parkinsonian symptoms (Schneider *et al.* 1998; Domino *et al.* 1999). An inverse relationship exists between smoking cigarettes and staving off the effects of PD. The occurrence of PD was decreased in smokers and non-smokers were two times as likely to contract PD (Fratiglioni and Wang 2000). Studies suggest that targeting heterologously expressed receptors, non-α7, may be a valuable treatment for PD (Quik *et al.* 2005). α6* nAChR subtypes involved in mediating DA release have recently been suggested as a therapeutic target for PD. Stimulation of these nAChR subtypes may result in relief from the PD symptoms without the side effects (O'Neill *et al.* 2002; Quik *et al.* 2004; Quik and McIntosh 2006). Nicotine is thought to be acting as a protective agent in the CNS (Morens *et al.* 1995; Baron 1996). SIB-1508Y (Sibia) has entered Phase 2 trials as a possible drug treatment for PD, due to its lower toxicity and increased potency for various nicotinic receptors (Sacaan *et al.* 1997; Arneric and Brioni 1999).

Schizophrenia

An excess of dopamine in the CNS has been hypothesized to cause Schizophrenia. Symptoms of this disease include delusions, hallucinations, blunt affect, and chaotic thinking and speech (Arnold and Trojanowski 1996). Schizophrenics have sensory imbalances, thereby making it difficult to regulate auditory and visual stimuli. Smoking is pervasive among the schizophrenic community (Lohr and Flynn 1992). It is postulated that those suffering from this disease smoke cigarettes in order to self-medicate

themselves with nicotine (Freedman *et al.* 1997; Sacco *et al.* 2005). Nicotine normalizes the gating deficit seen in patients participating in the P50 auditory-evoked response test (Adler *et al.* 1993; Bencherif and Schmitt 2002). Due to this finding, it has been suggested that nAChRs may be involved in schizophrenia. α7* receptors are decreased in schizophrenics (Freedman *et al.* 1995). Additionally, α7* antagonists impair auditory gating in rodents, indicating a possible loss, or reduced function of α7* nAChRs in schizophrenics' gating response (Luntz-Leybman *et al.* 1992; Lena and Changeux 1997). A genetic polymorphism in the a7* nicotinic receptor D15S1360 has been linked to a deficiency in the normal inhibition of the P50 auditory-evoked response (Freedman *et al.* 1997). De Luca *et al.* (2004) demonstrated a genetic difference in the D15S1360 marker between Parkinson's patients who smoke and those that do not, though larger studies are still needed to determine the relevance of these findings (De Luca *et al.* 2004).

Pain Management

Pain therapies have traditionally centered around two classes of compounds, nonsteroidal anti-inflammatory drugs (NSAIDs) and opioids. Nicotine in higher doses, however, affords a moderate and short-lived antinociceptive effect (Sahley and Berntson 1979; Tripathi *et al.* 1982). The discovery of the non-selective nAChR agonist, epibatidine, stimulated interest in the pain management aspect of nicotinic receptors. Epibatidine has demonstrated a potent mecamylamine-sensitive antinociceptive effect in animals (Badio and Daly 1994; Sullivan *et al.* 1994). However, due to its non-selectivity, epibatidine is not considered a drug candidate for the treatment of pain (Decker and Meyer 1999). Specific nAChR subtypes involved in analgesia have yet to be identified, although α4β2*

and α3β4* ganglionic receptor subtypes have been implicated (Badio *et al.* 1997; Badio *et al.* 1997; Marubio *et al.* 1999). Additionally, nicotinic agonist-induced antinociceptive behavior is most likely resulting from involvement of the α4β2* subtype causing or mediating neurotransmitter release in the spinal cord (Hogg and Bertrand 2004). Affinity for the α4β2* subtype, however, does not necessarily denote antinociceptive activity in a compound (Meyer *et al.* 2000). Studies assessing the possible role of α7* nAChRs in pain therapy have had mixed results. MLA and α-Btx were unable to block the antinociceptive effects of nicotine, cytosine, and other nAChR agonists in the tail-flick latency test (Rao *et al.* 1996; Damaj *et al.* 1998). When choline, an α7-specific agonist, was used to elicit the effect of analgesia, MLA and α-Btx were able to block the antinociceptive effect (Damaj *et al.* 2000).

Tourette's Syndrome

Tourette's syndrome is a hyperkinetic motor disorder characterized by involuntary movements and vocalizations. Although the exact mechanism of action is unknown, antipsychotics (e.g. haloperidol) are used to attenuate the symptoms of the condition. However, this treatment is not effective in ~30% of the cases and the drug causes some side effects (Erenberg *et al.* 1987; Shapiro *et al.* 1989). Nicotine reduces the symptoms of Tourette's syndrome in animal models, as well as in human subjects (Moss *et al.* 1989; Sanberg *et al.* 1989; Sanberg *et al.* 1997). Presently, the nicotinic mechanism of these therapies is thought to be the inactivation of α4β2* or α7* receptor subtypes, as well as a prolonged desensitization period (Lindstrom 1997; Sanberg *et al.* 1997). Mecamylamine

has also been used as a potential therapy for the attenuation of the tics associated with this disease (Silver *et al.* 2000; Young *et al.* 2001).

Smoking Cessation

Due to the addictive properties of NIC, the active alkaloid in tobacco products, smoking cessation has long been associated with the nicotinic receptors (Benowitz 1996; Rose 1996). Nicotine replacement therapy has been employed *via* nicotine gums, patches, and nasal sprays in order to achieve abatement of smoking (Hajek *et al.* 1999). Further research has also shown that the combination of the channel blocker mecamylamine with nicotine patches decreases cravings for cigarettes (Rose *et al.* 1994; Rose *et al.* 1998; Rose *et al.* 2001). Researchers uses the Rose *et al.* studies as the basis for using a partial agonist, which combines agonist and antagonist properties, to provide relief to smoking cessation patients. Cystine analogs, including varenicline, a $\alpha 4\beta 2^*$ nicotinic receptor subtype partial agonist, have been evaluated as agents for smoking cessation by Pfizer Laboratories (Coe *et al.* 2005; Coe *et al.* 2005). The alkaloid (-)-lobeline was in clinical trials as treatment for smoking cessation (Schneider and Olsson 1996). However, further study revealed that lobeline use in patient groups was not statistically different than those of the placebo group, though one of three sites did demonstrate significant improvements (Glover *et al.* 1998). Therefore, the use of lobeline as a smoking cessation agent is not fully understood and not a viable option currently (Dwoskin and Crooks 2002). Bupropion, a phenylaminoketone atypical antidepressant, has been utilized as a sustained release therapy for smoking cessation (George and O'Malley 2004). The mechanism of action is not known but Bupropion is a nicotinic antagonist at a3ß2, a4ß2, and a7

receptor subtypes expressed in *Xenopus* oocytes (IC_{50} = 1.3, 8.0, and 60 μM, respectively) (Slemmer *et al.* 2000). However, given its limited effectiveness and cost, Bupropion is not considered a long term solution (Sweet 2003).

Chapter 3: Synthesis and Evaluation of *mono*- and *bis*-Alkylated Quaternary Ammonium Salts

3.1. Introduction

The neuronal nicotinic acetylcholine receptor (nAChR) belongs to a superfamily of ligand gated ion channel receptors, and has several diverse and complicated substructures. Each receptor is composed of five individual subtypes either heterologously or homologously expressed. Selected heterogeneous subtypes include combinations of α3, α4, α5, α6 and β2 or β4 (e.g. α4β2*) subunits, while the predominant homologous subtype is composed of α7 subunits (α7*) (Holladay *et al.* 1997). The endogenous ligand, acetylcholine (ACh), as well as NIC are agonists at the receptor binding site. NIC has been studied as a potential treatment in several pathologies (e.g. Alzheimer's and Parkinson's disease, schizophrenia, and analgesia) and has been used as a treatment in smoking cessation programs (Lindstrom 1997). However, NIC is a nonspecific agonist interacting with several receptor subtypes, both in the periphery, as well as in the central nervous system (CNS). Therefore, a large amount of research has been devoted to the discovery of agonists that may increase the potential beneficial therapeutic effects and decrease the side effects of NIC (Holladay *et al.* 1997). These efforts have afforded a number of agonist compounds that are both potent and selective for nAChR subtypes. Surprisingly, very little research has focused on structure activity relationships (SARs) involving nAChR antagonists that are subtype selective (Dwoskin *et al.* 2000; Dwoskin and Crooks 2001).

mono-Substituted Quaternary Ammonium Molecules

Crooks *et al*. (1995) synthesized a small series of *N*-alkylated nicotinium compounds that demonstrated selective antagonist activities at different neuronal nAChR subtypes. Alkylating the pyridino *N*-atom of the NIC molecule with an *n*-octyl carbon chain afforded a compound that was both potent and selective for the nAChRs mediating dopamine (DA) release, a purported α6 containing receptor (Crooks *et al*. 1995). Incorporating an *n*-decyl carbon chain was later shown to afford an analog that was a selective antagonist at the α4β2* receptor subtype (Dwoskin *et al*. 1999). Thus, subtle changes in the alkyl chain length of these *N*-*n*-alkylnicotinium analogs produced a surprising difference in the antagonist activities of the compounds. Conformationally restricted analogs of the NIC molecule were also *N*-*n*-alkylated and these compounds retained antagonist activity at the nAChRs mediating DA release, with chain lengths of 8-12 carbons in the *syn*-conformation (**24a-e**) and 8-11 carbons in the *anti*-conformation (**25a-d**) affording various degrees of antagonist activity (Xu *et al*. 2001). Unlike the *N*-*n*-alkylnicotinium analogs, none of these conformationally restricted molecules antagonized the α4β2* nAChR subtype. Therefore, structural modification of the nicotine molecule can result in compounds with potent and selective nAChR antagonist characteristics.

bis-Substituted Quaternary Ammonium Molecules

bis-Quaternary ammonium salts have also been used as ligands in several receptor systems. For example, *bis*-quinolinium cyclophans have been used to block Apamin-sensitive Ca^{2+}-activated K^{+} channels (Chen *et al*. 2000). Investigators determined that altering the chain lengths of alkane spacers between the quaternary ammonium centers

could effectively afford analogs that inhibit receptor function. Additionally, like the *mono*-substituted *N*-alkyl quaternized ammonium salts, *bis*-substituted quaternized ammonium salts have demonstrated selective inhibition of peripheral nicotinic acetylcholine receptor subtypes. Peripheral nicotinic receptor antagonists, such as hexamethonium (HEX, **46**) and decamethonium (DEC), were originally prepared as simple analogs of the neuromuscular blocking agent, *d*-tubocurarine (*d*-Tub, **16**). The ten carbon analog, DEC, demonstrated competitive inhibition of nicotinic receptors at the neuromuscular junction, while HEX primarily antagonized nerve-nerve terminals (ganglionic receptors). These two *bis*-quaternary ammonium compounds were among the first to be used to differentiate between the different subtypes of peripheral nicotinic receptors, muscle and ganglionic. Although their mechanisms of action are quite different, DEC and HEX have been shown to have the optimum chain lengths for binding to their respective receptor subtypes in the periphery. In the CNS, HEX and DEC have been evaluated for NIC binding at a4ß2* receptors and found to exhibit weak affinities (Ki = 31.9 and 4.27, respectively) for the receptor subtype (Ayers *et al.* 2005). *d*-Tub, a more complex *bis*-quaternary structure, also has activity at the muscle-type peripheral nAChR subtype, but it also has activities at the ganglionic receptor subtypes and at a4ß2* subtypes (Ascher *et al.* 1979; Colquhoun *et al.* 1979; Ogden and Colquhoun 1985; Bertrand *et al.* 1990). Therefore, *bis*-quaternary ammonium structures have been used mainly as antagonists peripherally, and have the potential to differentiate between these nAChR subtypes by both altering the chain length and the quaternary ammonium headgroup.

In order to assess the pyrrolidine moiety's importance to the antagonist activity of these interesting series of compounds, a series of quaternized aza-aromatic compounds (e.g. pyridine, 3-picoline, nicotinamide, and NIC) were evaluated (**53-56**). In addition to the assessment of the importance of the pyrrolidine ring, alkyl chain lengths of between one to twenty carbon units were attached to the pyridino functionality to evaluate the relationship between alkyl chain length and inhibition of and selectivity for various nAChR subtypes.

Figure 3.1 *mono*-Alkylated Quaternary Ammonium Salts

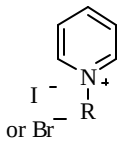

53a	NMPI	R= CH_3
53b	NEPI	R= CH_2CH_3
53c	NPrPI	R= $(CH_2)_2CH_3$
53d	NBuPI	R= $(CH_2)_3CH_3$
53e	NPePI	R= $(CH_2)_4CH_3$
53f	NHxPI	R= $(CH_2)_5CH_3$
53g	NHpPI	R= $(CH_2)_6CH_3$
53h	NOPI	R= $(CH_2)_7CH_3$
53i	NNPI	R= $(CH_2)_8CH_3$
53j	NDPI	R= $(CH_2)_9CH_3$
53k	NUPI	R= $(CH_2)_{10}CH_3$
53l	NDDPI	R= $(CH_2)_{11}CH_3$
53m	NPeDPB	R= $(CH_2)_{14}CH_3$
53n	NEcPB	R= $(CH_2)_{19}CH_3$

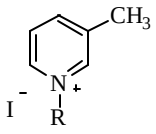

54a	NOPiI	R= $(CH_2)_7CH_3$
54b	NNPiI	R= $(CH_2)_8CH_3$
54c	NDPiI	R= $(CH_2)_9CH_3$
54d	NUPiI	R= $(CH_2)_{10}CH_3$
54e	NDDPiI	R= $(CH_2)_{11}CH_3$

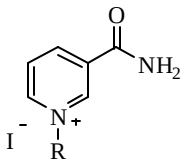

55a	NONAI	R= $(CH_2)_7CH_3$
55b	NNNAI	R= $(CH_2)_8CH_3$
55c	NDNAI	R= $(CH_2)_9CH_3$
55d	NUNAI	R= $(CH_2)_{10}CH_3$
55e	NDDNAI	R= $(CH_2)_{11}CH_3$

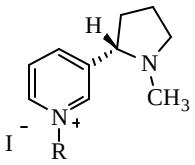

56a	NMNI	R= CH_3
56b	NENI	R= CH_2CH_3
56c	NPNI	R= $(CH_2)_2CH_3$
56d	NnBNI	R= $(CH_2)_3CH_3$
56e	NPeNI	R= $(CH_2)_4CH_3$
56f	NHxNI	R= $(CH_2)_5CH_3$
56g	NHpNI	R= $(CH_2)_6CH_3$
56h	NONI	R= $(CH_2)_7CH_3$
56i	NNNI	R= $(CH_2)_8CH_3$
56j	NDNI	R= $(CH_2)_9CH_3$
56k	NUNI	R= $(CH_2)_{10}CH_3$
56l	NDDNI	R= $(CH_2)_{11}CH_3$

Additionally, *bis*-quaternary ammonium salts (**57-61**) were evaluated for their effect on various nAChR subtypes as analogs of the existing peripheral antagonists HEX, DEC, and *d*-Tub to determine if such analogs antagonized neuronal nicotine receptors. Varying

chain lengths and different pyridinium moieties (e.g. pyridinium, 3-picolinium, quinolinium, isoquinolinium, and nicotinium) were utilized to determine if selective nicotinic receptor subtype antagonism could be achieved.

Figure 3.2 *bis*-Alkylated Quaternary Ammonium Salts

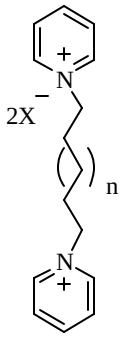

57a	bPPeI	n = 1; X = I
57b	bPHxI	n = 2; X = I
57c	bPOI	n = 4; X = I
57d	bPNB	n = 5; X = Br
57e	bPDI	n = 6; X = I
57f	bPUB	n = 7; X = Br
57g	bPDDB	n = 8; X = Br

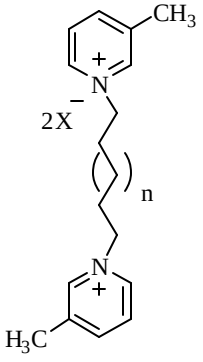

58a	bPiHxI	n = 2; X = I
58b	bPiOI	n = 4; X = I
58c	bPiNB	n = 5; X = Br
58d	bPiDI	n = 6; X = I
58e	bPiUB	n = 7; X = Br
58f	bPiDDB	n = 8; X = Br

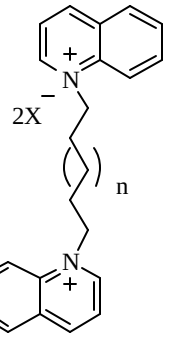

59a	bQHxI	n = 2; X = I
59b	bQOI	n = 4; X = I
59c	bQNB	n = 5; X = Br
59d	bQDI	n = 6; X = I
59e	bQUB	n = 7; X = Br
59f	bQDDB	n = 8; X = Br

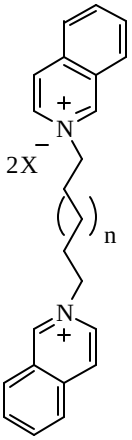

60a	bIQHxI	n = 2; X = I
60b	bIQOI	n = 4; X = I
60c	bIQNB	n = 5; X = Br
60d	bIQDI	n = 6; X = I
60e	bIQUB	n = 7; X = Br
60f	bIQDDB	n = 8; X = Br

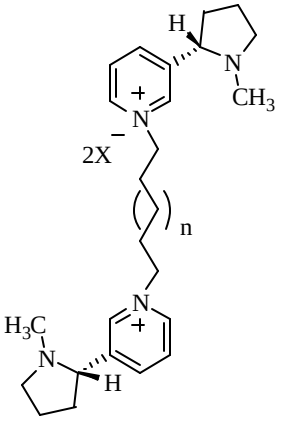

61a	bNHxI	n = 2; X = I
61b	bNOI	n = 4; X = I
61c	bNNB	n = 5; X = Br
61d	bNDI	n = 6; X = I
61e	bNUB	n = 7; X = Br
61f	bNDDB	n = 8; X = Br

3.2. Experimental

3.2.1. Chemicals

S-(-)-Nicotine, pyridine, 3-picoline, nicotinamide, quinoline, isoquinoline, iodomethane, iodoethane, 1-iodopropane, 1-iodobutane, 1-iodopentane, 1-iodohexane, 1-iodoheptane, 1-iodooctane, 1-iodononane, 1-iododecane, 1-iodoundecane, 1-iodododecane, 1-bromopentadecane, 1-bromoecosane, 1,5-diiodopentane, 1,6-diiodohexane, 1,8-diiodooctane, 1,9-dibromononane, 1,10-diiododecane, 1,11-dibromoundecane, 1,12-dibromododecane, diethylether, chloroform, deuterium oxide (100% atom D), deuterium chloride solution (20% W/W solution in D_2O, 99.5% atom D), 3-(trimethylsilyl)-2,2,3,3-d_4-propionate, and α-D-glucose were purchased from Aldrich Chemical Company Inc. (Milwaukee, WI). Acetic acid, was obtained from Fisher Scientific (Pittsburgh, PA). S-(-)-Nicotine ditartrate, nomifensine maleate, and mecamylamine hydrochloride (MEC) were purchased from Research Biochemicals, Inc. (Natick, MA). S-(-)-Cytisine, pargyline hydrochloride, *N*-[2-hydroxyethyl]piperazine-*N*'-[2-ethanesulfonic acid] (HEPES), Tris[hydroxymethyl]-aminomethane hydrochloride (Trizma HCl), Tris[hydroxymethyl]aminomethane (Trizma base), polyethylenimine (PEI), and dihydroxy-β-erythroidine hydrobromide (DHβE) were purchased from Sigma Chemical Co. (St. Louis, MO). Ascorbic acid, and TS-2 tissue solubilizer were purchased from Fluka (Ronkonkona, NY), AnalaR (BHD Ltd., Poole, U.K.), and Research Products International (Mount Prospect, IL), respectively. [^{3}H]Dopamine ([^{3}H]DA); 3,4-ethyl-2-[N-^{3}H]dihydroxyphenylethylamine; specific activity, 25.6 Ci/mmol) and [^{3}H]nicotine (L-(–)-[N-methyl-^{3}H]; specific activity, 78.4 Ci/mmol) were obtained from New England Nuclear (Boston, MA).

3.2.2. Synthetic Procedures

3.2.3. Synthetic Procedures for the Preparation of *mono*-Substituted Pyridinium Derivatives

3.2.3.1. Pyridinium Salts

The appropriate 1-iodoalkane or 1-bromoalkane (5.01-16.1 mmol) was added to a solution (30 mL) of dry pyridine and the solution was heated for 24 h at 65°C. The resulting solid precipitates were filtered and washed five times with dry diethyl ether. For liquid products, the excess pyridine was decanted off, the resulting liquid precipitates were washed with diethyl ether five times, and the remaining liquid was dried under vacuum. The resulting solids or liquids were isolated in 56-95% yields.

N-Methylpyridinium Iodide (NMPI, **53a**)

^{1}H NMR (300 MHz, DMSO-D_6), δ 9.01 (2H, d, C2&C6-H), 8.58 (1H, t, C4-H), 8.13 (2H, t, C3&C5-H), 4.37 (3H, s, C'1-CH_3); ^{13}C NMR (75 MHz, DMSO-D_6), δ 145.3, 144.8, 127.5, 48.0. The resulting tan solid was isolated in 95% yield, with a melting point of 117°C. Combustion Analysis: calculated for C_6H_8IN, C, 32.60; H, 3.65; N, 6.35. Found: C, 32.51; H, 3.62; N, 6.34.

N-Ethylpyridinium Iodide (NEPI, **53b**)

^{1}H NMR (300 MHz, DMSO-D_6), δ 9.14 (2H, d, C2&C6-H), 8.60 (1H, t, C4-H), 8.16 (2H, t, C3&C5-H), 4.67 (2H, q, C'1-CH_2), 1.53 (3H, t, C'2-CH_3); ^{13}C NMR (75 MHz,

DMSO-D_6), δ 145.5, 144.0, 127.8, 56.0, 16.0. The resulting yellow solid was isolated in 92% yield, with a melting point of 88-89°C. Combustion Analysis: calculated for $C_7H_{10}IN$, C, 35.77; H, 4.29; N, 5.96. Found: C, 35.86; H, 4.33; N, 5.94.

N-*n*-Propylpyridinium Iodide (NPrPI, **53c**)

^{1}H NMR (300 MHz, DMSO-D_6), δ 9.19 (2H, d, C2&C6-H), 8.63 (1H, t, C4-H), 8.17 (2H, t, C3&C5-H), 4.64 (2H, t, C'1-CH_2), 1.89 (2H, m, C'2-CH_2), 0.80 (3H, t, C'3-CH_3); ^{13}C NMR (75 MHz, DMSO-D_6), δ 144.7, 143.8, 127.1, 61.1, 23.4, 9.4. The resulting brown liquid was isolated in 87% yield. Combustion Analysis: calculated for $C_8H_{12}IN$, C, 38.57; H, 4.86; N, 5.62. Found: C, 38.73; H, 4.92; N, 5.61.

N-*n*-Butylpyridinium Iodide (NBuPI, **53d**)

^{1}H NMR (300 MHz, DMSO-D_6), δ 9.19 (2H, d, C2&C6-H), 8.64 (1H, t, C4-H), 8.18 (2H, t, C3&C5-H), 4.67 (2H, t, C'1-CH_2), 1.90 (2H, p, C'2-CH_2), 1.25 (2H, m, C'3-CH_2), 0.86 (3H, t, C'4-CH_3); ^{13}C NMR (75 MHz, DMSO-D_6), δ 146.2, 144.5, 127.9, 60.4, 32.4, 18.4, 13.1. The resulting orange liquid was isolated in 90% yield, with a melting point of 59-62°C. Combustion Analysis: calculated for $C_9H_{14}IN$, C, 41.08; H, 5.36; N, 5.32. Found: C, 41.14; H, 5.41; N, 5.32.

N-*n*-Pentylpyridinium Iodide (NPePI, **53e**)

^{1}H NMR (300 MHz, DMSO-D_6), δ 9.16 (2H, d, C2&C6-H), 8.62 (1H, t, C4-H), 8.17 (2H, t, C3&C5-H), 4.83 (2H, t, C'1-CH_2), 1.89 (2H, p, C'2-CH_2), 1.23 (4H, m, C'3&C'4-CH_2), 0.80 (3H, t, C'5-CH_3); ^{13}C NMR (75 MHz, DMSO-D_6), δ 146.2, 144.5, 127.9,

60.4, 30.0, 27.2, 21.3, 13.7. The resulting orange solid was isolated in 93% yield, with a melting point of 62°C. Combustion Analysis: calculated for $C_{10}H_{16}IN$, C, 43.34; H, 5.82; N, 5.05. Found: C, 43.47; H, 5.87; N, 5.04.

N-*n*-Hexylpyridinium Iodide (NHxPI, **53f**)

^{1}H NMR (300 MHz, DMSO-D_6), δ 9.17 (2H, d, C2&C6-H), 8.63 (1H, t, C4-H), 8.19 (2H, t, C3&C5-H), 4.85 (2H, t, C'1-CH_2), 2.00 (2H, p, C'2-CH_2), 1.24 (6H, m, C'3-C'5-CH_2), 0.80 (3H, t, C'6-CH_3); ^{13}C NMR (75 MHz, DMSO-D_6), δ 145.5, 144.6, 128.1, 60.6, 30.6, 30.4, 24.9, 21.8, 13.8. The resulting yellow solid was isolated in 94% yield, with a melting point of 62°C. Combustion Analysis: calculated for $C_{11}H_{18}IN$, C, 45.37; H, 6.23; N, 4.81. Found: C, 45.30; H, 6.20; N, 4.85.

N-*n*-Heptylpyridinium Iodide (NHpPI, **53g**)

^{1}H NMR (300 MHz, DMSO-D_6), δ 9.17 (2H, d, C2&C6-H), 8.63 (1H, t, C4-H), 8.18 (2H, t, C3&C5-H), 4.65 (2H, t, C'1-CH_2), 1.90 (2H, p, C'2-CH_2), 1.22 (8H, m, C'3-C'6-CH_2), 0.80 (3H, t, C'7-CH_3); ^{13}C NMR (75 MHz, DMSO-D_6), δ 145.5, 144.6, 128.1, 60.6, 31.1, 30.6, 27.9, 25.2, 21.8, 13.9. The resulting yellow solid was isolated in 89% yield, with a melting point of 63°C. Combustion Analysis: calculated for $C_{12}H_{20}IN$, C, 47.22; H, 6.61; N, 4.59. Found: C, 47.40; H, 6.72; N, 4.58.

N-*n*-Octylpyridinium Iodide (NOPI, **53h**)

^{1}H NMR (300 MHz, DMSO-D_6), δ 9.16 (2H, d, C2&C6-H), 8.62 (1H, t, C4-H), 8.17 (2H, t, C3&C5-H), 4.83 (2H, t, C'1-CH_2), 1.89 (2H, p, C'2-CH_2), 1.22 (10H, m, C'3-C'7-

CH_2), 0.80 (3H, t, C'8-CH_3); ^{13}C NMR (75 MHz, DMSO-D_6), δ 145.0, 144.2, 127.6, 60.1, 30.6, 30.2, 27.9, 27.8, 24.8, 21.4, 13.4. The resulting brown liquid was isolated in 87% yield. Combustion Analysis: calculated for $C_{13}H_{22}IN$, C, 48.91; H, 6.95; N, 4.39. Found: C, 49.01; H, 7.08; N, 4.39.

N-*n*-Nonylpyridinium Iodide (NNPI, **53i**)

^{1}H NMR (300 MHz, DMSO-D_6), δ 9.14 (2H, d, C2&C6-H), 8.62 (1H, t, C4-H), 8.17 (2H, t, C3&C5-H), 4.62 (2H, t, C'1-CH_2), 1.90 (2H, p, C'2-CH_2), 1.22 (12H, m, C'3-C'8-CH_2), 0.82 (3H, t, C'9-CH_3); ^{13}C NMR (75 MHz, DMSO-D_6), δ 145.5, 144.6, 128.1, 60.7, 31.3, 30.6, 28.6, 28.5, 28.3, 25.3, 22.0, 13.9. The resulting yellow solid was isolated in 88% yield, with a melting point of 76°C. Combustion Analysis: calculated for $C_{14}H_{24}IN$, C, 50.46; H, 7.26; N, 4.20. Found: C, 50.42; H, 7.34; N, 4.21.

N-*n*-Decylpyridinium Iodide (NDPI, **53j**)

^{1}H NMR (300 MHz, DMSO-D_6), δ 9.15 (2H, d, C2&C6-H), 8.62 (1H, t, C4-H), 8.17 (2H, t, C3&C5-H), 4.82 (2H, t, C'1-CH_2), 1.92 (2H, p, C'2-CH_2), 1.22 (14H, m, C'3-C'9-CH_2), 0.82 (3H, t, C'10-CH_3); ^{13}C NMR (75 MHz, DMSO-D_6), δ 145.5, 144.7, 128.1, 60.8, 31.2, 30.7, 28.8, 28.7, 28,6, 28.4, 25.3, 22.0, 13.9. The resulting pale yellow solid was isolated in 84% yield, with a melting point of 71°C. Combustion Analysis: calculated for $C_{15}H_{26}IN$, C, 51.88; H, 7.55; N, 4.03. Found: C, 51.91; H, 7.54; N, 4.00.

N-*n*-Undecylpyridinium Iodide (NUPI, **53k**)

^{1}H NMR (300 MHz, DMSO-D_6), δ 9.12 (2H, d, C2&C6-H), 8.61 (1H, t, C4-H), 8.17 (2H, t, C3&C5-H), 4.61 (2H, t, C'1-CH_2), 2.00 (2H, p, C'2-CH_2), 1.24 (16H, m, C'3-C'10-CH_2), 0.83 (3H, t, C'11-CH_3); ^{13}C NMR (75 MHz, DMSO-D_6), δ 145.2, 144.4, 127.8, 60.1, 31.0, 30.3, 28.6 (x2), 28.4, 28,3, 28.1, 25.0, 21.7, 13.6. The resulting pale yellow solid was isolated in 82% yield, with a melting point of 91°C. Combustion Analysis: calculated for $C_{16}H_{28}IN$, C, 53.19; H, 7.81; N, 3.88. Found: C, 53.24; H, 7.80; N, 3.89.

N-*n*-Dodecylpyridinium Iodide (NDDPI, **53l**)

^{1}H NMR (300 MHz, DMSO-D_6), δ 9.13 (2H, d, C2&C6-H), 8.62 (1H, t, C4-H), 8.18 (2H, t, C3&C5-H), 4.73 (2H, t, C'1-CH_2), 1.89 (2H, p, C'2-CH_2), 1.24 (18H, m, C'3-C'11-CH_2), 0.84 (3H, t, C'12-CH_3); ^{13}C NMR (75 MHz, DMSO-D_6), δ 145.4, 144.6, 128.0, 60.7, 31.2, 30.8, 28.9 (x3), 28.8, 28,7, 28.6, 25.4, 22.0, 13.9. The resulting yellow solid was isolated in 85% yield, with a melting point of 84°C. Combustion Analysis: calculated for $C_{17}H_{30}IN$, C, 54.40; H, 8.06; N, 3.73. Found: C, 54.59; H, 7.97; N, 3.73.

N-*n*-Pentadecylpyridinium Bromide (NPeDPB, **53m**)

^{1}H NMR (300 MHz, $CDCl_3$), δ 9.44 (2H, d, C2&C6-H), 8.49 (1H, t, C4-H), 8.11 (2H, t, C3&C5-H), 5.02 (2H, t, C'1-CH_2), 2.01 (2H, p, C'2-CH_2), 1.35 (24H, m, C'3-C'14-CH_2), 0.86 (3H, t, C'15-CH_3); ^{13}C NMR (75 MHz, $CDCl_3$), δ 145.2, 145.1, 128.4, 62.6, 32.3, 32.2, 30.0, 29.9(x3), 29.8, 29.7, 29.6, 29.3, 26.4, 22.1, 14.5. The resulting tan solid was

isolated in 65% yield, with a melting point of 76°C. Combustion Analysis: calculated for $C_{20}H_{36}BrN$. 1.0 H_2O, C, 61.84; H, 9.86; N, 3.61. Found: C, 61.73; H, 9.62; N, 3.60.

N-Ecosylpyridinium Bromide (NEcPB, **53n**)

^{1}H NMR (300 MHz, DMSO-D_6), δ 9.13 (2H, d, C2&C6-H), 8.62 (1H, t, C4-H), 8.17 (2H, t, C3&C5-H), 4.61 (2H, t, C'1-CH_2), 1.80 (2H, p, C'2-CH_2), 1.25 (34H, m, C'3-C'19-CH_2), 0.85 (3H, t, C'20-CH_3); ^{13}C NMR (75 MHz, DMSO-D_6), δ 145.3, 144.6, 127.9, 60.7, 31.3, 30.7, 29.0 (x10), 28.9, 28.8, 28.7, 28.4, 25.4, 22.1, 14.0. The resulting white solid was isolated in 56% yield, with a melting point of 73°C. Combustion Analysis: calculated for $C_{25}H_{46}BrN$. 1.75 H_2O, C, 63.61; H, 10.57; N, 2.97. Found: C, 63.45; H, 10.27; N, 3.00.

3.2.3.2. Picolinium Salts

The appropriate 1-iodoalkane (5.01-16.1 mmol) was added to a solution (30 mL) of 3-picoline, and the solution heated for 24 h at 65°C. The resulting liquid precipitates had the excess picoline decanted off and the resulting oil precipitates were washed with diethyl ether five times, and the remaining oil was dried under vacuum. The resulting oil was isolated in yields ranging from 89-94%.

N-*n*-Octylpicolinium Iodide (NOPiI, **54a**)

^{1}H NMR (300 MHz, DMSO-D_6), δ 9.04 (1H, s, C2 -H), 8.94 (1H, s, C6-H), 8.45 (1H, d, C4-H), 8.06 (1H, t, C5-H), 4.55 (2H, t, C'1-CH_2), 2.50 (3H, s, C3-CH_3), 1.91 (2H, p, C'2-CH_2), 1.25 (10H, m, C'3-C'7-CH_2), 0.85 (3H, t, C'8-CH_3); ^{13}C NMR (75 MHz,

DMSO-D_6), δ 145.5, 144.0, 141.8, 138.5, 127.2, 60.5, 31.1, 30.6, 28.4 (x2), 25.4, 22.1, 17.9, 14.0. The resulting dark brown oil was isolated in 92% yield. Combustion Analysis: calculated for $C_{14}H_{24}IN$, C, 50.46; H, 7.26; N, 4.20. Found: C, 50.26; H, 7.28; N, 4.18.

N-*n*-Nonylpicolinium Iodide (NNPiI, **54b**)

^{1}H NMR (300 MHz, DMSO-D_6), δ 9.00 (1H, s, C2 -H), 8.94 (1H, s, C6-H), 8.45 (1H, d, C4-H), 8.06 (H, t, C5-H), 4.55 (2H, t, C'1-CH_2), 2.50 (3H, s, C3-CH_3), 1.91 (2H, p, C'2-CH_2), 1.25 (10H, m, C'3-C'7-CH_2), 0.85 (3H, t, C'8-CH_3); ^{13}C NMR (75 MHz, DMSO-D_6), δ 145.5, 144.0, 141.8, 138.5, 127.2, 60.5, 31.2, 30.6, 28.7, 28.6, 28.4, 25.4, 22.1, 17.9, 14.0. The resulting dark brown oil was isolated in 94% yield. Combustion Analysis: calculated for $C_{15}H_{26}IN$, C, 51.88; H, 7.55; N, 4.03. Found: C, 51.99; H, 7.54; N, 4.04.

N-*n*-Decylpicolinium Iodide (NDPiI, **54c**)

^{1}H NMR (300 MHz, DMSO-D_6), δ 9.02 (1H, s, C2 -H), 8.93 (1H, s, C6-H), 8.45 (1H, d, C4-H), 8.06 (1H, t, C5-H), 4.53 (2H, t, C'1-CH_2), 2.50 (3H, s, C3-CH_3), 1.91 (2H, p, C'2-CH_2), 1.23 (14H, m, C'3-C'9-CH_2), 0.84 (3H, t, C'10-CH_3); ^{13}C NMR (75 MHz, DMSO-D_6), δ 145.5, 144.0, 141.8, 138.5, 127.2, 60.5, 31.3, 30.6, 28.9, 28.8, 28.7, 28.4, 25.4, 22.1, 17.9, 14.0. The resulting dark brown oil was isolated in 90% yield. Combustion Analysis: calculated for $C_{16}H_{28}IN$, C, 53.19; H, 7.81; N, 3.88. Found: C, 53.24; H, 7.79; N, 3.89.

N-*n*-Undecylpicolinium Iodide (NUPiI, **54d**)

^{1}H NMR (300 MHz, DMSO-D_6), δ 9.04 (1H, s, C2 -H), 8.94 (1H, s, C6-H), 8.46 (1H, d, C4-H), 8.07 (1H, t, C5-H), 4.55 (2H, t, C'1-CH_2), 2.50 (3H, s, C3-CH_3), 1.91 (2H, p, C'2-CH_2), 1.24 (18H, m, C'3-C'11-CH_2), 0.85 (3H, t, C'12-CH_3); ^{13}C NMR (75 MHz, DMSO-D_6), δ 145.5, 144.0, 141.7, 138.5, 127.2, 60.5, 31.3, 30.6, 29.0, 28.9, 28.8, 28.7, 28.4, 25.4, 22.1, 17.9, 14.0. The resulting dark brown oil was isolated in 89% yield. Combustion Analysis: calculated for $C_{17}H_{30}IN$, C, 54.40; H, 8.06; N, 3.73. Found: C, 54.53; H, 7.99; N, 3.75.

N-*n*-Dodecylpicolinium Iodide (NDDPiI, **54e**)

^{1}H NMR (300 MHz, DMSO-D_6), δ 9.03 (1H, s, C2 -H), 8.94 (1H, s, C6-H), 8.46 (1H, d, C4-H), 8.17 (1H, t, C5-H), 4.54 (2H, t, C'1-CH_2), 2.50 (3H, s, C3-CH_3), 1.92 (2H, p, C'2-CH_2), 1.25 (18H, m, C'3-C'11-CH_2), 0.86 (3H, t, C'12-CH_3); ^{13}C NMR (75 MHz, DMSO-D_6), δ 145.7, 144.1, 141.9, 138.7, 127.3, 60.6, 31.2, 30.5, 28.9 (x2), 28.8, 28.7, 28.6, 28.3, 25.3,22.0, 17.8, 13.9. The resulting dark brown oil was isolated in 91% yield. Combustion Analysis: calculated for $C_{18}H_{32}IN$, C, 55.53; H, 8.28; N, 3.60. Found: C, 55.70; H, 8.20; N, 3.59.

3.2.3.3. *N*-Alkylated Nicotinamide Salts

The appropriate 1-iodoalkane (5.01-16.1 mmol) was added to a solution (30 mL) of nicotinamide (40.94 mmol) in methanol. The solution was heated for 24 h at 65°C. The resulting precipitate was filtered, and the product washed five times with dry diethyl ether. The remaining solid was then dissolved in water and extracted with chloroform (3

x 25 mL). The organic layer was dried over anhydrous magnesium sulfate, filtered, and the solvent removed. The resulting solid was isolated in yields ranging from 70-83%.

N-*n*-Octylnicotinamide Iodide (NONAI, **55a**)

^{1}H NMR (300 MHz, DMSO-D_6), δ 9.47 (1H, s, C2 -H), 9.20 (1H, d, C6-H), 8.92 (1H, d, C4-H), 8.54 (1H, s, N1'-H), 8.27 (2H, t, C5-H), 8.18 (1H, s, N1'-H), 4.64 (2H, t, C'1-CH_2), 1.93 (2H, p, C'2-CH_2), 1.27 (10H, m, C'3-C'7-CH_2), 0.87 (3H, t, C'8-CH_3); ^{13}C NMR (75 MHz, DMSO-D_6), δ 162.6, 146.2, 144.6, 143.0, 133.7, 127.7, 61.1, 31.1, 30.6, 28.4 (x2), 25.4, 22.1, 14.0. The resulting golden solid was isolated in 83% yield, with a melting point of 154-155°C. Combustion Analysis: calculated for $C_{14}H_{23}IN_2O$ 0.25 H_2O, C, 45.85; H, 6.46; N, 7.64. Found: C, 45.60; H, 6.36; N, 7.71.

N-*n*-Nonylnicotinamide Iodide (NNNAI, **55b**)

^{1}H NMR (300 MHz, DMSO-D_6), δ 9.48 (1H, s, C2 -H), 9.22 (1H, d, C6-H), 8.92 (1H, d, C4-H), 8.54 (1H, s, N1'-H), 8.28 (2H, t, C5-H), 8.17 (1H, s, N1'-H), 4.63 (2H, t, C'1-CH_2), 1.93 (2H, p, C'2-CH_2), 1.25 (12H, m, C'3-C'8-CH_2), 0.85 (3H, t, C'9-CH_3); ^{13}C NMR (75 MHz, DMSO-D_6), δ 162.6, 146.2, 144.6, 143.0, 133.7, 127.7, 61.1, 31.2, 30.6, 28.7, 28.6, 28.4, 25.4, 22.1, 14.0. The resulting yellow solid was isolated in 80% yield, with a melting point of 164°C. Combustion Analysis: calculated for $C_{15}H_{25}IN_2O$ 0.5 H_2O, C, 46.76; H, 6.80; N, 7.27. Found: C, 46.55; H, 6.69; N, 7.30.

N-*n*-Decylnicotinamide Iodide (NDNAI, **55c**)

^{1}H NMR (300 MHz, DMSO-D_6), δ 9.48 (1H, s, C2 -H), 9.22 (1H, d, C6-H), 8.92 (1H, d, C4-H), 8.54 (1H, s, N1'-H), 8.28 (2H, t, C5-H), 8.18 (1H, s, N1'-H), 4.65 (2H, t, C'1-CH_2), 1.92 (2H, p, C'2-CH_2), 1.24 (14H, m, C'3-C'9-CH_2), 0.86 (3H, t, C'10-CH_3); ^{13}C NMR (75 MHz, DMSO-D_6), δ 162.6, 146.1, 144.5, 143.1, 133.7, 127.7, 61.1, 31.3, 30.6, 28.9, 28.8, 28.7, 28.4, 25.4, 22.1, 14.0. The resulting yellow solid was isolated in 77% yield, with a melting point of 170°C. Combustion Analysis: calculated for $C_{16}H_{27}IN_2O$ 0.33 H_2O, C, 48.49; H, 7.04; N, 7.07. Found: C, 48.38; H, 6.85; N, 6.95.

N-*n*-Undecylnicotinamide Iodide (NUNAI, **55d**)

^{1}H NMR (300 MHz, DMSO-D_6), δ 9.48 (1H, s, C2 -H), 9.21 (1H, d, C6-H), 8.92 (1H, d, C4-H), 8.54 (1H, s, N1'-H), 8.28 (2H, t, C5-H), 8.18 (1H, s, N1'-H), 4.64 (2H, t, C'1-CH_2), 1.93 (2H, p, C'2-CH_2), 1.25 (16H, m, C'3-C'10-CH_2), 0.85 (3H, t, C'11-CH_3); ^{13}C NMR (75 MHz, DMSO-D_6), δ 162.6, 146.1, 144.6, 143.0, 133.7, 127.7, 61.1, 31.3, 30.6, 29.0, 28.9, 28.8, 28.7, 28.4, 25.4, 22.1, 14.0. The resulting dark yellow solid was isolated in 70% yield, with a melting point of 175°C. Combustion Analysis: calculated for $C_{17}H_{29}IN_2O$ 0.25 H_2O, C, 49.94; H, 7.27; N, 6.85. Found: C, 49.81; H, 7.33; N, 6.83.

N-*n*-Dodecylnicotinamide Iodide (NDDNAI, **55e**)

^{1}H NMR (300 MHz, DMSO-D_6), δ 9.47 (1H, s, C2 -H), 9.21 (1H, d, C6-H), 8.92 (1H, d, C4-H), 8.54 (1H, s, N1'-H), 8.27 (2H, t, C5-H), 8.18 (1H, s, N1'-H), 4.64 (2H, t, C'1-CH_2), 1.92 (2H, p, C'2-CH_2), 1.23 (18H, m, C'3-C'11-CH_2), 0.84 (3H, t, C'12-CH_3); ^{13}C NMR (75 MHz, DMSO-D_6), δ 162.6, 146.1, 144.5, 143.1, 133.7, 127.7, 61.2, 31.3, 30.6,

29.0 (x2), 28.9, 28.8, 28.7, 28.4, 25.4, 22.1, 14.0. The resulting golden solid was isolated in 72% yield, with a melting point of 181°C. Combustion Analysis: calculated for $C_{18}H_{31}IN_2O$ 0.33 H_2O, C, 50.95; H, 7.52; N, 6.60. Found: C, 50.73; H, 7.48; N, 6.43.

3.2.3.4. Nicotinium Salts

S-(-)-Nicotine (30.8 mmol) was dissolved in glacial acetic acid (35 mL) and the solution was stirred at ambient temperature for five minutes. The appropriate 1-iodoalkane (30.8 mmol) was added to the solution, and the mixture was refluxed for three days. The mixture was then evaporated under reduced pressure to remove the solvent, and the resulting oil was treated with an aqueous solution of sodium bicarbonate. Diethyl ether (3 x 50 mL) and chloroform (3 x 50 mL) were added successively to the resulting mixture to extract the unreacted NIC and quaternized analog, respectively. The chloroform layers were collected, combined, and dried over magnesium sulfate. The chloroform was then filtered and evaporated to dryness on a rotary evaporator. The resulting oil was triturated with dry diethyl ether as needed, and the ether washings discarded. The remaining residue was utilized as a homogenous viscous oil in the pharmacological assays. The resulting oil was isolated in yields ranging from 60-72%.

N-*n*-Butylnicotinium Iodide (NnBNI, **56d**)

^{1}H NMR (300 MHz, DMSO-D_6),δ 9.05 (1H, s, C2-H), 8.99 (1H, d, C6-H), 8.54 (1H, d, C4-H), 8.12 (1H, t, C3-H), 4.61 (2H, t, C''1-CH_2), 3.43 (1H, t, pyrrolidine CH_2), 3.18 (1H, t, pyrrolidine CH_2), 2.34 (2H, m, C''2-CH_2), 2.15 (3H, s, pyrrolidine N-CH_3), 1.88 (4H, m, pyrrolidine CH_2CH_2), 1.65 (1H, m, pyrrolidine CH), 1.30 (2H, m, C''3-CH_2), 0.92 (3H, t, C"-CH_3); ^{13}C NMR (75 MHz, DMSO-D_6) δ 144.3, 143.9, 143.3, 127.8, 66.5,

60.5, 56.3, 34.7, 32.8 (x2), 22.6, 18.8, 13.4. The resulting dark brown oil was isolated in 60% yield. Combustion Analysis: calculated for $C_{14}H_{23}IN_2$ 0.125 H_2O, C, 48.25; H, 6.72; N, 8.04. Found: C, 48.02; H, 6.58; N, 8.02.

N-*n*-Pentylnicotinium Iodide (NPeNI, **56e**)

^{1}H NMR (300 MHz, $CDCl_3$) δ 9.37 (1H, d, C6-H), 9.18 (1H, s, C2-H), 8.50 (1H, d, C4-H), 8.11 (1H, t, C3-H), 4.92 (2H, t, C''1-CH_2), 3.64 (1H, t, pyrrolidine CH_2), 3.25 (1H, t, pyrrolidine CH_2), 2.46 (2H, m, C''2-CH_2), 2.25 (3H, s, pyrrolidine N-CH_3), 1.80- 2.02 (4H, m, pyrrolidine CH_2CH_2), 1.67 (1H, m, pyrrolidine CH), 1.36 (4H, m, C''3&''4-CH_2), 0.87 (3H, t, C"-CH_3); ^{13}C NMR (75 MHz, $CDCl_3$) δ 146.7, 144.3, 143.7, 143.2, 128.6, 67.1, 62.4, 57.0, 40.9, 36.1, 31.9, 28.4, 23.6, 22.5, 14.2. The resulting light brown oil was isolated in 72% yield. Combustion Analysis: calculated for $C_{15}H_{25}IN_2$ 0.25 H_2O, C, 45.93; H, 6.49; N, 7.14. Found: C, 45.76; H, 6.34; N, 7.15.

N-*n*-Dodecylnicotinium Iodide (NDDNI, **56l**)

^{1}H NMR (300 MHz, $CDCl_3$) δ 9.30 (1H, d, C6-H), 9.08 (1H, s, C2-H), 8.52 (1H, d, C4-H), 8.11 (1H, t, C5-H), 4.90 (2H, t, C''1-CH_2), 3.69 (1H, t, pyrrolidine CH_2), 3.30 (1H, t, pyrrolidine CH_2), 2.50 (2H, m, C''2-CH_2), 2.30 (3H, s, pyrrolidine N-CH_3), 1.65-2.12 (5H, m, pyrrolidine CH_2CH_2CH), 1.18-1.50 (18H, m, C''3-11-CH_2), 0.89 (3H, t, C"12-CH_3); ^{13}C NMR (75 MHz, $CDCl_3$) δ 146.7, 144.3, 143.6, 143.0, 128.6, 67.1, 62.6, 56.9, 40.9, 36.1, 32.1 (x2), 29.8 (x2), 29.7, 29.6 (x2), 29.3, 26.3, 23.5, 23.0, 14.4. The resulting dark brown oil was isolated in 65% yield. Combustion Analysis: calculated for $C_{22}H_{39}IN_2$ 0.25 HI, C, 53.88; H, 8.07; N, 5.71. Found: C, 53.74; H, 8.04; N, 5.58.

3.2.4. Synthetic Procedures for the Preparation of *bis*-Pyridinium Derivatives

3.2.4.1. *bis*-Pyridinium Salts

1,X-dihalogenoalkane, where X denotes the appropriate carbon length, (6.09-12.13 mmol) was added to a solution (30 mL) of dry pyridine, and the solution heated for 24 h at 65°C. The resulting solid precipitates were filtered and washed five times with dry diethyl ether. For liquid products, the excess pyridine was decanted off, the resulting liquid precipitates were washed with diethyl ether five times, and the remaining liquid was dried under vacuum. The resulting solid or liquid was isolated yields ranging from 87-93%.

N,*N'*-Pentane-1,5-diyl-*bis*-pyridinium Diiodide (bPPeI, **57a**)

^{1}H NMR (300 MHz, DMSO-D_6) δ 9.14 (2H, d, C2&C6-H), 8.62 (1H, t, C4-H), 8.19 (2H, t, C3&C5-H), 4.62 (2H, t, C'1-CH_2), 1.92 (2H, m, C'2-CH_2), 1.25 (1H, m, C'3-CH_2); ^{13}C NMR (75 MHz, DMSO-D_6) δ 145.3, 144.5, 127.9, 60.1, 29.9, 21.7. The resulting yellow solid was isolated in 90% yield, with a melting point of 146-147°C. Combustion Analysis: calculated for $C_{15}H_{20}I_2N_2$, C, 37.37; H, 4.18; N, 5.81. Found: C, 37.51; H, 4.20; N, 5.73.

N,*N'*-Hexane-1,6-diyl-*bis*-pyridinium Diiodide (bPHxI, **57b**)

^{1}H NMR (300 MHz, DMSO-D_6) δ 9.13 (2H, d, C2&C6-H), 8.63 (1H, t, C4-H), 8.18 (2H, t, C3&C5-H), 4.52 (2H, t, C'1-CH_2), 1.93 (2H, m, C'2-CH_2), 1.34 (2H, m, C'3-CH_2); ^{13}C

NMR (75 MHz, DMSO-D_6) δ 145.3, 144.5, 127.9, 60.5, 30.7, 24.8. The resulting pale yellow solid was isolated in 92% yield, with a melting point of 242-243°C. Combustion Analysis: calculated for $C_{16}H_{22}I_2N_2$, C, 38.73; H, 4.47; N, 5.65. Found: C, 38.62; H, 4.53; N, 5.87.

N,N'-Octane-1,8-diyl-*bis*-pyridinium Diiodide (bPOI, **57c**)

^{1}H NMR (300 MHz, DMSO-D_6) δ 9.11 (2H, d, C2&C6-H), 8.63 (1H, t, C4-H), 8.18 (2H, t, C3&C5-H), 4.59 (2H, t, C'1-CH_2), 1.89 (2H, m, C'2-CH_2), 1.28 (4H, m, C'3&4-CH_2); ^{13}C NMR (75 MHz, DMSO-D_6) δ 145.3, 144.5, 127.9, 60.5, 30.6, 28.1, 25.2. The resulting pale yellow solid was isolated in 93% yield, with a melting point of 203-204°C. Combustion Analysis: calculated for $C_{18}H_{26}I_2N_2$, C, 41.24; H, 5.00; N, 5.43. Found: C, 41.20; H, 5.08; N, 5.68.

N,N'-Nonane-1,9-diyl-*bis*-pyridinium Dibromide (bPNB, **57e**)

^{1}H NMR (300 MHz, DMSO-D_6) δ 9.17 (2H, d, C2&C6-H), 8.61 (1H, t, C4-H), 8.18 (2H, t, C3&C5-H), 4.63 (2H, t, C'1-CH_2), 1.89 (2H, m, C'2-CH_2), 1.22 (5H, m, C'3-5-CH_2); ^{13}C NMR (75 MHz, DMSO-D_6) δ 145.3, 144.5, 127.9, 60.5, 30.7, 28.4, 28.2, 25.3, $C_{19}H_{28}Br_2N_2$. The resulting clear liquid was isolated in 87% yield. Combustion Analysis: calculated for $C_{19}H_{28}Br_2N_2$, C, 51.37; H, 6.35; N, 6.31. Found: C, 51.42; H, 6.31; N, 6.25.

N,N'-Decane-1,10-diyl-*bis*-pyridinium Diiodide (bPDI, **57f**)

^{1}H NMR (300 MHz, DMSO-D_6) δ 9.10 (2H, d, C2&C6-H), 8.63 (1H, t, C4-H), 8.19 (2H, t, C3&C5-H), 4.60 (2H, t, C'1-CH_2), 1.89 (2H, m, C'2-CH_2), 1.24 (6H, m, C'3-5-CH_2); ^{13}C NMR (75 MHz, DMSO-D_6) δ 145.3, 144.5, 127.9, 60.6, 30.6, 28.8, 28.1, 25.2. The resulting pale yellow solid was isolated in 90% yield, with a melting point of 162-163°C. Combustion Analysis: calculated for $C_{20}H_{30}I_2N_2$, C, 43.50; H, 5.48; N, 5.07. Found: C, 43.53; H, 5.67; N, 5.29.

N,*N*'-Undecane-1,11-diyl-*bis*-pyridinium Dibromide (bPUB, **57g**)

^{1}H NMR (300 MHz, DMSO-D_6) δ 9.18 (2H, d, C2&C6-H), 8.62 (1H, t, C4-H), 8.19 (2H, t, C3&C5-H), 4.63 (2H, t, C'1-CH_2), 1.88 (2H, m, C'2-CH_2), 1.22 (7H, m, C'3-6-CH_2); ^{13}C NMR (75 MHz, DMSO-D_6) δ 145.3, 144.6, 127.9, 60.6, 30.8, 28.8 (x2), 28.4, 25.4. The resulting amber liquid was isolated in 91% yield. Combustion Analysis: calculated for $C_{21}H_{32}Br_2N_2$, C, 53.40; H, 6.83; N, 5.93. Found: C, 53.39; H, 6.91; N, 5.88.

N,*N*'-Dodecane-1,12-diyl-*bis*-pyridinium Dibromide (bPDDB, **57h**)

^{1}H NMR (300 MHz, DMSO-D_6) δ 9.15 (2H, d, C2&C6-H), 8.62 (1H, t, C4-H), 8.19 (2H, t, C3&C5-H), 4.61 (2H, t, C'1-CH_2), 1.88 (2H, m, C'2-CH_2), 1.22 (8H, m, C'3-6-CH_2); ^{13}C NMR (75 MHz, DMSO-D_6) δ 145.3, 144.6, 127.9, 60.7, 30.8, 28.9, 28.8, 28.5, 25.4. The resulting white solid was isolated in 93% yield, with a melting point of 222-223°C. Combustion Analysis: calculated for $C_{22}H_{34}Br_2N_2$, C, 54.33; H, 7.05; N, 5.76. Found: C, 54.40; H, 7.00; N, 5.86.

3.2.4.2. *bis*-Picolinium Salts

1,X-dihalogenoalkane, where X denotes the appropriate carbon length, (6.09-12.13 mmol) was added to a solution (30 mL) of 3-picoline, and the solution heated for 24 h at 65°C. The resulting precipitate was filtered, and the product washed five times with dry diethyl ether. The precipitate was then dissolved in water (30 mL) and extracted with chloroform (3 x 30 mL). The organic layer was collected and evaporated to dryness on a rotary evaporator. The resulting solid or liquid was isolated in yields ranging from 90-94%.

N,*N'*-Hexane-1,6-diyl-*bis*-picolinium Diiodide (bPiHxI, **58a**)

^{1}H NMR (300 MHz, DMSO-D_6) δ 9.06 (1H, s, C2-H), 8.94 (1H, d, C6-H), 8.46 (1H, d, C4-H), 8.07 (1H, t, C5-H), 4.56 (2H, t, C'1-CH_2), 2.50 (3H, s, C3-CH_3), 1.86 (2H, m, C'2-CH_2), 1.33 (2H, m, C'3-CH_2); ^{13}C NMR (75 MHz, DMSO-D_6) δ 145.6, 144.0, 141.7, 138.5, 127.1, 60.3, 30.3, 24.8, 17.9. The resulting pale yellow solid was isolated in 91% yield, with a melting point of 214-215°C. Combustion Analysis: calculated for $C_{18}H_{26}I_2N_2$, C, 41.24; H, 5.00; N, 5.34. Found: 41.03; H, 5.32; N, 5.22.

N,*N'*-Octane-1,8-diyl-*bis*-picolinium Diiodide (bPiOI, **58b**)

^{1}H NMR (300 MHz, DMSO-D_6) δ 9.18 (1H, s, C2-H), 8.96 (1H, d, C6-H), 8.46 (1H, d, C4-H), 8.07 (1H, t, C5-H), 4.62 (2H, t, C'1-CH_2), 2.50 (3H, s, C3-CH_3), 1.94 (2H, m, C'2-CH_2), 1.27 (4H, m, C'3&4-CH_2); ^{13}C NMR (75 MHz, DMSO-D_6) δ 145.5, 143.9, 141.7, 138.5, 127.1, 60.4, 30.5, 28.1, 25.2, 17.9. The resulting canary yellow solid was

isolated in 94% yield, with a melting point of 161-162°C. Combustion Analysis: calculated for $C_{20}H_{30}I_2N_2$, C, 43.50; H, 5.48; N, 5.07. Found: C, 43.32; H, 5.47; N, 4.98.

N,N'-Nonane-1,9-diyl-*bis*-picolinium Dibromide (bPiNB, **58c**)

^{1}H NMR (300 MHz, DMSO-D_6) δ 9.17 (1H, s, C2-H), 9.04 (1H, d, C6-H), 8.47 (1H, d, C4-H), 8.08 (1H, t, C5-H), 4.60 (2H, t, C'1-CH_2), 2.50 (3H, s, C3-CH_3), 1.92 (2H, m, C'2-CH_2), 1.27 (5H, m, C'3-5-CH_2); ^{13}C NMR (75 MHz, DMSO-D_6) δ 145.5, 144.1, 141.8, 138.5, 127.1, 60.4, 30.7, 28.5, 28.3, 25.4, 17.9. The resulting tan liquid was isolated in 90% yield. Combustion Analysis: calculated for $C_{21}H_{32}Br_2N_2$. 0.5 H_2O, C, 52.40; H, 6.91; N, 5.82. Found: C, 52.26; H, 6.89; N, 5.70.

N,N'-Decane-1,10-diyl-*bis*-picolinium Diiodide (bPiDI, **58d**)

^{1}H NMR (300 MHz, $CDCl_3$) δ 9.04 (1H, s, C2-H), 8.94 (1H, d, C6-H), 8.46 (1H, d, C4-H), 8.06 (1H, t, C5-H), 4.58 (2H, t, C'1-CH_2), 2.50 (3H, s, C3-CH_3), 1.90 (2H, m, C'2-CH_2), 1.27 (6H, m, C'3-5-CH_2) ; ^{13}C NMR (75 MHz, DMSO-D_6) δ 145.6, 144.0, 141.7, 138.6, 127.2, 60.5, 30.6, 28.7, 28.4, 25.4, 18.0. The resulting tan solid was isolated in 92% yield, with a melting point of 161-162°C. Combustion Analysis: calculated for $C_{22}H_{34}I_2N_2$. 1.5 H_2O, C, 43.51; H, 6.14; N, 4.61. Found: C, 43.82; H, 6.02; N, 4.61.

N,N'-Undecane-1,11-diyl-*bis*-picolinium Dibromide (bPiUB, **58e**)

^{1}H NMR (300 MHz, DMSO-D_6) δ 9.10 (1H, s, C2-H), 8.98 (1H, d, C6-H), 8.46 (1H, d, C4-H), 8.07 (1H, t, C5-H), 4.58 (2H, t, C'1-CH_2), 2.50 (3H, s, C3-CH_3), 1.90 (2H, m, C'2-CH_2), 1.26 (7H, m, C'3-6-CH_2); ^{13}C NMR (75 MHz, DMSO-D_6) δ 145.5, 144.0,

141.8, 138.5, 127.1, 60.5, 30.7, 28.8, 28.7, 28.4, 25.4, 17.9. The resulting tan liquid was isolated in 90% yield. Combustion Analysis: calculated for $C_{23}H_{36}Br_2N_2$. 0.33 H_2O, C, 54.56; H, 7.30; N, 5.53. Found: C, 54.23; H, 7.43; N, 5.41.

N,*N'*-Dodecane-1,12-diyl-*bis*-picolinium Dibromide (bPiDDB, **58f**)

^{1}H NMR (300 MHz, $CDCl_3$) δ 9.04 (1H, s, C2-H), 8.94 (1H, d, C6-H), 8.46 (1H, d, C4-H), 8.16 (1H, t, C5-H), 4.55 (2H, t, C'1-CH_2), 2.50 (3H, s, C3-CH_3), 1.90 (2H, m, C'2-CH_2), 1.25 (8H, m, C'3-6-CH_2); ^{13}C NMR (75 MHz, DMSO-D_6) δ 145.5, 144.1, 141.8, 138.5, 127.2, 60.4, 30.7, 28.9, 28.8, 28.4, 25.4, 17.9. The resulting tan liquid was isolated in 92% yield. Combustion Analysis: calculated for $C_{24}H_{38}Br_2N_2$, C, 56.04; H, 7.45; N, 5.45. Found: C, 55.89; H, 7.62; N, 5.32.

3.2.4.3. *bis*-Quinolinium Salts

1,X-dihalogenoalkane, where X denotes the appropriate carbon length, (6.09-12.13 mmol) was added to a solution (30 mL) of dry quinoline, and the solution heated for 24 h at 65°C. The resulting precipitate was filtered, and the product washed five times with dry diethyl ether. The resulting solid was isolated in yields ranging from 87-92%.

N,*N'*-Hexane-1,6-diyl-*bis*-quinolinium Diiodide (bQHxI, **59a**)

^{1}H NMR (300 MHz, DMSO-D_6) δ 9.53 (1H, d, C2-H), 9.29 (1H, d, C3-H), 8.61 (1H, d, C8-H), 8.50 (1H, d, C4-H), 8.29 (1H, t, C7-H), 8.18 (1H, t, C5-H), 8.07 (1H, d, C6-H), 5.09 (2H, t, C'1-CH_2), 1.96 (2H, m, C'2-CH_2), 1.25 (2H, m, C'3-CH_2); ^{13}C NMR (75 MHz, DMSO-D_6) δ 149.4, 147.2, 137.2, 135.5, 130.6, 129.7, 129.6, 122.0, 118.8, 57.2,

29.3, 25.3. The resulting mustard yellow solid was isolated in 89% yield, with a melting point of 234-235°C. Combustion Analysis: calculated for $C_{24}H_{26}I_2N_2$, C, 48.34; H, 4.39; N, 4.70. Found: C, 48.29; H, 4.43; N, 4.85.

N,N'-Octane-1,8-diyl-*bis*-quinolinium Diiodide (bQOI, **59b**)

^{1}H NMR (300 MHz, DMSO-D_6) δ 9.53 (1H, d, C2-H), 9.29 (1H, d, C3-H), 8.61 (1H, d, C8-H), 8.50 (1H, d, C4-H), 8.29 (1H, t, C7-H), 8.18 (1H, t, C5-H), 8.07 (1H, d, C6-H), 5.09 (2H, t, C'1-CH_2), 1.96 (2H, m, C'2-CH_2), 1.25 (4H, m, C'3&4-CH_2); ^{13}C NMR (75 MHz, DMSO-D_6) δ 149.5, 147.4, 137.4, 135.6, 130.7, 129.9, 129.7, 122.1, 118.9, 57.3, 29.5, 28.5, 25.7. The resulting canary yellow solid was isolated in 89% yield, with a melting point of 222-223°C. Combustion Analysis: calculated for $C_{26}H_{30}I_2$ N_2. 0.25 H_2O, C, 49.54; H, 4.90; N, 4.44. Found: C, 49.41; H, 5.19; N, 4.11.

N,N'-Nonane-1,9-diyl-*bis*-quinolinium Dibromide (bQNB, **59c**)

^{1}H NMR (300 MHz, DMSO-D_6) δ 9.68 (1H, d, C2-H), 9.34 (1H, d, C3-H), 8.67 (1H, d, C8-H), 8.55 (1H, d, C4-H), 8.27 (2H, m, C5&C7-H), 8.07 (1H, d, C6-H), 5.09 (2H, t, C'1-CH_2), 1.95 (2H, m, C'2-CH_2), 1.19-1.45 (5H, m, C'3-5-CH_2); ^{13}C NMR (75 MHz, DMSO-D_6) δ 149.5, 147.2, 137.2, 135.5, 130.6, 129.7, 129.5, 122.0, 118.9, 57.2, 29.6, 28.6, 28.4, 25.7. The resulting dark purple solid was isolated in 92% yield, with a melting point of 185-186°C. Combustion Analysis: calculated for $C_{27}H_{32}Br_2N_2$. 0.25 H_2O, C, 59.08; H, 5.97; N, 5.10. Found: C, 59.01; H, 6.09; N, 5.05.

N,N'-Decane-1,10-diyl-*bis*-quinolinium Diiodide (bQDI, **59d**)

^{1}H NMR (300 MHz, DMSO-D_6) δ 9.53 (1H, d, C2-H), 9.29 (1H, d, C3-H), 8.61 (1H, d, C8-H), 8.50 (1H, d, C4-H), 8.29 (1H, t, C7-H), 8.18 (1H, t, C5-H), 8.06 (1H, d, C6-H), 5.04 (2H, t, C'1-CH_2), 1.96 (2H, m, C'2-CH_2), 1.32 (6H, m, C'3-5-CH_2); ^{13}C NMR (75 MHz, DMSO-D_6) δ 149.5, 147.4, 137.4, 135.6, 130.7, 129.9, 129.7, 122.1, 118.9, 57.3, 29.5,28.9, 28.5, 25.7. The resulting canary yellow solid was isolated in 91% yield, with a melting point of 235-236°C. Combustion Analysis: calculated for $C_{28}H_{34}I_2N_2$. 0.66 H_2O, C, 50.62; H, 5.36; N, 4.22. Found: C, 50.48; H, 5.52; N, 4.19.

N,N'-Undecane-1,11-diyl-*bis*-quinolinium Dibromide (bQUB, **59e**)

^{1}H NMR (300 MHz, $CDCl_3$) δ 9.54 (1H, d, C2-H), 9.28 (1H, d, C3-H), 8.60 (1H, d, C8-H), 8.48 (1H, d, C4-H), 8.27 (1H, t, C7-H), 8.16 (1H, t, C5-H), 8.05 (1H, d, C6-H), 5.03 (2H, t, C'1-CH_2), 1.95 (2H, m, C'2-CH_2), 1.15-1.48 (7H, m, C'3-6-CH_2); ^{13}C NMR (75 MHz, DMSO-d_6) δ 149.5, 147.4, 137.4, 135.6, 130.7, 129.9, 129.7, 122.1, 118.9, 57.3, 29.5,28.9, 28.8, 28.5, 25.7. The resulting dark purple solid was isolated in 87% yield, with a melting point of 188-189°C. Combustion Analysis: calculated for $C_{29}H_{36}Br_2N_2$. 1.0 H_2O, C, 58.99; H, 6.49; N, 4.75. Found: C, 59.23; H, 6.56; N, 4.62.

N,N'-Dodecane-1,12-diyl-*bis*-quinolinium Dibromide (bQDDB, **59f**)

^{1}H NMR (300 MHz, DMSO-D_6) δ 9.58 (1H, d, C2-H), 9.29 (1H, d, C3-H), 8.61 (1H, d, C8-H), 8.50 (1H, d, C4-H), 8.29 (1H, t, C7-H), 8.18 (1H, t, C5-H), 8.04 (1H, d, C6-H), 5.04 (2H, t, C'1-CH_2), 1.95 (2H, m, C'2-CH_2), 1.2-1.4 (8H, m, C'3-6-CH_2); ^{13}C NMR (75 MHz, DMSO-D_6) δ 149.5, 147.4, 137.4, 135.6, 130.7, 129.9, 129.7, 122.1, 118.9,

57.3, 29.5,28.9, 28.8, 28.5, 25.7. The resulting dark purple solid was isolated in 92% yield, with a melting point of 187-188°C. Combustion Analysis: calculated for $C_{30}H_{38}Br_2N_2$. 0.33 H_2O, C, 60.82; H, 6.58; N, 4.73. Found: C, 61.01; H, 6.63; N, 4.64.

3.2.4.4. ***bis*-Isoquinolinium Salts**

1,X-dihalogenoalkane, where X denotes the appropriate carbon length, (6.09-12.13 mmol) was added to a solution (30 mL) of isoquinoline, and the solution heated for 24 h at 65°C. The resulting precipitate was filtered, and the product washed five times with dry diethyl ether. The resulting solid was isolated in yields ranging from 89-92%.

N,N'-Hexane-1,6-diyl-*bis*-isoquinolinium Diiodide (bIQHxI, **60a**)

^{1}H NMR (300 MHz, DMSO-D_6) δ 10.09 (1H, d, C1-H), 8.80 (1H, d, C3-H), 8.61 (1H, d, C8-H), 8.48 (1H, d, C4-H), 8.36 (1H, d, C7-H), 8.27 (1H, t, C5-H), 8.08 (1H, t, C6-H), 4.71 (2H, t, C'1-CH_2), 2.03 (2H, m, C'2-CH_2), 1.40 (4H, m, C'3&4-CH_2); ^{13}C NMR (75 MHz, DMSO-D_6) δ 149.7, 136.7 (x2), 134.7, 131.0, 130.1, 127.1, 127.0, 125.7, 60.6, 30.2, 25.0. The resulting pale yellow solid was isolated in 87% yield, with a melting point of 233°C. Combustion Analysis: calculated for $C_{24}H_{26}I_2N_2$, C, 48.34; H, 4.39; N, 4.70. Found: C, 48.46; H, 4.57; N, 4.98.

N,N'-Octane-1,8-diyl-*bis*-isoquinolinium Diiodide (bIQOI, **60b**)

^{1}H NMR (300 MHz, DMSO-D_6) δ 10.05 (1H, d, C1-H), 8.77 (1H, d, C3-H), 8.58 (1H, d, C8-H), 8.48 (1H, d, C4-H), 8.35 (1H, d, C7-H), 8.26 (1H, t, C5-H), 8.07 (1H, t, C6-H), 4.68 (2H, t, C'1-CH_2), 2.00 (2H, m, C'2-CH_2), 1.30 (4H, m, C'3&4-CH_2); ^{13}C NMR (75

MHz, DMSO-D_6) δ 149.7, 136.9 (x2), 134.8, 131.3, 130.3, 127.3, 127.2, 125.9, 60.9, 30.6, 28.4, 25.6. The resulting yellow solid was isolated in 92% yield, with decomposition at 250°C. Combustion Analysis: calculated for $C_{26}H_{30}I_2N_2$, C, 50.02; H, 4.84; N, 4.49. Found: C, 50.22; H, 4.61; N, 4.53.

N,N'-Nonane-1,9-diyl-*bis*-isoquinolinium Dibromide (bIQNB, **60c**)

^{1}H NMR (300 MHz, DMSO-D_6) δ 10.17 (1H, d, C1-H), 8.85 (1H, d, C3-H), 8.62 (1H, d, C8-H), 8.49 (1H, d, C4-H), 8.36 (2H, d, C7-H), 8.26 (2H, t, C5-H), 8.08 (1H, t, C6-H), 4.72 (2H, t, C'1-CH_2), 2.02 (2H, m, C'2-CH_2), 1.11-1.45 (5H, m, C'3-5-CH_2); ^{13}C NMR (75 MHz, DMSO-D_6) δ 149.8, 136.7 (x2), 134.8, 131.0, 130.1, 127.1, 127.1, 125.7, 60.7, 30.5, 28.6, 28.4, 25.5. The resulting light purple solid was isolated in 92% yield, with a melting point of 162°C. Combustion Analysis: calculated for $C_{27}H_{32}Br_2N_2$. 0.33 H_2O C, 58.92; H, 5.98; N, 5.09. Found: C, 58.76; H, 5.92; N, 4.90.

N,N'-Decane-1,10-diyl-*bis*-isoquinolinium Diiodide (bIQDI, **60d**)

^{1}H NMR (300 MHz, DMSO-D_6) δ 10.07 (1H, d, C1-H), 8.78 (1H, d, C3-H), 8.58 (1H, d, C8-H), 8.48 (1H, d, C4-H), 8.36 (1H, d, C7-H), 8.26 (1H, t, C5-H), 8.07 (1H, t, C6-H), 4.69 (2H, t, C'1-CH_2), 2.0 (2H, m, C'2-CH_2), 1.15-1.50 (6H, m, C'3-5-CH_2); ^{13}C NMR (75 MHz, DMSO-D_6) δ 149.7, 136.9 (x2), 134.9, 131.2, 130.0, 127.3, 127.2, 125.9, 60.9, 30.7, 28.9, 28.6, 25.7. The resulting dark yellow solid was isolated in 92% yield, with a melting point of 192°C. Combustion Analysis: calculated for $C_{28}H_{34}I_2N_2$. 0.33 H_2O C, 51.08; H, 5.31; N, 4.25. Found: C, 50.88; H, 5.42; N, 4.13.

N,N'-Undecane-1,11-diyl-*bis*-isoquinolinium Dibromide (bIQUB, **60e**)

^{1}H NMR (300 MHz, DMSO-D_6) δ 10.07 (1H, d, C1-H), 8.78 (1H, d, C3-H), 8.57 (1H, d, C8-H), 8.48 (1H, d, C4-H), 8.35 (1H, d, C7-H), 8.25 (1H, t, C5-H), 8.07 (1H, t, C6-H), 4.69 (2H, t, C'1-CH_2), 2.0 (2H, m, C'2-CH_2), 1.05-1.45 (7H, m, C'3-6-CH_2); ^{13}C NMR (75 MHz, DMSO-D_6) δ 149.8, 136.7 (x2), 134.8, 131.0, 130.2, 127.1 (x2), 125.7, 60.7, 30.5, 28.9, 28.8, 28.5, 25.6. The resulting purple solid was isolated in 89% yield, with a melting point of 166°C. Combustion Analysis: calculated for $C_{29}H_{36}Br_2N_2$, C, 60.85; H, 6.34; N, 4.89. Found: C, 60.65; H, 6.43; N, 4.92.

N,N'-Dodecane-1,12-diyl-*bis*-isoquinolinium Dibromide (bIQDDB, **60f**)

^{1}H NMR (300 MHz, DMSO-D_6) δ 10.06 (1H, d, C1-H), 8.78 (1H, d, C3-H), 8.58 (1H, d, C8-H), 8.48 (1H, d, C4-H), 8.35 (1H, d, C7-H), 8.25 (1H, t, C5-H), 8.07 (1H, t, C6-H), 4.70 (2H, t, C'1-CH_2), 2.0 (2H, m, C'2-CH_2), 1.15-1.40 (8H, m, C'3-6-CH_2); ^{13}C NMR (75 MHz, DMSO-D_6) δ 149.8, 136.7 (x2), 134.8, 131.0, 130.1, 127.1 (x2), 125.7, 60.6, 30.5, 28.9, 28.8, 28.5, 25.5. The resulting gray-purple solid was isolated in 91% yield, with a melting point of 225°C. Combustion Analysis: calculated for $C_{30}H_{38}Br_2N_2$. 0.5 H_2O, C, 60.51; H, 6.60; N, 4.70. Found: C, 60.75; H, 6.56; N, 4.54.

3.2.4.5. *bis*-Nicotinium Salts

S-(-)-Nicotine (30.8 mmol) was dissolved in glacial acetic acid (35 mL) and the solution was stirred at ambient temperature for five minutes. The 1,X-dihalogenoalkane, where X denotes the appropriate carbon length, (15.4 mmol) was added to the solution and the mixture stirred with refluxing for three days. The mixture was then evaporated under

reduced pressure to remove the solvent, and the resulting oil was treated with an aqueous solution of sodium bicarbonate. The resulting aqueous mixture was extracted with diethyl ether (3 x 50 mL), and then chloroform (3 x 50 mL) and the remaining aqueous layer separated and evaporated to dryness on a rotary evaporator. The resulting solid was dissolved in chloroform (200 mL) and filtered. The filtrate was collected and evaporated to dryness under pressure. The resulting oil was isolated in yields ranging from 15-35%.

N,N'-Hexane-1,6-diyl-*bis*-nicotinium Diiodide (bNHxI, **61a**)

^{1}H NMR (300 MHz, $CDCl_3$),δ 9.44 (1H, s, C2-H), 9.38 (1H, d, C6-H), 8.44 (1H, d, C4-H), 8.13 (1H, m, C5-H), 4.95 (2H, t, C''1-CH_2), 4.03 (1H, t, pyrrolidine CH_2), 3.25 (1H, t, pyrrolidine CH_2), 2.49 (2H, m, C''2-CH_2), 2.23 (3H, s, pyrrolidine N-CH_3), 1.60-2.19 (5H, m, pyrrolidine CH_2CH_2), 1.30-1.55 (2H, m, C''3-CH_2); ^{13}C NMR (75 MHz, $CDCl_3$) δ 146.8, 143.9, 143.7 (x2), 128.2, 66.8, 61.1, 57.0, 40.8, 36.0, 31.3, 24.7, 23.5. The resulting brown viscous oil was isolated in 25% yield. Combustion Analysis: calculated for $C_{26}H_{40}I_2N_4$. 0.75 H_2O, C, 46.20; H, 6.19; N, 8.29. Found: C, 46.08; H, 6.27; N, 8.23.

N,N'-Octane-1,8-diyl-*bis*-nicotinium Diiodide (bNOI, **61b**)

^{1}H NMR (300 MHz, $CDCl_3$),δ 9.58 (1H, s, C2-H), 9.50 (1H, d, C6-H), 8.47 (1H, d, C4-H), 8.03 (1H, m, C5-H), 4.96 (2H, t, C''1-CH_2), 3.65 (1H, t, pyrrolidine CH_2), 3.24 (1H, t, pyrrolidine CH_2), 2.49 (2H, m, C''2-CH_2), 2.25 (3H, s, pyrrolidine N-CH_3), 1.60-2.19 (5H, m, pyrrolidine CH_2CH_2), 1.40-1.60 (4H, m, C''3&4-CH_2); ^{13}C NMR (75 MHz, $CDCl_3$) δ 146.9, 143.8, 143.6, 143.5, 128.3, 66.8, 61.7, 57.0, 40.8, 36.1, 32.0, 27.7, 25.2, 23.5. The resulting yellow viscous oil was isolated in 15% yield. Combustion Analysis:

calculated for $C_{28}H_{44}I_2N_4$. 0.25 H_2O, C, 48.39; H, 6.45; N, 8.06. Found: C, 48.13; H, 6.61; N, 7.98.

N,N'-Nonane-1,9-diyl-*bis*-nicotinium Dibromide (bNNB, **61c**)

^{1}H NMR (300 MHz, $CDCl_3$),δ 9.75 (1H, s, C2-H), 9.56 (1H, d, C6-H), 8.49 (1H, d, C4-H), 8.08 (1H, m, C5-H), 5.05 (2H, t, C''1-CH_2), 3.65 (1H, t, pyrrolidine CH_2), 3.25 (1H, t, pyrrolidine CH_2), 2.48 (2H, m, C''2-CH_2), 2.25 (3H, s, pyrrolidine N-CH_3), 1.60-2.23 (5H, m, pyrrolidine CH_2CH_2), 1.30-1.60 (5H, m, C''3-5-CH_2); ^{13}C NMR (75 MHz, $CDCl_3$) δ 146.5, 144.2, 143.7, 143.6, 128.3, 66.9, 61.7, 56.9, 40.7, 36.0, 32.1, 28.2, 28.0, 25.5, 23.4. The resulting yellow viscous oil was isolated in 27% yield. Combustion Analysis: calculated for $C_{29}H_{46}Br_2N_4$. 0.33 H_2O, C, 56.50; H, 7.63; N, 9.09. Found: C, 56.18; H, 7.81; N, 9.01.

N,N'-Decane-1,10-diyl-*bis*-nicotinium Diiodide (bNDI, **61d**)

^{1}H NMR (300 MHz, $CDCl_3$) δ 9.55 (1H, s, C2-H), 9.44 (1H, d, C6-H), 8.53 (1H, d, C4-H), 8.09 (1H, m, C5-H), 4.98 (2H, t, C''1-CH_2), 3.74 (1H, t, pyrrolidine CH_2), 3.30 (1H, t, pyrrolidine CH_2, 2.50 (2H, m, C''2-CH_2), 2.29 (3H, s, pyrrolidine N-CH_3), 1.65-2.20 (5H, m, pyrrolidine CH_2CH_2), 1.30-1.57 (6H, m, C''3-5-CH_2); ^{13}C NMR (75 MHz, $CDCl_3$) δ 146.6, 143.9 x 2, 143.4, 128.4, 66.9, 61.9, 57.0, 40.8, 36.1, 32.1, 28.5, 28.2, 25.8, 23.5. The resulting yellow viscous oil was isolated in 27% yield. Combustion Analysis: calculated for $C_{30}H_{48}I_2N_4$. 1.0 H_2O, C, 48.92; H, 6.84; N, 7.61. Found: C, 48.64; H, 6.58; N, 7.48.

N,N'-Undecane-1,11-diyl-*bis*-nicotinium Dibromide (bNUB, **61e**)

^{1}H NMR (300 MHz, $CDCl_3$) δ 9.70 (1H, s, C2-H), 9.47 (1H, d, C6-H), 8.49 (1H, d, C4-H), 8.12 (1H, m, C5-H), 5.02 (2H, t, C''1-CH_2), 3.65 (1H, t, pyrrolidine CH_2), 3.26 (1H, t, pyrrolidine CH_2), 2.49 (2H, m, C''2-CH_2), 2.25 (3H, s, pyrrolidine N-CH_3), 1.60-2.20 (5H, m, pyrrolidine CH_2CH_2), 1.20-1.50 (8H, m, C''3-6-CH_2); ^{13}C NMR (75 MHz, $CDCl_3$) δ 146.5, 144.2, 143.7, 143.5, 128.4, 66.9, 61.9, 56.9, 40.7, 36.1, 32.2, 28.8, 28.7, 28.6, 25.9, 23.4. The resulting yellow viscous oil was isolated in 30% yield. Combustion Analysis: calculated for $C_{31}H_{50}Br_2N_4$. 0.33 H_2O, C, 57.76; H, 7.92; N, 8.69. Found: C, 57.55; H, 7.99; N, 8.61.

N,N'-Dodecane-1,12-diyl-*bis*-nicotinium Dibromide (bNDDB, **61f**)

^{1}H NMR (300 MHz, $CDCl_3$) δ 9.66 (1H, s, C2-H), 9.38 (1H, d, C6-H), 8.46 (1H, d, C4-H), 8.10 (1H, t, C5-H), 5.01 (2H, t, C''1-CH_2), 3.61 (1H, t, pyrrolidine CH_2), 3.25 (1H, t, pyrrolidine CH_2), 2.45 (2H, m, C''2-CH_2), 2.23 (3H, s, pyrrolidine N-CH_3), 1.60-2.19 (5H, m, pyrrolidine CH_2CH_2), 1.20-1.50 (8H, m, C''3-6-CH_2); ^{13}C NMR (75 MHz, $CDCl_3$) δ 146.6, 144.2, 143.7, 143.4, 128.5, 67.0, 62.0, 60.0, 40.8, 36.1, 32.4, 29.0, 28.8, 28.7, 26.0, 23.5. The resulting yellow viscous oil was isolated in 35% yield. Combustion Analysis: calculated for $C_{32}H_{52}Br_2N_4$. 0.5 H_2O, C, 58.09; H, 8.07; N, 8.47. Found: C, 57.86; H, 8.12; N, 8.39.

3.2.5. Binding Assays for α4β2* and α7* Nicotinic Receptor Subtypes

[^{3}H]Nicotine Binding Assay (α4β2*)

The interaction of the compounds with the high affinity [^{3}H]NIC binding site of the α4β2* nAChR was studied utilizing a modification of the methodology of Marks *et al.* (1986). Rat striata were dissected, pooled, and homogenized in 10 vol ice-cold modified Krebs-HEPES buffer (in mM: 20 HEPES, 118 NaCl, 4.8 KCl, 2.5 $CaCl_2$, 1.2 $MgSO_4$, pH 7.5). Homogenates were incubated at 37°C for 5 min, and then centrifuged at 27,000 g for 20 min at 4°C. The pellets were resuspended in 10 vol ice-cold MilliQ water and incubated for 5 min at 37°C, followed by centrifugation at 27,000 g for 20 min at 4°C. The second and third pellets were resuspended in 10 vol fresh, ice-cold 10% KRH buffer, incubated for 5 min at 37°C, and centrifuged as above. The final pellets were resuspended in 20 vol of ice-cold MilliQ water, which afforded ~200 µg membrane protein/100 µL aliquot [Bradford, 1976], using BSA as the protein standard. Binding assays were performed in duplicate in a final vol of 200 µL Krebs-HEPES buffer containing 200 mM Tris (pH 7.5 at 4°C). Assays were initiated by the addition of 100 µL of membrane suspension to assay tubes containing final concentrations of 3 nM [^{3}H]-NIC (50 µL) and one of 9 concentrations of compound being evaluated. Nonspecific binding was defined in the presence of 10 µM NIC. After a 90 min incubation at 4°C, reactions were terminated by dilution with 3 mL ice-cold Krebs-HEPES buffer, followed immediately by filtration through Schleicher and Schuell #32 glass fiber filters (pre-soaked in 0.5% polyethyleneimine) using a Brandel cell harvester (Biomedical Research

and Development Laboratories, Inc., Gaithersburg, MD). Filters were rinsed three times with 3 mL of ice-cold Krebs-HEPES buffer and transferred to scintillation vials, 3 mL of scintillation cocktail was added, and radioactivity was determined by liquid scintillation spectroscopy (Marks *et al.* 1986).

[^{3}H]MLA Binding Assay (a **7*)**

[^{3}H]MLA binding probes the α7 nAChR subtype, and assays were carried out using a modification of the method of Davies *et al.* (1999). Whole brain minus cortex, striatum and cerebellum was homogenized in 20 vol of ice-cold hypotonic buffer (in mM: 2 HEPES, 14.4 NaCl, 0.15 KCl, 0.2 $CaCl_2$ and 0.1 $MgSO_4$, pH 7.5). Homogenates were incubated at 37°C for 10 min and centrifuged at 29,000 g for 17 minutes at 4°C. Pellets were washed three times by resuspension in 20 vol of the same buffer followed by centrifugation as described above. Final pellets were resuspended in the incubation buffer to yield ~150 µg membrane protein/100 µL membrane suspension. Binding assays were performed in duplicate, in a final volume of 250 µL of incubation buffer (in mM: 20 HEPES, 144 NaCl, 1.5 KCl, 2 $CaCl_2$, and 1 $MgSO_4$, pH 7.5). Binding assays were initiated by the addition of 100 µL of membrane suspension to 150 µL of sample containing 2.5 nM [^{3}H]MLA and the desired concentration of the test compound, and incubated for 2 hrs at ambient temperature. Nonspecific binding was determined in the presence of 1 mM nicotine. Assays were terminated by dilution of samples with 3 mL of ice-cold incubation buffer, followed by immediate filtration through Schleicher and Schuell #32 glass fiber filters (pre-soaked in 0.5% polyethyleneimine) using a Brandel

cell harvester (Davies *et al.* 1999). Filters were processed as described above for the [^{3}H]NIC binding assay.

3.2.6. Functional Assays for the Nicotinic Receptors Modulating DA Release and a4b2* Nicotinic Receptor Subtype

[^{3}H]Dopamine Overflow Assay

Quaternary ammonium analog effects on [^{3}H]overflow from rat striatal slices preloaded with [^{3}H]DA, were determined using a modification of a previously published method (Dwoskin and Zahniser 1986; Wilkins *et al.* 2002). Briefly, rat striata were dissected and coronal slices (500 µm, 6-8 mg) were obtained using a McIlwain tissue chopper. Slices were incubated for 30 min in Krebs buffer (in mM: 118 NaCl, 4.7 KCl, 1.3 $CaCl_2$, 1.2 $MgCl_2$, 1.0 NaH_2PO_4, 11.1 α-D-glucose, 25 $NaHCO_3$, 0.11 L-ascorbic acid and 0.004 disodium EDTA; pH 7.4, saturated with 95% O_2 / 5% CO_2) at 34°C in a metabolic shaker. Slices were then incubated for an additional 30 min in fresh buffer containing 0.1 µM [^{3}H]DA, after rinsing, each slice was transferred to a glass superfusion chamber, maintained at 34 °C and superfused (1.0 mL/min) with oxygenated Krebs' buffer containing nomifensine (10 µM), a DA reuptake inhibitor), and pargyline (10 µM), a monoamine oxidase inhibitor, to ensure that [^{3}H]overflow represented [^{3}H]DA, rather than [^{3}H]DA metabolites.

Following superfusion for 60 min, three 5-min samples (5 mL/sample) were collected to determine basal [^{3}H]outflow. After collection of the third basal sample, slices from an

individual rat were superfused for 60 min in the absence (0 nM; control) or presence of analog (1 nM-10 μM) to determine the intrinsic activity of the analog, e.g., ability of the analog to evoke [^{3}H]overflow. Each slice was exposed to only one concentration of analog, which remained in the buffer through the completion of the experiment. After a 60 min superfusion in the absence or presence of analog, NIC (10 μM) was added to the superfusion buffer and samples were collected for an additional 60 min to determine the ability of the analog to inhibit NIC-evoked [^{3}H]DA overflow. At least one striatal slice in each experiment was superfused for 60 min in the absence of analog, followed by superfusion with only NIC (10 μM) to determine a NIC control for NIC-evoked [^{3}H]DA overflow in the absence of analog. Using a repeated-measures design, striata from a single rat were used to determine the ability of an analog to evoke [^{3}H]DA release (intrinsic activity) and to determine analog-induced inhibition of NIC-evoked [^{3}H]DA overflow (antagonist activity).

After collection of the superfusate samples, slices were retrieved from the chambers and solubilized using 1 mL TS-2 tissue solubilizer. Scintillation cocktail (10 mL) was added to the superfusate samples. The pH and volume of the solubilized tissue samples were adjusted to those of the superfusate samples. Radioactivity in the superfusate and tissue samples was determined by liquid scintillation spectroscopy (Packard model B1600 TR Scintillation Counter, Downer's Grove, IL).

$^{86}Rb^{+}$ Efflux Assay (a 4b 2*)

Quaternary ammonium analog effects on $^{86}Rb^{+}$ efflux were determined using a previously published method (Marks *et al.* 1995). Rat thalamus was homogenized and centrifuged at 1000xg for 10 min at 4°C. The supernatant fraction was centrifuged at 12,000xg for 20 min at 4°C to obtain the synaptosomal fraction. Synaptosomes were incubated for 30 min in 35 µl of uptake buffer (140 mM NaCl, 1.5 mM KCl, 2.0 mM $CaCl_2$, 1.0 mM $MgSO_4$, 20 mM α-D-glucose; pH 7.5) containing 4 µCi of $^{86}Rb^{+}$. $^{86}Rb^{+}$ uptake was terminated by filtration of the synaptosomes onto glass fiber filters (6 mm; Type A/E, Gelman Sciences, Ann Arbor, MI) under gentle vacuum (0.2 atm), followed by three washes with superfusion buffer (0.5 ml each). Subsequently, each filter containing the $^{86}Rb^{+}$-loaded synaptosomes (39 ± 4.8 µg protein/µl) was placed on a 13 mm glass fiber filter (Type A/E) mounted on a polypropylene platform. $^{86}Rb^{+}$ efflux assay buffer (125 mM NaCl, 5 mM CsCl, 1.5 mM KCl; 2 mM $CaCl_2$, 1 mM $MgSO_4$, 25 mM HEPES, 20 mM α-D-glucose, 0.1 µM TTX, 1.0 g/l bovine serum albumin; pH 7.5) was superfused onto the synaptosomes at a rate of 2.5 ml/min. TTX and CsCl were included in the buffer to block voltage-gated Na^{+} and K^{+} channels, respectively, and to reduce the rate of basal $^{86}Rb^{+}$ efflux (Marks *et al.* 1995).

The intrinsic activity of the quaternary ammonium analog as well as the ability to inhibit $^{86}Rb^{+}$ efflux evoked by 1 µM NIC was determined. After 8 min of superfusion, samples were collected (sample/18 s) for 5 min to determine basal $^{86}Rb^{+}$ efflux. Subsequently, synaptosomes were superfused for 3 min with the quaternary ammonium analog to determine the intrinsic properties of the analog. The exposure to the analog was followed

by superfusion with buffer containing both the quaternary ammonium analog and NIC for an additional 3 min, to determine the ability of the analog to inhibit NIC-evoked $^{86}Rb^{+}$ efflux. Each aliquot part of thalamic synaptosomes was exposed to only one concentration of quaternary ammonium analog. In each experiment, one synaptosomal aliquot part was superfused in the absence of either compound to determine basal $^{86}Rb^{+}$ efflux over the course of the superfusion period, and another aliquot was superfused with NIC (1 μM) to determine the effect of NIC on $^{86}Rb^{+}$ efflux in the absence of the quaternary ammonium analog. Samples were analyzed by liquid scintillation spectroscopy (Packard model B1600 TR Scintillation Counter).

3.2.7. Data Analysis

For analog induced inhibition of [^{3}H]NIC and [^{3}H]MLA binding, data were expressed as specific [^{3}H]NIC or [^{3}H]MLA bound as a percentage of control and plotted as a function of log analog concentration. The concentration (IC_{50}) of analog that inhibited specific [^{3}H]NIC or [^{3}H]MLA binding by 50% were fit by a one-site binding competition model, using nonlinear least-squares regression, such that $Y = Bt + (Tp - Bt)/[1 + 10^{(\log IC50 - X)\bullet n}]$, where Y is the specific [^{3}H]NIC or [^{3}H]MLA binding expressed as a percentage, X is the logarithm of analog concentration, Bt and Tp are the minimum and maximum specific [^{3}H]NIC and [^{3}H]MLA binding densities, respectively, and n is the pseudo-Hill coefficient. The inhibition constant (Ki) for each analog was calculated from IC_{50} values using the Cheng-Prusoff equation [$K_i = IC_{50}/(1 + \text{ligand}/K_d)$], where c is the concentration of free radioligand and K_d is the equilibrium dissociation constant of the ligand.

In [^{3}H]DA overflow assays, fractional release of each superfusate sample was calculated by dividing the total [^{3}H] collected in each sample by the total [^{3}H] present in the tissue at the time of sample collection and was expressed as a percentage of total tissue tritium. Basal [^{3}H]outflow was calculated from the average of the fractional release in three five minute samples collected prior to the addition of analog to the superfusion buffer. Total [^{3}H]overflow was calculated by summing the increases of [^{3}H] above the basal [^{3}H]outflow, resulting from exposure to the analog, NIC, or both and subtracting the basal [^{3}H]outflow for an equivalent period of analog exposure. The data were expressed as percent of control and were fitted by non-linear, non-weighted least-squares regression using the sigmoidal function, $Y = Bt + (Tp - Bt)/[1 + 10^{(\log IC50 - X)}]$, where Y is the total [^{3}H]overflow expressed as a percentage of NIC-evoked response, X is the logarithm of analog concentration, Bt and Tp are the minimum response (held constant at 0%) and maximum response (held constant at 100%), respectively, and log IC_{50} value represents the logarithm of analog concentration required to decrease NIC (10 μM)-evoked [^{3}H]DA overflow by 50% of control levels. The effect of each analog on [^{3}H]DA overflow (intrinsic activity) and its ability to inhibit NIC-evoked [^{3}H]DA overflow (inhibition effect) was analyzed by one-way repeated-measure analysis of variance (ANOVA), where analog concentration was a within subject factor (SPSS version 9.0, Chicago, IL); where appropriate, Dunnett's *post hoc* tests were performed to determine the concentration of analog that significantly evoked or inhibited [^{3}H]DA overflow relative to the control (buffer or NIC-evoked [^{3}H]DA overflow, respectively). A two-way repeated-measures ANOVA was performed to analyze the time course of the NIC-

induced increase in the fractional release (within-subjects factor) for different concentrations of the analog (within-subject factor). IC_{50} values for analog-induced inhibition of NIC-evoked [^{3}H]DA overflow were determined using an iterative non-linear least squares curve-fitting program, (PRISM version 3.0, Graph PAD Software, Inc., San Diego, CA).

3.3. Results and Discussion

Chemistry

Several *N*-*n*-alkyl quaternized ammonium salts were successfully synthesized. *mono*-Substituted *N*-*n*-alkylpyridinium, *N*-*n*-alkylpicolinium, and *N*-*n*-alkylnicotinamide salts were prepared in similar manners, however, their purification work-up varied. All three precipitated from solution upon reaction and were filtered to afford the crude salts. The *N*-*n*-alkylpyridinium and *N*-*n*-alkylpicolinium salts were triturated with diethyl ether to afford the pure quaternary ammonium salts. The nicotinamide series were isolated differently, due to the low solubility of the nicotinamide starting material in the diethyl ether. These salts were isolated using both an initial diethyl ether wash, followed by an aqueous dissolution and subsequent extraction with chloroform. The *N*-*n*-alkylnicotinium salts were synthesized in a different manner to ensure that the pyridino nitrogen was selectively alkylated over the pyrrolidino nitrogen. Previous research by Menshutkin demonstrated that tertiary amines react with alkyl halides resulting in quaternary ammonium salt (Figure 3.3a) (Menshutkin 1890). In the nicotine molecule, the pyrrolidine nitrogen is more reactive than the pyridine nitrogen. Therefore, the pyridine nitrogen would be quaternized only after, or at the same time as, the pyrrolidine nitrogen, causing a doubly quaternized species (Figure 3.3b). Due to the reactive nature

of both nitrogens and to avoid the double quaternization, a protection of the pyrrolidino nitrogen was necessary. Using the higher reactivity of the pyrrolidino nitrogen, a simple acid protection step may be utilized to direct the Menshutkin towards the pyridine nitrogen. Acetic acid was used by Crooks *et al.* (1995) to achieve this selective alkylation of the pyridino nitrogen with excellent results (Figure 3.3c).

Figure 3.3 The Menshutkin reaction and its use in quaternizing nicotine

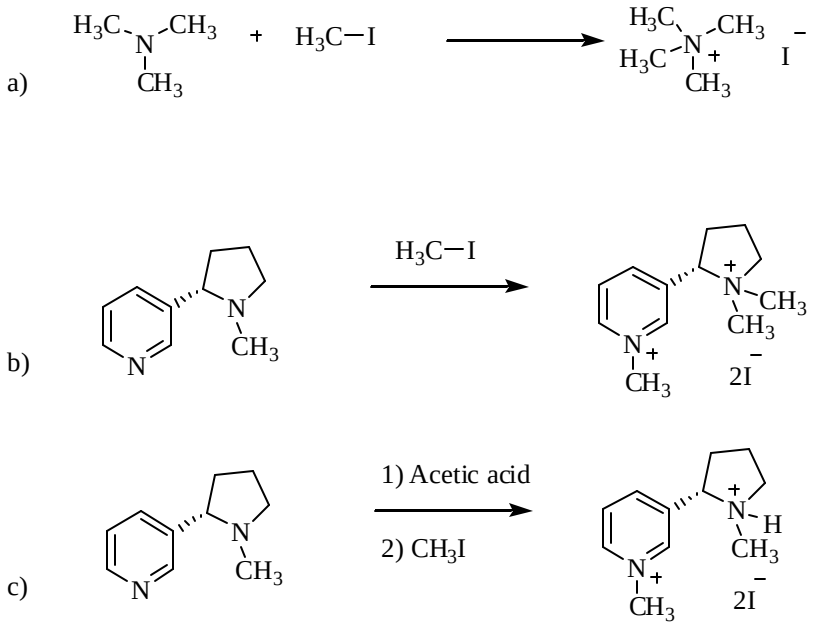

However, the resulting work-up was modified in the current synthesis to increase the yield and decrease the labor-intensive work-up. The existing synthetic route called for the protonated NIC molecule and the iodoalkane reactant to be stirred for three days at room temperature. The increase in the reaction temperature due to the refluxing increased the yield of the reaction in the present synthesis. The previous synthesis also involved a time-consuming basification and subsequent removal of water at increased

temperature followed by a 24-hour reflux in chloroform to remove the excess NIC. This resulted in a loss of the *N*-*n*-alkylnicotinium salt due to the salt having some solubility in chloroform. In the current synthesis, after the basification step, the mixture was sequentially treated with diethyl ether and chloroform to remove the excess NIC and the corresponding *N*-*n*-alkylnicotinium salt, respectively, without evaporating the aqueous layer. This procedure removed the two previous time-consuming steps, and increased the overall yield of the product.

The *bis*-*N*,*N'*-alkyl quaternary ammonium salts were prepared similarly to their corresponding *mono*-alkyl quaternized ammonium salts. *bis*-*N*,*N'*-Alkylpyridinium salts and *bis*-*N*,*N'*-alkylpicolinium salts, as well as *bis*-*N*,*N'*-alkylquinolinium salts and *bis*-*N*,*N'*-alkylisoquinolinium salts, were isolated in high yields when diethyl ether was utilized to remove the excess reactant. The *bis*-*N*,*N'*-alkylnicotinium salts were synthesized via a similar synthetic route to that utilized for the corresponding *mono*-alkylnicotinium salts, although the final purification step was modified. The diethyl ether extraction step removed the unreacted NIC, but the subsequent chloroform extraction revealed the presence of a product from an unexpected side reaction; a *mono*-substituted *N*-alkylnicotinium salt with an acetate terminating the carbon chain instead of another NIC molecule was synthesized and had greater solubility than the *bis*-*N*,*N'*-alkylnicotinium salt in chloroform. During the reaction, it is possible that the acetate ion displaced the iodide or bromide causing the impurity. Alternatively, the *bis*-*N*,*N'*-alkylnicotinium salt may have formed but over the course of the reaction the a carbon to the quaternized pyridine nitrogen could have been attacked by the acetate ion, resulting in

the *mono*-substituted *N*-alkylnicotinium salt with the terminal acetate moiety (Figure 3.4). The aqueous layer containing the *bis*-*N*,*N'*-alkylnicotinium salt was evaporated under reduced pressure and chloroform was added to extract the *bis*-*N*,*N'*-alkylnicotinium salt. The chloroform layer was dried using magnesium sulfate, filtered, and evaporated under reduced pressure to afford the final product.

Figure 3.4 Formation of the acetate impurity

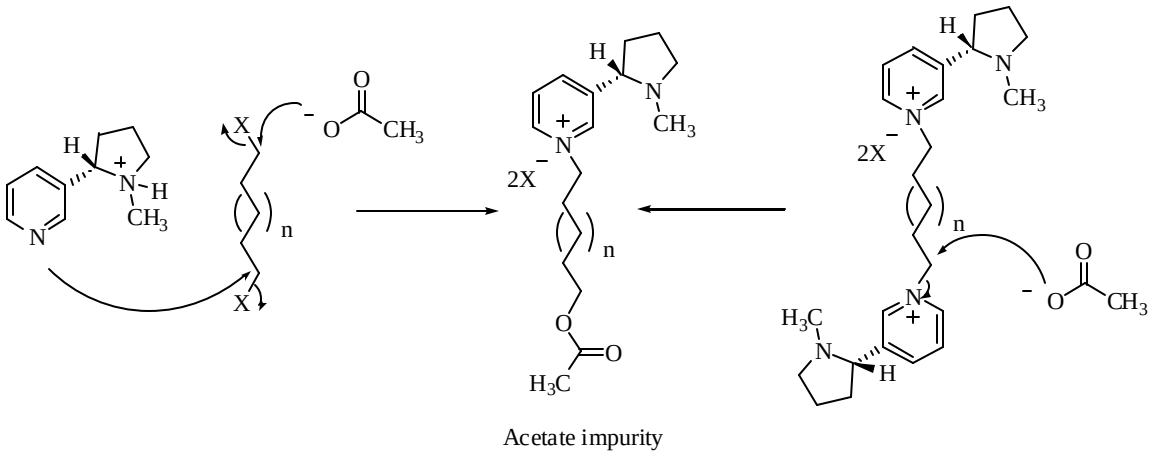

Acetate impurity

It is important to note, that despite several different functionalities and charges on the molecules, the *mono*- and *bis*-quaternary ammonium salts all demonstrated chloroform solubility.

Pharmacology of the *mono*-Substituted Quaternary Ammonium Salts

N-*n*-Alkylpyridinium salts

N-*n*-Alkylpyridinium salts with chain lengths ranging from one to twenty carbon units weakly inhibited [^{3}H]NIC binding to rat striatal membranes (see Table 3.1 for affinity values). Salts with chain lengths less than 15 carbons completely inhibited [^{3}H]NIC

binding. The C_{20} analog NEcPB inhibited binding by only 25%. The binding affinities (Ki) at the a4ß2* nAChR subtypes ranged from 9-20 µM for the C_1-C_{11} and C_{15} analogs. The C_{12} and C_{20} chain length salts were not active (Ki > 100). No significant linear relationship was found between compound affinity and carbon chain length. The *N*-n-alkylpyridinium salts did not inhibit [^{3}H]MLA binding, and thus had no significant affinity at the α7* nAChR subtype (Table 3.1).

Initial screens at two concentrations, i.e. 0.1 and 1.0 µM, of analog, C_1-C_{12}, were determined for the *N*-*n*-alkylpyridinium series in the [^{3}H]DA overflow assay. Chain lengths of nine or less carbons were not active; however, carbon chain lengths greater than nine were found to significantly inhibit NIC-evoked [^{3}H]DA overflow by 70-90%. Evaluation of the activities of these compounds, for both intrinsic and inhibitory activity, over the full concentration range (0.01-100 µM) was performed. NUPI (C_{11}), NDDPI (C_{12}), and NPDPB (C_{15}) increased [^{3}H]DA overflow at 10 µM and NDPI (C_{10}), NEcPB (C_{20}) increase overflow at 100 µM. Concentrations that elicited intrinsic activity were not included in the analysis of inhibition of NIC-evoked DA overflow. Carbon chain lengths greater than nine carbons, i.e. NDPI, NUPI, NDDPI, NPDPB, and NEcPB all inhibited NIC-evoked [^{3}H]DA overflow in the high nanomolar concentration range (IC_{50} values = 120 – 490 nM, Table 3.1). For each analog, repeated measures one-way ANOVA revealed significant concentration-dependent inhibition of nicotine-evoked [^{3}H]DA overflow: NDPI (C10), $F_{5,35} = 29.44$, $p < 0.0001$; NUPI (C11), $F_{4,29} = 24.58$, $p < 0.0001$; NDDPI (C12), $F_{3,23} = 11.07$, $p < 001$; NPDPB (C15), $F_{5,18} = 24.31$, $p < 0.001$; NEcPB (C20), $F_{5,15} = 9.29$, $p < 0.001$. NDPI, NUPI, and NDDPI all inhibited overflow

completely (I_{max} = 100%), whereas NPDPB and NEcPB only inhibited overflow by a maximum of 45-55%.

N-*n*-Alkylpicolinium salts

N-*n*-Alkylpicolinium salts exhibited similar properties to the *N*-*n*-alkylpyridinium salts in their binding affinities at $\alpha4\beta2$* and $\alpha7$* nAChR subtypes. Analogs with chain lengths of C_8-C_{12} had weak or no affinity in the [^{3}H]NIC binding assay, and had no affinity in the [^{3}H]MLA binding assay (Table 3.2). In the NIC-evoked [^{3}H]DA overflow assay, NOPiI (C_8) and NDPiI (C_{10}) did not exhibit intrinsic activity up to 1.0 μM, but NDDPiI (C_{12}) did evoke overflow at $\geq$ 1.0 μM. Due to the intrinsic activity, the concentration 1.0 μM of NDDPiI was not used in determining the inhibitory concentration of the compound. In this series of compounds, NDDPiI was the most potent of the *N*-*n*-alkylpicolinium salts tested at the nAChR subtypes mediating NIC-evoked DA overflow (IC_{50} = 30 nM) and there was an increase of inhibitory activity in this series as the carbon chain increased (Table 3.2). Interestingly, NDDPiI only inhibited overflow by 63%.

N-*n*-alkylnicotinamide salts

N-*n*-alkylnicotinamide salts were not active in either of the binding assays and were not tested in the NIC-evoked DA release assay (Table 3.3).

Table 3.1 Pharmacological Data Derived from the *mono*-Alkylated Pyridinium Salts

Compound			Pharmacological Assays		
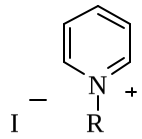	Name	R	[^{3}H]NIC Binding Assay, Ki (μM)	[^{3}H]MLA Binding Assay, Ki (μM)	[^{3}H]DA Release Assay, IC_{50} (μM)
53a	NMPI	Methyl	20.1 (15.6 – 25.9)[a]	>100	>1.0
53b	NEPI	Ethyl	28.7 (22.3 – 37.0)	>100	>1.0
53c	NPrPI	Propyl	42.3 (30.2 – 59.3)	>100	>1.0
53d	NBuPI	Butyl	9.65 (7.57 - 12.3)	>100	>1.0
53e	NPePI	Pentyl	8.72 (5.68 – 13.4)	67.7 (2.31 -1980)	>1.0
53f	NHxPI	Hexyl	9.07 (6.12 – 13.5)	>100	>1.0
53g	NHpPI	Heptyl	15.0 (13.0 – 17.2)	>100	>1.0
53h	NOPI	Octyl	20.1 (16.3 – 24.8)	>100	>1.0
53i	NNPI	Nonyl	19.0 (19.0 – 22.1)	61.8 (3.35 – 1142)	>1.0

Table 3.1 (continued) Pharmacological Data Derived from the *mono*-Alkylated Pyridinium Salts

Compound			Pharmacological Assays		
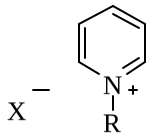	Name	R	[^{3}H]NIC Binding Assay, Ki (μM)	[^{3}H]MLA Binding Assay, Ki (μM)	[^{3}H]DA Release Assay, IC_{50} (μM)
53j	NDPI	Decyl	16.7 (13.6 – 20.4)	>100	0.13 (0.02 – 0.87)
53k	NUPI	Undecyl	17.0 (14.4 – 20.1)	>100	0.49 (0.01 – 16.9)
53l	NDDPI	Dodecyl	>100	>100	0.26 (0.02 – 4.23)
53m	NPeDPB	Pentdecyl	38.0 (28.2 – 51.3)	>100	0.32 (0.11 – 0.87)
53n	NEcPB	Ecosinyl	>100	>100	0.12 (0.01 – 2.38)

[a] Data represent mean (95% confidence intervals)

Table 3.2 Pharmacological Data Derived from the *mono*-Alkylated 3-Picolinium Salts

Compound			Pharmacological Assays		
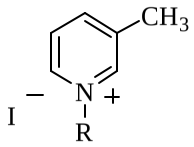	Name	R	[^{3}H]NIC Binding Assay, Ki (μM)	[^{3}H]MLA Binding Assay, Ki (μM)	[^{3}H]DA Release Assay, IC_{50} (μM)
54a	NOPiI	Octyl	>100	>100	1.0 + 0.09
54b	NNPiI	Nonyl	62 $\pm$ 17[a]	>100	ND[c]
54c	NDPiI	Decyl	26 $\pm$ 3.6[b]	>100	0.3 $\pm$ 0.05
54d	NUPiI	Undecyl	>100	>100	ND
54e	NDDPiI	Dodecyl	>100	>100	0.03 $\pm$ 0.02

[a] Data represent mean $\pm$ S.E.M [b] From 3 concentrations, [c] ND = Not Determined

Table 3.3 Pharmacological Data Derived from the *mono*-Alkylated Nicotinamide Salts

			Pharmacological Assays		
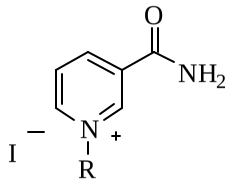					
	Name	R	[^{3}H]NIC Binding Assay, Ki (μM)	[^{3}H]MLA Binding Assay, Ki (μM)	[^{3}H]DA Release Assay, IC_{50} (μM)
55a	NONAI	Octyl	>100	>100	ND[a]
55b	NNNAI	Nonyl	>100	>100	ND
55c	NDNAI	Decyl	>100	>100	ND
55d	NUNAI	Undecyl	>100	>100	ND
55e	NDDNAI	Dodecyl	>100	>100	ND

[a] ND = Not Determined

Table 3.4 Pharmacological Data Derived from the *mono*-Alkylated Nicotinium Salts

Compound			Pharmacological Assays		
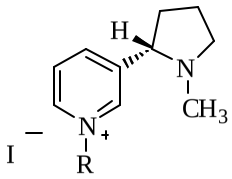	Name	R	[^{3}H]NIC Binding Assay, Ki (μM)	[^{3}H]MLA Binding Assay, Ki (μM)	[^{3}H]DA Release Assay, IC_{50} (μM)
56a	NMNI	Methyl	3.53 (2.77 – 4.48)	>100	24.6 (1.65 – 367)
56b	NENI	Ethyl	1.04 (0.76 – 1.43)	≤100	ND
56c	NPNI	Propyl	21.5 (18.2 – 25.3)	>100	37.4 (9.88 – 141)
56d	NnBNI	Butyl	10.9 (9.70 – 12.3)	>100	9.07 (3.15 – 26.3)
56e	NPeNI	Pentyl	ND[a]	>100	ND
56f	NHxNI	Hexyl	0.53 (0.46 – 0.60)	92.4 (24.0 –375)	3.45 (3.15 – 26.3)
56g	NHpNI	Heptyl	2.06 (1.85 – 2.28)	76.0 (13.5 – 429)	0.80 (0.37 – 1.71)
56h	NONI	Octyl	19.7 (15.4 – 25.1)	28.3 (18.4 – 43.5)	0.62 (0.20 – 1.94)
56i	NNNI	Nonyl	0.84 (0.73 – 0.95)	≤ 100	0.21 (0.09 – 0.48)

Table 3.4 continued Pharmacological Data Derived from the *mono*-Alkylated Nicotinium Salts

Compound			Pharmacological Assays		
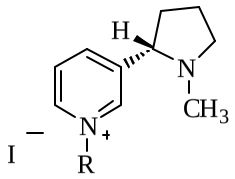	Name	R	[^{3}H]NIC Binding Assay, Ki (μM)	[^{3}H]MLA Binding Assay, Ki (μM)	[^{3}H]DA Release Assay, IC_{50} (μM)
56j	NDNI	Decyl	0.09 (0.08 – 0.11)[a]	~100	>100
56k	NUNI	Undecyl	ND[b]	$\underline{<}$100	ND
56l	NDDNI	Dodecyl	0.14 (0.11 – 0.17)	>100	0.009 (0.003 – 0.03)

[a] Data represent mean (95% confidence intervals) [b] ND = Not Determined

***N*-*n*-Alkylnicotinium salts**

N-*n*-Alkylnicotinium salts demonstrated a wide range of affinities in the [^{3}H]NIC binding assay (90 nM –20 μM, Table 3.4). The C_{10} and C_{12} analogs (NDNI and NDDNI) had the highest affinities, Ki = 90 nm and 140 nm, respectively. A linear relationship between *N*-*n*-alkyl chain length and analog affinity was determined, with the exception of the *N*-*n*-octyl compound, NONI, which had one of the lowest affinities in the series. The *N*-*n*-alkylnicotinium salts all demonstrated low affinity in the [^{3}H]MLA binding assay (Table 3.4).

In the evaluation of the *N*-*n*-alkylnicotinium salts to inhibit NIC-evoked [^{3}H]DA overflow, analogs with chain lengths greater than six carbons demonstrated intrinsic activity at concentrations greater than 1 μM. Longer chain compounds were more likely to evoke significant amounts of [^{3}H]overflow. NDNI (C_{10}) had the lowest concentration necessary for evoking [^{3}H]overflow at 1 μM, followed by NDDNI (C_{12}) at 10 μM, and NONI (C_8), NHpNI (C_7), and NHxNI (C_6) at 100 μM. NNNI (C_9) did not evoke [^{3}H]overflow at any concentration tested. For each analog, repeated measures one-way ANOVA revealed significant concentration-dependent inhibition of nicotine-evoked [^{3}H]DA overflow: NMNI (C_1), $F_{3,15} = 5.02$, $p < 0.05$; NPNI (C_3), $F_{6,38} = 4.33$, $p < 0.005$; NnBNI (C_4), $F_{3,19} = 8.83$, $p < 0.005$; NHxNI (C_6), $F_{5,20} = 3.81$, $p < 0.05$; NHpNI (C_7), $F_{5,24} = 26.3$, $p < 0.0001$; NONI (C_8), $F_{5,27} = 10.5$, $p < 0.0001$; NNNI (C_9), $F_{5,23} = 4.58$, $p < 0.01$; and NDDNI (C_{12}), $F_{4,18} = 9.00$, $p < 0.001$. Evaluation of the inhibition of NIC-evoked [^{3}H]DA overflow by the *N*-*n*-alkylnicotinium salts revealed that NPNI was the least potent of the *N*-*n*-alkylnicotinium analogs (IC_{50} = 37 μM), while NnBNI and

NHxNI also exhibited low micromolar activity (IC_{50} = 9 and 3 μM, respectively). NHpNI, NONI, and NNNI had IC_{50} values in the range 0.2 - 0.8 μM. NDDNI, the C_{12} analog, had the highest inhibitory potency with an IC_{50} value of 9 nM (Table 3.4).

Structure Activity Relationship of the *mono*-Substituted Quaternary Ammonium Salts

The affinities of *N*-*n*-alkylnicotinium compounds in the [^{3}H]NIC binding assay revealed that as the carbon chain was increased so was the affinity for the α4β2* receptor. Subsequent evaluation of these compounds in the functional Rb^{86+} efflux assay demonstrated that *N*-*n*-alkylnicotinium compounds with good affinity in the [^{3}H]NIC binding assay, were receptor antagonists at the α4β2* nAChR subtype. Analogs with longer *n*-alkyl chain lengths of nine, ten, and twelve all had nanomolar affinities for the α4β2* nAChR subtype, with the *N*-*n*-decylnicotinium (NDNI) and *N*-*n*-dodecylnicotinium (NDDNI) having the highest affinities for the receptor with Ki values of 90 nM and 140 nM, respectively. These Ki values are comparable to that of the classical nAChR antagonist DHβE, which has a Ki value of 149 nM at the α4β2* receptor subtype (Wilkins *et al.* 2003). Interestingly, a one-carbon deletion from the nine-carbon chain analog, to afford the *N*-*n*-nonylnicotinium salt (NNNI), results in a twenty-fold decrease in affinity for the α4β2* receptor subtype. Therefore, a subtle change to the length of the carbon chain may cause a large difference in activity. This is further supported by the inactivity of the C_8 compound, *N*-*n*-octylnicotinium, which had low affinity in the [^{3}H]NIC binding assay. The higher affinities in the longer chain compounds may be due to an increase in the lipophilic interaction of the carbon chain and

the hydrophobic regions of the binding site. This interaction may have a stabilizing effect on the compound-receptor complex, increasing the affinity for the C_9-C_{12} compounds of this series of compounds.

In addition to the carbon chain length, the pyrrolidine ring of this series of compounds also appears to play an important role in the interaction at the binding site. The *N*-*n*-alkylnicotinium salts with increased numbers of carbon units all demonstrated a greater affinity for the $\alpha4\beta2^*$ binding site over their corresponding *N*-*n*-alkylpyridinium, *N*-n-alkylpicolinium, and *N*-*n*-alkylnicotinamide salts. Complete removal of the pyrrolidine ring in the *N*-*n*-alkylpyridinium series resulted in a complete loss in affinity for the $\alpha4\beta2^*$ receptor. In the *N*-*n*-alkylpicolinium series, the importance of a 3-substituent was explored. However, the low affinity of these salts in the [^{3}H]NIC binding assay indicates that a simple methyl group in the three position of the pyridine ring does not afford compounds with high affinity for the $\alpha4\beta2^*$ binding site. The nicotinamide moiety is a somewhat larger and more polar substituent that incorporates a second nitrogen atom into the receptor-ligand model. Due to the lack of activity of these molecules at the $\alpha4\beta2^*$ binding site, and since the nicotinamide nitrogen is not basic in nature, it can be assumed that it is not necessarily the size of the 3-substituent that promotes interaction with the receptor but rather the incorporation of an appropriate functional moiety. Therefore, a basic nitrogen, such as that in the pyrrolidine ring may be important for recognition by the high affinity [^{3}H]NIC binding site on the $\alpha4\beta2^*$ receptor subtype.

Several of the quaternized ammonium salts were potent antagonists in the NIC-evoked [^{3}H]DA overflow assay, with the *N*-*n*-dodecylnicotinium analog (NDDNI) exhibiting the greatest activity at the nAChR subtypes mediating DA release (IC_{50} = 9 nM); this inhibition is significantly greater than that exhibited by DHβE (IC_{50} = 1.6 μM). However, the *N*-*n*-alkylpyridinium and *N*-*n*-alkylpicolinium salts with similar *N*-*n*-alkyl chain lengths also antagonized the receptor subtype at higher nanomolar concentrations, with IC_{50} values of 260 nM (NNDPI) and 30 nM (NDDPiI). The *N*-*n*-alkylpicolinium and *N*-*n*-alkylnicotinium salts both demonstrate a linear relationship between antagonist activity and carbon chain length at the nAChR subtypes that mediate DA release. The removal of the pyrrolidine ring did not completely eliminate the ability of these *N*-*n*-alkylpyridinium salts to interact with this class of nAChR subtypes

The quaternary ammonium salts demonstrated low activities in the [^{3}H]MLA binding assay. The *N*-*n*-alkylnicotinium molecules only inhibited binding with carbon chain lengths of C_6, C_7, C_8 (Ki = 28.3-92.4 μM). These values are at least ten fold less active at the receptor than NIC, a weak agonist. The *N*-*n*-alkylpyridinium compounds also did not exhibit affinity for α7* nAChRs, with only two compounds, NPePI (C_6) and NNPI (C_9), having Ki values below 100 μM (67.7 and 61.8 μM, respectively). Therefore, these compounds are not active at the α7* receptor subtype.

Pharmacology of the *bis*-Substituted Quaternary Ammonium Salts

N,N'-bis-Alkylpyridinium salts

N,N'-bis-Alkylpyridinium salts with *n*-alkyl chain lengths ranging from six to twelve carbon atoms were evaluated in the [^{3}H]NIC binding assay and had weak affinities for the $\alpha4\beta2$* nAChR subtype binding site (Table 3.5). These compounds did show a general trend of increasing affinity as the *n*-alkyl carbon chain length was increased. Compound bPDDB, had the highest affinity for the $\alpha4\beta2$* receptor subtype with a Ki value of 9.15 μM. The *N,N'-bis*-alkylpyridinium salts with chain lengths ranging from C_6-C_{12} demonstrated low affinity or no affinity with respect to [^{3}H]MLA binding, and thus exhibited no significant interaction with the $\alpha7$* nAChR subtype (Table 3.5).

The C_{12} analog, bPDDB, had no intrinsic activity at any of the concentrations tested (0.001-10 μM) in the [^{3}H]DA overflow assay. bPDDB inhibited NIC-evoked [^{3}H]DA overflow with an IC_{50} value of 1.0 μM. No other *N,N'-bis*-alkylpyridinium compounds were evaluated at nAChR subtypes mediating DA release (Table 3.5).

N,N'-bis-Alkylnicotinium salts

N,N'-bis-Alkylnicotinium salts were also evaluated in the [^{3}H]NIC binding assay. The C_{10} (bNDI) and C_{11} (bNUB) analogs had the highest affinities for the $\alpha4\beta2$* receptor subtype, with Ki values of 330 and 430 nM, respectively (Table 3.6). Moreover, bNDI and bNUB inhibited NIC-evoked $^{86}Rb^+$ efflux from rat thalamic synaptosomes (IC_{50} = 3.76 $\pm$ 1.1 μM and 5.22 $\pm$ 1.4 μM, respectively), without producing intrinsic activity. Several other compounds, i.e. the C_6-C_9 and C_{12} analogs, had low micromolar affinities (Ki = 1.54 - 20.0 μM). None of the *N,N'-bis*-alkylnicotinium salts were active in the [^{3}H]MLA binding assay (Table 3.6).

In addition to the α4β2* and α7 receptor subtype assays, the *N,N'-bis*-alkylnicotinium C_{12} analog, bNDDB, was evaluated for both intrinsic and inhibitory activity in the [^{3}H]DA overflow assay. bNDDB had intrinsic activity at 10 μM. The C_{12} salt afforded an IC_{50} value of 3.30 μM in the NIC-evoked [^{3}H]DA overflow assay (Table 3.6).

***N,N'-bis*-Alkylpicolinium salts**

N,N'-bis-Alkylpicolinium salts generally did not exhibit high affinities at the α4β2* nAChR subtype, with Ki values for the C_9, C_{11}, C_{12} analogs in the high micromolar range (48.6-79.9 μM) and the C_6, C_{10} and C_{11} compounds had no affinity at this nAChR subtype (>100 μM). The *N,N'-bis*-alkylpicolinium salts were not active in the [^{3}H]MLA binding assay (Table 3.7).

The C_{12} *N,N'-bis*-alkylpicolinium analog, bPiDDB, was evaluated for its intrinsic and inhibitory behavior in the [^{3}H]DA overflow assay. bPiDDB had no intrinsic activity in [^{3}H]DA overflow assay at any of the concentrations tested (0.001-10 μM). The compound was very potent in inhibiting NIC-evoked [^{3}H]DA overflow. With an IC_{50} value of 2 nM, this compound is one of the most potent compounds in inhibiting NIC-evoked DA release (Table 3.7). Interestingly, bPiDDB inhibited NIC-evoked [^{3}H]DA overflow by a maximum of only 50%.

Due to the high potency of bPiDDB to inhibit NIC-evoked [^{3}H]DA overflow, all the *N,N'-bis*-alkylpicolinium analogs were tested for intrinsic activity and for their ability to

inhibit [^{3}H]DA overflow. Generally, *N,N'-bis*-alkylpicolinium analogs did not exhibit intrinsic activity in this assay. One-way ANOVAs revealed significant concentration-dependent inhibition for each analog: bPiOI (C_8), $F_{5,19} = 4.441$, $p = 0.007$; bPiNB (C_9), $F_{5,19} = 4.053$, $p = 0.011$; bPiDI (C_{10}), $F_{5,23} = 7.346$, $p < 0.001$; bPiUB (C_{11}), $F_{5,28} = 11.750$, $p < 0.001$, bPiDDB (C_{12}), $F_{5,23} = 13.282$, $p < 0.001$. Contrary to what was observed in the pyridinium series, the shorter chain length compounds, i.e. C_8 and C_{10}, were potent antagonists at the nAChR subtype responsible for mediating DA release. However, the antagonism pattern did not seem to increase as carbon chain length increased, as has been observed in several of the other series. The C_8 (bPiOI) and C_{10} (bPiDI), analogs had low nanomolar activities (IC_{50} = 10 and 30 nM, respectively), while the C_9 (bPiNB) and C_{11} (bPiUB), analogs had low micromolar activities (IC_{50} = 1.5 - 1.6 μM) and the C_6 analog (bPiHxI), was inactive (Table 3.7). All the active *N,N'-bis*-alkylpicolinium salts inhibited NIC-evoked [^{3}H]DA overflow similar to bPiDDB, with a maximum of ~50% (I_{max} = 50%).

N,N'-bis-Alkylisoquinolinium and *N,N'-bis*-alkylquinolinium salts

N,N'-bis-Alkylisoquinolinium and *N,N'-bis*-alkylquinolinium salts were evaluated in the [^{3}H]NIC binding assay and generally had low affinities for the α4β2* nAChR (Tables 3.8 and 3.9). The C_6, C_8, C_9, C_{11}, and C_{12} *N,N'-bis*-alkylisoquinolinium analogs had low to moderate micromolar affinities (Ki = 6.10-65.5 μM) for the α4β2* nAChR subtype, while the C_{10} analog had no affinity (Ki > 100 μM). The pharmacological profile of the *N,N'-bis*-alkylquinolinium salts was similar to that of the *N,N'-bis*-alkylisoquinolinium salts in the [^{3}H]NIC binding assay, with the C_6, C_9, and C_{11} analogs exhibiting only

moderate micromolar affinities (Ki = 22.5-39.3 μM) for the α4β2* nAChR subtype, while the C_8, C_{10}, and C_{12} analogs had no affinity (Ki > 100 μM). Interestingly, analogs in both the *N,N'-bis*-alkylisoquinolinium series and the *N,N'-bis*-alkylquinolinium series were all active in the [^{3}H]MLA binding assay, with Ki values in the low micromolar range (1.61-16.0 μM, Tables 3.8 and 3.9); the two most potent analogs in these two groups were the C_{12} analogs, bQDDB and bIQDDB (Ki = 1.61 and 2.21 μM, respectively).

Table 3.5 Pharmacological Data Derived from the *bis*-Alkylpyridinium Salts

Compound			Pharmacological Assays		
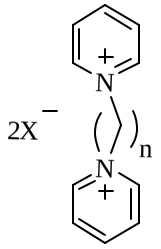	Name	n	[^{3}H]NIC Binding Assay, Ki (μM)	[^{3}H]MLA Binding Assay, Ki (μM)	[^{3}H]DA Release Assay, IC_{50} (μM)
57a	bPPeI	5	>100	>100	>1.0
57b	bPHxI	6	97.8 ± 17.5[a]	>100	ND[b]
57c	bPOI	8	34.3 ± 2.74	>100	>1.0
57d	bPNB	9	24.2 ± 1.19	>100	ND
57e	bPDI	10	18.7 ± 3.09	>100	>1.0
57f	bPUB	11	14.0 ± 3.21	57.0 ± 4.89	ND
57g	bPDDB	12	9.15 ± 0.17	33 ± 4.6	1.0 ± 0.38

[a] Data represent mean ± S.E.M [b]ND = Not Determined

Table 3.6 Pharmacological Data Derived from the *bis*-Alkylnicotinium Salts

Compound			Pharmacological Assays		
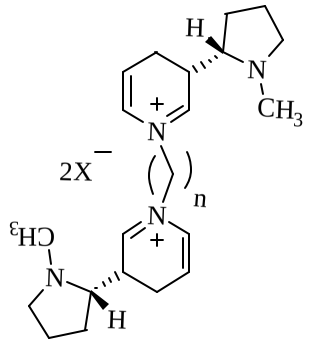	Name	n	[^{3}H]NIC Binding Assay, Ki (μM)	[^{3}H]MLA Binding Assay, Ki (μM)	[^{3}H]DA Release Assay, IC_{50} (μM)
61a	bNHxI	6	20.0 ± 2.84[a]	>100	ND[b]
61b	bNOI	8	1.54 ± 0.17	>100	ND
61c	bNNB	9	5.03 ± 0.80	>100	ND
61d	bNDI	10	0.33 ± 0.01	>100	ND
61e	bNUB	11	0.43 ± 0.06	>100	ND
61f	bNDDB	12	1.95 ± 0.19	>100	0.17 ± 0.13

[a] Data represent mean ± S.E.M [b]ND = Not Determined

Table 3.7 Pharmacological Data Derived from the *bis*-Alkylpicolinium Salts

Compound			Pharmacological Assays		
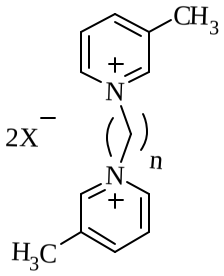	Name	n	[^{3}H]NIC Binding Assay, Ki (μM)	[^{3}H]MLA Binding Assay, Ki (μM)	[^{3}H]DA Release Assay, IC_{50} (μM)
58a	bPiHxI	6	>100	>100	>100
58b	bPiOI	8	>100	>100	0.30 ± 0.18
58c	bPiNB	9	79.9 ± 16.6[a]	>100	5.81 ± 5.07
58d	bPiDI	10	>100	>100	0.18 ± 0.11
58e	bPiUB	11	69.2 ± 28.9	>100	1.12 ± 0.65
58f	bPiDDB	12	48.6 ± 17.2	>100	0.002 ± 0.001

[a] Data represent mean ± S.E.M

Table 3.8 Pharmacological Data Derived from the *bis*-Alkylisoquinolinium Salts

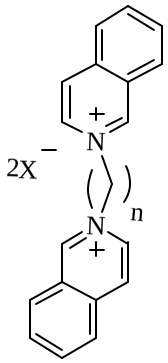

Compound			Pharmacological Assays		
	Name	n	[^{3}H]NIC Binding Assay, Ki (μM)	[^{3}H]MLA Binding Assay, Ki (μM)	[^{3}H]DA Release Assay, IC_{50} (μM)
60a	bIQHxI	6	17.9 ± 3.59[a]	16.0 ± 1.92	1.87 ± 1.11
60b	bIQOI	8	65.5 ± 14.5	11.7 ± 5.63	1.69 ± 1.18
60c	bIQNB	9	7.89 ± 0.92	5.95 ± 1.01	>100
60d	bIQDI	10	>100	7.25 ± 3.02	0.09 ± 0.04
60e	bIQUB	11	9.02 ± 1.56	5.46 ± 0.78	0.05 ± 0.03
60f	bIQDDB	12	6.10 ± 0.73	2.21 ± 0.25	0.04 ± 0.03

[a] Data represent mean ± S.E.M

Table 3.9 Pharmacological Data Derived from the *bis*-Alkylquinolinium Salts

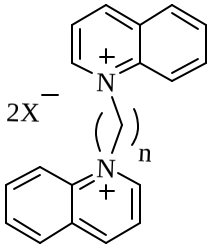

Compound			Pharmacological Assays		
	Name	n	[^{3}H]NIC Binding Assay, Ki (μM)	[^{3}H]MLA Binding Assay, Ki (μM)	[^{3}H]DA Release Assay, IC_{50} (μM)
59a	bQHxI	Hexyl	39.3 ± 5.59[a]	13.3 ± 2.12	0.50 ± 0.46
59b	bQOI	Octyl	>100	2.39 ± 0.69	0.06 ± 0.03
59c	bQNB	Nonyl	22.5 ± 1.30	3.58 ± 0.45	0.24 ± 0.17
59d	bQDI	Decyl	>100	7.81 ± 1.90	>1
59e	bQUB	Undecyl	37.8 ± 8.65	2.58 ± 0.46	0.21 ± 0.18
59f	bQDDB	Dodecyl	>100	1.61 ± 0.25	0.02 ± 0.008

[a] Data represent mean ± S.E.M

The compounds in the *N,N'-bis*-alkylisoquinolinium and *N,N'-bis*-alkylquinolinium series were evaluated for both intrinsic activity and their ability to inhibit NIC-evoked [^{3}H]DA overflow. The C_8 and C_{12} *N,N'-bis*-alkylquinolinium salts, bQOI and bQDDB, and the C_{10} *N,N'-bis*-alkylisoquinolinium salt, bIQDDB, elicited [^{3}H]DA overflow at 10 μM. The other *N,N'-bis*-alkylquinolinium and *N,N'-bis*-alkylisoquinolinium salts, did not exhibit intrinsic activity at any concentration tested *N,N'-bis*-alkylquinolinium. One-way ANOVA revealed significant concentration-dependent inhibition for bQHxI (C_6), $F_{5,24} = 5.055$, $p = 0.002$; bIQOI (C_8), $F_{4,14} = 6.428$, $p = 0.003$; bQNB (C_9), $F_{5,19} = 4.872$, $p = 0.004$; bQDI (C_{10}), $F_{4,14} = 3.294$, $p = 0.033$; bQUB (C_{11}), $F_{5,19} = 7.873$, $p < 0.001$; bQDDB (C_{12}), $F_{5,24} = 9.16$, $p < 0.001$; bIQOI (C_8), $F_{5,20} = 4.141$, $p = 0.01$; bIQDI (C_{10}), $F_{4,16} = 4.835$, $p < 0.001$, bIQUB (C_{11}), $F_{5,20} = 4.157$, $p < 0.001$; bIQDDB (C_{12}), $F_{5,22} = 3.827$, $p < 0.05$. *N,N'-bis*-alkylisoquinolinium salts exhibited antagonist activity at nAChR subtypes that mediate DA release (IC_{50} = 20-90 nM). In addition, the analogs only partially inhibited NIC-evoked [^{3}H]DA overflow (I_{max} = 62-78%).

, $F_{5,19} = 4.441$, $p = 0.007$; bPiNB (C_9), $F_{5,19} = 4.053$, $p = 0.011$; bPiDI (C_{10}), $F_{5,23} = 7.346$, $p < 0.001$; bPiUB (C_{11}), $F_{5,28} = 11.750$, $p < 0.001$, bPiDDB (C_{12}),

Structure Activity Relationship of the *bis*-Substituted Quaternary Ammonium Salts

At muscle-type peripheral receptors, the compounds with only a trimethylammonium headgroup, were found to require an optimum chain length of ten carbon units (DEC). Although DEC had three orders of magnitude lower affinity for the α4β2* subtype compared to NIC (Ki = 5.73 ± 0.76 μM versus 0.0014 ± 0.0001 μM) for the α4β2* subtype and had no affinity for the α7* subtype, it is apparent that replacing the *N,N'-*

trimethylammonium moieties of DEC with azaaromatic moieties, such as nicotinium moieties ($\alpha4\beta2^*$) and quinolinium and isoquinolinium moieties ($\alpha7^*$), affords molecules with good affinity for nAChR subtypes.

Of particular interest is the finding that two compounds in this study exhibited high selectivity at the $\alpha4\beta2^*$ nAChR subtype. In this respect, the *N,N'-bis*-alkylnicotinium analogs, bNDI and bNUB exhibit low nanomolar affinities (330 and 430 nM, respectively) for the $\alpha4\beta2^*$ nAChR subtype, and functionally inhibited NIC-evoked $^{86}Rb^+$ efflux, while demonstrating no affinity for the $\alpha7^*$ nAChR subtype, these data indicate that these two analogs are selective $\alpha4\beta2^*$ nAChR subtype antagonists. As seen in the *mono*-quaternary ammonium series, the importance of the pyrrolidino moiety to achieve activity at the $\alpha4\beta2^*$ subtype is also seen in the *bis*-quaternary ammonium series. The *N,N'-bis*-alkylnicotinium series, when compared to the *N,N'-bis*-alkylpyridinium and *N,N'-bis*-alkylpicolinium series, demonstrates a two-fold decrease in affinity in the [^{3}H]NIC binding assay for the most potent compounds. Additionally, the *N,N'-bis*-alkylisoquinolinium and *N,N'-bis*-alkylquinolinium series had low affinity for the $\alpha4\beta2^*$ subtype, indicating that increased aromaticity, i.e. 6π system to 10π system, is not necessarily an important requirement for binding.

In contrast, replacing the *bis*-nicotinium headgroups with *bis*-quinolinium and *bis*-isoquinolinium moieties afforded compounds with no affinity for the $\alpha4\beta2^*$ nAChR, but which had similar affinity to NIC and d-TBC (Ki values = 0.45 $\pm$ 0.09 μM and 4.79 $\pm$ 0.20 μM, respectively) at the $\alpha7^*$ nAChR subtype. Although no correlation between

carbon chain length and affinity was observed in either series, the C_{12} analogs in the *N,N'-bis*-alkylisoquinolinium (bIQDDB) and *N,N'-bis*-alkylquinolinium (bQDDB) series had the highest affinities, and when the *bis*-quinolinium and *bis*-isoquinolinium headgroups were replaced with simple *bis*-pyridinium moieties, only the longer chain molecules were active (C_{11} and C_{12} analogs). The presence of a 3-position methyl substituent in the pyridinium ring in the *N,N'-bis*-alkylpicolinium series appears to decrease the affinity for the α7* nAChR subtype, as is seen in the loss of α7* affinity in the *bis*-nicotinium and *bis*-picolinium series. The *bis*-quinolinium analog, bQDDB exhibited a Ki value of 1.61 μM for the α7* nAChR subtype and this compound had no affinity for the $\alpha4\beta2$* nAChR subtype. Therefore, it appears that increased aromaticity is an important structural requirements for the α7* nAChR subtype and not for the $\alpha4\beta2$* nAChR subtype. The *N,N'-bis*-alkylisoquinolinium and *N,N'-bis*-alkylquinolinium series is the first active compound in both the *mono*- and *bis*-azaaromatic series for the a7* nAChR subtype.

In initial experiments, the C_{12} analogs of the *bis*- azaaromatic series were evaluated in the NIC-evoked [^{3}H]DA overflow, because the C_{12} *N-n*-alkylnicotinium analog, NDDNI, was the most potent antagonist at the nAChR subtypes mediating DA release. In all of the *bis*-azaaromatic series, the C_{12} analogs were able to inhibit NIC-evoked [^{3}H]DA overflow at low micromolar or low nanomolar concentrations. The most potent antagonist in the series was the C_{12} analog in the *N,N'-bis*-alkylpicolinium series. Taken together with the data from the $\alpha4\beta2$* and α7* assays, this compound is highly selective as an antagonist at the nAChR subtype mediating DA release. Four to five orders of

magnitude separate the affinity for the nAChR subtypes mediating DA release with those for the $\alpha4\beta2$* and $\alpha7$* nAChR subtypes. Additionally, other analogs in the *N,N'-bis*-alkylpicolinium series of compounds were evaluated and all were found to have inhibitory activity in the NIC-evoked [^{3}H]DA overflow assay, although none were as potent as bPiDDB. The simple C_8 and C_{10} analogs *N,N'-bis*-alkylpyridinium series were also tested to determine their activity and surprisingly, none of the *N,N'-bis*-alkylpyridinium analogs had any activity at concentrations below 1 μM. This represents a 10-fold decrease in potency for the corresponding C_8 and C_{10} *N,N'-bis*-alkylpicolinium analogs and a 1000-fold decrease for the C_{12} analogs. Surprisingly, the C_{12} *N,N'-bis*-alkylnicotinium analog was not as active as bPiDDB, indicating that the bulky pyrrolidino moiety maybe hindering binding at the nAChR subtypes mediating DA release and therefore decreasing the activity. The increased aromaticity of the *N,N'-bis*-alkylisoquinolinium and *N,N'-bis*-alkylquinolinium series also led to an increase in antagonist activity at nAChR subtypes mediating NIC-evoked DA release but none of the analogs in these series of compounds approached the inhibitory activity of bPiDDB. Thus, the 3-methyl substituent on the picolinium ring is important for determining NIC-evoked [^{3}H]DA overflow at these receptor subtypes.

As stated previously, there is currently considerable debate as to the exact subunit composition of nAChR subtypes mediating NIC-evoked DA release (Klink *et al.* 2001; Azam *et al.* 2002; Champtiaux *et al.* 2002; Whiteaker *et al.* 2002; Zoli *et al.* 2002). The discovery and use of the α-conotoxins (α-ctx), particularly the α-ctx MII, has greatly increased our understanding of this receptor class. Two receptor subtypes, α-ctx MII

sensitive and α-ctx MII resistant, have been determined as the nAChR subtypes responsible for NIC-evoked DA release. Using knockout mice data coupled with the α-ctx MII data, Luetje (2004) has identified four distinct DA releasing subtypes, α-ctx MII sensitive subtypes, α6β2β3 and α6α4β2β3, where α6 and α4 form with the β2 subunit to form a functional receptor; and α-ctx MII resistant subtypes consist of α4β2 and α4α5β2 with the α4 and β2 subunits forming the agonist binding sites (Luetje 2004). Interestingly, bPiDDB only partially blocks the effects of NIC-evoked [^{3}H]DA overflow (I_{max}~50%), indicating that it is only antagonizing select subtypes that mediate DA release, similar to α-ctx MII. The observed low affinity of bPiDDB for the α4β2* nAChR subtype, in addition to the partial antagonism activity demonstrated by bPiDDB in the NIC-evoked [^{3}H]DA overflow assay, indicates that bPiDDB most likely antagonizes the α-ctx MII sensitive subtypes, α6β2β3 and α6α4β2β3 and not the ctx MII resistant subtypes, α4β2 and α4α5β2.

Binding Model of Quaternized Azaaromatic Compounds at the nAChR subtypes mediating DA release

In order to propose a binding model for these quaternary ammonium compounds, it is important to identify if these antagonists are competing for the same receptor binding site. It was determined that the C_8 *N*-*n*-alkylnicotinium salt, NONI, was a competitive antagonist in the NIC-evoked [^{3}H]DA overflow assay (Wilkins *et al.* 2002). Crooks *et al.* (1995) reported that *N*-*n*-alkylation of the pyridyl nitrogen of NIC resulted in a change in the physical properties of both the pyridyl nitrogen atom as well as the pyrrolidine nitrogen atom of the molecule. The pyridyl alkylation caused the pKa of the pyrrolidine

nitrogen to fall 2 pH units, resulting in it being mostly unprotonated at physiological pH. Therefore, a nAChR binding model was hypothesized for the nAChR subtypes mediating DA release, wherein the nAChR recognition points of the quaternized molecule were reversed from those in the protonated NIC molecule, resulting in a novel interaction of such molecules at the nAChR binding site (Crooks *et al.* 1995). In this model, the cationic binding area of the nAChR receptor recognizes the quaternary ammonium moiety of the *N*-*n*-alkylnicotinium compound, while the hydrogen-bonding site accommodates the unprotonated pyrrolidine nitrogen (lone pair) (Figure 3.5).

Figure 3.5 Illustration of the different modes of interaction of protonated NIC and NDDNI at the nAChR

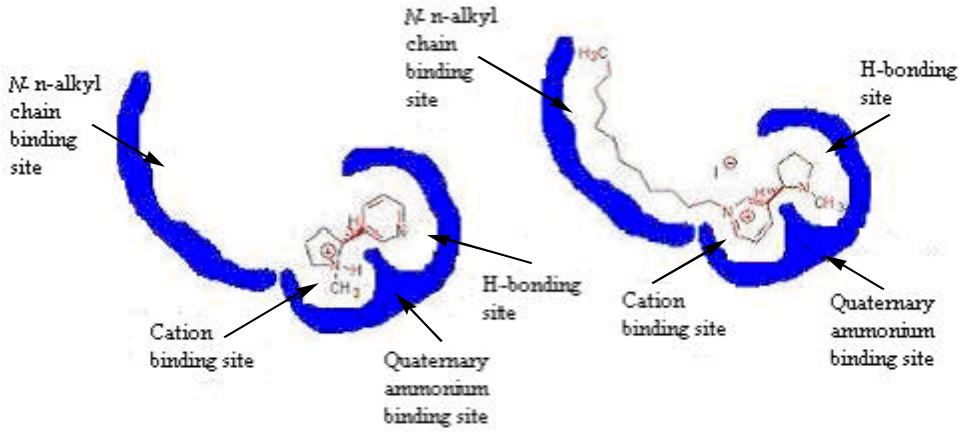

Many compounds belonging to the *mono*- and *bis*-azaaromatic series were active in the NIC-evoked [^{3}H]DA release assay. Therefore, a flexible model should be examined for the nAChR subtypes mediating DA release. Because of the fact that the quaternized pyridinium moiety is a constant structural feature in many compounds of the *mono*-azaaromatic series, there must still be a cationic binding site that interacts with these types of molecules. This interaction is not sufficient to inhibit release, as evidenced by

the lack inhibition exhibited by the smaller chain *N*-*n*-alkyl analogs; therefore, the carbon chain length is also an important structural feature. The length of the carbon chain in active molecules is found to be variable, depending on the substituent in the three position of the pyridyl moiety. It is hypothesized that the *N*-*n*-alkylnicotinium molecules fit into the receptor binding site at a unique angle, which allows the pyrrolidino moiety to interact with a nearby H-bonding site, and an *n*-alkyl moiety with critical carbon chain length is necessary to complete the strong interaction of the molecule with the DA-releasing nAChR at the *N*-*n*-alkyl binding site. The *n*-alkyl chain would likely interact with residues adjacent to the binding site itself that are of a hydrophobic nature. This hydrophobic interaction may also explain the observed decrease in activity seen with C_{10} *N*-*n*-alkylnicotinium salt, NDNI. In this case, the ten-carbon alkyl chain may not fit the binding area due to a negative interaction of the chain with the receptor protein, leading to a decrease in affinity. The C_{12} *n*-alkyl analog was a potent antagonist in the NIC-evoked DA release assay. This may be due to an interaction that overcomes the disruption that NDNI encounters. The longer alkyl chain may be able to bend to a conformation that minimizes the interaction or that moves around the amino acid causing the issue.

The recognition site also allows the *N*-*n*-alkylpyridinium and *N*-*n*-alkylpicolinium molecules to interact with the binding site. However, the *N*-*n*-alkylpyridinium and *N*-*n*-alkylpicolinium molecules still have a decreased affinity when compared to the *N*-*n*-alkylnicotinium series. This points to the importance of the absence of the pyrrolidine ring, decreasing the strength of the interaction with the binding site. Without the

pyrrolidine ring, these series of compounds may lack the ability to seat into the cationic binding site as strongly as the *N*-*n*-alkylnicotinium molecules. Therefore, they require longer chain lengths to create a more favorable ionic interaction at the cationic site while maintaining the ability to interact at the *N*-*n*-alkyl binding site. However, the effect of the increase in carbon chain length does not fully compensate for the loss of the pyrrolidine ring, as the *N*-*n*-alkylpyridinium and *N*-*n*-alkylpicolinium series demonstrated at least 10 fold decreased affinities (0.12 and 0.03 µM, respectively) when compared to the *N*-*n*-alkylnicotinium series (0.009 µM). Taken overall, these data underline the importance of the *N*-*n*-alkyl binding site, the H-binding site, and the cationic binding site in the binding of this series of compounds.

The activity of compounds in the *bis*-azaaromatic series provides additional information on the interaction of these quaternary ammonium compounds with nAChR subtypes mediating DA release. Due to the presence of the second quaternized headgroup, the carbon chain length and the quaternary ammonium center are not the only factors in determining interaction between the molecule and the receptor. The inclusion of a second quaternary ammonium headgroup increases antagonist activity at the nAChR subtypes mediating DA release for the *N*,*N'*-*bis*-alkylpicolinium series. This increased activity is likely due to interaction of these molecules with a second quaternary ammonium binding area remote from the first quaternary ammonium binding site. Due to the poor activity of the C_{12} *N*,*N'*-*bis*-alkylnicotinium analog in the DA release assay, the second quaternary ammonium binding site may be different than the first quaternary ammonium binding site. It is possible that site has a smaller area that cannot

accommodate the entire nicotine molecule, but a smaller 3-position substituent may be fit into the second binding site (Figure 3.6C).

Figure 3.6 Potential binding pocket of the α6β2β3 nAChR subtype with NDDPiI, NDDNI, bPiDDB, and bNDDB

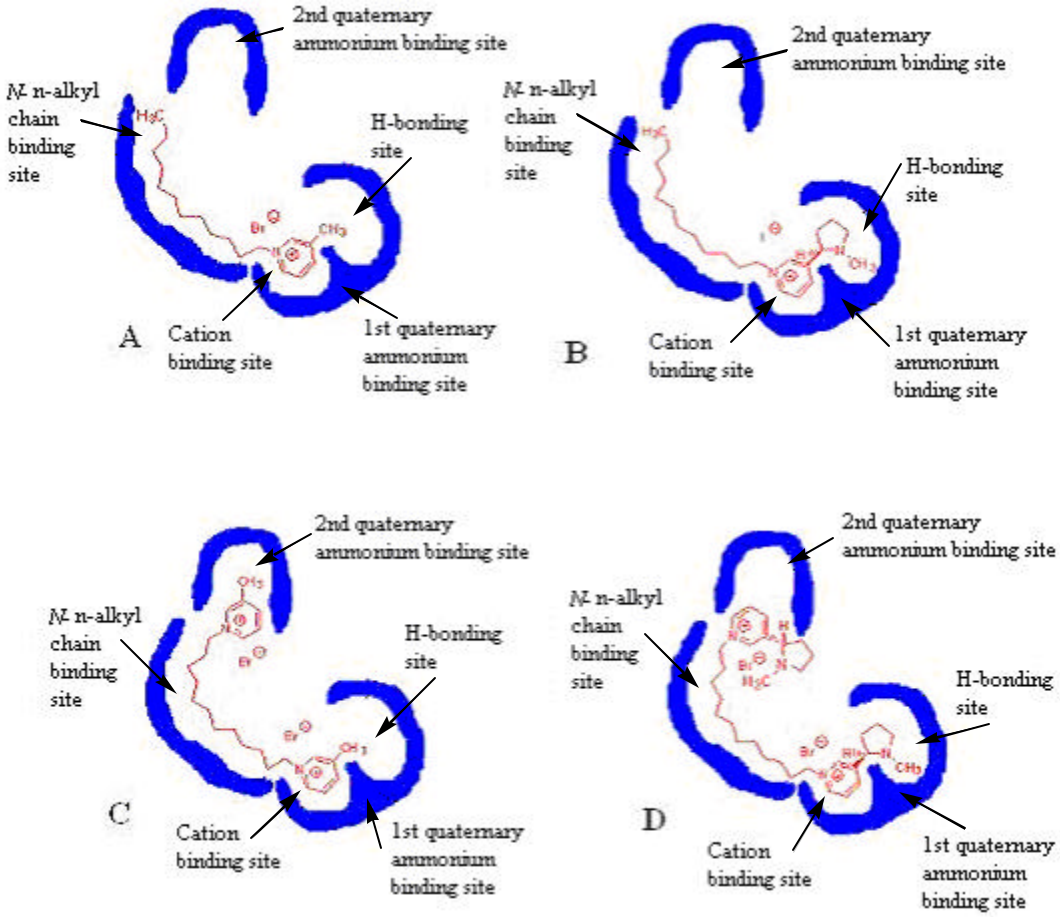

Even though the exact sub-unit composition is not known, the heterologously assembled DA-releasing nAChR subtype binding sites utilize an α-β interface (Kuo *et al.* 2005). The main binding pocket of the mostly resides in the α subunit of the receptor site (Karlin 2002; Unwin 2005). Recently, it was determined that the ß subunits may play a dominant role in receptor inactivation (Fenster *et al.* 1997; Gentry *et al.* 2003). Therefore, the β-subunit must be integral to the strong inhibitory activity of this series of compounds at the nAChR subtypes mediating DA release. If the second binding pocket, as well as, some of the hydrophobic residues that interact with the carbon chain of quaternized molecule, resides on the β-subunit interface, the interaction of the molecule

could prevent a conformational shift of the binding pocket and not allow the ionic pore to open, inactivating the receptor.

3.4. Conclusions

Several interesting *mono*- and *bis*-azaaromatic quaternary ammonium compounds have emerged from this structure-activity study. bPiDDB was found to be a potent and selective antagonist at the nAChRs mediating DA release, indicating it to be a possible $\alpha6\beta2\beta3$ or $\alpha6\alpha4\beta2\beta3$ nAChR subtype antagonist. The C_{10} *mono*- and *bis*-nicotinium analogs, NDNI and bNDI, both had good antagonist activity and selectivity for $\alpha4\beta2$* nAChR subtypes. Additionally, bQDDB and bIQDDB have been shown to be the first members of these series of quaternary ammonium molecules that have affinity for $\alpha7$* nAChR subtypes. The selectivity of these series of compounds for nAChR subtypes demonstrates that these agents may be useful for both basic and clinical research aimed at determining the pharmacological role of nAChR subtypes and their potential use as therapeutic agents.

Chapter 4: Molecular Modeling of *mono*- and *bis*-Quaternary Ammonium Salts at $\alpha 4\beta 2^*$ Receptor Subtypes

4.1. Introduction

Over the past decade, the nAChR has become a target for drug development. The most prevalent nAChR subtype in the mammalian brain is the heterologously expressed $\alpha 4\beta 2^*$ receptor subtype, which is the primary high affinity [^{3}H]nicotine binding site. Ligands that specifically interact with this nAChR subtype are of interest in a number of pathologies, including tobacco dependence and drug addiction, Alzheimer's disease, Parkinson's disease, Tourette's syndrome, schizophrenia, and pain (Lindstrom 1997; Dwoskin *et al.* 2000; Lloyd and Williams 2000; Dwoskin and Crooks 2001; Dani *et al.* 2004; Hogg and Bertrand 2004). NIC and other nAChR agonists (e.g., epibatidine) are not selective for $\alpha 4\beta 2^*$ receptor subtypes, and produce significant side effects, making these compounds less attractive as drug candidates. Consequently, previous studies have generated quantitative structure-activity relationships (QSAR) in an attempt to understand the interactions of these agonists with their recognition sites on nAChRs (Barlow and McLeod 1969; Barlow and Johnson 1989; Dukat *et al.* 1996; Nielsen *et al.* 2000; Nicolotti *et al.* 2001).

To date, several of these QSAR studies have utilized linear regression analysis of ligand-receptor binding or function, in order to elucidate the nature of the ligand interactions within several nAChR receptor subtypes (Barlow and McLeod 1969; Dukat *et al.* 1996; Nielsen *et al.* 2000). Of note, QSAR studies have been used to investigate ligand interactions at the $\alpha 4\beta 2^*$ nAChR subtype (Dukat *et al.* 1996; Tonder and Olesen 2001;

Tonder *et al.* 2001). Though generalities for the ligand interactions were drawn from the SARs generated, insufficient model validation limited the ability of the previously used models to recognize the training set of compounds. As such, generation of a nAChR pharmacophore has proven difficult. In this respect the earlier pharmacophore model generated by Sheridan *et al.* (1986), despite being based on crude pharmacological data, still constitutes an approach worthy of further exploration (Sheridan *et al.* 1986; Schmitt 2000; Glennon *et al.* 2004).

Another model surmises that a water molecule may mediate binding of a ligand to the receptor, perhaps through an interaction with the protonated nitrogen atom of the ligand or the hydrogen bonding acceptor moiety in the ligand molecule (Glennon *et al.* 2004). The crystallization of an acetylcholine binding protein (AChBP) from snail glia has also provided insight into the binding domain of the nAChR. Brejc *et al.* (2001) have determined that the loop C (Changeux's nomenclature) of the acetylcholine binding site was crystallographically less well resolved than the rest of the binding site (Brejc *et al.* 2001), leading to the possibility that part of the binding site may take on different conformations, depending on ligand shape and size. This represents a plausible challenge to the notion of a static pharmacophore. Due to the complexity of the nAChR molecular recognition process and the difficulty in obtaining high-resolution (e.g. microscopic kinetics) data for specific receptor subtypes, unambiguous models defining specific nAChR subtype pharmacophores do not yet exist.

It has been established previously that QSAR descriptor data has non-linear characteristics (Zupan and Gasteiger 1993; Rogers and Hopfinger 1994; Kohonen 2001). Therefore, alternative approaches such as self-organizing maps (SOMs) and the genetic functional approximation (GFA) algorithm have been utilized to generate QSAR for several biological systems (Gokhale and Kulkarni 2000; So *et al.* 2000; Yuan and Parrill 2002; Schneider and Nettekoven 2003; von Korff and Steger 2004), and may be better suited for analysis of ligand interactions with $\alpha4\beta2^*$ nAChRs. Regression analysis typically employed in QSAR, such as Partial Least Squares (PLS) or Multiple Least Squares (MLS) are limited to relating linear descriptor trends to a given activity or property. Considering the complexity in the modeling of the *mono*- and *bis*-quaternary ammonium salt interactions with nAChRs described in this study, we elected to use SOMs and GFAs in the QSAR analysis described below as one valid modeling approach.

4.2. Experimental

4.2.1. Biological Data

Biological data were obtained from the [^{3}H]NIC binding assay using rat striatal membranes, a well established assay reported to identify the $\alpha4\beta2^*$ subtype (Xu *et al.* 2001; Ayers *et al.* 2002; Grinevich *et al.* 2003; Wilkins *et al.* 2003). The data set consisted of ninety-three *mono*- and *bis*-substituted quaternary ammonium compounds together with other related compounds developed in the Crooks laboratory, many of which are described in earlier section of this dissertation. The chemical structures are presented in Figure 1. Activities (e.g. $\alpha4\beta2^*$ receptor affinities) are expressed as experimentally determined Ki values as explained in Chapter three.

4.2.2. Descriptor Generation

Descriptors were generated using the chemical modeling program Cerius2 (Accelrys, Inc. San Diego CA) and QSARIS (MDL Information Systems Inc., San Liandro CA). Descriptors were divided into one of several physical property categories: conformational, electronic, information, molecular shape analysis (MSA), quantum mechanical, receptor, spatial, structural, thermodynamic, and topological. The descriptors were used for the generation of both the SOMs and GFAs.

4.2.3. Self-Organizing Maps with Descriptor Selection

In order to relate bioactivity and molecular features, a set of computational models were developed using a custom-built stepwise descriptor selection algorithm coupled to a supervised SOM (Bayram *et al.* 2004). The algorithm was developed using Matlab 6.1 with the SOM Toolbox 2.0 (http://www.cis.hut.fi/projects/somtoolbox/). Table 4.1 contains a description of the descriptors employed in the various models.

Table 4.1 Descriptors utilized in the generation of SOM and GFA models

Descriptors	Description
Area	Molecular area
CIC	Complementary informational content
E-DIST-mag	Entropy of the matrix
Fh2o	Desolvation free energy for water
Foct	Desolvation free energy for octanol
IC	Informational content
Jurs-FNSA-3	Fractional negatively charged partial surface areas
Jurs-PNSA-1	Partial negative surface area
Jurs-RASA	Relative hydrophobic surface area
Jurs-RPCS	Relative positive charge surface area
Jurs-WNSA-2	Surface weighted, partial negative charge
Jurs-WNSA-3	Partial weighting of the surface accessible portions of the molecule
Jurs-WPSA-1	Surface-weighted charged partial surface areas
LogP	Octanol/water partition coefficient
Log Z	Logarithm of the Hosoya index
MW	Molecular weight
PHI	Kier flexibility index
S_aaCH	Energy states of aromatic CH bonds
S_aasC	Energy states of the C bonds
S_dCH2	Energy states of all CH_2 groups
S_dO	Energy states of all carbonyl moieties
S_sCH3	Energy states of all CH_3
S_ssCH2	Energy states of the CH_2 bonds
S_sssNH	Energy states of all NH bonds
S_tCH	Energy states of total CH bonds
SC-3_P	Molecular connectivity index of longer chain lengths
SIC	Structural informational content
Vm	Molecular volume

Datasets

Three data sets were created: (1) both *mono*- and *bis*-salts (92 molecules; the 'ALL' data set); (2) *mono*-quaternary ammonium salts (69 molecules; the 'MONO' data set); and (3) *bis*-quaternary ammonium salts (23 molecules; the 'BIS' data set). A binning scheme was created to convert the numerical bioactivity into categorical data since our implementation of SOMs works on categorical data. The scheme assigned roughly the same number of molecules to each of three bins.

Figure 4.1 *N*-Alkyl quaternary ammonium salts and their affinities (Ki) at α4β2* nAChRs used in SOM and GFA studies

***N*-Alkylpyridinium Salts**

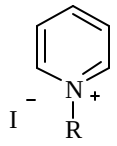

			Ki
53a	NMPI	R= Methyl	20
53b	NEPI	R= Ethyl	28
53c	NPrPI	R= Propyl	42
53d	NBuPI	R= Butyl	9.7
53e	NPePI	R= Pentyl	8.7
53f	NHxPI	R= Hexyl	9.1
53g	NHpPI	R= Heptyl	15
53h	NOPI	R= Octyl	20
53i	NNPI	R= Nonyl	19
53j	NDPI	R= Decyl	17
53k	NUPI	R= Undecyl	17
53l	NDDPI	R= Dodecyl	120
53m	NPeDPI	R= Pentadecyl	49.7
53n	NEcPI	R= Eicosonyl	>100

			Ki
62a	NAPB	R= Allyl	56.0
62b	JTO	R= *trans*-Oct-2-enyl	13.1
62c	JCO	R= *cis*-Oct-2-enyl	19.0
62d	LO	R= Oct-2-ynyl	17.4
62e	MO	R= Oct-7-enyl	11.1
62f	LN	R= Non-2-ynyl	28.9
62g	JTN	R= *trans*-Non-2-enyl	25.4
62h	JCN	R= *cis*-Non-2-enyl	23.8
62i	LD	R= Dec-2-ynyl	9.52
62j	MU	R= Undec-10-enyl	12.3
62k	NU	R= Undec-10-ynyl	8.57

***N*-Alkylpicolinium Salts**

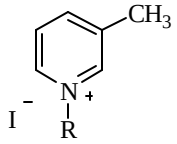

			Ki
54a	NOPiI	R= Octyl	>100
54e	NDDPiI	R= Dodecyl	>100

***N*-Alkylnicotinamide Salts**

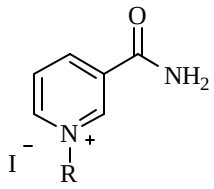

			Ki
55a	NONAI	R= Octyl	>100
55b	NNNAI	R= Nonyl	>100
55c	NDNAI	R= Decyl	>100
55d	NUNAI	R= Undecyl	>100

_N_-Alkylnicotinium Salts

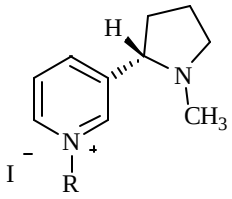

			Ki
56a	NMNI	R= Methyl	3.5
56b	NENI	R= Ethyl	1.0
56c	NPNI	R= Propyl	22
56d	NnBNI	R= Butyl	10.9
56f	NHxNI	R= Hexyl	0.53
56g	NHpNI	R= Heptyl	2.1
56h	NONI	R= Octyl	20
56i	NNNI	R= Nonyl	0.84
56j	NDNI	R= Decyl	0.093
56l	NDDNI	R= Dodecyl	0.14

			Ki
63a	NONB-7M	R= 7-Methyloctyl	0.44
63b	NCyNB-4	R= Octyl-cyclobutyl	4.56
63c	NCyNB-5	R= Octyl-cyclopentyl	5.54
63d	NCyNB-6	R= Octyl-cyclohexyl	7.20
63e	NBzNB	R= Benzyl	2.67
63f	NANI	R= Allyl	2.1
63g	NONB-3c	R= *cis*-Oct-3-enyl	0.075
63h	NONB-3t	R= *trans*-Oct-3-enyl	3.97
63i	NONB-7e	R= Oct-7-enyl	0.45
63j	NONB-3y	R= Oct-3-ynyl	0.20
63k	NONB-6e7M	R= 7-Methyl-oct-6-enyl	0.45
63l	NDNB-4c	R= *cis*-Dec-4-enyl	7.39
63m	NDNB-4t	R= *trans*-Dec-4-enyl	0.32
63n	NDNB-9e	R= Dec-9-enyl	0.049
63o	NDNB-3y	R= Dec-3-ynyl	0.49
63p	NUNB-10e	R= Undec-10-enyl	0.54

Conformationally Restricted _N_-Alkylnicotinium Salts

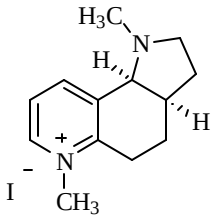

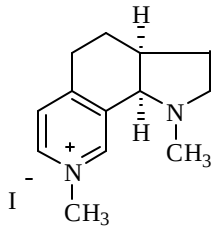

			Ki
25a	BCO	R= Octyl	>100
25b	BCN	R= Nonyl	>100
25c	BCD	R= Decyl	>100
25d	BCUD	R= Undecyl	>100
25e	BCDD	R= Dodecyl	>100

			Ki
26a	ACO	R= Octyl	>100
26b	ACN	R= Nonyl	>100
26c	ACD	R= Decyl	>100
26d	ACUD	R= Undecyl	>100
26e	ACDD	R= Dodecyl	>100

bis-Quaternary Ammonium Salts

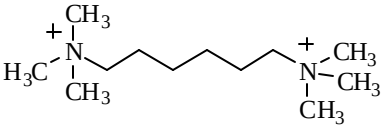

45 HEX Ki = 31.9

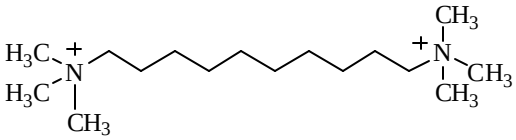

63 DEC Ki = 4.27

bis-N,N'-Alkylpyridinium Salts

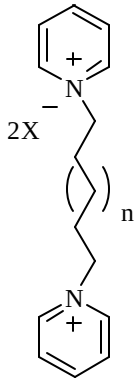

			Ki
56a	bPPeI	n = 1; X = I	>100
56c	bPOI	n = 4; X = I	33.9
56d	bPNB	n = 5; X = Br	24.1
56e	bPDI	n = 6; X = I	18.6
56f	bPUB	n = 7; X = Br	14.4
56g	bPDDB	n = 8; X = Br	9.14

bis-N,N'-Alkylpicolinium Salts

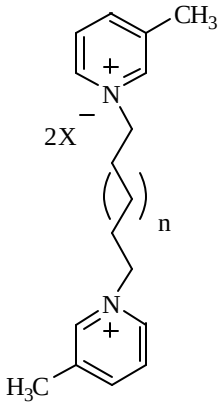

			Ki
57b	bPiOI	n = 4; X = I	>100
57c	bPiNB	n = 5; X = Br	66.7
57d	bPiDI	n = 6; X = I	>100
57e	bPiUB	n = 7; X = Br	82.0
57f	bPiDDB	n = 8; X = Br	33.0

bis-N,N'-Alkylquinolinium Salts

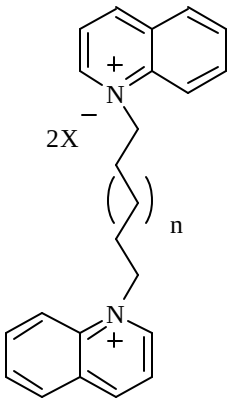

			Ki
58b	bQOI	n = 4; X = I	>100
58c	bQNB	n = 5; X = Br	20.1
58d	bQDI	n = 6; X = I	>100
58e	bQUB	n = 7; X = Br	38.3
58f	bQDDB	n = 8; X = Br	>100

bis-N,N'-Alkylnicotinium Salts

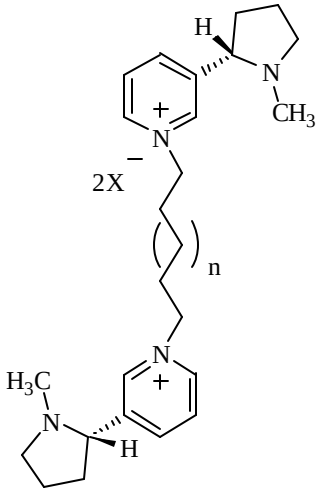

			Ki
60b	bNOI	n = 4; X = I	1.50
60c	bNNB	n = 5; X = Br	4.31
60d	bNDI	n = 6; X = I	0.28
60e	bNUB	n = 7; X = Br	0.37
60f	bNDDB	n = 8; X = Br	1.43

In using the supervised SOM learning algorithm provided in the toolbox, this binning scheme allowed for a more accurate clustering of the data sets and for extracting the underlying commonalities of the molecules.

Bin 1: $0 < x = 5$

Bin 2: $5 < x = 50$

Bin 3: $50 < x = 100$

The data set being modeled was partitioned into a set of test molecules (20%) and training molecules (80%). Membership in the test or training set was random, with the one requirement that the proportion of molecular population in each bin be identical in both test and training sets. The descriptor blocks for each data set were normalized to unit variance and mapped to a logistic function. Descriptors with zero variance were removed, as were pairs with linear correlation above 0.90, retaining the most representative of the pair.

The SOM-Stepwise Feature Reduction Algorithm

Finally, a SOM-oriented variation of a forward entry stepwise regression algorithm was employed, to select a small number of independent variables from which the SOM model was constructed. The algorithm used is identical to the forward entry stepwise method with the following variations:

(1) the entry statistic was defined to be the percent of training set molecules correctly classified by the model, any increase of which resulted in the inclusion of the descriptors being tested;

(2) the entry statistic was calculated by constructing a SOM using a supervised learning algorithm; and,

(3) descriptors to be entered into the model were chosen in pairs, one from each of two randomized lists of the full set of descriptors.

Algorithm training was conducted iteratively until some convergence criteria were met.

Experimental Design

For each of the three data sets, ten independent runs were conducted, each with distinct training set/test set samplings. At the end of each training process, the test set molecules were predicted with the trained SOM model, providing the benchmark statistic, e.g., 'percentage correctly classified'. Averaging these statistics over the ten runs produced an estimate of the algorithm's success in both learning the training data and generalizing to the test data. Conducting multiple runs to some extent minimizes sampling bias, as well as bias arising from the stochastic SOM initialization process. The best model for each of the three data sets was further examined using custom visualization tools, as shown in the Figures 4.2-4.4.

4.2.4. Genetic Functional Activity Algorithms

Genetic functional algorithms (GFAs) as described by Rogers and Hopfinger (Rogers and Hopfinger 1994) were implemented using Cerius^2 (version 4.6) software (Accelrys Inc., San Diego, CA). GFAs were conducted using static 100 member populations; linear, quadratic, and offset quadratic basis functions; the mutation probability for both additions

and deletions was set at 0.2%. Lack of fit criterion was set at 1.0 and initial equation length was set to three. Models were evolved over 50,000-80,000 generations using standard convergence criterion.

4.3. Results and Discussion

Self-Organizing Maps

U-matrix maps represent the descriptor-based relationships of the training set of molecules by the SOM, and are constructed by projecting all selected descriptor's contributions to the mapping.

D-matrix maps indicate the classification mapping of the SOM, as learned from the corresponding training sets. All three maps illustrate strong clustering.

The color level, in all the maps seen below (see Figures 4.2-4.4) describes the relative clustering in the data; the darker areas indicate small distances, while the lighter areas indicate larger distances. The colored hexagons indicate the points on the map corresponding to training molecules, and are colored by the affinity classification and labeled with the corresponding training molecule names.

SOM models of the ALL data set

The ten models learned the training set with high classification accuracy (93% $\pm$ 0.02) and were able to correctly classify the test compounds with a percent accuracy of 68% $\pm$ 0.08. The average number of descriptors chosen *via* the stepwise SOM was 11, which

were selected from a total number of 47 descriptors. False negative values, where the model placed the compound two bins removed from its actual value, were low, accounting for less than 2% of the failures generated by the model. There were no false positives reported for any of the models. Figure 4.2 is a graphical representation of the best model of the ten models generated from the ALL data set. The descriptors selected by the best model were, S_dO, S_aaCH, IC, S_sCH3, S_sssNH, S_tCH, and PHI.

Figure 4.2 (A) D-matrix generated from the ALL data set, red numbers indicate the classification mapping of each node; (B) U-matrix SOM generated from the ALL data set. Key: red- class 1, green- class 2, blue- class 3. Inter-node distances are shown in grey-scale coloring, the closer the distance the darker the shading.

A)

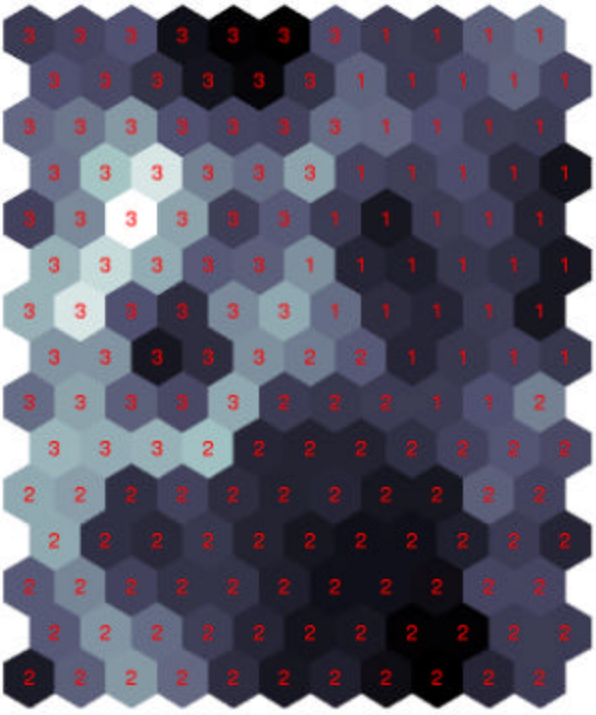

B)

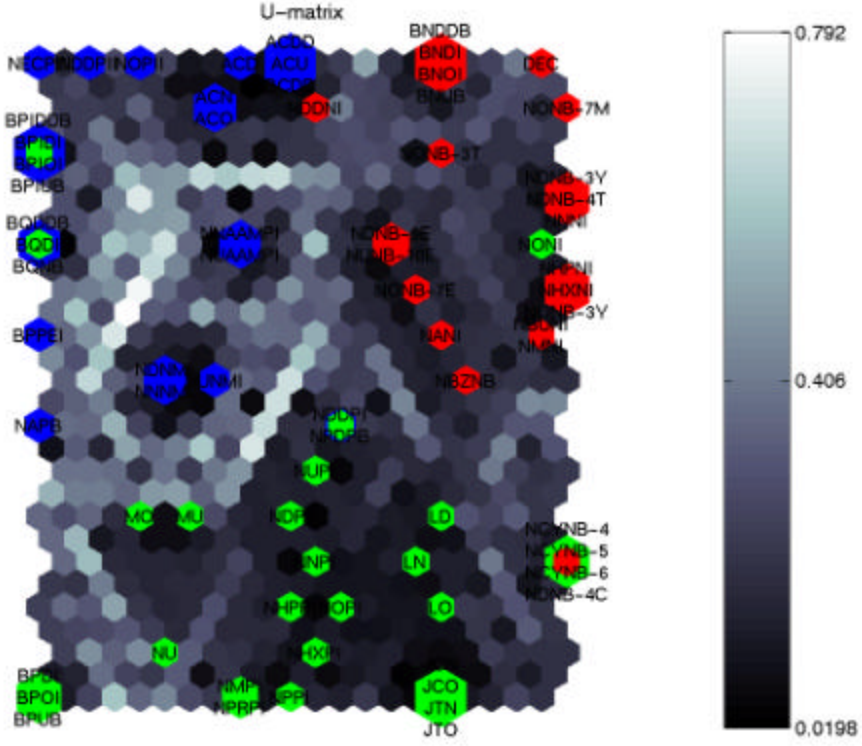

The D-matrix (Figure 4.2A) shows that there are three general clusters for the full complement of compounds in the ALL data set. The descriptor, IC (informational content), is an information-theoretic topological index and may be identifying steric qualities of the molecules. The descriptors utilized, S_dO, S_aaCH, IC, S_sCH3, S_sssNH, S_tCH, and PHI, by the model mostly correspond to the electrotopological (E-Top) indices. S_dO describes the sum of the energies of carbonyl moieties in the set from the *N*-*n*-alkylnicotinamide series. As the carbonyl-containing compounds of this family are inactive, S_dO may be acting largely as a binary classifier. Additionally, the best model used descriptors for the energy states of all CH_3, aromatic CH, total CH, and NH bonds, e.g. S_sCH_3, S_aaCH, S_tCH, and S_sssNH, respectively. These descriptors may differentiate the C3-functionality of the pyridine ring; the S_dO and S_sssNH descriptors together likely map the SAR relative to the inclusion of the amide functionality at the C3-position of the pyridine ring, leading to a decrease in affinity. Another descriptor that may demonstrate the importance of the C3-position functionality is the Kier flexibility index, PHI. The compounds in the *N*-*n*-alkylpicolinium series, which contain a methyl group at the C3-position of the pyridine ring, were also inactive and grouped with the *N*-*n*-alkylnicotinamide salts. The active *N*-*n*-alkylnicotinium salts, with a 2-N-methylpyrrolidino functionality at the C3-position of the pyridine ring, however, were separated from the inactive compounds. The rigidity of the methyl and amide functionalities when compared to the more flexible pyrrolidine ring may also be key to the observed affinity of these compounds at the a4ß2* nAChR.

The U-matrix (Figure 4.2B) reflects chemically intuitive trends; the longer saturated *N*-*n*-alkylnicotinium salts were clustered together. Additionally, the unsaturated *N*-*n*-alkylnicotinium compounds, NONB-3y, NDNB-4t, and NDNB-3y, were similar in bioactivity and clustered near the saturated *N*-*n*-alkylnicotinium compound NNNI. However, NONI, the less active eight-carbon analog, was clustered among the active compounds, pointing to a limitation in the SOM or the descriptors. Shorter carbon chain *N*-*n*-alkylnicotinium compounds and *N*-*n*-alkylpyridinium compounds were likewise clustered together. Interestingly, rotationally restricted analogs were not found in the freely rotating *N*-*n*-alkylnicotinium compound cluster. This reflects a bias toward their different affinities, as the model does not recognize the two classes as structurally similar, but actually classifies the restricted rotation analogs as being structurally similar to the longer chain *N*-*n*-alkylpyridinium analogs (NEcPB and NDDPI).

A strong distinction is observed between the different structural classes of *bis*-substituted quaternary ammonium compounds. The active *bis*-quaternary ammonium salts are closely associated with the *N*-*n*-alkylnicotinium compounds, as well as the classical muscle nAChR antagonist, decamethonium bromide (DEC). The *bis*-quaternary ammonium compounds were clustered nearer to the mono-substituted *N*-*n*-alkylpyridinium salts. This clustering may indicate that the *bis*-quaternary ammonium compounds bind to the receptor in similar fashion as the *N*-*n*-alkylnicotinium compounds.

SOM models of the MONO data set

The ten models learned the training set with high accuracy (95% ± 0.03) and were able to predict test compound affinities with 72% ± 0.10 accuracy. The average number of descriptors chosen *via* the stepwise SOM regression method was 7.8 descriptors, selected from a total number of 42. A 7.2 percentile of the missed assignments by the model were false positives. False negatives accounted for less than 1% of the failures generated by the model. Figure 4.3 is a graphical demonstration of the best model generated from the mono-substituted series of compounds. From the model generated, the descriptors used to create the model were S_aaCH, Jurs-RASA, Jurs-PNSA-1, Foct, S_dCH2, Fh2o, and LogP.

Figure 4.3 (A) D-matrix generated from the MONO data set; (B) the U-matrix representation.

A)

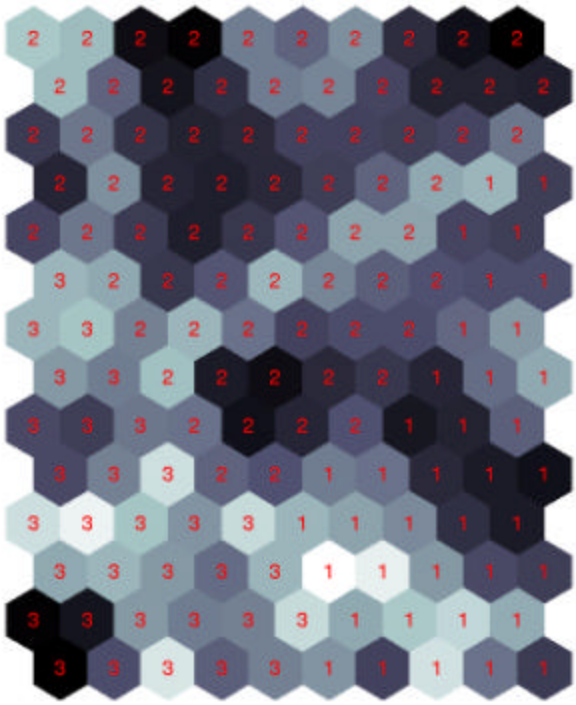

B)

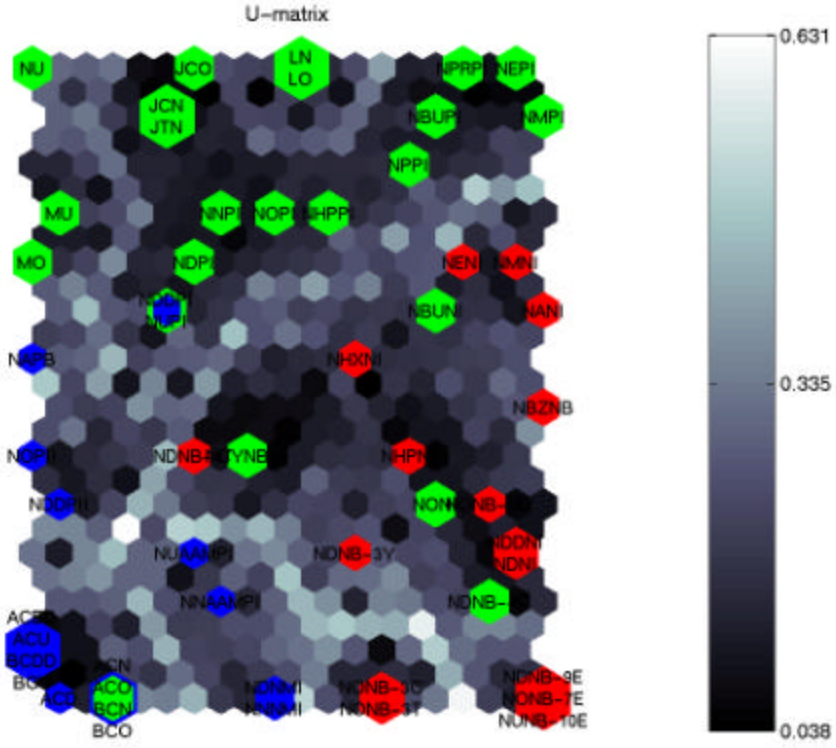

The *mono*-substituted quaternary ammonium salt model based on the MONO data set also demonstrated three distinct areas of clustering (Figure 4.3A) and used different descriptors, S_aaCH, Jurs-RASA, Jurs-PNSA-1, Foct, S_dCH2, Fh2o, and LogP, than those used in the ALL compound set, with only one similar descriptor, e.g. S_aaCH. The model did use a similar descriptor, S_dCH2, to describe the importance of the energy states of all of the CH_2 groups in the molecule. One of the new descriptors, Jurs-PNSA-1 describes the partial negative surface area (e.g. the sum of the solvent-accessible surface areas of all negatively charged atoms). Also included in the model is the related Jurs-RASA descriptor, which indicates the relative hydrophobic surface area, defined as the total hydrophobic surface area divided by the total molecular solvent-accessible surface area. The hydrophobic character of compounds in this series appears to be a major determining factor for their affinity, and is supported by the three additional related descriptors, e.g. Foct, Fh2o, and LogP. These descriptors are thermodynamic descriptors that estimate the desolvation free energy for octanol, water, and the octanol/water partition coefficient, respectively.

The long chain *N*-*n*-alkylnicotinium salts and the unsaturated *N*-*n*-alkenylnicotinium salts were clustered together in the SOM model (Figure 4.3B). These compounds share similar structures and similar a4ß2* nAChR affinities. The unsaturated and saturated *N*-alkylpyridinium salts were grouped together with the shorter chained *N*-*n*-alkylnicotinium compounds, which indicates, according to the descriptors chosen, that both the *N*-alkyl chain and the pyridine C3-position substituent are important for determining a4ß2* nAChR affinity. The longer chain *N*-*n*-alkylnicotinium salts

exhibited the highest affinities, which correlate with a larger number of lipophilic group (e.g. CH_2 groups in the alkyl chains and in the *N*-methylpyrrolidine ring), whereas the longer chain *N*-*n*-alkylpyridinium salts and the shorter chain *N*-*n*-alkylnicotinium salts have fewer numbers of CH_2 groups and therefore, lower affinities for the a4ß2* nAChR receptor.

The third cluster contains two interesting compound families: *N*-*n*-alkylnicotinamide salts, which were inactive in the [^{3}H]NIC binding assay, and the conformationally restricted *N*-*n*-alkylnicotinium analogs, which were also inactive. The *N*-*n*-alkylnicotinamide salts possess a hydrophilic moiety at the 3-position of the pyridinium ring. Similar to many nAChR ligands, affinity at the $\alpha4\beta2$* nAChR subtype is positively influenced by a hydrophobic interaction, whereas a hydrophilic moiety at the 3-position of the pyridinium ring serves to decrease affinity. The low-affinity, conformationally-restricted *N*-*n*-alkylnicotinium analogs have a high degree of hydrophobicity, and the model was able to differentiate them from other nicotinium molecules. Although it is unclear exactly which descriptor or descriptors may map this phenomenon, it is clear that the SOMs can differentiate in a manner that takes into account both distributed (hydropathy) and localized (functional groups) determinants of the observed SAR.

SOM models of the BIS data set

The ten models learned the training set with high accuracy (98% ± 0.03) and predicted the test compounds with a percentage accuracy of 58% ± 0.15. The average number of descriptors chosen *via* the stepwise SOM was 4.8 selected from a total number of 30

descriptors. False positive and negative values were not observed in this model. Figure 4.4 is a graphical representation of the best model generated from the *bis*-substituted series of compounds. From the model generated, the descriptors used to create the model were S_ssCH2, CIC, S_aasC, Jurs-RPCS, and Jurs-WNSA-3.

Figure 4.4 (A) D-matrix generated from the BIS dataset; (B) the U-matrix representation.

A)

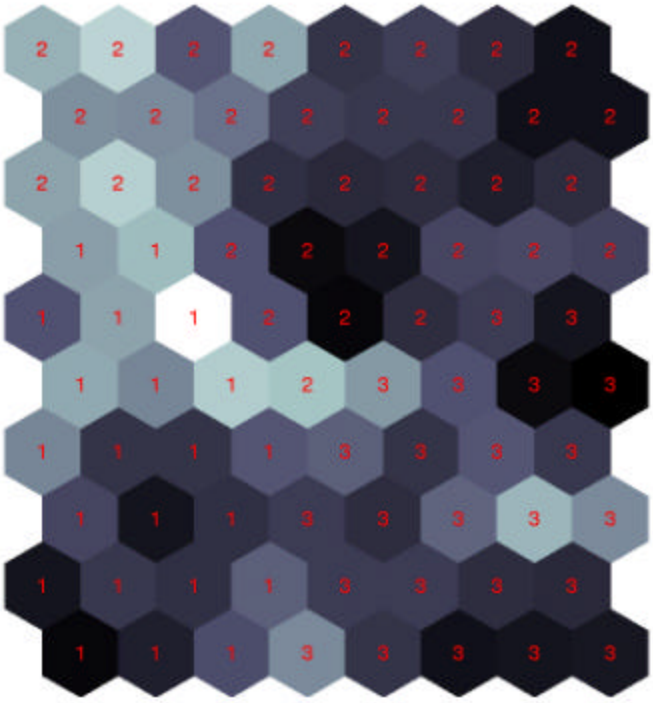

B)

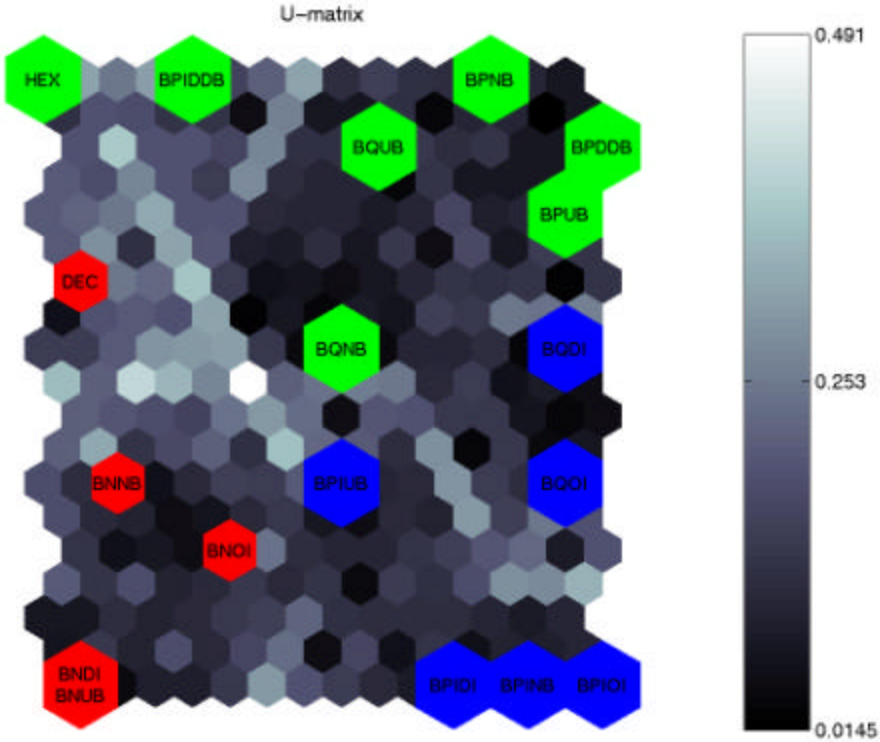

The model developed for the *bis*-quaternary ammonium salts based on the BIS data set also shows three distinct clustering areas (Figure 4.4A and 4.4B). This model contains the descriptors S_ssCH2 (energy states of the CH_2 bonds) and S_aasC (energy states of the C bonds), again stressing the importance of the lipophilic nature of these compounds. The model also contained the descriptor, CIC (complementary informational content), which is an information-theoretic topological index similar to IC and may be identifying steric interactions of the molecules. The *bis*-quaternary ammonium salt model utilized the Jurs spatial descriptors to generate the model. However, unlike the *mono*-*N*-*n*-alkylated quaternary ammonium salt model, which uses a hydrophobic interaction descriptor, the *bis*-quaternary ammonium salt SOM used a positive charge surface area descriptor, Jurs-RPCS. This descriptor represents the most positively charged atom and its relative accessible surface area. Since these *bis*-molecules possess two positive charges, the selected descriptors may indicate an increased importance of charge distribution within the series. The model also uses the Jurs-WNSA-3 descriptor, which is similar to the Jurs-PNSA-1 descriptor used in the *mono*-*N*-*n*-alkylated quaternary ammonium salt model, except that it represents only a partial weighting of the surface accessible portions of the molecule. The highest affinity members of this data set, the *bis*-quaternary ammonium salts, were clustered together. DEC was also clustered in the high affinity bin, whereas the classical ganglionic nAChR antagonist, hexamethonium bromide (HEX), was clustered with the lower affinity compounds, *viz*. the *bis*-quinolinium and the *bis*-pyridinium salts. Additionally, the *bis*-picolinium compounds were grouped with two of the *bis*-quinolinium salts in the weakest affinity set. Therefore, the presence of the 2-*N*-methylpyrrolidine ring of the *bis*-nicotinium salts plays an

important role in determining the affinities of this series of compounds for the a4ß2* nAChR receptor. It was demonstrated that a pKa shift occurs in the pyrrolidino nitrogen when the pyridino functionality in the NIC molecule is quaternized (Crooks *et al.* 1995). Therefore, the importance of the 2-*N*-methylpyrrolidine may be due to increased lipophilicity and/or to the possibility that the less basic nitrogen may act as a hydrogen bond acceptor.

Genetic Functional Activity Algorithms

Genetic Functional Algorithm Models

N-Alkylpyridinium and *N*-Alkyl-3-substituted pyridinium salts

The resulting equation was derived using the GFA methods:

$$K_i = 161.582 + 0.004244\ (\text{Area})^2 - 2.7e\text{-}5\ (\text{E-DIST-mag})^2 - 5.12623\ (\text{Vm}) + 36.4862\ (\text{SC-3\_P}) + 0.001581\ (\text{Jurs-WPSA-1})^2 \quad \textbf{(1)}$$

r^2: 0.835734

q^2: 0.720

The GFA methodology was applied to generate three equations for the prediction of the quaternary ammonium compound's affinity at the $\alpha 4\beta 2^*$ nAChR subtype. Equation (**1**) was generated to correlate the descriptors to the bioactivity of all of the *N*-*n*-alkylpyridinium salts, *N*-*n*-alkylpicolinium salts and *N*-*n*-alkylnicotinamide salts (MONO dataset). The equation reveals a positive correlation with increased molecular volume (Vm) and area (Area), while the molecular connectivity index of longer chain lengths (SC-3_P) has a negative correlation. Interestingly, the compounds in the *N*-*n*-alkylnicotinamide series, which have larger molecular volumes than their corresponding

pyridinium cousins, possess less affinity toward this nAChR subtype. Additionally, the affinities of the *N*-*n*-alkylnicotinamide salts were also decreased when compared to the simpler *N*-*n*-alkylpyridinium salts. The GFA also had a negative correlation with the E-DIST-mag descriptor, which describes the entropy of the matrix. The Jurs-WPSA-1 descriptor describes the surface-weighted charged partial surface areas; an indication that the positive charge distribution plays a role in receptor recognition (note that the converse descriptor, Jurs-PNSA-1 was used in the corresponding SOM model).

<u>*N*-Alkylnicotinium salts</u>

The resulting equation was derived using the GFA methods:

$$K_i = 43.5762 + 1.0e\text{-}6\ (\text{E-DIST-mag})^2 - 3.03532\ (\text{Jurs-RPCS})^2 - 6862.5\ (\text{Jurs-FNSA-3})^2 + 0.000602\ (\text{MW})^2 \quad \textbf{(2)}$$

r^2: 0.592152

q^2: 0.369

Equation (**2**) models the SAR of the *N*-*n*-alkylnicotinium salts only. As can be seen in equation (**1**), the E-DIST-mag descriptor was utilized, however, a positive correlation was found with this set of data. Jurs-RPCS, a measurement of the relative positive surface charge, and Jurs-FNSA-3, fractional negatively charged partial surface areas, positively correlate with affinity for the $\alpha4\beta2^*$ nAChR binding site, with the latter descriptor having the most weight. Interestingly, molecular weight (MW) is also negatively correlated. Since the highest affinity analogs NDDNI and NDNI (C_{12} and the C_{10} *N*-*n*-alkylnicotinium compounds, respectively) possess the highest molecular weight, the spatial partial charge interactions described by the Jurs descriptors must be more

heavily weighted in this case. Additionally, this data set did not include NONI, the C_8 *N*-*n*-alkylnicotinium analog. The GFA was unable to generate a reliable model with NONI included, indicating that the descriptor set was likely insufficient to fully describe the SAR of this series.

bis-Quaternary Ammonium salts

The resulting equation was derived using the GFA methods:

$$K_i = -141.363 + 1449.55\,(SIC)^2 + 0.000602\,(Jurs\text{-}WNSA\text{-}2)^2 - 47.5526\,(IC)^2 + 2.43134\,(Log\ Z) \quad \textbf{(3)}$$

r^2: 0.810622

q^2: 0.657

The affinity of the *bis*-quaternary ammonium compounds is modeled by equation (**3**). Similar to the *N*-*n*-alkylnicotinium salts and the SOM maps, the *bis*-quaternary ammonium salts utilized a surface weighted, partial charge descriptor. Again, the information-theoretic topological indices are found in the model equation. IC and SIC (structural informational content) are present and may be identifying steric qualities of the molecules and Log Z (logarithm of the Hosoya index), which deals with connectivity of the molecule. It also appears that the Jurs descriptors are effective in describing the SAR of the quaternary ammonium salts. The GFA selected a surface weighted, partial negative charge descriptor, Jurs-WNSA, which is most likely related to a portion of the molecule, possibly the aromatic pyridinium ring.

It is important to note that although the SOM and GFA methodologies were provided the same set of descriptors at the outset of training, not surprisingly, models resulting from the two methods utilize different subsets of these descriptors. A combination of three factors is thought to underlie this observation: 1) GFAs and SOMs model nonlinearity in fundamentally different ways; 2) each method approaches descriptor selection in fundamentally different ways and; 3) each have different susceptibilities to getting stuck in local minima.

4.4. Conclusion

Two different computational modeling methodologies were used to model the SAR of the interaction of quaternary ammonium compounds with the $\alpha 4\beta 2^*$ nAChR subtype. The SOM methodology was effective in appropriately grouping compounds with diverse structures and activities. GFAs were also able to predict compound activities from a set of physical descriptions. Taken together, the charge distribution and the hydrophobic free energies seem to be important indicators of bioactivity for this particular class of molecules. However, both methodologies exhibited limitations when compounds with similar physical properties, but vastly different biological activities were evaluated. Nevertheless, the current work demonstrates that non-linear *in silico* methodologies can be used to screen large series of compounds, and successful models can be generated to aide in the selection of active compounds from larger compound libraries to be further evaluated.

Chapter 5: Enantioselective Synthesis of Nicotine Analogs as Precursors for the Preparation of Novel Quaternary Ammonium Analogs

5.1. Introduction

The principal tobacco alkaloid, NIC, is a potent agonist at nAChRs, and interacts with all known nAChR subtypes. nAChR ligands modulate a number of functions within both the peripheral and the central nervous systems, mediated by a diversity of nAChR subtypes containing a2-a10 and ß2-ß4 subunits. Interestingly, leaves from *Nicotiana tobaccum* contain a number of other minor alkaloids structurally related to nicotine, e.g., nornicotine, anabasine, and anatabine. *S*-(-)-Nicotine is biosynthesized in the tobacco plant from nicotinic acid and *L*-ornithine or *L*-arginine. Nornicotine, the second most abundant tobacco alkaloid, is biosynthesized via enzymatic *N*-demethylation of *S*-(-)-nicotine; the minor alkaloid, anabasine, is generally believed to be biosynthesized from nicotinic acid and lysine, via a similar pathway to that described above for nicotine (Bush *et al.* 1999). Anatabine is derived biosynthetically solely from nicotinic acid, which is decarboxylated to 1, 2-dihydropyridine and 2, 5-dihydropyridine followed by condensation of these two molecules to form 3, 6-dihydroanatabine (Bush *et al.* 1999). Aromatization of 3, 6-dihydroanatabine then affords anatabine.

While nicotine in tobacco is found almost exclusively in the *S*-(-)-enantiomeric form (Crooks *et al.* 1992; Armstrong *et al.* 1999), the minor tobacco alkaloids are present as mixtures of their respective optical isomers (Armstrong *et al.* 1999). In this respect, unlike nicotine, nornicotine exists as a mixture of its *S*-(-)- and *R*-(+)-enantiomeric forms in various ratios, depending on the species of *Nicotiana* from which it was isolated. Even

different sources of tobacco, e.g. Burley, Turkish, or Virginia, contain different ratios of nornicotine enantiomers (Armstrong *et al.* 1999). The presence of both enantiomeric forms of nornicotine in the tobacco plant results from the enzymatic *N*-demethylation of *S*-(-)-nicotine in the plant. Biosynthetic studies with 2'-[^{3}H]-nicotine have shown that the 2'-[^{3}H]-label is lost during formation of *R*-(+)-nornicotine, but is retained in the formation of *S*-(-)-nornicotine (Bush *et al.* 1999). These observations suggest the formation of a planar intermediate in the formation of the *R*-(+)-isomer, and the likely existence of two distinct *N*-demethylase enzymes.

The minor tobacco alkaloids are also known to possess nAChR agonist activity, and may contribute to the neuropharmacological effects of smoking, although they are generally relatively less pharmacologically active than *S*-(-)-nicotine (Crooks and Dwoskin 1997). Pharmacological investigations and structure-activity studies with these minor tobacco alkaloids have been somewhat limited, due to the lack of availability of their optically pure forms. Previous structure-activity studies have demonstrated that the optical isomers of nornicotine show significant differences in their ability to bind to nicotinic receptors in rat brain and generally are less potent compared with nicotine (Reavill *et al.* 1988; Copeland *et al.* 1991). For example, *S*-(-)-nornicotine inhibits [^{3}H]-nicotine binding to rat brain membranes with a 50-fold lower affinity (Ki= 47 nM) compared with nicotine (Ki = 1.0 nM) (Xu *et al.* 2001). In contrast, *S*-(-)-nicotine and *S*-(-)-nornicotine exhibit similar affinities for the [^{3}H]methyllycaconitine binding site (Ki = 770 nM and 1340 nM, respectively) in brain (Xu *et al.* 2001). These results indicate interaction of nornicotine with both a4ß2* and a7* nAChR subtypes. Evidence has also accumulated

demonstrating that nornicotine enantiomers differ in their neurochemical and behavioral effects (Bardo *et al.* 1997; Crooks and Dwoskin 1997; Green *et al.* 2000; Green *et al.* 2001). Similar to nicotine, both enantiomers of nornicotine evoke a concentration-dependent, Ca^{2+}-dependent and mecamylamine-sensitive increase in DA release from rat striatal and nucleus accumbens slices (Dwoskin *et al.* 1993; Teng *et al.* 1997; Green *et al.* 2001), indicating that nornicotine acts as an agonist at nAChR subtypes modulating DA release. Interestingly, *R*-(+)-nornicotine was more potent than the *S*-(-)-enantiomer in evoking [^{3}H]dopamine overflow from rat nucleus accumbens slices, whereas both isomers were equipotent in this respect in experiments with rat striatal slices, suggesting the involvement of different nicotinic receptor subtypes in these brain regions. Whereas, *S*-(-)-nicotine and *S*-(-)-nornicotine were equipotent in releasing DA from striatal slices, nicotine was 43-fold more potent than nornicotine (EC_{50} = 70 nM and 3.0 μM, respectively) in releasing DA from nucleus accumbens slices (Green *et al.* 2001). Interestingly, nornicotine has a longer half-life than nicotine in both rodent and non-human primate plasma and brain (Kyerematen *et al.* 1990; Crooks *et al.* 1997; Ghosheh *et al.* 1999; Valette *et al.* 2003); and following chronic treatment with *S*-(-)-nicotine, nornicotine (of unknown chirality) accumulates in rodent brain reaching pharmacologically relevant concentrations (Ghosheh *et al.* 2001).

Behavioral studies using animal models also provide support for the use of nornicotine as a tobacco use cessation agent. Nornicotine produces nicotine-like discriminative stimulus effects (Bardo *et al.* 1997), as well as nicotine-like effects on schedule-controlled operant responding (Risner *et al.* 1988). Recent results indicate that

nornicotine functions as a positive reinforcer (Bardo *et al.* 1999); however, under similar experimental conditions, nornicotine is associated with a lower rate of responding in comparison with nicotine (Corrigall and Coen 1989; Bardo *et al.* 1999), suggesting that nornicotine has a lower reinforcing efficacy. Moreover, nornicotine has been shown to decrease nicotine self-administration in rats (Green *et al.* 2000). Furthermore, across repeated nornicotine pretreatments, tolerance did not develop to nornicotine-induced decrease in nicotine self-administration. Importantly, nornicotine has been recently found to inhibit dopamine transporter (DAT) function (Middleton *et al.* 2005), and thus, acts similarly to bupropion, which is a currently available smoking cessation agent. In summary, nornicotine increases DA release and inhibits DAT function, both mechanisms being beneficial in the treatment of tobacco use. Thus, a simple structural change, e.g., removal of the *N*-methyl moiety from the pyrrolidine ring of nicotine, which affords nornicotine, may be beneficial with respect to its pharmacological profile. Taken together, these current preclinical neurochemical and behavioral results suggest that nornicotine could be a promising candidate for development as a tobacco cessation agent (Middleton *et al.* 2005). In this respect, it should be noted that *R*-(+)-nornicotine is currently being investigated as a potential smoking cessation agent (Crooks *et al.* 1998).

Dwoskin *et al*. (1995) have shown that *S*-(-)-anabasine increases fractional [^{3}H] release in a concentration-dependent manner from rat striatal slices preloaded with [^{3}H]-dopamine (EC_{50} = 19.3 ± 3.2 μM), but was less potent than *S*-(-)-nicotine (EC_{50} = 3.0 ± 2.2 μM) (Dwoskin *et al.* 1995). Similar results have been reported by Grady *et al*. (1992), who demonstrated that (±)-anabasine stimulates [^{3}H]-dopamine release from mouse striatal

synaptosomes, and (±)-anabasine has been reported to inhibit high affinity binding of [^{3}H]-*S*-(-)-nicotine to rat and mouse striatal membranes (Reavill *et al.* 1988; Grady *et al.* 1992). Thus far, direct comparisons of these pharmacological properties between the enantiomers of anabasine and anatabine have not been determined due to difficulties in obtaining the pure optical isomers of each compound.

Early efforts to develop synthetic routes to racemic minor tobacco alkaloids have utilized a variety of methods (for a comprehensive review, see Crooks, 1999). However, few examples of general preparative methods for these alkaloids have been reported. Deo and Crooks (1996) have utilized a benzophenone imine intermediate for the general synthesis of racemic nornicotine, anabasine, and anatabine, while a number of strategies have been developed for the enantioselective synthesis of nornicotine, anabasine and anatabine optical isomers (Deo and Crooks 1996; Crooks 1999; Loh *et al.* 1999; Yus *et al.* 2001), few of these are of general utility. Recently, the *S*-(-)-isomers of nornicotine, anabasine and anatabine have been synthesized via a 5-step enantioselective synthesis that utilizes a ring-closing metathesis route (Felpin *et al.* 2001); also, Amat *et al*. (2002) have reported a chiral synthesis of *S*-(-)-anabasine from a chiral lactam intermediate (Amat *et al.* 2002). Additionally, *S*-(-)-anatabine has been synthesized by reacting an allylsulfone with an azaaromatic chiral sulfinimine (Balasubramanian and Hassner 1998).

Aiqiao *et al*. (1991) have reported a rapid and convenient use of a 2-hydroxy-3-pinanone intermediate for the enantioselective synthesis of 2-pyridyl methylamines; this method was subsequently adapted by Swango *et al*. (1999) for the efficient synthesis of *S*-(-)- and *R*-(+)-nornicotine isomers in three steps, with a reported ee of 91% and 81%, respectively

(Aiqiao *et al.* 1991; Swango *et al.* 1999). This current study describes a general synthetic procedure for the facile preparation of the optical isomers of nornicotine, anabasine, and anatabine, utilizing modifications of the Swango *et al.* (1999) synthetic methodology (Figure 5.1), and more importantly, establishes this synthetic route as a convenient method for the preparation of the enantiomerically pure minor tobacco alkaloids.

5.2. Experimental

5.2.1. Materials

The chemicals utilized in the synthesis of the enantiomers of nornicotine, anabasine, and anatabine were obtained from Aldrich Chemical Company (Milwaukee, WI), or from Acros Organics (Somerville, NJ), and were used without further purification. Flash column chromatography was carried out using ICN SILITECH 32-63, 60Å silica gel. Melting points were determined on a Fisher Scientific melting point apparatus and are uncorrected. ^{1}H-NMR and ^{13}C-NMR spectra were recorded on a Varian 300 MHz NMR. All Spectra were referenced, and chemical shifts were determined using tetramethylsilane (TMS) as the internal standard. Mass spectra were recorded on a JEOL JMS-700T Mstation, or on a Bruker Autoflex MALDI-TOF mass spectrometer. Specific rotation measurements were carried out on a Perkin-Elmer Model 241 Polarimeter. Microanalyses were carried out by Atlantic Microlabs, Inc. (Atlanta, GE).

5.2.2. Synthetic Procedures

Enantioselective NIC Alkaloid Synthesis

(1R,2R,5R)- and (1S,2S,5S)- 2,6,6-Trimethyl-3-(pyridin-3-ylmethylimino)-bicyclo[3.1.1]heptan-2-ol (**67 and 67R**)

Boron trifluoride diethyl etherate (0.3 mL) was added to a solution of 3-(aminomethyl) pyridine (3.30 g, 30.6 mmol) and 1*R*, 2*R*, 5*R*-(+)-2-hydroxy-3-pinanone (5.00 g, 29.8 mmol). The reaction mixture was refluxed for 2.5 h under N_2 using a Dean-Stark apparatus. After cooling, the solvent was evaporated under reduced pressure. The residue was purified by flash silica gel column chromatography using $CHCl_3$:hexane:methanol, 12:2:1 as the elution solvent to afford the (+)-2-hydroxy-3-pinanone ketimine **67** (6.24 g, 81%) as white crystals after removal of solvent: $[a_D]$ = $+3.8^o$ (c = 1.0, methanol); ^{1}H NMR (300 MHz, $CDCl_3$) δ 8.58 (1H, d, J = 2.4 Hz), 8.48 (1H, dd, J = 4.8, 1.8 Hz), 7.70 (1H, d, J = 7.8 Hz), 7.25 (1H, dd, J = 7.8, 4.8 Hz), 4.48 (2H, s), 2.80 (1H, br s), 2.58 (2H, m), 2.34 (1H, m), 2.06 (2H, m), 1.56 (1H, d, J = 10.8 Hz), 1.50 (3H, s), 1.31 (3H, s), 0.84 (3H, s) ppm.; ^{13}C NMR (75 MHz, $CDCl_3$) δ 178.19, 149.33, 148.28, 135.81, 135.52, 123.60, 51.83, 50.46, 38.75, 38.50, 34.12, 28.56, 28.37, 27.51, 23.11 ppm. m/z 258 (M^+, base peak).

The same procedure was utilized for the synthesis of 1*S*, 2*S*, 5*S*-(-)-2-hydroxy-3-pinanone ketimine (6.58 g, 85%), which was obtained as white crystals from the reaction of 1*S*, 2*S*, 5*S*-(-)-2-hydroxy-3-pinanone with 3-(aminomethyl)pyridine; $[a_D]$ = -3.6^o (c = 1.0, methanol).

Figure 5.1 Enantioselective Synthesis of S-(-)-Nornicotine, S-(-)-Anabasine, and S-(-)-Anatabine

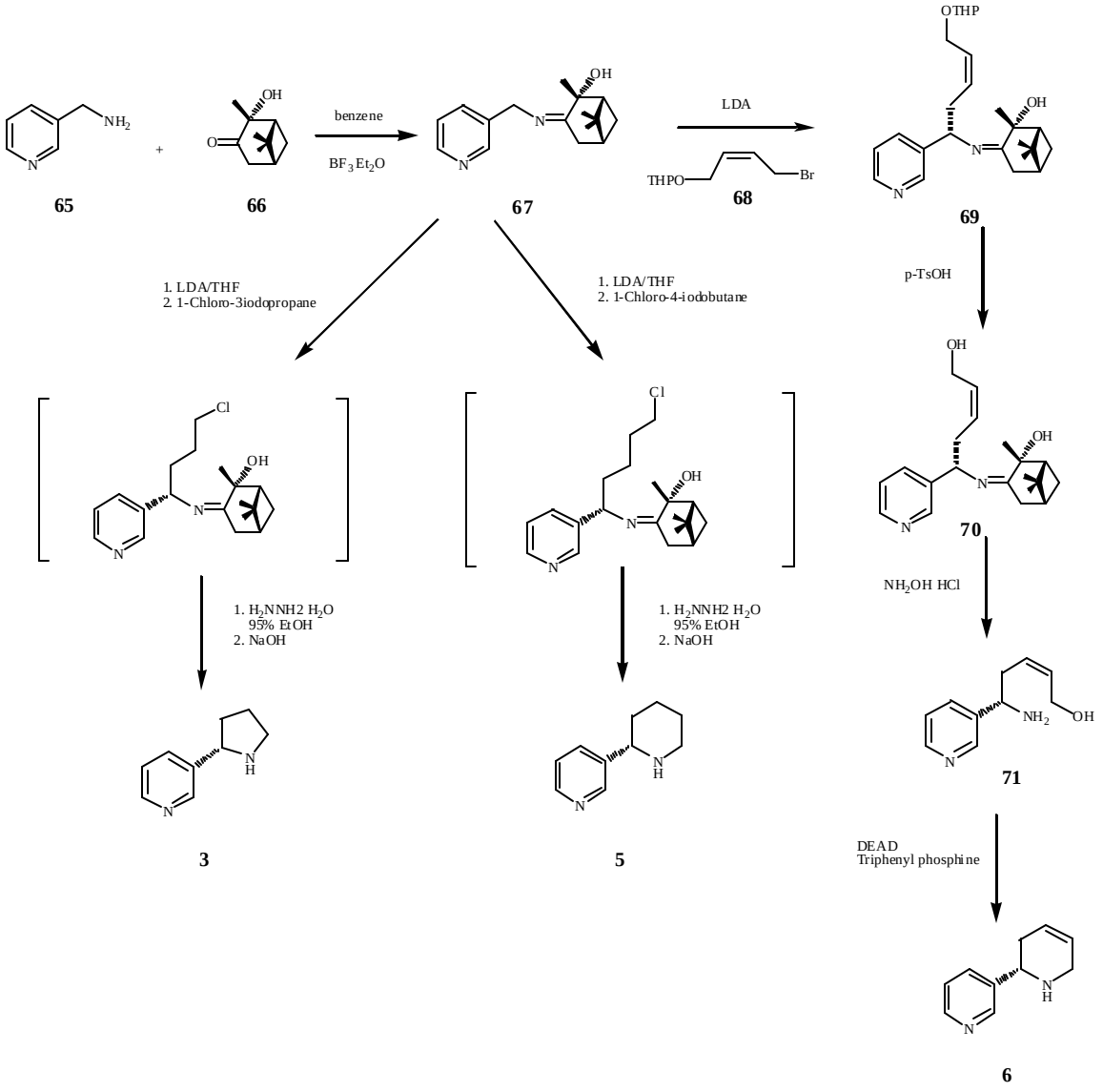

65 **66** **67** **68** **69** **70** **71** **3** **5** **6**

(S)-(-)-Nornicotine and (R)-nornicotine (**3 and 3R**)

To a stirred solution of ketimine **67** (258 mg, 1.00 mmol) in THF (8 mL) was added dropwise LDA (1.50 mL, 2.0 M solution in THF, 3.00 mmol) at 0°C. The purple solution was stirred at 0°C for 15 min then cooled to –78°C. 1-Chloro-3-iodopropane (0.32 mL, 3.00 mmol) in THF (2 mL) was then added dropwise. The reaction mixture was stirred for an additional 30 min at –78°C, and then quenched with saturated aqueous

NH_4Cl solution. The solution was extracted with diethyl ether (3x10 mL). The combined organic layers were washed with brine, dried over anhydrous magnesium sulfate, filtered, and the solvent evaporated. The residue was passed through a short silica gel column, eluting with hexane, followed by $CHCl_3$:MeOH (20:1) to give the C-alkylated intermediate as a yellow oil. The crude product was not purified, but immediately added to a mixture of 95% EtOH (6 mL), hydrazine monohydrate (4 mL) and acetic acid (2 mL). The mixture was stirred overnight at room temperature and 10% aqueous NaOH solution (10 mL) was added. The solution was then extracted with $CHCl_3$ (3x20 mL), the combined organic liquors were dried over anhydrous magnesium sulfate, filtered, and the solvent evaporated. The residue was purified by flash column chromatography on silica gel, eluting with $CHCl_3$:MeOH:Et_3N (100:10:1) to afford *S*-(-)-nornicotine **(3)** (118 mg, 79% overall) as a pale yellow oil; $[a_D]$ = -32.6^o (c = 1.0, methanol); ^{1}H NMR (300 MHz, $CDCl_3$) δ 8.60 (1H, d, J = 1.8 Hz), 8.45 (1H, dd, J = 4.8, 1,7 Hz), 7.74 (1H, "dt", J = 7.8, 1.9 Hz), 7.25 (1H, dd, J = 7.8, 4.8 Hz), 4.14 (1H, dd, J=7.3, 2.1 Hz), 3.11 (2H, m), 2.20 (1H, m), 2.11 (1H, m), 1.91 (2H, m), 1.66 (1H, m) ppm.; ^{13}C NMR (75 MHz, $CDCl_3$) δ 148.3, 148.0, 140.1, 134.2, 123.2, 59.7, 46.7, 34.0, 25.2 ppm; m/z 148 (M^+).

The same procedure was utilized for the synthesis of *R*-(+)-nornicotine (110 mg, 76% overall) from 1*S*, 2*S*, 5*S*-(-)-2-hydroxy-3-pinanone ketimine and 1-chloro-3-iodopropane, and the product was obtained as a pale yellow oil; $[a_D]$ = +32.8^o (c = 1.0, methanol).

(S)-(-)-Anabasine and (R)-(+)-anabasine (**5 and 5R**)

A similar procedure used to synthesize **3** was also utilized for the synthesis of *S*-(-)-anabasine **(5)**, which was obtained in 72% yield from 1*R*, 2*R*, 5*R*-(-)-2-hydroxy-3-pinanone ketimine **(67)** using 1-chloro-4-iodobutane as the alkylating agent instead of 1-chloro-3-iodopropane. The product was obtained as a light-yellow oil; $[a_D] = -79.8^o$ (c = 0.9, methanol); ^{1}H NMR (300 MHz, $CDCl_3$) δ 8.60 (1H, s), 8.50 (1H, dt, J = 4.8, 1,7 Hz), 7.74 (1H, dm, J = 7.8, 1.8 Hz), 7.25 (1H, dd, J = 7.8, 4.8 Hz), 3.65 (2H, dd, J=11, 2.2 Hz), 3.22 (1H, dm, J= 11 Hz), 2.75-2.85 (1H, m), 2.00 (1H, s), 1.46-1.95 (6H, m) ppm.; ^{13}C NMR (75 MHz, $CDCl_3$) δ 148.0, 148.2, 139.9 133.7, 122.8, 59.2, 47.0, 34.00, 24.9, 24.6 ppm. m/z 163 (M^+).

Additionally, *R*-(+)-anabasine was synthesized in a similar manner, utilizing 1*S*, 2*S*, 5*S*-(-)-2-hydroxy-3-pinanone ketimine as the chiral intermediate, and was obtained as a pale yellow oil (75% yield); $[a_D] = +80.2^o$ (c = 1.0, methanol).

_S_-(-)-Anatabine and _R_-(+)-anatabine

cis-2-(4-Bromobut-2-enyloxy)tetrahydropyran **(68)**

p-Toluenesulfonic acid monohydrate (0.13 g) was added to a stirred solution of *cis*-but-2-ene-1,4-diol (2.64 g, 30.0 mmol) and THP (2.53 g, 30.0 mmol) in CH_2Cl_2 (10 mL) and THF (25 mL) at 0°C. After stirring at 0 °C for 2 h, the reaction mixture was stirred at room temperature for a further 20 min. Water was added, and the aqueous phase was extracted with diethyl ether (3x20 mL). The combined organic layers were dried over anhydrous magnesium sulfate, filtered, and the solvent evaporated. The residue was purified by flash column chromatography on silica gel, eluting with hexane:EtOAc, (2:1)

to give *cis*-4-(tetrahydropyran-2-yloxy)but-2-en-1-ol (2.66 g, 52%) as a colorless oil: ^{1}H NMR (300 MHz, $CDCl_3$) δ 5.81 (1H, m), 5.67 (1H, m), 4.64 (1H, m), 4.15 (4H, m), 3.82 (1H, m), 3.49 (1H, m), 1.42-1.84 (6H, m) ppm; ^{13}C NMR (75 MHz, $CDCl_3$) δ 132.54, 128.11, 97.68, 62.63, 62.31, 58.50, 30.71, 25.59, 19.49 ppm.

To a solution of *cis*-4-(tetrahydropyran-2-yloxy)but-2-en-1-ol (2.44 g, 14.2 mmol) in DMF (40 mL) was added triphenylphosphine (4.17 g, 15.9 mmol). The solution was cooled to 0°C and NBS (2.73 g, 15.5 mmol) was added in portions. After stirring for 30 min at room temperature, the reaction was quenched with methanol (2 mL). The solution was diluted with diethyl ether (200 mL), and washed with water, saturated aqueous $NaHCO_3$, and brine, successively. The organic layer was dried over anhydrous magnesium sulfate, filtered, and concentrated. The residue was purified by flash chromatography on silica gel, eluting with hexane to afford the bromide **68** (2.24 g, 67%) as a colorless oil: ^{1}H NMR (300 MHz, $CDCl_3$) δ 5.86 (1H, m), 5.69 (1H, m), 4.61 (1H, dd, J = 4.2, 3.0 Hz), 4.31 (1H, m), 4.14 (1H, m), 4.01 (2H, d, J = 7.8 Hz), 3.84 (1H, m), 3.51 (1H, m), 1.40-1.90 (6H, m) ppm; ^{13}C NMR (75 MHz, $CDCl_3$) δ 130.95, 128.41, 98.15, 62.49, 62.08, 30.80, 26.84, 25.65, 19.67 ppm. m/z: 155 (M^+-81), 133/135, 85, 53.

1*R*, 1'*S*, 2*R*, 5*R*-2,6,6-Trimethyl-3-[1'-pyridin-3''-yl-5'-(tetrahydro-pyran-2''-yloxy)pent-3'-enylimino]bicyclo[3.1.1]heptan-2-ol **(69)**

To a stirred solution of ketimine **67** (1.94 g, 7.50 mmol) in THF (60 mL) was added dropwise LDA (11.3 mL, 2.0 M solution in THF, 22.6 mmol) at 0°C. The purple solution was stirred at 0°C for 15 min then cooled to –78°C. The bromide **68** (2.12 g,

9.00 mmol) in THF (8 mL) was added dropwise. The reaction mixture was stirred for an additional 30 min at –78°C, and then quenched with saturated aqueous NH_4Cl solution. The aqueous phase was extracted with diethyl ether (3x20 mL). The combined organic layers were washed with brine, dried over anhydrous magnesium sulfate, filtered, and evaporated. The residue was flash chromatographed on silica gel, eluting with $CHCl_3$:hexane:MeOH (100:20:2) to give **69** (2.80 g, 91%) as a colorless oil: ^{1}H NMR (300 MHz, $CDCl_3$) δ 8.56 (1H, d, J = 2.1 Hz), 8.48 (1H, dd, J = 5.1, 1.8 Hz), 7.72 (1H, d, J = 7.5 Hz), 7.25 (1H, dd, J = 7.5, 4.8 Hz), 5.61 (1H, m), 5.50 (1H, m), 4.59 (2H, m), 4.19 (1H, m), 4.01 (1H, m), 3.84 (1H, m), 3.49 (1H, m), 2.63 (3H, m), 2.44 (1H, m), 2.26 (1H, m), 2.06 (1H, t, J = 6.3 Hz), 1.99 (1H, m), 1.62-1.88 (2H, m), 1.52 (3H, s), 1.44-1.60 (4H, m), 1.39 (1H, d, J = 10.5 Hz), 1.31 (3H, s), 0.90 (3H, s) ppm; ^{13}C NMR (75 MHz, $CDCl_3$) shows signals for two diastereomers δ 176.13, 148.77, 148.53, 138.73 (138.70), 134.69, 129.13 (128.98), 128.80 (128.74), 123.70, 98.17 (97.99), 62.94 (62.85), 62.46, 61.10 (61.06), 50.26, 38.63, 37.08, 33.91, 30.90, 28.79, 28.26, 27.60, 25.71, 23.32, 19.77 ppm. m/z: 412 (M^+), 327, 311, 257, 162, 144, 85; Anal. Calcd for $C_{25}H_{36}N_2O_3 \cdot H_2O$: C, 69.74; H, 8.90; N, 6.51. Found: C, 69.80; H, 8.58; N, 6.33.

1*R*, 1'*S*, 2*R*, 5*R*-3-(5'-Hydroxy-1'-pyridin-3''-yl-pent-3'-enylimino)-2,6,6-trimethyl-bicyclo[3.1.1]heptan-2-ol **(70)**

To a solution of THP ether **69** (1.45 g, 3.52 mmol) in MeOH (90 mL) was added p-toluenesulfonic acid (1.37 g, 7.04 mmol). The mixture was stirred at room temperature for 3 h and then concentrated. Saturated aqueous $NaHCO_3$ solution (20 mL) was added, and the aqueous phase was extracted with diethyl ether (3x20 mL). The combined

organic layers were washed with brine, dried over anhydrous magnesium sulfate, and evaporated. The residue was flash chromatographed on silica gel, eluting with $CHCl_3$:MeOH (25:1) to give **70** (1.05 g, 90%) as a colorless oil: $[a_D] = -33.1°$ (c = 1.0, MeOH); ^1H NMR (200 MHz, $CDCl_3$) δ 8.51 (1H, br s), 8.44 (1H, d, J = 4.0 Hz), 7.66 (1H, dt, J = 8.0, 2.0 Hz), 7.22 (1H, dd, J = 8.0, 5.0 Hz), 5.71 (1H, m), 5.42 (1H, m), 4.55 (1H, dd, J = 8.4, 4.8 Hz), 4.08 (2H, m), 2.42-2.84 (4H, m), 2.16-2.38 (2H, m), 20.1 (1H, t, J = 6.0 Hz), 1.94 (1H, m), 1.50 (3H, s), 1.33 (1H, d, J = 11.4 Hz), 1.27 (3H, s), 0.85 (3H, s) ppm; ^{13}C NMR (75 MHz, $CDCl_3$) δ 177.81, 148.78, 148.69, 138.69, 134.68, 131.98, 128.25, 123.85, 76.79, 60.45, 58.64, 50.55, 38.52, 38.46, 37.23, 34.15, 28.52, 28.13, 27.41, 23.13 ppm. m/z: 329 (M^++1); Anal. Calcd for $C_{20}H_{28}N_2O_2 \cdot 0.3CHCl_3$: C, 66.93; H, 7.83; N, 7.69. Found: C, 67.16; H, 7.94; N, 7.77.

S-5-Amino-5-pyridin-3-yl-pent-2-en-1-ol **(71)**

To a solution of **70** (0.86 g, 2.6 mmol) in MeOH (40 mL) was added hydroxylamine hydrochloride (1.39 g, 20.0 mmol). The mixture was stirred at room temperature for 18 h. Ammonia gas was bubbled into the solution to adjust the pH to 9. The MeOH was then evaporated and $CHCl_3$ (15 mL) was added to the residue. The resulting mixture was filtered and the filtrate was concentrated. The resulting residue was flash chromatographed on silica gel, eluting with $CHCl_3$:MeOH:Et_3N (100:10:1) to give **71** (0.34 g, 74%) as a colorless oil: $[a_D] = -44.3°$ (c = 1.0, MeOH); ^1H NMR (200 MHz, $CDCl_3$) δ 8.53 (1H, d, J = 2.4 Hz), 8.46 (1H, dd, J = 4.8, 1.6 Hz), 7.68 (1H, dt, J = 7.6, 1.8 Hz), 7.24 (1H, dd, J = 7.4, 5.0 Hz), 5.85 (1H, m), 5.47 (1H, m), 3.90-4.20 (3H, m), 2.30-2.60 (5H, m) ppm; ^{13}C NMR (50 MHz, $CDCl_3$) δ 149.00, 148.65, 140.70, 134.10,

133.01, 128.43, 123.80, 57.84, 52.73, 37.42 ppm. m/z: 179 (M^++1); Anal. Calcd for $C_{10}H_{14}N_2O \cdot 0.2H_2O$: C, 66.05; H, 7.98; N, 15.41. Found: C, 66.23; H, 7.91; N, 15.37.

S-(-)-Anatabine and *R*-(+)-anatabine **(6 and 6R)**

Diethyl azodicarboxylate (DEAD, 0.23 mL, 1.40 mmol) was added dropwise to a stirred solution of triphenyl phosphine (365 mg, 1.40 mmol) in THF (6 mL) at 0°C under N_2. The reaction mixture was stirred at 0°C for 20 min. A solution of **71** (178 mg, 1.00 mmol) in THF (3 mL) was then added dropwise. The mixture was stirred at 0°C for 30 min, and then at room temperature for 2 h. Evaporation of the solvent followed by purification of the residue by flash column chromatography on silica gel ($CHCl_3$:MeOH, 20:1) gave *S*-(-)-anatabine (**6**) (124 mg, 77%) as a colorless oil: $[a_D] = -180^o$ (c = 1.0, methanol); ^{1}H NMR (300 MHz, $CDCl_3$) δ 8.56 (1H, d, J = 1.6 Hz), 8.46 (1H, dd, J = 4.8, 1.6 Hz), 7.68 (1H, dt, J = 8.0, 1.8 Hz), 7.23 (1H, dd, J = 4.0, 2.8 Hz), 5.79 (2H, m), 3.84 (1H, t, J = 7.0 Hz), 3.33-3.65 (2H, m), 2.21 (2H, m), 2.00 (1H, br s) ppm; ^{13}C NMR (75 MHz, $CDCl_3$) δ 148.93, 148.82, 140.05, 134.29, 126.46, 125.26, 123.71, 55.44, 46.12, 34.01 ppm. m/z: 160 (M^+, base peak), 159, 145, 131, 118, 105, 80, 54.

The same procedure was utilized for the synthesis of *R*-(+)-anatabine from 1*S*, 2*S*, 5*S*-(-)-2-hydroxy-3-pinanone ketimine and *cis*-2-(4-bromobut-2-enyloxy)tetrahydropyran, which was obtained as a pale yellow oil (70% yield); $[a_D] = +177^o$ (c = 1.0, methanol).

5.3. Results and Discussion

The *R*- and *S*-enantiomers of nornicotine, anabasine, and anatabine were successfully synthesized in good to moderate yields, and in good enantiomeric purity. The stereo-controlled C-alkylation of the 2-hydroxy-3-pinanone-3-(aminomethyl)pyridine ketimine intermediate is the key step in the reaction sequence. Experimental evidence from the crystal structure of the ketimine (Ayers *et al*., 2005) formed during the C-alkylation step supports the findings that the (+)-ketimine is C-alkylated from the *re* face of the (-)-ketimine-lithium complex. This alkylation affords the *S*-isomer exclusively, while the C-alkylated product with the *R*-configuration is generated from the (-)-ketimine-lithium complex. LDA was chosen from a number of possible catalytic bases, including K*t*BuOH, due to the higher yields obtained, and because of the improvement in purity of the isolated products when using this base. As determined by Aiqiao *et al.*, the base (LDA) forms a stable complex with the ketimine, effectively blocking the *si* face of the molecule and opening the *re* face of the molecule to addition of an alkyl halide (Figure 5.2) (Aiqiao *et al.* 1991).

Figure 5.2 Stable carbanion (+)-ketimine intermediate.

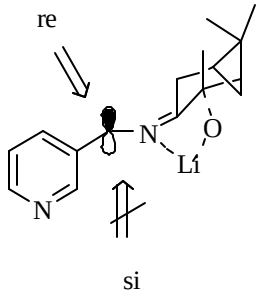

An advantage in the above procedure over previously reported literature syntheses of *R*-(+)- and *S*-(-)-nornicotine, and *R*-(+)- and *S*-(-)-anabasine isomers is the small number of overall steps to achieve the formation of the desired alkaloids. In an earlier approach to that outlined above, Swango *et al*. (1999) utilized the 2-hydroxy-3-pinanone-3-(aminomethyl)pyridine ketimine reagent in the synthesis of nornicotine isomers, but C-alkylation was carried out with a halogenoalcohol, to afford an intermediate *N*-alkylhydroxy analog, which had to be isolated and converted to the corresponding *N*-alkylbromo analog, prior to cyclization to afford the final product. The current synthesis outlined in this paper constitutes a two-step, general procedure for the synthesis of the optical isomers of both nornicotine and anabasine, by utilizing a 1, 4-dihalogeno alkane instead of a halogenoalcohol in the C-alkylation of the ketimine. This change reduces the number of steps in the reaction sequence from three to two, and significantly simplifies the work-up procedure for obtaining the final chiral product. Attempts at utilizing diiodopropane or diiodobutane in the reaction resulted in lower yields of reaction products. The use of a chloroiodoalkane reactant affords rapid and more efficient C-alkylation of the ketimine, but slow solvolytic degradation at the chloro-terminus. This allows for flash silica gel column purification to be performed, thereby obtaining a stable intermediate for the final cyclization event of the reaction sequence in the presence of hydrazine and water.

In addition to Swango *et al.*, other groups have successfully synthesized nornicotine and anabasine enantiomerically pure (Felpin *et al.* 2001; Amat *et al.* 2002). However, both these syntheses are five steps and result in lower overall yields. Felpin *et al.*, utilize a

novel approach, employing ring closuring metathesis. Though this synthesis resulted in high enantioselective yields the metal used in the final cyclization step is expensive and the final step is significantly longer than the ketimine synthesis.

The above procedure can also be utilized for the synthesis of anatabine enantiomers. However, three steps are required to introduce the C-hydroxy-*cis*-alkene substituent at the α-carbon of the 2-hydroxy-3-pinanone-3-(aminomethyl)pyridine ketimine, followed by a final cyclization step using a Mitsunobu reaction. Nevertheless, this synthetic route is very favorably comparable to previously reported enantioselective syntheses of anatabine described by Balasubramanian and Hassner (1998), and by Mehmandoust *et al*. (1989), both of which involve five steps overall (Mehmandoust *et al*. 1989; Balasubramanian and Hassner 1998). The methodology outlined by Balasubramanian and Hassner could not definitively rule out the presence of an enantiomer in the final steps. The resulting enantiomeric yields were only 70% and the overall yield was 60%.

5.4. Conclusions

Successful adaptation and improvement of an existing methodology has allowed for a streamlined approach in the stereoselective synthesis of the enantiomers of the nicotinic analogs, nornicotine, anabasine, and anatabine. A two-step synthetic procedure for the enantioselective synthesis of the optical isomers of nornicotine and anabasine, and a modified procedure for the synthesis of anatabine enantiomers have been successfully developed, and all compounds were synthesized in good yields and high enantiomeric purity. Due to this purity, these compounds are ideal to use as precursors for another generation of quaternary ammonium analogs.

Chapter 6: Summary and Future Directions

6.1. Summary

This research project successfully utilized the introductory phases of the drug discovery process in order to explore neuronal nAChR subtypes. Previous research indicated that NONI and NDNI were selective and potent antagonists for the nAChRs that mediate DA release and for $\alpha 4\beta 2^*$ nAChR subtypes, respectively. Synthetic analogs of NONI and NDNI were synthesized and evaluated at a4ß2*, a7* and nAChRs that mediate DA release to create a structure activity relationship and afforded potent and selective antagonists. The [^{3}H]NIC binding data were also used to create predictive models for the binding of these series of compounds to a4ß2* receptor subtypes. Additionally, new enantioselective synthetic routes were developed to afford optically pure NIC analogs.

6.1.1. Quaternary Ammonium Analogs

In order to begin the drug discovery process, a series of compounds were designed based on initial work on NONI and NDNI and synthesized. Many of the compounds were isolated in high yields, and all were obtained in high purity and fully characterized. In the *N*-n-alkylnicotinium series, in order to selectively *N*-alkylate the pyridyl *N*-atom of S-(-)-nicotine, a protonation of the pyrrolidine *N*-atom, using an adaptation on the Menshutkin reaction using acetic acid, was necessary. Purification of the resulting compounds was especially important, due to the need to eliminate nicotine completely from the product, as it would interfere with pharmacological evaluation in the binding and release assays. Additionally, the *N-N-bis*-compounds, although similar in structure,

proved difficult to isolate and purify, and several different work-up techniques had to be developed.

The *mono*-quaternary ammonium compounds evaluated had a variety of nAChR antagonist activities, depending on the length of the chain, as well as the nature of the 3-pyridyl substituent. *N*-*n*-Alkylnicotinium salts exhibited antagonist activity at both $\alpha4\beta2^*$ receptor subtypes and nAChR subtypes that mediate DA release depending on alkyl chain length, while having little to no affinity for the $\alpha7^*$ receptor subtype. From these studies, NDDNI has emerged as a potential tool for antagonism of the $\alpha4\beta2^*$ receptor subtype. The activities of the *N*-*n*-alkylpyridinium, *N*-*n*-alkylpicolinium, and *N*-*n*-alkylnicotinamide salts have also led to a better understanding of how the *N*-*n*-nicotinium series of compounds may be interacting with the $\alpha4\beta2^*$ binding site, and has highlighted the importance of the pyrrolidine ring as a necessary component to obtain antagonist activity. The length of the *N*-*n*-alkyl substituent is also an important determinant of the antagonist activity of these molecules, as evidenced by the increased activities when the chain length increased for the *N*-*n*-alkylpicolinium and *N*-*n*-alkylnicotinium salts.

In contrast to the $\alpha4\beta2^*$ receptor subtype, the pyrrolidine ring of the NONI molecule was found not to be critical for binding to and inactivation of nAChR subtypes that mediate DA release. However, the presence of the pyrrolidine ring did afford the most potent antagonist, NDDNI. In addition to the *N*-*n*-alkylnicotinium compounds, the *N*-*n*-alkyl pyridinium and *N*-*n*-alkylpicolinium compounds were generally active in inhibiting NIC-

evoked DA release from rat striatal slices, and had relatively lower affinity for α4β2* and α7* nAChR subtypes. Thus, removal of the pyrrolidine ring from the *N*-*n*-alkylnicotinium series afforded a series of compounds which exhibited an increase in antagonist potency for the nAChR subtypes that mediate DA release, while having little or no activity in α4β2* and α7* nAChR subtypes. This supports the idea that there is a difference in the binding domains of α4β2* nAChR subtypes, α7* nAChR subtypes, and certain nAChRs that mediate DA release.

The *bis*-quaternary ammonium compounds also demonstrated activity at the various nAChR subtypes. *N,N*-*bis*-alkylnicotinium compounds were found to be selective antagonists at a4ß2* receptor subtypes, similar to the *N*-*n*-alkylnicotinium series. However, unlike the *N*-*n*-alkylnicotinium series, the *N,N*-*bis*-alkylnicotinium compounds were not the most potent antagonists at the receptors that mediate NIC-evoked DA release. *N,N*-*bis*-Dodecylpicolinium (bPiDDB) proved to be the most potent antagonist at the receptors that mediate NIC-evoked DA release. That, coupled with it inactivity at a4ß2* and a7* receptor subtypes, make this compound the most potent and selective compound in the all the series tested. Furthermore, the lack of a4ß2* activity and the partial antagonist effect of bPiDDB in the NIC-evoked DA overflow assay, allows for a putative assignment of the antagonist activity occurring at α6β2β3 and α6α4β2β3 nAChR subtypes. bPiDDB is an excellent lead candidate for exploring the these nAChR subtypes due to it pharmacological profile. In addition to its laboratory utility, acute dosing of bPiDDB has recently been shown to decrease nicotine self-administration in

rats and may be used as a lead compound for clinical development (Neugebauer *et al.* 2006).

The only compounds that were found to be active in the α7* MLA binding assay were the heteroaromatic analogs (i.e. *N,N-bis*-isoquinolinium and *N,N-bis*-quinolinium salts). Within these series of compounds, the most potent analog was bQDDB, the twelve-carbon quinoline analog, suggesting that the position of the extended aromatic ring is an important aspect to the binding of these compounds.

6.1.2. Modeling

Using several different classes of quaternary ammonium salts, two different established molecular modeling techniques were applied to create a novel approach to SAR studies. Three self-organizing map (SOMs) models were generated from three different sets of compounds. The groups consisted of the *mono*-substituted compounds, the *bis*-substituted compounds, and both sets combined. The models were able to successfully "bin" the test set of compounds after developing a model from a similar set of training compounds. Additionally, using genetic functional activity (GFA) algorithms an evolutionary approach to generating predictive model equations was applied to the compounds. Three separate equations were generated in order to form a predictive method for evaluating affinities at the α4β2* receptor subtype.

6.1.3. Synthesis of Enantiomerically Pure Nicotinic Analogs

In addition to the modeling and SAR work of the quaternary ammonium compounds, novel synthetic methods were also employed to develop enantiomerically pure nicotine analogs. Efficient enantioselective syntheses of (S)- and R-(+)-nornicotine, (S)-and R-(+)-anabasine, and (S)-and R-(+)-anatabine have been developed, affording isomers in high enantiomeric excess.

6.2. Future Directions

The three areas of focus of this project can all be expanded. Evaluation of the quaternary ammonium pyridinium analogs in the functional [^{3}H]DA release assay, as well as in the $^{86}Rb^+$ efflux assay, is necessary for a complete functional profile to be obtained on each compound in each of these series. Additionally, those compounds that had affinity for the α7* nAChR subtype should be tested for their functional activities. Once the functional profile was complete for these compounds, further study of their mode of action would be important. Of considerable interest would also be the functional activity of the nicotinamide analogs at nAChRs that mediate DA release. The compounds provide a different functional 3-position substituent with different electronic properties. This would allow probing the H-bonding binding area of the nAChRs that mediate DA release.

In addition to further testing, novel pyridinium compounds could also be preformed on those compounds that were synthesized in Chapter 5. S-(-)- and R-(+)-Nornicotine (**3** and **3R**), S-(-)- and R-(+)-anabasine (**5** and **5R)**, S-(-)- and R-(+)-anatabine (**6** and **6R)**, as

well as their *N*-methylated derivatives, could be quaternized with various chain lengths, (Figure 6.1).

Figure 6.1 *N*-Alkylated quaternary ammonium salts of S-(-)- and R-(+)-Nornicotine (**72** and **73**), S-(-)- and R-(+)-anabasine (**74** and **75)**, S-(-)- and R-(+)- anatabine (**76** and **77)**, and their methylated derivatives **(78, 79**, **80**, **81**, and **82)**.

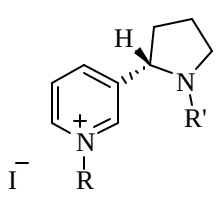

72 R'= H

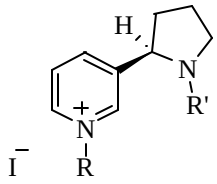

73 R'= H
78 R'= CH_3

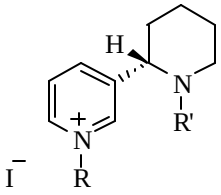

74 R'= H
79 R'= CH_3

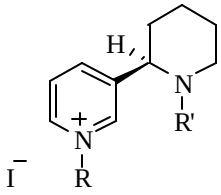

75 R'= H
80 R'= CH_3

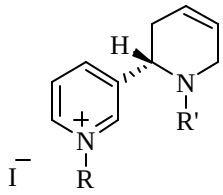

76 R'= H
81 R'= CH_3

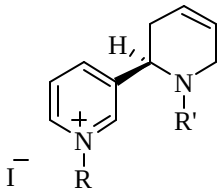

77 R'= H
82 R'= CH_3

R= $(CH_2)_7CH_3$
$(CH_2)_8CH_3$
$(CH_2)_9CH_3$
$(CH_2)_{10}CH_3$
$(CH_2)_{11}CH_3$

Novel synthetic compounds may also be synthesized using the techniques outlined in Chapter 5. Although the racemic forms of azetidine and azepine NIC analogs have been synthesized, no enantioselective syntheses of these compounds have so far been reported. Using the enantioselective synthetic route developed for nornicotine, anabasine, and anatabine, synthesis of enantiomerically pure forms of these compounds may be possible.

To better direct the next generation of compounds in these series, the computational models developed from the initial SAR study of the $\alpha 4\beta 2^*$ may be used predictively to determine active compounds *in silico*. Additionally, predictive models could be developed for nAChR subtypes that mediate DA release and $\alpha 7^*$ nAChR subtypes, as more data become available.

One of the advantages of the peripheral antagonists, DEC and HEX, is that their quaternary ammonium cationic nature does not allow for their passage into the central nervous system (CNS), therefore isolating their antagonist activity to nAChRs in the periphery. Although several of these compounds have excellent chloroform solubility and could theoretically pass into the CNS, it is not certain if a quaternary ammonium molecule can passively enter the blood-brain barrier (BBB). Active transport into the CNS, via the choline transporter may allow the passage of such quaternary ammonium molecules. Allen et al. (2003) have investigated NONI, NDNI, NOPI, binding to the BBB choline transporter and found that these salts do have affinity (27 – 49 μM) for the transporter binding site. Research on the *bis*-azaaromatic quaternary ammonium analogs, revealed that bPiDDB also had affinity for the BBB choline transporter (1.57 μM). Furthermore, it was determined that radiolabeled NONI and bPiDDB are both transported via the BBB choline transporter into the CNS (Allen *et al.* 2003; Geldenhuys *et al.* 2005). Another possible strategy for delivery of these pyridinium compounds across the BBB into the CNS involves the synthesis of a pyridinium head group designed to be a bioprecursor of these compounds. Bodor *et al.* (1990) have designed uncharged stable dihydropyridine analogs that do not rearomatize due to the presence of a C_3 or C_5

electron withdrawing substitution. Once the reduced product passes the BBB, the CNS enzyme monoamine oxidase-B (MAO-B) oxidizes the dihydropyridine analog to the quaternary ammonium compound that is active at neuronal nAChRs. This could be important in establishing a delivery method for this class of compounds, and would further the potential use of these compounds in nAChR related pathologies.

6.3. Conclusion

There is much to explore regarding the pharmacology of the neuronal nAChRs and the interaction of potential drug molecules with these receptors. The studies described herein have provided initial useful information that may be helpful in determining the functional properties of the individual nAChR subtypes, as well as in developing new synthetic methods for the preparation of novel compounds to add to the library of ligands available for probing the function of the various nAChR subtypes. Additionally, using established modeling techniques, new predictive models could be developed and utilized to increase the probability of success in the discovery of biologically active compounds with clinical potential. Using these methodologies allows for the successful identification of potent and selective nAChR ligands, of utility in unraveling the complexities of neuronal nAChRs, as well as having potential therapeutic uses in the clinic.

List of Abbreviations

α-Btx	α-Bungarotoxin
α-CBT	α-Cobratoxin
α-ctx	α-Conotoxins
5-HT	Serotonin
ACh	Acetylcholine
AChBP	Acetylcholine binding protein
AD	Alzheimer's disease
ADME	Absorption, distribution, metabolism, and elimination
AMPA	α-amino-3-hydroxy-5-methyl-4-isoxazolepropionate
ANOVA	One-way repeated-measure analysis of variance
Atx	(+)-Anatoxin-a
BBB	Blood-brain barrier
$CHCl_3$	Chloroform
CNS	Central nervous system
CoMFA	Comparative molecular field analysis
Cyt	Cytisine
DA	Dopamine
DAT	Dopamine transporter
DCEH	(R)-descholoroepibatidine
DEAD	Diethyl azodicarboxylate
DEC	Decamethonium
DHβE	Dihydro-β-erythroidine
DMF	*N*,*N*-Dimethylformamide
d-TC	*d*-Tubocurarine
Epi	Epibatidine
Et_3N	Triethylamine
EtOAc	Ethyl acetate
EtOH	Ethanol
ETX-a	Erabutoxin-a
ETX-b	Erabutoxin-b
FDA	Food and Drug Administration
$GABA_A$	Gamma-aminobutyric acid
GFA	Genetic functional approximation algorithm
HEK	Human embryonic kidney
HEPES	*N*-[2-Hydroxyethyl]piperazine-*N*'-[2-ethanesulfonic acid]
HEX	Hexamethonium
IND	Investigational new drug application
K*t*BuOH	Potassium *tert*-butoxide
LDA	Lithium diisopropylamide
L-DOPA	L-Dihydroxyphenylanine
LOB	Lobeline
LTX	Lophotoxin
MAO-B	Monoamine oxidase-B
MEC	Mecamylamine

MeOH	Methanol
MLA	Methyllycaconitine
MLS	Multiple least squares
MSA	Molecular shape analysis
nAChR	Nicotinic acetylcholine receptor
$NaHCO_3$	Sodium bicarbonate
NBS	*N*-bromosuccinimide
n-Btx	Neuronal bungarotoxin
NDA	New drug application
NIC	Nicotine
NMDA	*N*-Methyl-D-aspartate
NSAID	Nonsteroidal anti-inflammatory drug
NSTX	Neosurugatoxin
NT	Neurotransmitter
OCB	Open channel blockers
PD	Parkinson's disease
PEI	Polyethylenimine
PLS	Partial least squares
QSAR	Quantitative structure-activity relationship
R-NIC	R-(+)-Nicotine
SAR	Structure-activity relationship
SOM	Self-organizing map
THF	Tetrahydrofuran
THP	Tetrahydropyran
Trizma HCl	Tris[hydroxymethyl]-aminomethane hydrochloride

References

Abood, L. G., K. Shahid Salles and A. Maiti (1988). "Structure-activity studies of carbamate and other esters: agonists and antagonists to nicotine." Pharcol Biochem Behav **30**(2): 403-408.

Abramson, S. N., P. Culvert, T. Kline, L. Ying, P. Guest, L. Gutman and P. Taylor (1988). "Lophotoxin and related coral toxins covalently label the alpha-subunit of the nicotinic acetylcholine receptor." J Biol Chem **263**(34): 18568-18573.

Adams, M. E. and B. M. Olivera (1994). "Neurotoxins: overview of an emerging research technology." Trends Neurosci **17**(4): 151-5.

Adcock, C., G. R. Smith and M. S. Sansom (1998). "Electrostatics and the ion selectivity of ligand-gated channels." Biophys J **75**(3): 1211-22.

Adler, L. E., L. D. Hoffer, A. Wiser and R. Freedman (1993). "Normalization of auditory physiology by cigarette smoking in schizophrenic patients." Am J Psychiatry **150**(12): 1856-61.

Aiqiao, M., X. Xun, W. Lanjun and J. Yaozhong (1991). "Asymmetric synthesis XV: enantioselective sytheses of (R) or (S) -alpha-substituted -(2-pyridyl) methylamines via chiral pinanone ketimine template." Synth Comm **21**(21): 2207-2212.

Alkondon, M., E. F. Pereira, S. Wonnacott and E. X. Albuquerque (1992). "Blockade of nicotinic currents in hippocampal neurons defines methyllycaconitine as a potent and specific receptor antagonist." Mol Pharmacol **41**(4): 802-8.

Allen, D. D., P. R. Lockman, K. E. Roder, L. P. Dwoskin and P. A. Crooks (2003). "Active transport of high-affinity choline and nicotine analogs into the central nervous system by the blood-brain barrier choline transporter." J Pharmacol Exp Ther **304**(3): 1268-1274.

Amat, M., M. Canto, N. Llor and J. Bosch (2002). "Enantioselective synthesis of 2-arylpiperidines from chiral lactams. A concise synthesis of (-)-anabasine." Chem Comm: 526-527.

Anand, R., W. G. Conroy, R. Schoepfer, P. Whiting and J. Lindstrom (1991). "Neuronal nicotinic acetylcholine receptors expressed in Xenopus oocytes have a pentameric quaternary structure." J Biol Chem **266**(17): 11192-8.

Armstrong, D. W., X. Wang, J. T. Lee and Y. S. Liu (1999). "Enantiomeric composition of nornicotine, anatabine, and anabasine in tobacco." Chirality **11**: 82-84.

Arneric, S. P. and J. D. Brioni, Eds. (1999). Neuronal nicotinic receptors: pharmacology and therapeutic opportunities. New York, Wiley-Liss.

Arnold, S. E. and J. Q. Trojanowski (1996). "Recent advances in defining the neuropathology of schizophrenia." Acta Neuropathol (Berl) **92**(3): 217-31.

Ascher, P., W. A. Large and H. P. Rang (1979). "Studies on the mechanism of action of acetylcholine antagonists on rat parasympathetic ganglion cells." J Physiol **295**: 139-70.

Astles, P. C., S. R. Baker, J. R. Boot, L. M. Broad, C. P. Dell and M. Keenan (2002). "Recent progress in the development of subtype selective nicotinic acetylcholine receptor ligands." Curr Drug Targets -CNS & Neuro Disorders **1**: 337-348.

Ayers, J. T., A. Clauset, J. D. Schmitt, L. P. Dwoskin and P. A. Crooks (2005). "Molecular Modeling of mono- and bis-Quaternary Ammonium Salts as Ligands at the alpha4beta2* Nicotinic Acetylcholine Receptor Subtype Using Nonlinear Techniques." AAPS Journal **7**(3): Article 68.

Ayers, J. T., L. P. Dwoskin, A. G. Deaciuc, V. P. Grinevich, J. Zhu and P. A. Crooks (2002). "bis-Azaaromatic quaternary ammonium analogues: ligands for alpha4beta2* and alpha7* subtypes of neuronal nicotinic receptors." Bioorg & Med Chem Lett **12**(21): 3067-3071.

Azam, L., C. Dowell, M. Watkins, J. A. Stitzel, B. M. Olivera and J. M. McIntosh (2005). "Alpha-conotoxin BuIA, a novel peptide from Conus bullatus, distinguishes among neuronal nicotinic acetylcholine receptors." J Biol Chem **280**(1): 80-87.

Azam, L., U. H. Winzer-Serham, Y. Chen and F. M. Leslie (2002). "Expression of neuronal acetylcholine receptor subunit mRNAs within midbrain dopamine neurons." J Comp Neurol **444**: 260-274.

Badio, B. and J. W. Daly (1994). "Epibatidine, a potent analgetic and nicotinic agonist." Mol Pharmacol **45**(4): 563-9.

Badio, B., H. M. Garraffo, C. V. Plummer, W. L. Padgett and J. W. Daly (1997). "Synthesis and nicotinic activity of epiboxidine: an isoxazole analogue of epibatidine." Eur J Pharmacol **321**(2): 189-94.

Badio, B., W. L. Padgett and J. W. Daly (1997). "Ibogaine: a potent noncompetitive blocker of ganglionic/neuronal nicotinic receptors." Mol Pharmacol **51**(1): 1-5.

Balasubramanian, T. and A. Hassner (1998). "Asymmetric synthesis of functionalized piperidine derivatives: synthesis of (S)-anatabine." Tetrahedron: Asymmetry **9**: 2201-2205.

Bardo, M. T., R. A. Bevins, J. E. Klebaur, P. A. Crooks and L. P. Dwoskin (1997). "Nornicotine partially substitutes for (+)-amphetamine in a drug discrimination paradigm in rats." Pharmacol Biochem Behav **58**: 1083-1087.

Bardo, M. T., T. A. Green, P. A. Crooks and L. P. Dwoskin (1999). "Nornicotine is self-administered intravenously by rats." Psychopharmacology **146**: 290-296.

Barlow, R. B. and O. Johnson (1989). "Relations between structure and nicotine-like activity: X-ray crystal structure analysis of (-)-cytisine and (-)-lobeline hydrochloride and a comparison with (-)-nicotine and other nicotine-like compounds." Br J Pharmacol **98**(3): 799-808.

Barlow, R. B. and L. J. McLeod (1969). "Some studies on cytisine and its methylated derivatives." Br J Pharmacol **35**(1): 161-74.

Baron, J. A. (1996). "Beneficial effects of nicotine and cigarette smoking: the real, the possible and the spurious." Br Med Bull **52**(1): 58-73.

Bayram, E., P. Santago, R. Harris, Y.-D. Xiao, A. J. Clauset and J. D. Schmitt (2004). "Genetic algorithms and self-organizing maps: a powerful combination for modeling complex QSAR and QSPR problems." J Comp-Aided Mol Design **18**(7-9): 483-493.

Beers, W. H. and E. Reich (1970). "Structure and activity of acetylcholine." Nature **228**(275): 917-22.

Bencherif, M., C. M. Eisenhour, R. J. Prince, P. M. Lippiello and R. J. Lukas (1995). "The "calcium antagonist" TMB-8 [3,4,5-trimethoxybenzoic acid 8-

(diethylamino)octyl ester] is a potent, non-competitive, functional antagonist at diverse nicotinic acetylcholine receptor subtypes." J Pharmacol Exp Ther **275**(3): 1418-26.

Bencherif, M., K. Fowler, R. J. Lukas and P. M. Lippiello (1995). "Mechanisms of up-regulation of neuronal nicotinic acetylcholine receptors in clonal cell lines and primary cultures of fetal rat brain." J Pharmacol Exp Ther **275**(2): 987-94.

Bencherif, M. and J. D. Schmitt (2002). "Targeting neuronal nicotinic receptors: a path to new therapies." Curr Drug Targets -CNS & Neuro Disorders **1**: 349-357.

Bencherif, M., J. D. Schmitt, B. S. Bhatti, P. Crooks, W. S. Caldwell, M. E. Lovette, K. Fowler, L. Reeves and P. M. Lippiello (1998). "The heterocyclic substituted pyridine derivative (+/-)-2-(-3-pyridinyl)- 1-azabicyclo[2.2.2]octane (RJR-2429): a selective ligand at nicotinic acetylcholine receptors." J Pharmacol Exp Ther **284**(3): 886-94.

Benowitz, N. L. (1996). "Pharmacology of nicotine: addiction and therapeutics." Annu Rev Pharmacol Toxicol **36**: 597-613.

Bergmeier, S. C., D. J. Lapinsky, R. B. Free and D. B. McKay (1999). "Ring E analogs of methyllycaconitine (MLA) as novel nicotinic antagonists." Bioorg Med Chem Lett **9**(15): 2263-6.

Bertrand, D., M. Ballivet and D. Rungger (1990). "Activation and blocking of neuronal nicotinic acetylcholine receptor reconstituted in Xenopus oocytes." Proc Natl Acad Sci U S A **87**(5): 1993-7.

Bhat, R. V., M. J. Marks and A. C. Collins (1991). "Effects of chronic nicotine infusion on kinetics of high-affinity nicotine binding." J Neurochem **62**(2): 574-581.

Blackman, J. G., B. L. Ginsberg and C. Ray (1963). "Synaptic transmission in the sympathetic ganglion of the frog." 167 **J Physiol (Lond)**: 355-373.

Boulter, J., J. Connolly, E. Deneris, D. Goldman, S. Heinemann and J. Patrick (1987). "Functional expression of two neuronal nicotinic acetylcholine receptors from cDNA clones identifies a gene family." Proc Natl Acad Sci U S A **84**(21): 7763-7.

Boulter, J., A. O'Shea-Greenfield, R. M. Duvoisin, J. G. Connolly, E. Wada, A. Jensen, P. D. Gardner, M. Ballivet, E. S. Deneris, D. McKinnon and et al. (1990). "Alpha 3, alpha 5, and beta 4: three members of the rat neuronal nicotinic acetylcholine receptor-related gene family form a gene cluster." J Biol Chem **265**(8): 4472-82.

Brejc, K., W. J. van Dijk, R. V. Klaassen, M. Schuurmans, J. van Der Oost, A. B. Smit and T. K. Sixma (2001). "Crystal structure of an ACh-binding protein reveals the ligand-binding domain of nicotinic receptors." Nature **411**(6835): 269-76.

Briggs, C. A., D. J. Anderson, J. D. Brioni, J. J. Buccafusco, M. J. Buckley, J. E. Campbell, M. W. Decker, D. Donnelly-Roberts, R. L. Elliott, M. Gopalakrishnan, M. W. Holladay, Y. H. Hui, W. J. Jackson, D. J. Kim, K. C. Marsh, A. O'Neill, M. A. Prendergast, K. B. Ryther, J. P. Sullivan and S. P. Arneric (1997). "Functional characterization of the novel neuronal nicotinic acetylcholine receptor ligand GTS-21 in vitro and in vivo." Pharmacol Biochem Behav **57**(1-2): 231-41.

Briggs, C. A. and D. G. McKenna (1996). "Effect of MK-801 at the human alpha 7 nicotinic acetylcholine receptor." Neuropharmacology **35**(4): 407-14.

Brioni, J. D., M. W. Decker, J. P. Sullivan and S. P. Arneric (1997). "The pharmacology of (-)-nicotine and novel cholinergic channel modulators." Adv Pharmacol **37**: 153-214.

Buisson, B. and D. Bertrand (1998). "Open-channel blockers at the human alpha4beta2 neuronal nicotinic acetylcholine receptor." Mol Pharmacol **53**(3): 555-63.

Bush, L., H. W.P. and B. H. (1999). Chemical properties of nicotine and other tobacco-related compounds. Analytical determination of nicotine and related compounds and their metabolites. J. W. G. a. P. Jacob. New York, Elsevier**:** 69-147.

Cachelin, A. B. and G. Rust (1994). "Unusual pharmacology of (+)-tubocurarine with rat neuronal nicotinic acetylcholine receptors containing beta 4 subunits." Mol Pharmacol **46**(6): 1168-74.

Cachelin, A. B. and G. Rust (1995). "Beta-subunits co-determine the sensitivity of rat neuronal nicotinic receptors to antagonists." Pflugers Arch **429**(3): 449-51.

Cartier, G. E., D. Yoshikami, W. R. Gray, S. Luo, B. M. Olivera and J. M. McIntosh (1996). "A new alpha-conotoxin which targets alpha3beta2 nicotinic acetylcholine receptors." J Biol Chem **271**(13): 7522-8.

Castro, N. G. and E. X. Albuquerque (1993). "Brief-lifetime, fast-inactivating ion channels account for the alpha- bungarotoxin-sensitive nicotinic response in hippocampal neurons." Neurosci Lett **164**(1-2): 137-40.

Champtiaux, N., C. Gotti, M. Cordero-Erausquin, D. J. David, C. Przybylski, C. Lena, F. Clementi, M. Moretti, F. M. Rossi, N. Le Novere, J. M. McIntosh, A. M. Gardier and J. P. Changeux (2003). "Subunit composition of functional nicotinic receptors in dopaminergic neurons investigated with knock-out mice." J Neurosci **23**(21): 7820-7829.

Champtiaux, N., Z. Y. Han, A. Bessis, F. M. Rossi, M. Zoli, L. Marubio, J. M. McIntosh and J. P. Changeux (2002). "Distribution and pharmacology of alpha6-containing nicotinic acetylcholine receptors analyzed with mutant mice." J Neurosci **22**: 1208-1217.

Changeux, J. and S. J. Edelstein (2001). "Allosteric mechanisms in normal and pathological nicotinic acetylcholine receptors." Curr Opin Neurobiol **11**(3): 369-77.

Changeux, J. P., D. Bertrand, P. J. Corringer, S. Dehaene, S. Edelstein, C. Lena, N. Le Novere, L. Marubio, M. Picciotto and M. Zoli (1998). "Brain nicotinic receptors: structure and regulation, role in learning and reinforcement." Brain Res Brain Res Rev **26**(2-3): 198-216.

Charnet, P., C. Labarca, B. N. Cohen, N. Davidson, H. A. Lester and G. Pilar (1992). "Pharmacological and kinetic properties of alpha 4 beta 2 neuronal nicotinic acetylcholine receptors expressed in Xenopus oocytes." J Physiol **450**: 375-94.

Charpantier, E., P. Barneoud, P. Moser, F. Besnard and F. Sgard (1998). "Nicotinic acetylcholine subunit mRNA expression in dopaminergic neurons of the rat substantia nigra and ventral tegmental area." Neuroreport **9**(13): 3097-101.

Chavadarian, C. G., J. I. Seeman and J. B. Wooten (1983). "Synthesis of cis-2,3,3a,4,5,9b-hexahydro-1-methyl-1H- pyrrolo-[2,3-f]quinoline." J Org Chem **48**: 492-494.

Chavez-Noriega, L. E., J. H. Crona, M. S. Washburn, A. Urrutia, K. J. Elliott and E. C. Johnson (1997). "Pharmacological characterization of recombinant human neuronal nicotinic acetylcholine receptors h alpha 2 beta 2, h alpha 2 beta 4, h alpha 3 beta 2, h alpha 3 beta 4, h alpha 4 beta 2, h alpha 4 beta 4 and h alpha 7 expressed in Xenopus oocytes." J Pharmacol Exp Ther **280**(1): 346-56.

Chen, D. and J. W. Patrick (1997). "The alpha-bungarotoxin-binding nicotinic acetylcholine receptor from rat brain contains only the alpha7 subunit." J Biol Chem **272**(38): 24024-9.

Chen, J. Q., D. Galanakis, C. R. Ganellin, P. M. Dunn and D. H. Jenkinson (2000). "bis-Quinolinium cyclophanes: 8,14-diaza-1,7(1, 4)- diquinolinacyclotetradecaphane (UCL 1848), a highly potent and selective, nonpeptidic blocker of the apamin-sensitive Ca(2+)-activated K(+) channel." J Med Chem **43**(19): 3478-81.

Chiappinelli, V. A. (1983). "Kappa-bungarotoxin: a probe for the neuronal nicotinic receptor in the avian ciliary ganglion." Brain Res **277**(1): 9-22.

Chiappinelli, V. A., K. M. Wolf, C. Feng, L. Yum and L. L. McMahon (1993). "Different responses to opioids measured in terminals and somas of Edinger-Westphal neurons." Neuroscience **57**(2): 425-32.

Clarke, P. B., R. D. Schwartz, S. M. Paul, C. B. Pert and A. Pert (1985). "Nicotinic binding in rat brain: autoradiographic comparison of [3H]acetylcholine, [3H]nicotine, and [125I]-alpha-bungarotoxin." J Neurosci **5**(5): 1307-15.

Claudio, T., M. Ballivet, J. Patrick and S. Heinemann (1983). "Nucleotide and deduced amino acid sequences of Torpedo californica acetylcholine receptor gamma subunit." Proc Natl Acad Sci U S A **80**(4): 1111-5.

Co., R. J. R. T. (1999). US5952239. United States.

Co., R. J. R. T. (1999). Azatricyclic compounds with antinicotinic activity. US5986100. United States.

Co., R. J. R. T. (1999). Preparation of azatricyclo[3.3.1.13,7]decanes and related compounds as nicotinic antagonists. WO1999051602. World.

Co., R. J. R. T. (2000). Preparation of azatricyclo[3.3.1.13,7]decanes and related compounds as nicotinic antagonists. US6057446. United States.

Coe, J. W., P. R. Brooks, M. G. Vetelino, M. C. Wirtz, E. P. Arnold, J. Huang, S. B. Sands, T. I. Davis, L. A. Lebel, C. B. Fox, A. Shirkhande, J. H. Heym, E. Schaeffer, H. Rollema, Y. Lu, R. S. Mansbach, L. K. Chambers, C. C. Rovetti, D. W. Schulz, F. D. Tingley and B. T. O'Neill (2005). "Varenicline: an alpha4beta2 nicotinic receptor partial agonist for smoking cessation." J Med Chem **48**: 3474-3477.

Coe, J. W., M. G. Vetelino, C. G. Bashore, M. C. Wirtz, P. R. Brooks, E. P. Arnold, L. A. Lebel, C. B. Fox, S. B. Sands, T. I. Davis, D. W. Schulz, H. Rollema, F. D. Tingley and B. T. O'Neill (2005). "In pursuit of alpha4beta2 nicotinic receptor partial agonists for smoking cessation: carbon analogs of (-)-cystine." Bioorg Med Chem Lett **15**: 2974-2979.

Cohen, J. B., S. D. Sharp and W. S. Liu (1991). "Structure of the agonist-binding site of the nicotinic acetlycholine receptor. [3H]acetylcholine mustard identifies residues in the cation-binding subsite." J Biol Chem **266**: 23354-23364.

Collins, A. C., Y. Luo, S. Selvaag and M. J. Marks (1994). "Sensitivity to nicotine and brain nicotinic receptors are altered by chronic nicotine and mecamylamine infusion." J Pharmacol Exp Ther **271**: 125-133.

Colquhoun, D., F. Dreyer and R. E. Sheridan (1979). "The actions of tubocurarine at the frog neuromuscular junction." J Physiol **293**: 247-84.

Colquhoun, L. M. and J. W. Patrick (1997). "Pharmacology of neuronal nicotinic acetylcholine receptor subtypes." Adv Pharmacol **39**: 191-220.

Conroy, W. G., A. B. Vernallis and D. K. Berg (1992). "The alpha 5 gene product assembles with multiple acetylcholine receptor subunits to form distinctive receptor subtypes in brain." Neuron **9**(4): 679-91.

Cooper, E., S. Couturier and M. Ballivet (1991). "Pentameric structure and subunit stoichiometry of a neuronal nicotinic acetylcholine receptor." Nature **350**(6315): 235-8.

Copeland, J. R., A. Adem, P. Jacob III and A. Nordberg (1991). "A comparison of the binding of nicotine and nornicotine stereoisomers to nicotinic binding sites in rat brain cortex." Arch pharmacol **343**: 123-127.

Corrigall, W. A. and K. M. Coen (1989). "Nicotine maintains robust self-administration in rats on a limited-access schedule." Psychopharmacology **99**: 473-478.

Corringer, P. J., S. Bertrand, S. Bohler, S. J. Edelstein, J. P. Changeux and D. Bertrand (1998). "Critical elements determining diversity in agonist binding and desensitization of neuronal nicotinic acetylcholine receptors." J Neurosci **18**(2): 648-57.

Corringer, P. J., N. Le Novere and J. P. Changeux (2000). "Nicotnic receptors at the amino-acid level." Annu Rev Phamacol Toxicol **40**: 431-458.

Court, J. A., E. K. Perry, D. Spurden, S. Lloyd, J. I. Gillespie, P. Whiting and R. Barlow (1994). "Comparison of the binding of nicotinic agonists to receptors from human and rat cerebral cortex and from chick brain (alpha 4 beta 2) transfected into mouse fibroblasts with ion channel activity." Brain Res **667**(1): 118-22.

Creasy, K. R., M. I. Damaj, K. R. Dimen, W. S. Glassco, E. L. May and B. R. Martin (1996). "Structure-activity relationships for mecamylamine's antagonism of nicotine in the central nervous system." Med Chem Res: 535-542.

Crooks, P. A. (1999). Chemical properties of nicotine and other tobacco-related compounds. Analytical determination of nicotine and related compounds and their metabolites. J. W. Gorrod and P. Jacob. New York, Elsevier**:** 69-147.

Crooks, P. A., B. S. Bhatti, N. M. Deo, J. D. Schmitt, M. Bencherif and W. S. Caldwell (1998). Sythesis and structure-activity relationship of analogs of 2-(3-pyridyl-)-1-azabicyclo[2.2.2]octane, RJR-2429, a selective ligand at nicotinic acetylcholine receptors. Proceedings of the 216th American Chemical Society, Boston, MA.

Crooks, P. A. and L. P. Dwoskin (1997). "Contribution of CNS nicotine metabolites to the neuropharmacological effects of nicotine and tobacco smoking." Biochem Pharmacol **54**: 743-753.

Crooks, P. A., L. P. Dwoskin and M. T. Bardo (1998). Nornicotine enantiomers for use as a treatment for dopamine-related conditions and disease states. United States.

Crooks, P. A., C. S. Godin and W. F. Pool (1992). "Enantiomeric purity of nicotine in tobacco smoke." Med Sci Res **20**: 879-880.

Crooks, P. A., M. Li and L. P. Dwoskin (1997). "Metabolites of nicotine in rat brain after peripheral nicotine administration: cotinine, nornicotine and norcotinine." Drug Metab Disposit **25**: 47-54.

Crooks, P. A., A. Ravard, L. H. Wilkins, L. Teng, S. T. Buxton and L. P. Dwoskin (1995). "Inhibition of nicotine-evoked [3H]dopamine release by pyridino N-substituted nicotine analogues: a new class of nicotinic antagonist." Drug Dev Res **36**: 91-102.

Crooks, P. A., R. Xu, V. P. Grinevich, A. J. Haubner and L. P. Dwoskin (2000). "Conformationally restrained analogs of NONI and NDNI are selective antagonists at the putative alpha3beta2 nicotinic acetylcholine receptor (nAChR) subtype." Drug Alcohol Depend **60**(Supp 1): S46-S47.

Cui, C., T. K. Booker, R. S. Allen, S. R. Grady, P. Whiteaker, M. J. Marks, O. Salminen, T. Tritto, C. M. Butt, W. R. Allen, J. A. Stitzel, J. M. McIntosh, J. Boulter, A. C. Collins and S. F. Heinemann (2003). "The beta-3 nicotinic receptor subunit: a component of alpha-conotoxin MII-binding nicotinic acetylcholine receptors that modulate dopamine release and related behaviors." J Neurosci **23**(25): 11045-11053.

Dajas-Bailador, F., G. Costa, F. Dajas and S. Emmett (1998). "Effects of alpha-erabutoxin, alpha-bungarotoxin, alpha-cobratoxin and fasiculin on the nicotine-evoked release of dopamine in the rat striatum in vivo." Neurochem Int **33**: 307-312.

Daly, J. W., Y. Nishizawa, M. W. Edwards, J. A. Waters and R. S. Aronstam (1991). "Nicotinic receptor-elicited sodium flux in rat pheochromocytoma PC12 cells: effects of agonists, antagonists, and noncompetitive blockers." Neurochem Res **16**(4): 489-500.

Damaj, M. I., Fei-Yin, M. M. Dukat, W. Glassco, R. A. Glennon and B. R. Martin (1998). "Antinociceptive responses to nicotinic acetylcholine receptor ligands after systemic and intrathecal administration in mice." J Pharmacol Exp Ther **284**: 1058-1065.

Damaj, M. I., E. M. Meyer and B. R. Martin (2000). "The antinociceptive effects of alpha7 nicotinic agonists in an acute pain model." Neuropharmacology **39**(13): 2785-91.

Damaj, M. I., G. S. Patrick, K. R. Creasy and B. R. Martin (1997). "Pharmacology of lobeline, a nicotinic receptor ligand." J Pharmacol Exp Ther **282**(1): 410-9.

D'Andrea, M. R., R. Nagele, D. H. S. Lee and H.-Y. Wang (2002). "Targeting intracellular Abeta for Alzheimer's disease drug discovery." 56(194-200).

D'Andrea, M. R. and R. G. Nagele (2006). "Targeting the alpha 7 nicotinic acetylcholine receptor to reduce amyloid accumulation in Alzheimer's disease pyramidal neurons." Curr Pharm Design **12**(6): 677-684.

Dani, J. A., M. Biasi, Y. Liang, J. Peterson, L. Zhang, T. Zhang and F. M. Zhou (2004). "Potential applications of nicotinic ligands in the laboratory and clinic." Bioorg Med Chem Lett **14**: 1837-1839.

Davies, A. R., D. J. Hardick, I. S. Blagbrough, B. V. Potter, A. J. Wolstenholme and S. Wonnacott (1999). "Characterisation of the binding of [3H]methyllycaconitine: a new radioligand for labelling alpha 7-type neuronal nicotinic acetylcholine receptors." Neuropharmacology **38**(5): 679-90.

de Fiebre, C. M., E. M. Meyer, J. C. Henry, S. I. Muraskin, W. R. Kem and R. L. Papke (1995). "Characterization of a series of anabaseine-derived compounds reveals that the 3-(4)-dimethylaminocinnamylidine derivative is a selective agonist at neuronal nicotinic alpha 7/125I-alpha-bungarotoxin receptor subtypes." Mol Pharmacol **47**(1): 164-171.

De Luca, V., A. H. C. Wong, D. J. Muller, G. W. H. Wong, R. F. Tyndale and J. L. Kennedy (2004). "Evidence of association between smoking and alpha7 nicotinic

receptor subunit gene in schizophrenia patients." Neuropsychopharmacology **29**: 1522-1526.

Decker, M. W., D. J. Anderson, J. D. Brioni, D. L. Donnelly-Roberts, C. H. Kang, A. B. O'Neill, M. Piattoni-Kaplan, S. Swanson and J. P. Sullivan (1995). "Erysodine, a competitive antagonist at neuronal nicotinic acetylcholine receptors." Eur J Pharmacol **280**(1): 79-89.

Decker, M. W., J. D. Brioni, A. W. Bannon and S. P. Arneric (1995). "Diversity of neuronal nicotinic acetylcholine receptors: lessons from behavior and implications for CNS therapeutics." Life Sci **56**(8): 545-70.

Decker, M. W., P. Curzon, J. D. Brioni and S. P. Arneric (1994). "Effects of ABT-418, a novel cholinergic channel ligand, on place learning in septal-lesioned rats." Eur J Pharmacol **261**(1-2): 217-22.

Decker, M. W. and M. D. Meyer (1999). "Therapeutic potential of neuronal nicotinic acetylcholine receptor agonists as novel analgesics." Biochem Pharmacol **58**(6): 917-23.

Deneris, E. S., J. Boulter, L. W. Swanson, J. Patrick and S. Heinemann (1989). "Beta 3: a new member of nicotinic acetylcholine receptor gene family is expressed in brain." J Biol Chem **264**(11): 6268-72.

Deneris, E. S., J. Connolly, J. Boulter, E. Wada, K. Wada, L. W. Swanson, J. Patrick and S. Heinemann (1988). "Primary structure and expression of beta 2: a novel subunit of neuronal nicotinic acetylcholine receptors." Neuron **1**(1): 45-54.

Deo, N. M. and P. A. Crooks (1996). "Regioselective alkylation of N-(diphenylmethylidine)-3-(aminomethyl)pyridine: a simple route to minor tobacco alkaloids and related compounds." Tetrahedron Lett **37**: 1137-1140.

Domino, E. F., L. Ni and H. Zhang (1999). "Nicotine alone and in combination with L-DOPA methyl ester or the D2 agonist N-0923 in MPTP-induced chronic hemiparkinsonian monkeys." Exp Neurol **158**: 395-402.

Donnelly-Roberts, D. L., P. S. Puttfarcken, T. A. Kuntzweiler, C. A. Briggs, D. J. Anderson, J. E. Campbell, M. Piattoni-Kaplan, D. G. McKenna, J. T. Wasicak, M. W. Holladay, M. Williams and S. P. Arneric (1998). "ABT-594 [(R)-5-(2-azetidinylmethoxy)-2-chloropyridine]: a novel, orally effective analgesic acting via neuronal nicotinic acetylcholine receptors: I. In vitro characterization." J Pharmacol Exp Ther **285**(2): 777-86.

Dowell, C., B. M. Olivera, J. E. Garrett, S. T. Staheli, M. Watkins, A. Kuryatov, D. Yoshikami, J. M. Lindstrom and J. M. McIntosh (2003). "Alpha-conotoxin PIA is selective for alpha6 subunit-containing nicotinic acetylcholine receptors." J Neurosci **23**(24): 8445-8452.

Drasdo, A., M. Caulfield, D. Bertrand and S. Wonnacott (1992). "Methyllycaconitine: a novel nicotinic antagonist." Mol Cell Neurosci **3**: 237-243.

Dukat, M., W. Fiedler, D. Dumas, I. Damaj, B. R. Martin, J. A. Rosencrans, J. R. James and R. A. Glennon (1996). "Pyrrolidine-modified and 6-substituted analogs of nicotine: a structure-affinity investigation." Eur J Med Chem **31**: 875-888.

Dwoskin, L. P., S. T. Buxton, A. L. Jewell and P. A. Crooks (1993). "S(-)-Nornicotine increases dopamine release in a calcium-dependent manner from superfused rat striatal slices." J Neurochem **60**: 2167-2174.

Dwoskin, L. P. and P. A. Crooks (2001). "Competitive neuronal nicotinic receptor antagonists: a new direction for drug discovery." J Pharmacol Exp Ther **298**(2): 395-402.

Dwoskin, L. P. and P. A. Crooks (2002). "A novel mechanism of action and potential use for lobeline as a treatment for psychostimulant abuse." Biochem Pharmacol **63**: 89-98.

Dwoskin, L. P., L. Teng, S. T. Buxton and P. A. Crooks (1999). "(S)-(-)-Cotinine, the major brain metabolite of nicotine, stimulates nicotinic receptors to evoke [3H]dopamine release from rat striatal slices in a calcium-dependent manner." J Pharmacol Exp Ther **288**(3): 905-11.

Dwoskin, L. P., L. Teng, S. T. Buxton, A. Ravard, N. Deo and P. A. Crooks (1995). "Minor alkaloids of tobacco release [3H]dopamine from superfused rat striatal slices." Europ J Pharmacol **276**: 195-199.

Dwoskin, L. P., L. H. Wilkins, J. R. Pauly and P. A. Crooks (1999). "Development of a novel class of subtype-selective nicotinic receptor antagonist: pyridine-N-substituted nicotine analogs." Ann N Y Acad Sci **868**: 617-9.

Dwoskin, L. P., R. Xu, J. T. Ayers and P. A. Crooks (2000). "Recently developments in neuronal nicotinic acetylcholine receptor anatagonists." Curr Opin Ther Patents **10**(10): 1561-1581.

Dwoskin, L. P. and N. R. Zahniser (1986). "Robust modulation of [3H]dopamine release from rat striatal slices by D- 2 dopamine receptors." J Pharmacol Exp Ther **239**(2): 442-53.

el-Bizri, H. and P. B. Clarke (1994). "Blockade of nicotinic receptor-mediated release of dopamine from striatal synaptosomes by chlorisondamine administered in vivo." Br J Pharmacol **111**(2): 414-8.

el-Bizri, H. and P. B. Clarke (1994). "Blockade of nicotinic receptor-mediated release of dopamine from striatal synaptosomes by chlorisondamine and other nicotinic antagonists administered in vitro." Br J Pharmacol **111**(2): 406-13.

Elgoyhen, A. B., D. E. Vetter, E. Katz, C. V. Rothlin, S. F. Heinemann and J. Boulter (2001). "alpha10: a determinant of nicotinic cholinergic receptor function in mammalian vestibular and cochlear mechanosensory hair cells." Proc Natl Acad Sci U S A **98**(6): 3501-6.

Ellison, M., F. Gao, H.-L. Wang, S. M. Sine, J. M. McIntosh and B. M. Olivera (2004). "Alpha-conotoxins ImI and ImII target distinct regions of the human alpha7 nicotinic acetylcholine receptor and distinguish human nicotinic receptor subtypes." Biochem **43**: 16019-16026.

Ellison, M., J. M. McIntosh and B. M. Olivera (2003). "Alpha-conotoxins ImI and ImII." J Biol Chem **278**(2): 757-764.

Erenberg, G., R. P. Cruse and A. D. Rothner (1987). "The natural history of Tourette syndrome: a follow-up study." Ann Neurol **22**(3): 383-5.

Everhart, D., E. Reiller, A. Mirzoian, J. M. McIntosh, A. Malhotra and C. W. Luetje (2003). "Identification of residues that confer alpha-conotoxin PnIA sensitivity on the alpha3 subunit of neuronal nicotinic acetylcholine receptors." J Pharmacol Exp Ther **306**: 664-670.

Everitt, B. J. and T. W. Robbins (1997). "Central cholinergic systems and cognition." Annu Rev Psychol **48**: 649-84.

Felpin, F. X., S. Girard, G. Vo-Thanh, R. J. Robins, J. Villieras and J. Lebreton (2001). "Efficient enantiomeric synthesis of pyrrolidine and piperidine alkaloids from tobacco." J Org Chem **66**(19): 6305-12.

Fenster, C. P., M. F. Rains, B. Noerager, M. W. Quick and R. A. Lester (1997). "Influence of subunit composition on desensitization of neuronal acetylcholine receptors at low concentrations of nicotine." J Neurosci **17**(15): 5747-59.

Flores, C. M., S. W. Rogers, L. A. Pabreza, B. B. Wolfe and K. J. Kellar (1992). "A subtype of nicotinic cholinergic receptor in rat brain is composed of alpha 4 and beta 2 subunits and is up-regulated by chronic nicotine treatment." Mol Pharmacol **41**(1): 31-7.

Flynn, D. D. and D. C. Mash (1986). "Characterization of L-[3H]nicotine binding in human cerebral cortex: comparison between Alzheimer's disease and the normal." J Neurochem **47**(6): 1948-54.

Fratiglioni, L. and H.-X. Wang (2000). "Smoking and Parkinson's and Alzheimer's disease: review of the epidemiological studies." Behav Brain Res **113**: 117-120.

Frazier, C. J., A. V. Buhler, J. L. Weiner and T. V. Dunwiddie (1998). "Synaptic potentials mediated via alpha-bungarotoxin-sensitive nicotinic acetylcholine receptors in rat hippocampal interneurons." J Neurosci **18**(20): 8228-35.

Freedman, R., H. Coon, M. Myles-Worsley, A. Orr-Urteger, A. Olincy, A. Davis, M. Polymeropoulos, J. Holik, J. Hopkins, M. Hoff, J. Rosenthal, M. C. Waldo, F. Reimherr, P. Wender, J. Yaw, D. A. Young, C. R. Breese, C. Adams, D. Patterson, L. E. Alder, L. Kruglyak, S. Leonard and W. Byerley (1997). "Linkage of a neurophysiological deficit in schizophrenia to a chromosome 15 locus." Proc Natl Acad Sci USA **94**: 587-592.

Freedman, R., M. Hall, L. E. Adler and S. Leonard (1995). "Evidence in postmortem brain tissue for decreased numbers of hippocampal nicotinic receptors in schizophrenia." Biol Psychiatry **38**(1): 22-33.

Fruchart-Gaillard, C., B. Gilquin, S. Antil-Delbeke, N. Le Novere, T. Tamiya, P. J. Corringer, J. P. Changeux and A. Menez (2002). "Experimentally based model of a complex between a snake toxin and the alpha 7 nicotinic receptor." Proc Natl Acad Sci USA **99**: 3216-3221.

Garvey, D. S., J. T. Wasicak, R. L. Elliott, S. A. Lebold, A. M. Hettinger, G. M. Carrera, N. H. Lin, Y. He, M. W. Holladay, D. J. Anderson and et al. (1994). "Ligands for brain cholinergic channel receptors: synthesis and in vitro characterization of novel isoxazoles and isothiazoles as bioisosteric replacements for the pyridine ring in nicotine." J Med Chem **37**(26): 4455-63.

Geldenhuys, W. J., P. R. Lockman, T. H. Nguyen, C. J. Van der Schyf, P. A. Crooks, L. P. Dwoskin and D. D. Allen (2005). "3D-QSAR study of bis-azaaromatic quaternary ammonium analogs at the blood-brain barrier choline transporter." Bioorg Med Chem **13**: 4253-4261.

Gentry, C. L., L. H. Wilkins, Jr. and R. J. Lukas (2003). "Effects of prolonged nicotinic ligand exposure on function of heterologously expressed, human alpha4beta2- and alpha4beta4-nicotinic acetylcholine receptors." J Pharmacol Exp Ther **304**: 206-216.

George, T. P. and S. S. O'Malley (2004). "Current pharmacological treatments for nicotine dependence." Trends in Pharmacol Sciences **25**(1): 42-48.

German, D. C., K. Manaye, W. K. Smith, D. J. Woodward and C. B. Saper (1989). "Midbrain dopaminergic cell loss in Parkinson's disease: computer visualization." Ann Neurol **26**(4): 507-14.

Gerzanich, V., R. Anand and J. Lindstrom (1994). "Homomers of alpha 8 and alpha 7 subunits of nicotinic receptors exhibit similar channel but contrasting binding site properties." Mol Pharmacol **45**(2): 212-20.

Gerzanich, V., X. Peng, F. Wang, G. Wells, R. Anand, S. Fletcher and J. Lindstrom (1995). "Comparative pharmacology of epibatidine: a potent agonist for neuronal nicotinic acetylcholine receptors." Mol Pharmacol **48**(4): 774-82.

Gerzanich, V., F. Wang, A. Kuryatov and J. Lindstrom (1998). "alpha 5 Subunit alters desensitization, pharmacology, Ca++ permeability and Ca++ modulation of human neuronal alpha 3 nicotinic receptors." J Pharmacol Exp Ther **286**(1): 311-20.

Ghosheh, O., L. P. Dwoskin, W. K. Li and P. A. Crooks (1999). "Residence times and half-lives of nicotine metabolites in rat brain after acute peripheral administration of [2'-14C]nicotine." Drug Metab Disposit **27**: 1448-1455.

Ghosheh, O., L. P. Dwoskin, D. K. Miller and P. A. Crooks (2001). "Accumulation of nicotine and its metabolites in rat brain after intermittent or continuous peripheral administration of [2'-14C]-nicotine." Drug Metab Disposit **29**: 645-651.

Girod, R., G. Crabtree, G. Ernstrom, J. Ramirez-Latorre, D. McGehee, J. Turner and L. Role (1999). "Heteromeric complexes of alpha 5 and/or alpha 7 subunits. Effects of calcium and potential role in nicotine-induced presynaptic facilitation." Ann N Y Acad Sci **868**: 578-90.

Glassco, W., J. Suchocki, C. George, B. R. Martin and E. L. May (1993). "Synthesis, optical resolution, absolute configuration, and preliminary pharmacology of (+)- and (-)-cis-2,3,3a,4,5,9b-hexahydro-1-methyl-1H- pyrrolo-[3,2-h]isoquinoline, a structural analog of nicotine." J Med Chem **36**(22): 3381-5.

Glennon, R. A. and M. Dukat (2004). "alpha4beta2 nACh receptor pharmacophore models." Bioorg Med Chem Lett **14**: 1841-1844.

Glennon, R. A., M. Dukat and L. Liao (2004). "Musings on alpha4beta2 nicotinic acetylcholine (nACh) receptor pharmacophore models." Curr Topics Med Chem **4**: 631-644.

Glover, E. D., S. J. Leischow, S. I. Rennard, P. N. Glover, D. Daughton, J. N. Quiring, F. H. Schneider and P. J. Mione (1998). "A smoking cessation trial with lobeline sulfate: a pilot study." Am J Health Behave **22**: 62-74.

Gokhale, V. and V. Kulkarni (2000). "Understanding the antifungal activity of terbinafine analogues using structure-activity relationship (QSAR) models." Bioorg & Med Chem **8**(10): 2487-2499.

Goldman, D., E. Deneris, W. Luyten, A. Kochhar, J. Patrick and S. Heinemann (1987). "Members of a nicotinic acetylcholine receptor gene family are expressed in different regions of the mammalian central nervous system." Cell **48**(6): 965-73.

Goldner, F. M., K. T. Dineley and J. W. Patrick (1997). "Immunohistochemical localization of the nicotinic acetylcholine receptor subunit alpha6 to dopaminergic neurons in the substantia nigra and ventral tegmental area." Neuroreport **8**(12): 2739-42.

Gopalakrishnan, M., B. Buisson, E. Touma, T. Giordano, J. E. Campbell, I. C. Hu, D. Donnelly-Roberts, S. P. Arneric, D. Bertrand and J. P. Sullivan (1995). "Stable expression and pharmacological properties of the human alpha 7 nicotinic acetylcholine receptor." Eur J Pharmacol **290**(3): 237-46.

Gopalakrishnan, M., L. M. Monteggia, D. J. Anderson, E. J. Molinari, M. Piattoni-Kaplan, D. Donnelly-Roberts, S. P. Arneric and J. P. Sullivan (1996). "Stable expression, pharmacologic properties and regulation of the human neuronal nicotinic acetylcholine alpha 4 beta 2 receptor." J Pharmacol Exp Ther **276**(1): 289-97.

Gotti, C., E. Carbonnelle, M. Moretti, R. Zwart and F. Clementi (2000). "Drugs selective for nicotinic receptor subtypes: a real possibility or a dream?" Behav Brain Res **113**(1-2): 183-92.

Gotti, C., W. Hanke, K. Maury, M. Moretti, M. Ballivet, F. Clementi and D. Bertrand (1994). "Pharmacology and biophysical properties of alpha 7 and alpha 7-alpha 8 alpha-bungarotoxin receptor subtypes immunopurified from the chick optic lobe." Eur J Neurosci **6**(8): 1281-91.

Grady, S., M. J. Marks, S. Wonnacott and A. C. Collins (1992). "Characterization of nicotinic receptor-mediated [3H]dopamine release from synaptosomes prepared from mouse striatum." J Neurochem **59**(3): 848-56.

Grady, S. R., E. U. Grun, M. J. Marks and A. C. Collins (1997). "Pharmacological comparison of transient and persistent [3H]dopamine release from mouse striatal synaptosomes and response to chronic L- nicotine treatment." J Pharmacol Exp Ther **282**(1): 32-43.

Grady, S. R., N. M. Meinerz, J. Cao, A. M. Reynolds, M. R. Picciotto, J. P. Changeux, J. M. McIntosh, M. J. Marks and A. C. Collins (2001). "Nicotinic agonists stimulate acetylcholine release from mouse interpeduncular nucleus: a function mediated by a different nAChR than dopamine release from striatum." J Neurochem **76**(1): 258-68.

Gray, R., A. S. Rajan, K. A. Radcliffe, M. Yakehiro and J. A. Dani (1996). "Hippocampal synaptic transmission enhanced by low concentrations of nicotine." Nature **383**(6602): 713-6.

Green, T. A., P. A. Crooks, M. T. Bardo and L. P. Dwoskin (2001). "Contributory role for nornicotine neuropharmacology: nornicotine-evoked [3H]dopamine overflow from rat nucleus accumbens slices." Biochem Pharmacol **62**: 1597-1603.

Green, T. A., S. B. Phillips, P. A. Crooks, L. P. Dwoskin and M. T. Bardo (2000). "Nornicotine pretreatment decreases intravenous nicotine self-administration in rats." Psychopharmacology **152**: 289-294.

Grilli, M., M. Parodi, M. Raiteri and M. Marchi (2005). "Chronic nicotine differentially affects the function of nicotinic receptor subtypes regulating neurotransmitter release." J Neurochem **93**: 1353-1360.

Grinevich, V. P., P. A. Crooks, P. Sumithran, A. J. Haubner, J. T. Ayers and L. P. Dwoskin (2003). "N-n-Alkylpyridinium analogs, a novel class of nicotinic receptor antagonists: selective inhibition of nicotine-evoked [3H]dopamine overflow from superfused rat striatal." J Pharmacol Exp Ther **306**: 1011-1020.

Groebe, D. R. and S. N. Abramson (1995). "Lophotoxin is a slow binding irreversible inhibitor of nicotinic acetylcholine receptors." J Biol Chem **270**(1): 281-286.

Grutter, T. and J. P. Changeux (2001). "Nicotinic receptors in wonderland." Trends Biochem Sci **26**(8): 459-63.
Grutter, T., L. Ehret-Sabatier, F. Kotzyba-Hibert and M. Goeldner (2000). "Photoaffinity labeling of Torpedo nicotinic receptor with the agonist [3H]DCTA: identification of amino acid residues which contribute to the binding of the ester moiety of acetylcholine." Biochemistry **39**: 3034-3043.
Grutter, T., N. Le Novere and J. P. Changeux (2004). "Rational understanding of nicotinic receptors drug binding." Curr Top Med Chem **4**: 645-651.
Hacksell, U. and C. Mellin (1989). "Stereoselectivity of nicotinic receptors." Prog Brain Res **79**: 95-100.
Hajek, P., R. West, J. Foulds, F. Nilsson, S. Burrows and A. Meadow (1999). "Randomized comparative trial of nicotine polacrilex, a transdermal patch, nasal spray, and an inhaler." Arch Intern Med **159**(17): 2033-8.
Hardick, D. J., G. Cooper, T. Scott-Ward, I. S. Blagbrough, B. V. Potter and S. Wonnacott (1995). "Conversion of the sodium channel activator aconitine into a potent alpha 7-selective nicotinic ligand." FEBS Lett **365**(1): 79-82.
Harvey, S. C. and C. W. Luetje (1996). "Determinants of competitive antagonist sensitivity on neuronal nicotinic receptor beta subunits." J Neurosci **16**(12): 3798-806.
Harvey, S. C., J. M. McIntosh, G. E. Cartier, F. N. Maddox and C. W. Luetje (1997). "Determinants of specificity for alpha-conotoxin MII on alpha3beta2 neuronal nicotinic receptors." Mol Pharmacol **51**(2): 336-42.
Hey, P. (1952). "On relationships between structure and nicotine-like stimulant activity in choline esters and ethers." Br J Pharmacol **7**: 117-129.
Hogg, R. C. and D. Bertrand (2004). "Nicotinic acetylcholine receptors as drug targets." Current Drug Targets - CNS & Neurological Disorders **3**: 123-130.
Holladay, M. W., M. J. Dart and J. K. Lynch (1997). "Neuronal nicotinic acetylcholine receptors as targets for drug discovery." J Med Chem **40**(26): 4169-94.
Houghtling, R. A., M. I. Davila-Garcia and K. J. Kellar (1995). "Characterization of (+/-)(-)[3H]epibatidine binding to nicotinic cholinergic receptors in rat and human brain." Mol Pharmacol **48**(2): 280-7.
Huang, X., F. Zheng, P. A. Crooks, L. P. Dwoskin and C.-G. Zhan (2005). "Modeling multiple species of nicotine and deschloroepibatidine interacting with alpha4beta2 nicotinic acetylcholine receptor: from microscopic binding to phenomenological binding affinity." J Am Chem Soc**?????**: ????
Imoto, K., C. Busch, B. Sakmann, M. Mishina, T. Konno, J. Nakai, H. Bujo, Y. Mori, K. Fukuda and S. Numa (1988). "Rings of negatively charged amino acids determine the acetylcholine receptor channel conductance." Nature **335**(6191): 645-8.
Jacyno, J. M., J. S. Harwood, N. H. Lin, J. E. Campbell, J. P. Sullivan and M. W. Holladay (1996). "Lycaconitine revisited: partial synthesis and neuronal nicotinic acetylcholine receptor affinities." J Nat Prod **59**(7): 707-9.
Janes, R. W. (2005). "Alpha-conotoxins as selective probes for nicotinic acetylcholine receptor subclasses." Curr Opinion in Pharmacology **5**: 280-292.
Johnson, D. S., J. Martinez, A. B. Elgoyhen, S. F. Heinemann and J. M. McIntosh (1995). "alpha-Conotoxin ImI exhibits subtype-specific nicotinic acetylcholine receptor

blockade: preferential inhibition of homomeric alpha 7 and alpha 9 receptors." Mol Pharmacol **48**(2): 194-9.

Kaiser, S. A., L. Soliakov, S. C. Harvey, C. W. Luetje and S. Wonnacott (1998). "Differential inhibition by alpha-conotoxin-MII of the nicotinic stimulation of [3H]dopamine release from rat striatal synaptosomes and slices." J Neurochem **70**(3): 1069-76.

Kao, P. N. and A. Karlin (1986). "Acetylcholine receptor binding site contains a disulfide cross-link between adjacent half-cystinyl residues." J Biol Chem **261**: 2085-8088.

Karadsheh, M. S., M. S. Shah, X. Tang, R. I. Macdonald and J. A. Stitzel (2004). "Functional characterization of mouse alpha4beta2 nicotinic acetylcholine receptors stably expressed in HEK293T cells." J Neurochem **91**: 1138-1150.

Karlin, A. (2002). "Emerging structure of the nicotinic acetylcholine receptors." Nature Reviews **3**: 102-114.

Karlin, A. and M. H. Akabas (1995). "Toward a structural basis for the function of nicotinic acetylcholine receptors and their cousins." Neuron **15**(6): 1231-44.

Kem, W. R. (1997). "Alzheimer's drug design based upon an invertebrate toxin (anabaseine) which is a potent nicotinic receptor agonist." Invert Neurosci **3**(2-3): 251-9.

Kem, W. R., V. M. Mahnir, R. L. Papke and C. J. Lingle (1997). "Anabaseine is a potent agonist on muscle and neuronal alpha- bungarotoxin-sensitive nicotinic receptors." J Pharmacol Exp Ther **283**(3): 979-92.

Khiroug, S. S., L. Khiroug and J. L. Yakel (2004). "Rat nicotinic acetylcholine receptor alpha2beta2 channels: comparison of functional properties with alpha4beta2 channels in Xenopus oocytes." Neuroscience **124**: 817-822.

Kier, L. B. (1968). "A molecular orbital calculation of the preferred conformation of nicotine." Mol Pharmacol **4**(1): 70-6.

Klink, R., A. K. d'Exaerde, M. Zoli and J. P. Changeux (2001). "Molecular and physiological diversity of nicotinic acetylcholine receptors in the midbrain dopaminargic nuclei." J Neurosci **21**: 1452-1463.

Kohonen, T. (2001). Self-organizing maps. Berlin, Springer.

Kuo, Y.-P., L. Xu, J. B. Eaton, L. Zhao, J. Wu and R. J. Lukas (2005). "Roles of nicotinic acetylcholine receptor subunit large cytoplasmic loop sequences in receptor expression and function." J Phar Exp Ther **314**: 455-466.

Kuryatov, A., F. Olale, J. Cooper, C. Choi and J. Lindstrom (2000). "Human alpha6 AChR subtypes: subunit composition, assembly, and pharmacological responses." Neuropharmacol **39**(13): 2570-2590.

Kyerematen, G. A., M. Morgan, B. Chattopadhyay, J. D. deBethizy and E. S. Vesell (1990). "Disposition of nicotine and eight metabolites in smokers and nonsmokers: identification in smokers of two metabolites that are longer lived than cotinine." Clin Pharmacol Therap **48**: 641-651.

Lai, A., N. Parameswaran, M. Khwaja, P. Whiteaker, J. M. Lindstrom, H. Fan, J. M. McIntosh, S. R. Grady and M. Quik (2005). "Long-term nicotine treatment decreases striatal alpha6* nicotinic acetylcholine receptor sites and function in mice." Mol Pharmacol **67**(5): 1639-1647.

Lawrence, A. D. and B. J. Sahakian (1998). "The cognitive psychopharmacology of Alzheimer's disease: focus on cholinergic systems." Neurochem Res **23**(5): 787-94.

Le Novere, N., T. Grutter and J. P. Changeux (2002). "Models of the extracellular domain of the nicotinic receptors and of the agonist- and Ca2+-binding sites." Proc Nat Acad Sci USA **99**: 3210-3215.

Lee, C. Y. (1972). "Chemistry and pharmacology of polypeptide toxins in snake venoms." Annu Rev Pharmacol **12**: 265-86.

Lena, C. and J. P. Changeux (1997). "Pathological mutations of nicotinic receptors and nicotine-based therapies for brain disorders." Curr Opin Neurobiol **7**(5): 674-82.

Leonard, R. J., C. G. Labarca, P. Charnet, N. Davidson and H. A. Lester (1988). "Evidence that the M2 membrane-spanning region lines the ion channel pore of the nicotinic receptor." Science **242**(4885): 1578-81.

Lin, N. and M. D. Meyer (1998). "Recent developments in neuronal nicotinic acetylcholine receptor modulators." Exp Opin Ther Patents **8**(8): 991-1015.

Lindstrom, J. (1997). "Nicotinic acetylcholine receptors in health and disease." Mol Neurobiol **15**(2): 193-222.

Lippiello, P. M., M. Bencherif, J. A. Gray, S. Peters, G. Grigoryan, H. Hodges and A. C. Collins (1996). "RJR-2403: a nicotinic agonist with CNS selectivity II. In vivo characterization." J Pharmacol Exp Ther **279**(3): 1422-9.

Lloyd, G. K. and M. Williams (2000). "Neuronal nicotinic acetylcholine receptors as novel drug targets." J Pharmacol Exp Ther **292**(2): 461-7.

Lloyd, K. G., L. Davidson and O. Hornykiewicz (1975). "The neurochemistry of Parkinson's disease: effect of L-dopa therapy." J Pharmacol Exp Ther **195**(3): 453-64.

Loh, T., J. Zhou, X. Li and K. Sim (1999). "A novel reductive aminocyclization for the sytheses of chiral pyrrolidines: stereoselective syntheses of (S)-nornicotine adn 2-(2'-pyrrolidyl)-pyridines." Tetrahedron Lett **40**: 7847-7850.

Lohr, J. B. and K. Flynn (1992). "Smoking and schizophrenia." Schizophr Res **8**: 93-102.

Luetje, C. W. (2004). "Getting past the asterisk: the subunit composition of the presynaptic nicotinic receptors that modulate striatal dopamine release." Mol Pharmacol **65**: 1333-1335.

Luetje, C. W., N. M. Floyd and S. C. Harvey (1998). "Glycosylation within the cysteine loop and six residues near conserved cys192/cys193 are determinants of neuronal bungarotoxin sensitivity on the neuronal nicotinic receptor alpha3 subunit." Mol Pharmacol **53**(6): 1112-1119.

Luetje, C. W. and J. Patrick (1991). "Both alpha- and beta-subunits contribute to the agonist sensitivity of neuronal nicotinic acetylcholine receptors." J Neurosci **11**(3): 837-45.

Luetje, C. W., K. Wada, S. Rogers, S. N. Abramson, K. Tsuji, S. Heinemann and J. Patrick (1990). "Neurotoxins distinguish between different neuronal nicotinic acetylcholine receptor subunit combinations." J Neurochem **55**(2): 632-40.

Lukas, R. J. (1993). "Expression of ganglia-type nicotinic acetylcholine receptors and nicotinic ligand binding sites by cells of the IMR-32 human neuroblastoma clonal line." J Pharmacol Exp Ther **265**(1): 294-302.

Lukas, R. J., J. P. Changeux, N. Le Novere, E. X. Albuquerque, D. J. Balfour, D. K. Berg, D. Bertrand, V. A. Chiappinelli, P. B. Clarke, A. C. Collins, J. A. Dani, S. R. Grady, K. J. Kellar, J. M. Lindstrom, M. J. Marks, M. Quik, P. W. Taylor and S. Wonnacott (1999). "International Union of Pharmacology. XX. Current status of the nomenclature for nicotinic acetylcholine receptors and their subunits." Pharmacol Rev **51**(2): 397-401.

Luntz-Leybman, V., P. C. Bickford and R. Freedman (1992). "Cholinergic gating of response to auditory stimuli in rat hippocampus." Brain Res **587**(1): 130-6.

Macallan, D. R., G. G. Lunt, S. Wonnacott, K. L. Swanson, H. Rapoport and E. X. Albuquerque (1988). "Methyllycaconitine and (+)-anatoxin-a differentiate between nicotinic receptors in vertebrate and invertebrate nervous systems." FEBS Lett **226**(2): 357-63.

Marks, M. J., A. E. Bullock and A. C. Collins (1995). "Sodium channel blockers partially inhibit nicotine-stimulated 86Rb+ efflux from mouse brain synaptosomes." J Pharmacol Exp Ther **274**(2): 833-41.

Marks, M. J., D. A. Farnham, S. R. Grady and A. C. Collins (1993). "Nicotinic receptor function determined by stimulation of rubidium efflux from mouse brain synaptosomes." J Pharmacol Exp Ther **264**(2): 542-52.

Marks, M. J., J. R. Pauly, S. D. Gross, E. S. Deneris, I. Hermans-Borgmeyer, S. F. Heinemann and A. C. Collins (1992). "Nicotine binding and nicotinic receptor subunit RNA after chronic nicotine treatment." J Neurosci **12**(7): 2765-84.

Marks, M. J., S. F. Robinson and A. C. Collins (1996). "Nicotinic agonists differ in activation and desensitization of 86Rb+ efflux from mouse thalamic synaptosomes." J Pharmacol Exp Ther **277**(3): 1383-96.

Marks, M. J., K. W. Smith and A. C. Collins (1998). "Differential agonist inhibition identifies multiple epibatidine binding sites in mouse brain." J Pharmacol Exp Ther **285**(1): 377-86.

Marks, M. J., J. A. Stitzel, E. Romm, J. M. Wehner and A. C. Collins (1986). "Nicotinic binding sites in rat and mouse brain: comparison of acetylcholine, nicotine, and alpha-bungarotoxin." Mol Pharmacol **30**(5): 427-36.

Marubio, L. M., M. del Mar Arroyo-Jimenez, M. Cordero-Erausquin, C. Lena, N. Le Novere, A. de Kerchove d'Exaerde, M. Huchet, M. I. Damaj and J. P. Changeux (1999). "Reduced antinociception in mice lacking neuronal nicotinic receptor subunits." Nature **398**(6730): 805-10.

Matsubayashi, H., M. Alkondon, E. F. Pereira, K. L. Swanson and E. X. Albuquerque (1998). "Strychnine: a potent competitive antagonist of alpha-bungarotoxin-sensitive nicotinic acetylcholine receptors in rat hippocampal neurons." J Pharmacol Exp Ther **284**(3): 904-13.

McDonald, I. A., j. M. Vernier, N. Cosford and J. Corey-Naeve (1996). "Neuronal nicotinic acetylcholine receptor agoinsts." Curr Pharm Design **2**: 357-366.

McGehee, D. S. and L. W. Role (1995). "Physiological diversity of nicotinic acetylcholine receptors expressed by vertebrate neurons." Annu Rev Physiol **57**: 521-46.

Mehmandoust, M., C. Marazano and B. C. Das (1989). "A stereoselective route to enantiomeric 2-alkyl-1,2,3,6-tetrahydropyridines." J Chem Soc Chem Commun: 1185-1144.

Menshutkin, N. (1890). "Unknown." Z. Physik Chem **5**: 589.
Meyer, E. M., A. Kuryatov, V. Gerzanich, J. Lindstrom and R. L. Papke (1998). "Analysis of 3-(4-hydroxy, 2-Methoxybenzylidene)anabaseine selectivity and activity at human and rat alpha-7 nicotinic receptors." J Pharmacol Exp Ther **287**(3): 918-25.
Meyer, E. M., E. T. Tay, R. L. Papke, C. Meyers, G. L. Huang and C. M. de Fiebre (1997). "3-[2,4-Dimethoxybenzylidene]anabaseine (DMXB) selectively activates rat alpha7 receptors and improves memory-related behaviors in a mecamylamine-sensitive manner." Brain Res **768**(1-2): 49-56.
Meyer, E. M., E. T. Tay, J. A. Zoltewicz, C. Meyers, M. A. King, R. L. Papke and C. M. De Fiebre (1998). "Neuroprotective and memory-related actions of novel alpha-7 nicotinic agents with different mixed agonist/antagonist properties." J Pharmacol Exp Ther **284**(3): 1026-32.
Meyer, M. D., M. W. Decker, L. E. Rueter, D. J. Anderson, M. J. Dart, K. H. Kim, J. P. Sullivan and M. Williams (2000). "The identification of novel structural compound classes exhibiting high affinity for neuronal nicotinic acetylcholine receptors and analgesic efficacy in preclinical models of pain." Eur J Pharmacol **393**(1-3): 171-7.
Middleton, L. S., P. A. Crooks, P. J. Wedlund, W. A. Cass and L. P. Dwoskin (2005). "Nornicotine inhibition of striatal dopamine transporter function via nicotinic receptor activation." J Pharmacol Exp Therap **In press**.
Miller, D. K., P. A. Crooks and L. P. Dwoskin (2000). "Lobeline inhibits nicotine-evoked [(3)H]dopamine overflow from rat striatal slices and nicotine-evoked (86)Rb(+) efflux from thalamic synaptosomes." Neuropharmacology **39**(13): 2654-62.
Miyazawa, A., Y. Fujiyoshi, M. Stowell and N. Unwin (1999). "Nicotinic acetylcholine receptor at 4.6A resolution: transverse tunnels in the channel wall." J Mol Biol **288**: 765-786.
Miyazawa, A., Y. Fujiyoshi and N. Unwin (2003). "Structure and gating mechanism of the acetylcholine receptor pore."Nature **423**: 949-?
Mogg, A. J., P. Whiteaker, J. M. McIntosh, M. J. Marks, A. C. Collins and S. Wonnacott (2002). "Methyllycaconitine is a potent antagonist of alpha-conotoxin-MII-sensitive presynaptic nicotinic acetylcholine receptors in rat striatum." J Pharmacol Exp Ther **302**: 197-204.
Morens, D. M., A. Grandinetti, D. Reed, L. R. White and G. W. Ross (1995). "Cigarette smoking and protection from Parkinson's disease: false association or etiologic clue?" Neurology **45**(6): 1041-51.
Moss, D. E., P. Z. Manderscheid, S. P. Montgomery, A. B. Norman and P. R. Sanberg (1989). "Nicotine and cannabinoids as adjuncts to neuroleptics in the treatment of Tourette syndrome and other motor disorders." Life Sci **44**(21): 1521-5.
Neugebauer, N. M., Z. Zhang, P. A. Crooks, L. P. Dwoskin and M. T. Bardo (2006). "Effect of a novel nicotinic receptor antagonist, *N,N'*-dodecane-1,12-diyl-*bis*-3-picolinium dibromide, on nicotine self-administration and hyperactivity in rats." Psychopharmacology **184**: 426-434.
Nguyen, H. N., B. A. Rasmussen and D. C. Perry (2004). "Binding and functional activity of nicotinic cholinergic receptors in selected rat brain regions are

increased following long-term but not short-term nicotine treatment." J Neurochem **90**: 40-49.
Nicolotti, O., M. Pellegrini-Calace, A. Carrieri, C. Altomare, N. B. Centeno, F. Sanz and A. Carotti (2001). "Neuronal nicotinic receptor agonists: a multi-approach development of the pharmacophore." J Comput Aided Mol Des **15**(9): 859-72.
Nielsen, S. F., E. O. Nielsen, G. M. Olsen, T. Liljefors and D. Peters (2000). "Novel potent ligands for the central nicotinic acetylcholine receptor: synthesis, receptor binding, and 3D-QSAR analysis." J Med Chem **43**(11): 2217-26.
Nordberg, A., H. Lundqvist, P. Hartvig, A. Lilja and B. Langstrom (1995). "Kinetic analysis of regional (S)(-)11C-nicotine binding in normal and Alzheimer brains-in vivo assessment using positron emission tomography." Alzheimer Dis Assoc Disord **9**: 21-27.
Ogden, D. C. and D. Colquhoun (1985). "Ion channel block by acetylcholine, carbachol and suberyldicholine at the frog neuromuscular junction." Proc R Soc Lond B Biol Sci **225**(1240): 329-55.
Olanow, C. W. (2004). "The scientific basis for the current treatment of Parkinson's disease." Annu Rev Med **55**: 41-60.
O'Neill, M. J., T. K. Murray, V. Lakics, N. P. Visanji and S. Duty (2002). "The role of neuronal nicotinic acetylcholine receptorsin acute and chronic neurodegeneration." Curr Drug Targets -CNS & Neuro Disorders **1**: 399-411.
Orr-Urtreger, A., F. M. Goldner, M. Saeki, I. Lorenzo, L. Goldberg, M. De Biasi, J. A. Dani, J. W. Patrick and A. L. Beaudet (1997). "Mice deficient in the alpha7 neuronal nicotinic acetylcholine receptor lack alpha-bungarotoxin binding sites and hippocampal fast nicotinic currents." J Neurosci **17**(23): 9165-71.
Ortells, M. O. and G. G. Lunt (1995). "Evolutionary history of the ligand-gated ion-channel superfamily of receptors [see comments]." Trends Neurosci **18**(3): 121-7.
Palma, E., S. Bertrand, T. Binzoni and D. Bertrand (1996). "Neuronal nicotinic alpha 7 receptor expressed in Xenopus oocytes presents five putative binding sites for methyllycaconitine." J Physiol **491**(Pt 1): 151-61.
Papke, R. L., E. Meyer, T. Nutter and V. V. Uteshev (2000). "alpha7 receptor-selective agonists and modes of alpha7 receptor activation." Eur J Pharmacol **393**(1-3): 179-95.
Papke, R. L., P. R. Sanberg and R. D. Shytle (2001). "Analysis of mecamylamine stereoisomers on human nicotinic receptor subtypes." J Pharmacol Exp Ther **297**(2): 646-56.
Papke, R. L. and J. S. Thinschmidt (1998). "The correction of alpha7 nicotinic acetylcholine receptor concentration-response relationships in Xenopus oocytes." Neurosci Lett **256**(3): 163-6.
Paton, W. D. M. and E. J. Zaimis (1951). "Paralysis of autonomic ganglia by methonium salts." Br J Pharmacol Chemother **6**: 155-168.
Peng, X., V. Gerzanich, R. Anand, P. J. Whiting and J. Lindstrom (1994). "Nicotine-induced increase in neuronal nicotinic receptors results from a decrease in the rate of receptor turnover." Mol Pharmacol **46**(3): 523-30.
Perry, E. K., C. Martin-Ruiz, M. Lee, M. Griffiths, M. Johnson, M. Piggott, V. Haroutunian, J. D. Buxbaum, J. Nasland, K. Davis, C. Gotti, F. Clementi, S. Tzartos, O. Cohen, H. Sereq, E. Jaros, R. Perry, C. Ballard, I. McKeith and J.

Court (2000). "Nicotinic receptor subtypes in human brain aging, Alzheimer and Lewy body diseases." Eur J Pharmacol **393**: 215-222.

Picciotto, M. R., M. Zoli, C. Lena, A. Bessis, Y. Lallemand, N. LeNovere, P. Vincent, E. M. Pich, P. Brulet and J. P. Changeux (1995). "Abnormal avoidance learning in mice lacking functional high-affinity nicotine receptor in the brain." Nature **374**(6517): 65-7.

Picciotto, M. R., M. Zoli, R. Rimondini, C. Lena, L. M. Marubio, E. M. Pich, K. Fuxe and J. P. Changeux (1998). "Acetylcholine receptors containing the beta2 subunit are involved in the reinforcing properties of nicotine." Nature **391**(6663): 173-7.

Quik, M., T. Bordia, L. Forno and J. M. McIntosh (2004). "Loss of alpha-conotoxinMII- and A85380-sensitive nicotinic acetylcholine receptors in Parkinson's disease striatum." J Neurochem **88**: 668-679.

Quik, M., J. Choremis, J. Komourian, R. J. Lukas and E. Puchacz (1996). "Similarity between rat brain nicotinic alpha-bungarotoxin receptors and stably expressed alpha-bungarotoxin binding sites." J Neurochem **67**(1): 145-54.

Quik, M. and J. M. McIntosh (2006). "Striatal alpha 6* nicotinic acetylcholine receptors: potential targets for Parkinson's disease therapy." J Pharmacol Exp Ther **316**: 481-489.

Quik, M., S. Vailati, T. Bordia, J. M. Kulak, H. Fan, J. M. McIntosh, F. Clementi and C. Gotti (2005). "Subunit composition of nicotinic receptors in monkey striatum: effect of treatments with 1-methyl-4-phenyl-1,2,3,6-tetrahydropyridine or L-DOPA." Mol Pharmacol **67**(1): 32-41.

Rakhilin, S., R. C. Drisdel, D. Sagher, D. S. McGehee, Y. Vallejo and W. N. Green (1999). "alpha-bungarotoxin receptors contain alpha7 subunits in two different disulfide-bonded conformations." J Cell Biol **146**(1): 203-18.

Rao, T. S., L. D. Correa, R. T. Reid and G. K. Lloyd (1996). "Evaluation of anti-nociceptive effects of neuronal nicotinic acetylcholine receptor (NAChR) ligands in the rat tail-flick assay." Neuropharmacology **35**(4): 393-405.

Reavill, C., P. Jenner, R. Kumar and I. P. Stolerman (1988). "High affinity binding of [3H](-)-nicotine to rat brain membranes and its inhibition by analogues of nicotine." Neuropharmacology **27**: 235-241.

Reavill, C., B. Walther, I. P. Stolerman and B. Testa (1990). "Behavioral and pharmacokinetics studies on nicotine, cytisine and lobeline." Neuropharmacol **36**: 619-624.

Reuben, M., M. Louis and P. B. Clarke (1998). "Persistent nicotinic blockade by chlorisondamine of noradrenergic neurons in rat brain and cultured PC12 cells." Br J Pharmacol **125**(6): 1218-27.

Risner, M. E., E. J. Cone, N. L. Benowitz and P. J. Jacob (1988). "Effects of stereoisomers of nicotine and nornicotine on schedule controlled responding by beagle dogs and squirrel monkeys." J Pharmacol Exp Therap **234**: 807-813.

Rogers, D. and A. J. Hopfinger (1994). "Application of genetic function approximation to quantitative structure-activity relationships and quantitative structure-property relationships." J Chem Inf Comput Sci **34**: 854-866.

Rose, J. E. (1996). "Nicotine addiction and treatment." Annu Rev Med **47**: 493-507.

Rose, J. E., F. M. Behm, J. D. Lane, E. C. Westmen, E. D. Levin, R. M. Stein, J. D. Lane and G. V. Ripka (1998). "Nicotine-mecamylamine treatment for smoking cessation." Exp Clin Psychopharmacol **6**: 331-343.

Rose, J. E., F. M. Behm and E. C. Westman (2001). "Acute effects of nicotine and mecamylamine on tobacco withdrawal symptoms, cigarette reward and ad lib smoking." Pharmacol Biochem Behav **68**(2): 187-97.

Rose, J. E., F. M. Behm, E. C. Westman, E. D. Levin, R. M. Stein and G. V. Ripka (1994). "Mecamylamine combined with nicotine skin patch facilitates smoking cessation beyond nicotine patch treatment alone." Clin Pharmacol Ther **56**(1): 86-99.

Rowell, P. P. and J. A. Hillebrand (1994). "Characterization of nicotine-induced desensitization of evoked dopamine release from rat striatal synaptosomes." J Neurochem **63**(2): 561-9.

Rusted, J. M., P. A. Newhouse and E. D. Levin (2000). "Nicotinic treatment for degenerative neuropsychiatric disorders such as Alzheimer's disease and Parkinson's disease." Behav Brain Res **113**(1-2): 121-129.

Sabey, K., K. Paradiso, J. Zhang and J. H. Steinbach (1999). "Ligand binding and activation of rat nicotinic alpha4beta2 receptors stably expressed in HEK293 cells." Mol Pharmacol **55**(1): 58-66.

Sacaan, A. I., J. L. Dunlop and G. K. Lloyd (1995). "Pharmacological characterization of neuronal acetylcholine gated ion channel receptor-mediated hippocampal norepinephrine and striatal dopamine release from rat brain slices." J Pharmacol Exp Ther **274**(1): 224-30.

Sacaan, A. I., R. T. Reid, E. M. Santori, P. Adams, L. D. Correa, L. S. Mahaffy, L. Bleicher, N. D. Cosford, K. A. Stauderman, I. A. McDonald, T. S. Rao and G. K. Lloyd (1997). "Pharmacological characterization of SIB-1765F: a novel cholinergic ion channel agonist." J Pharmacol Exp Ther **280**(1): 373-83.

Sacco, K. A., A. Termine, A. Seyal, M. M. Dudas, J. C. Vessicchio, S. Krishnan-Sarin, P. I. Jatlow, B. E. Wexler and T. P. George (2005). "Effects of cigarette smoking on spatial working memory and attentional deficits in schizophrenia: involvement of nicotinic receptor mechanisms." Arch Gen Psychiatry **62**: 649-659.

Sahley, T. L. and G. G. Berntson (1979). "Antinociceptive effects of central and systemic administrations of nicotine in the rat." Psychopharmacology (Berl) **65**(3): 279-83.

Salminen, O., K. L. Murphy, J. M. McIntosh, J. Drago, M. J. Marks, A. C. Collins and S. R. Grady (2004). "Subunit composition and pharmacology of two classes of striatal presynaptic nicotinic acetylcholine receptors mediating dopamine release in mice." Mol Pharmacol **65**(6): 1526-1535.

Samii, A., J. G. Nutt and B. R. Ransom (2004). "Parkinson's disease." Lancet **363**: 1783-1793.

Sanberg, P. R., B. J. McConville, H. M. Fogelson, P. Z. Manderscheid, K. W. Parker, M. M. Blythe, W. M. Klykylo and A. B. Norman (1989). "Nicotine potentiates the effects of haloperidol in animals and in patients with Tourette syndrome." Biomed Pharmacother **43**(1): 19-23.

Sanberg, P. R., A. A. Silver, R. D. Shytle, M. K. Philipp, D. W. Cahill, H. M. Fogelson and B. J. McConville (1997). "Nicotine for the treatment of Tourette's syndrome." Pharmacol Ther **74**(1): 21-5.

Sargent, P. B. (1993). "The diversity of neuronal nicotinic acetylcholine receptors." Annu Rev Neurosci **16**: 403-43.

Sarkar, T. K., S. Basak, I. Wainer, R. Moaddel, R. Yamaguchi, K. Jozwiak, H.-T. Chen and C.-C. Lin (2004). "Coaxing a pyridine nucleus to give up its aromaticity: synthesis and pharmacological characterization of novel conformationally restricted analogues of nicotine and anabasine." J Med Chem **47**: 6691-6701.

Schapira, M., R. Abagyan and M. Totrov (2002). "Structural model of nicotinic aceylcholine receptor isotypes bound to acetylcholine and nicotine." BMC Structural Biology **2**: 1-8.

Schmitt, J. D. (2000). "Exploring the nature of molecular recognition in nicotinic acetylcholine receptors." Curr Med Chem **7**(8): 749-800.

Schneider, F. H. and T. A. Olsson (1996). "Clinical-experience with lobeline as a smoking cessation agent." Med Chem Res **6**: 562-570.

Schneider, G. and M. Nettekoven (2003). "Ligand-based combinatorial design of selective purinergic receptor (A2A) antagonists using self-organizing maps." J Comb Chem **5**(3): 233-237.

Schneider, J. S., A. Pope-Coleman, M. Van Velson, F. Menzaghi and G. K. Lloyd (1998). "Effects of SIB-1508Y, a novel neuronal nicotinic acetylcholine receptor agonist, on motor behavior in parkinsonian monkeys." Mov Disord **13**: 637-642.

Schulz, D. W., R. H. Loring, E. Aizenman and R. E. Zigmond (1991). "Autoradiographic localization of putative nicotinic receptors in the rat brain using 125I-neuronal bungarotoxin." J Neurosci **11**(1): 287-97.

Schulz, D. W. and R. E. Zigmond (1989). "Neuronal bungarotoxin blocks the nicotinic stimulation of endogenous dopamine release from rat striatum." Neurosci Lett **98**(3): 310-6.

Schwartz, R. D., R. McGee, Jr. and K. J. Kellar (1982). "Nicotinic cholinergic receptors labeled by [3H]acetylcholine in rat brain." Mol Pharmacol **22**(1): 56-62.

Seguela, P., J. Wadiche, K. Dineley-Miller, J. A. Dani and J. W. Patrick (1993). "Molecular cloning, functional properties, and distribution of rat brain alpha 7: a nicotinic cation channel highly permeable to calcium." J Neurosci **13**(2): 596-604.

Sekul, A. A. and W. C. Holland (1961). "Pharmacology of senecioylcholine." J Pharmacol Exp Ther **132**: 171-175.

Shapiro, E., A. K. Shapiro, G. Fulop, M. Hubbard, J. Mandeli, J. Nordlie and R. A. Phillips (1989). "Controlled study of haloperidol, pimozide and placebo for the treatment of Gilles de la Tourette's syndrome." Arch Gen Psychiatry **46**(8): 722-30.

Sharpless, C. G. V. and S. Wonnacott (2001). "Neuronal nicotinic receptors." Tocris Reviews **19**: 1-12.

Sheridan, R. P., R. Nilakantan, J. S. Dixon and R. Venkataraghavan (1986). "The ensemble approach to distance geometry: Application to the nicotinic pharmacophore." J Med Chem **29**: 899-906.

Silver, A. A., R. D. Shytle and P. R. Sanberg (2000). "Mecamylamine in Tourette's syndrome: a two-year retrospective case study." J Child Adolesc Psychopharmacol **10**(2): 59-68.

Slemmer, J. E., B. R. Martin and M. I. Damaj (2000). "Buproprion is a nicotinic antagonist." J Pharmacol Exp Ther **295**: 321-327.

Smit, A. B., K. Brejc, N. Syed and T. K. Sixma (2003). "Structure and function of AChRP, homologue of the ligand-binding domain of the nicotinic acetylcholine receptor." Ann N Y Acad Sci **998**: 81-92.

Smit, A. B., N. I. Syed, D. Schaap, J. van Minnen, J. Klumperman, K. S. Kits, H. Lodder, R. C. van der Schors, R. van Elk, B. Sorgedrager, K. Brejc, T. K. Sixma and W. P. Geraerts (2001). "A glia-derived acetylcholine-binding protein that modulates synaptic transmission." Nature **411**: 261-268.

So, S., S. van Helden, V. van Geerestein and M. Karplus (2000). "Quantitative structure-activity relationship studies of progesterone receptor binding steroids." J Chem Info & Comp Sci **40**(3): 762-772.

Spande, T. F., H. M. Garraffo, H. J. Yeh, Q. L. Pu, L. K. Pannell and J. W. Daly (1992). "A new class of alkaloids from a dendrobatid poison frog: a structure for alkaloid 251F." J Nat Prod **55**(6): 707-22.

Suchocki, J. A., E. L. May, T. J. Martin, C. George and B. R. Martin (1991). "Synthesis of 2-exo- and 2-endo-mecamylamine analogues. Structure- activity relationships for nicotinic antagonism in the central nervous system." J Med Chem **34**(3): 1003-10.

Sugaya, K., E. Giacobini and V. A. Chiappinelli (1990). "Nicotinic acetylcholine receptor subtypes in human frontal cortex: changes in Alzheimer's disease." J Neurosci Res **27**(3): 349-59.

Sullivan, J. P. and A. W. Bannon (1996). "Epibatidine: pharmacological properties of a novel nicotinic acetylcholine receptor agonist and analgesic agent." CNS Drug Rev **2**: 21-39.

Sullivan, J. P., M. W. Decker, J. D. Brioni, D. Donnelly-Roberts, D. J. Anderson, A. W. Bannon, C. H. Kang, P. Adams, M. Piattoni-Kaplan, M. J. Buckley and et al. (1994). "(+/-)-Epibatidine elicits a diversity of in vitro and in vivo effects mediated by nicotinic acetylcholine receptors." J Pharmacol Exp Ther **271**(2): 624-31.

Sumarithan, S. P., P. A. Crooks, R. Xu, J. Zhu, A. G. Deaciuc, L. H. Wilkins, Jr. and L. P. Dwoskin (2005). "Introduction of unsaturation into the *N*-*n*-alkyl chain of nicotinic receptor antagonists, NONI and NDNI: effect on affinity and selectivity." AAPS Journal **7**(1): Article 19.

Swango, J. H., B. S. Bhatti, M. M. Qureshi and P. A. Crooks (1999). "A novel enantioselective synthesis of (S)-(-)- and (R)-(+)-nornicotine via alkylation of a chiral 2-hydroxy-3-pinanone ketimine template." Chirality **11**(4): 316-8.

Sweet, M. (2003). "GlaxoSmithKline takes legal action to block new controls on its smoking cessation drug." Br Med J **326**: 952.

Teng, L., P. A. Crooks, S. T. Buxton and L. P. Dwoskin (1997). "Nicotinic-receptor mediation of S(-)nornicotine-evoked -3H-overflow from rat striatal slices preloaded with -3H-dopamine." J Pharmacol Exp Ther **283**(2): 778-87.

Thomas, P., M. Stephens, G. Wilkie, M. Amar, G. G. Lunt, P. Whiting, T. Gallagher, E. Pereira, M. Alkondon, E. X. Albuquerque and et al. (1993). "(+)-Anatoxin-a is a potent agonist at neuronal nicotinic acetylcholine receptors." J Neurochem **60**(6): 2308-11.

Tonder, J. E. and P. H. Olesen (2001). "Agonists at the alpha4beta2 nicotinic acetylcholine receptors: structure-activity relationships and molecular modelling." Curr Med Chem **8**(6): 651-74.

Tonder, J. E., P. H. Olesen, J. B. Hansen, M. Begtrup and I. Pettersson (2001). "An improved nicotinic pharmacophore and a stereoselective CoMFA-model for nicotinic agonists acting at the central nicotinic acetylcholine receptors labelled by." J Comput Aided Mol Des **15**(3): 247-58.

Tripathi, H. L., B. R. Martin and M. D. Aceto (1982). "Nicotine-induced antinociception in rats and mice: correlation with nicotine brain levels." J Pharmacol Exp Ther **221**(1): 91-6.

Tuppo, E. E. and H. R. Arias (2005). "The role of inflammation in Alzheimer's disease." Int J Biochem & Cell Biol **37**: 289-305.

Unwin, N. (2005). "Refined structure ofthe nicotinic acetylcholine receptor at 4A resolution." J Mol Biol **346**: 967-989.

Valette, H., M. Bottlaender, F. Dollé, C. Coulon, M. Ottaviani and A. Syrota (2003). "Long-lasting occupancy of central nicotine acetylcholine receptors after smoking: a PET study in monkeys." J Neurochem **84**: 105-111.

Virginio, C., F. Graziani and G. C. Terstappen (2005). "Differential inhibition of rat alpha3* and alpha7 nicotinic acetylcholine receptors by tetrandrine and closely related bis-benzylisoquinoline derivatives." Neurosci Lett **381**: 299-304.

von Korff, M. and M. Steger (2004). "GPCR-tailored pharmacophore pattern recognition of small molecular ligands." J Chem Info & Comp Sci **44**(3): 1137-1147.

Wada, E., K. Wada, J. Boulter, E. Deneris, S. Heinemann, J. Patrick and L. W. Swanson (1989). "Distribution of alpha 2, alpha 3, alpha 4, and beta 2 neuronal nicotinic receptor subunit mRNAs in the central nervous system: a hybridization histochemical study in the rat." J Comp Neurol **284**(2): 314-35.

Wada, K., M. Ballivet, J. Boulter, J. Connolly, E. Wada, E. S. Deneris, L. W. Swanson, S. Heinemann and J. Patrick (1988). "Functional expression of a new pharmacological subtype of brain nicotinic acetylcholine receptor." Science **240**(4850): 330-4.

Wang, F., V. Gerzanich, G. B. Wells, R. Anand, X. Peng, K. Keyser and J. Lindstrom (1996). "Assembly of human neuronal nicotinic receptor alpha5 subunits with alpha3, beta2, and beta4 subunits." J Biol Chem **271**(30): 17656-65.

Webster, J. C., M. M. Francis, J. K. Porter, G. Robinson, C. Stokes, B. Horenstein and R. L. Papke (1999). "Antagonist activities of mecamylamine and nicotine show reciprocal dependence on beta subunit sequence in the second transmembrane domain." Br J Pharmacol **127**(6): 1337-48.

Whiteaker, P., A. R. Davies, M. J. Marks, I. S. Blagbrough, B. V. Potter, A. J. Wolstenholme, A. C. Collins and S. Wonnacott (1999). "An autoradiographic study of the distribution of binding sites for the novel alpha7-selective nicotinic radioligand [3H]-methyllycaconitine in the mouse brain." Eur J Neurosci **11**(8): 2689-96.

Whiteaker, P., C. G. Peterson, W. Xu, J. M. McIntosh, R. Paylor, A. L. Beaudet, A. C. Collins and M. J. Marks (2002). "Involvement of the alpha3 subunit in central nicotinic binding populations." J Neurosci **22**: 2522-2529.

Whiteaker, P., C. G. Sharples and S. Wonnacott (1998). "Agonist-induced up-regulation of alpha4beta2 nicotinic acetylcholine receptors in M10 cells: pharmacological and spatial definition." Mol Pharmacol **53**(5): 950-62.

Whitehouse, P. J., A. M. Martino, M. V. Wagster, D. L. Price, R. Mayeux, J. R. Atack and K. J. Kellar (1988). "Reductions in [3H]nicotinic acetylcholine binding in Alzheimer's disease and Parkinson's disease: an autoradiographic study." Neurology **38**(5): 720-3.

Whiting, P. J., R. Liu, B. J. Morley and J. M. Lindstrom (1987). "Structurally different neuronal nicotinic acetylcholine receptor subtypes purified and characterized using monoclonal antibodies." J Neurosci **7**(12): 4005-16.

Wilkens, L. H. (2001). Pharmacological characterization of a series of novel *N*-alkyl nicotinium analogues as neuronal nicotinic receptor subtype-selective antagonists. Pharmaceutical Sciences. Lexington, University of Kentucky**:** 399.

Wilkins, L. H., Jr., V. P. Grinevich, J. T. Ayers, P. A. Crooks and L. P. Dwoskin (2003). "N-n-Alkylnicotinium analogs, a novel class of nicotinic receptor antagonists: interaction with alpha4beta2* and alpha7* neuronal nicotinic receptors." J Pharmacol Exp Ther **304**: 400-410.

Wilkins, L. H., Jr., A. J. Haubner, J. T. Ayers, P. A. Crooks and L. P. Dwoskin (2002). "*N*-n-Alkylnicotinium Analogs, A Novel Class of Nicotinic Receptor Antagonist: Inhibition of S-(-)-Nicotine-Evoked [3H]Dopamine Overflow from Superfused Rat Striatal Slices." J Phar Exp Ther **301**: 1088-1096.

Wonnacott, S. (1997). "Presynaptic nicotinic ACh receptors." Trends Neurosci **20**(2): 92-8.

Wonnacott, S., E. X. Albuquerque and D. Bertrand (1993). "Methyllycaconitine: a new probe that discriminates between nicotinic acetylcholine receptor subclasses." Meth Neurosci **12**: 263-275.

Wonnacott, S., A. Drasdo, E. Sanderson and P. Rowell (1990). "Presynaptic nicotinic receptors and the modulation of transmitter release." Ciba Found Symp **152**: 87-101.

Wonnacott, S., S. Jackman, K. L. Swanson, H. Rapoport and E. X. Albuquerque (1991). "Nicotinic pharmacology of anatoxin analogs. II. Side chain structure- activity relationships at neuronal nicotinic ligand binding sites." J Pharmacol Exp Ther **259**(1): 387-91.

Xiao, Y., E. L. Meyer, J. M. Thompson, A. Surin, J. Wroblewski and K. J. Kellar (1998). "Rat alpha3/beta4 subtype of neuronal nicotinic acetylcholine receptor stably expressed in a transfected cell line: pharmacology of ligand binding and function." Mol Pharmacol **54**(2): 322-33.

Xu, R., L. P. Dwoskin, V. P. Grinevich, G. Deaciuc and P. A. Crooks (2001). "Neuronal nicotinic acetylcholine receptor binding affinities of boron- containing nicotine analogues." Bioorg Med Chem Lett **11**(9): 1245-8.

Young, J. M., R. D. Shytle, P. R. Sanberg and T. P. George (2001). "Mecamylamine: new therapeutic uses and toxicity/risk profile." Clin Ther **23**(4): 532-65.

Yu, Z. J., D. G. Morgan and L. Wecker (1996). "Distribution of three nicotinic receptor alpha 4 mRNA transcripts in rat brain: selective regulation by nicotine administration." J Neurochem **66**(3): 1326-9.

Yuan, H. and A. Parrill (2002). "QSAR studies of HIV-1 integrase inhibition." Bioorg & Med Chem **10**(12): 4169-4183.

Yum, L., K. M. Wolf and V. A. Chiappinelli (1995). "Nicotinic acetylcholine receptors in separate brain regions exhibit different affinities for methyllycaconitine." Neuroscience **72**(2): 545-555.

Yus, M., T. Soler and F. Foubelo (2001). "A new and direct synthesis of 2-substituted pyrrolidines." J Org Chem **66**(18): 6207-8.

Zhong, W., J. P. Gallivan, Y. Zhang, L. Li and H. A. Lester (1998). "From ab initio quantum mechanics to molecular neurobiology: a cation-pi binding site in the nicotinic receptor." Proc Natl Acad Sci USA **95**: 12088-12093.

Zoli, M., C. Lena, M. R. Picciotto and J. P. Changeux (1998). "Identification of four classes of brain nicotinic receptors using beta2 mutant mice." J Neurosci **18**(12): 4461-72.

Zoli, M., M. Moretti, M. McIntoh, F. Clementi and C. Gotti (2002). "Indentification of the nicotinic receptor subtypes expressed on dopaminergic terminals in the rat striatum." J Neurosci **22**: 8785-8789.

Zoli, M., M. R. Picciotto, R. Ferrari, D. Cocchi and J. P. Changeux (1999). "Increased neurodegeneration during ageing in mice lacking high-affinity nicotine receptors." Embo J **18**(5): 1235-44.

Zupan, J. and J. Gasteiger (1993). Neuronal Networks for Chemists. New York, VCH.

Vita

GENERAL INFORMATION

Date of Birth: July 7, 1975

Place of Birth: Denver, CO

Citizenship: United States of America

EDUCATION

Trinity College, Hartford, CT

Bachelors of Science, May 1997

Major: Chemistry

FELLOWSHIPS

Target of Opportunity Research Assistantship (TORA), University of Kentucky, 1999

AWARDS AND HONORS

Peter Glavanos Travel Award Recipient, 2001

Undergraduate Research Grant Recipient,

Trinity College, 1996

PROFESSIONAL SOCIETIES

American Association of Pharmaceutical Sciences (AAPS) Member, 1997-present

President of AAPS Student Chapter, University of Kentucky, 2001-2002

American Chemical Society (ACS) Member, 1997-present

Rho Chi Honor Society, Alpha Xi Chapter, 1999-present

PRESENTATIONS

- “The Pharmacology of the Nicotinic Acetylcholine Receptor: An Overview” Guest Lecture for Dr. George Digenis PHR 924 Drug Design, University of Kentucky, College of Pharmacy, Lexington KY (2001)
- “The Pharmacology of the Nicotinic Acetylcholine Receptor: An Overview” Guest Lecture for Dr. George Digenis PHR 924 Drug Design, University of Kentucky, College of Pharmacy, Lexington KY (2000)
- “Synthesis and Delivery of Pyridinium Derivatives as Potent and Selective Antagonists at Central Nervous System Nicotinic Acetylcholine Receptor Subtypes” University of Kentucky, College of Pharmacy, Lexington KY (1999)
- “The Pharmacology of the Nicotinic Acetylcholine Receptor: An Overview” Guest Lecture for Dr. George Digenis PHR 924 Drug Design, University of Kentucky, College of Pharmacy, Lexington KY (1999)
- “Design of Centrally Active and Selective Nicotinic Receptor Antagonists” University of Kentucky, College of Pharmacy, Lexington KY (1998)

PATENTS

- "Bis-Pyridino-containing Compounds for Use in the Treatment of CNS Pathologies." By Peter A. Crooks, Linda P. Dwoskin, Joshua T. Ayers, Vladimir Grinevich, and Sangeetha P. Sumithran, International Patent No. WO 2005066129 A2, July 27th, 2005
- "Chain-Modified Pyridino-N-Substituted Nicotine Compounds for Use In the Treatment of CNS Pathologies." By Peter A. Crooks, Linda P. Dwoskin, Rui Xu,

and Joshua Ayers, U.S. Patent Application No. US 2003/0225142A1, December 4th, 2003.

- "N-Pyridinium Analogs for the Use in the Treatment of CNS Pathologies." By Peter A. Crooks, Joshua T. Ayers, Vladimir P. Grinevich and Linda P. Dwoskin, Deposition for U.S. patent to be filed: August 2001

PUBLISHED ABSTRACTS AND POSTER PRESENTATIONS

- S. P. Sumithran, P. A. Crooks, A. G. Deaciuc, **J. T. Ayers**, L. P. Dwoskin. *bis*-Quinolinium and *bis*-Isoquinolinium Quaternary Ammonium Analogs Potently Inhibit Nicotinic Receptors Mediating Nicotine-Evoked Striatal Dopamine Release.
- **J. T. Ayers**, A. Haubner, V. P. Grinevich, S. P. Sumithran, A. G. Deaciuc, O. Ghosheh, L. P. Dwoskin, P. A. Crooks. Synthesis and evaluation of *N*-alkylpyridinium analogs at the nicotinic acetylcholine receptor subtypes. *PharmSci.* 2001.
- **J. T. Ayers**, A. Haubner, V. P. Grinevich, S. P. Sumithran, A. G. Deaciuc, L. P. Dwoskin, P. A. Crooks. Synthesis and evaluation of *N*-alkylated *bis*-pyridinium, *bis*-nicotinium and *bis*-quinolinium analogs at the nicotinic acetylcholine receptor subtypes. *PharmSci.* 2001.
- **J. T. Ayers**, A. Haubner, S. P. Sumithran, V. P. Grinevich, A. G. Deaciuc, L. P. Dwoskin, P. A. Crooks. Synthesis and evaluation of *N*-alkylated pyridinium compounds as antagonists at nicotinic acetylcholine receptor subtypes". *American Chemical Society Annual Meeting*. 2001.

- **J. T. Ayers**, A. Haubner, V. P. Grinevich, O. Ghosheh, L. P. Dwoskin, P. A. Crooks. Evaluation of *N*-alkylated *bis*-pyridinium analogs at the putative α3β2 and α4β2 nicotinic acetylcholine receptor subtypes. *PharmSci.* 2000. S- 3240
- **J. T. Ayers**, A. Haubner, V. P. Grinevich, L. P. Dwoskin, P. A. Crooks. Synthesis and evaluation of N-alkylated pyridinium derivatives as antagonists at the nicotinic acetylcholine receptor. *American Chemical Society Annual Meeting*. 2000. S-275
- **J. T. Ayers**, A. Haubner, V.P. Grinevich, O. Ghosheh, L.P. Dwoskin, P.A. Crooks. Evaluation of *N*-alkylated pyridinium analogs as antagonists at the putative α3β2 nicotinic acetylcholine receptor subtype. *PharmSci.* 1999. S-3137
- **J. T. Ayers**, A. Haubner, L. H. Wilkins, V. P. Grinevich, O. Ghosheh, L. P. Dwoskin, P. A. Crooks. Synthesis of *N*-alkylated pyridinium molecules and their pharmacology at the nicotinic receptor. *IBC Nicotinic Acetylcholine Receptor Conference*. 1999. S-2

PUBLICATIONS

- F. Zheng, E. Bayram, S. P. Sumithran, **J. T. Ayers**, C-G Zhan, J. D. Schmitt, L. H. Wilkins, A. G. Deaciuc, D. D. Allen, L. P. Dwoskin, and P. A. Crooks. QSAR Modeling of *mono*- and *bis*-Quaternary Ammonium Salts that Act as Antagonists at Neuronal Nicotinic Acetylcholine Receptors Mediating Dopamine Release. *Bioorg & Med Chem* 14: 3017-3037 (2006).
- L. H. Wilkins, Jr., D. Miller, **J. T. Ayers**, P. A. Crooks, and L. P. Dwoskin. *N*-n-Alkylnicotinium Analogs, a Novel Class of Antagonists at a4ß2* Nicotinic

Acetylcholine Receptors: Inhibition of S(-)-Nicotine-Evoked 86Rb+ Efflux from Rat Thalamic Synaptosomes. *AAPS Journal* 7(4): Article 90 (2006).

- **J. T. Ayers**, S. Parkin, L. P. Dwoskin, and P. A. Crooks. A 1R, 2R, 5R-(+)-2a-hydroxypinanone Ketimine. Acta Crystallogr: Section E, E61: o2682-o2684 (2005).
- **J. T. Ayers**, R. Xu, L. P. Dwoskin, and P. A. Crooks. A General Procedure for the Enantioselective Synthesis of the Minor Tobacco Alkaloids Nornicotine, Anabasine, and Anatabine. *AAPS Journal* 7(3): Article 75 (2005).
- **J. T. Ayers**, A. Clauset, J. D. Schmitt, L. P. Dwoskin, and P. A. Crooks. Molecular Modeling of mono- and bis-Quaternary Ammonium Salts as Ligands at the a4ß2* Nicotinic Acetylcholine Receptor Subtype Using Nonlinear Techniques. *AAPS Journal* 7(3): Article 68 (2005).
- P. A. Crooks, **J. T. Ayers**, R. Xu, S. P. Sumithran, V. P. Grinevich, L. H. Wilkins, A. G. Deaciuc, D. D. Allen, and L. P. Dwoskin. Development of Subtype-Selective Ligands as Antagonists at Nicotinic Receptors Mediating Nicotine-Evoked Dopamine Release. *Bioorg & Med Chem Lett* 14(8): 1869-1874 (2004).
- L. P. Dwoskin, S. P. Sumithran, J. Zhu, A. G. Deaciuc, **J. T. Ayers**, and P. A. Crooks. Subtype-Selective Nicotinic Receptor Antagonists: Potential as Tobacco Use Cessation Agents. *Bioorg & Med Chem Lett* 14(8): 1863-1867 (2004).
- J. Zhu, P. A. Crooks, **J. T. Ayers**, S. P. Sumithran, and L. P. Dwoskin. *N*-n-Alkylnicotinium and *N*-n-Alkylpyridinium Analogs Inhibit the Dopamine

Transporter: Selectivity as Nicotinic Receptor Antagonists. *Drug Dev Res* 60: 270-284 (2003).

- L. H. Wilkins, Jr., V. P. Grinevich, **J. T. Ayers**, P. A. Crooks, and L. P. Dwoskin. *N*-n-Alkylnicotinium Analogs, a Novel Class of Nicotinic Receptor Antagonists: Interaction with alpha4beta2* and alpha7* Neuronal Nicotinic Receptors. *J Pharmacol Exp Ther* 304: 400-410 (2003).
- V.P. Grinevich, P.A. Crooks, P. Sumithran, A.J. Haubner, **J. T. Ayers**, and L. P. Dwoskin. *N*-n-Alkylpyridinium Analogs, a Novel Class of Nicotinic Receptor Antagonists: Selective Inhibition of Nicotine-Evoked [3H]Dopamine Overflow from Superfused Rat Striatal. *J Pharmacol Exp Ther* 306: 1011-1020 (2003).
- **J. T. Ayers**, L. P. Dwoskin, A. G. Deaciuc, V. P. Grinevich, J. Zhu, and P. A. Crooks. *bis*-Azaaromatic quaternary ammonium analogues: ligands for alpha4beta2* and alpha7* subtypes of neuronal nicotinic receptors. *Bioorg & Med Chem Lett* 12(21): 3067-3071 (2002).
- L. H. Wilkins, Jr., A. J. Haubner, **J. T. Ayers**, P. A. Crooks, and L. P. Dwoskin. *N-n*-Alkylnicotinium Analogs, A Novel Class of Nicotinic Receptor Antagonist: Inhibition of S-(-)-Nicotine-Evoked [3H]Dopamine Overflow from Superfused Rat Striatal Slices. *J Pharmacol Exp Ther* 301: 1088-1096 (2002).
- L. P. Dwoskin, R. Xu, **Ayers, J. T.**, P. A. Crooks. Recent developments in neuronal nicotinic acetylcholine receptor antagonists. *Exp Opin Ther Patents* 10 (10), 1-21 (2000).
- S. R. Anderson, **J. T. Ayers,** K. M. DeVries, F. Ito, D.Mendenhall, B. C. Vanderplas. The preparation of -substituted amines from mixtures of epoxide

opening products via a common aziridinium ion intermediate. *Tetrahedron Asymmetry*. 10(14), 2655-2663 (1999).

- **J. T Ayers** and S. R Anderson. A Preparative Scale Reduction of Alkyl Disulfides with Tributyl Phosphine and Water. *Synth. Comm.* 29(3), 351-358 (1999).

Joshua T. L. Ayers

07 July 2006